Mikel Armendia · Mani Ghassempouri
Erdem Ozturk · Flavien Peysson *Editors*

Twin-Control

A Digital Twin Approach to Improve Machine Tools Lifecycle

OPEN

Springer

Twin-Control

Mikel Armendia · Mani Ghassempouri
Erdem Ozturk · Flavien Peysson
Editors

Twin-Control

A Digital Twin Approach to Improve Machine Tools Lifecycle

OPEN

Springer

Editors
Mikel Armendia
Parke Teknologikoa
IK4-TEKNIKER
Eibar, Guipúzcoa, Spain

Erdem Ozturk
Advanced Manufacturing Park
University of Sheffield
Catcliffe, South Yorkshire, UK

Mani Ghassempouri
Z.I. de Melou
Comau
Castres, France

Flavien Peysson
Predict
Six-Fours-les-Plages, France

ISBN 978-3-030-02202-0 ISBN 978-3-030-02203-7 (eBook)
https://doi.org/10.1007/978-3-030-02203-7

Library of Congress Control Number: 2018957671

This Springer imprint is published by the registered company Springer Nature Switzerland AG
The registered company address is: Gewerbestrasse 11, 6330 Cham, Switzerland

Foreword

Recent digitalization developments and the ever-increasing global competitiveness have made the utilization of virtual simulation tools and the collaboration between the physical world and the virtual world a key enabler for quality assurance as well as productivity.

European economy is relying on a strong industrial base. Europe cannot compete with low price and low-quality product due to scarce natural and energy resources as well as ambitious social and environmental goals. European-based industries need to focus on innovation, productivity and resource efficiency criterions to create added value on global markets. The competitive advantage, which is essential for any global player, falls on high value-added goods and services when it comes to the European industry. To maintain the advantage, European industry needs to rely on innovation and technological advancement as its main source of competitiveness.

Twin-Control is a EUR 5.6 million industrial project funded by the Public–Private Partnership (PPP) for Factories of the Future (FoF) within the European Framework Programme for Research and Innovation, Horizon 2020 supported under the European Commission's over the last 36 months. It has aimed at utilizing the digital world for better controlling the real-world manufacturing processes. Twin-Control has investigated the development of a simulation and control system that integrates the different aspects that affect machine tool and machining performance. This holistic approach allows a better estimation of machining performance than single featured simulation packages.

Apart from the regular model-based simulation and assessment purposes, the developed tool can be installed within machine tool CNCs and allows a direct control of the process through monitoring. The monitored data combined by the model-based estimations allows an improved performance of the manufacturing process. These are achieved by controlling component degradation and optimizing maintenance actions, increasing energy efficiency and modifying process parameters to both increase productivity to protect a degraded component until the next planned maintenance.

The Twin-Control approach developed in this project was mainly tested and implemented within two of the key industries for European economy: aerospace and automotive. The integrated concept adopted by Twin-Control enhances the necessary collaboration between machine tool builders and part manufacturers to improve the productivity of the manufacturing processes.

The project focuses on several smaller developments and tests to incrementally achieve the complete radical goal of monitoring and controlling CNC machines with virtual predictive models. It has shown itself to be a successful set-up for development work in a project such as Twin-Control.

The project outcomes are promising as it can show increased control and performance of the CNCs operations. I recommend the study of the material contained in this book.

Gothenburg, Sweden
July 2018

Dr. Björn Johansson
Division of Production Systems
Chalmers University of Technology

Acknowledgements

Twin-Control project (www.twincontrol.eu) was kindly funded in H2020 by the European Commission (Grant agreement No. 680725), as part of the Factories of the Future initiative.

The editors of the book would like to thank all authors and industrial partners of Twin-Control project!

Contents

Abbreviations

AC	Adaptive control
API	Application programming interface
CAD	Computer-aided design
CAE	Computer-aided engineering
CAM	Computer-aided manufacturing
CAN	Controller Area Network
CAS	Collision avoidance system
CL	Cutter location
CMMS	Computer maintenance management system
CNC	Computer numeric control
CPS	Cyber-physical system
CSV	Comma separated value
DLL	Dynamic link library
DOF	Degree of freedom
EER	Energy efficiency ratio
FE	Finite element
FEA	Finite element analysis
FFT	Fast Fourier transform
FMECA	Failure modes, effects, and criticality analysis
FRF	Frequency response function
FTP	File Transfer Protocol
GUI	Graphical user interface
HMI	Human–machine interface
HP	High pressure
HTTP	Hypertext Transfer Protocol
ICT	Information and communication technology
ISO	International Standard Organization
IT	Information technology
KER	Key exploitable results
KPI	Key performance indicators

LAN	Local area network
MBS	Multi-body software
MDA	Machine data acquisition
MES	Manufacturing execution system
MT	Machine tool
MVC	Model view controller
NC	Numerical control
NILM	Non-intrusive load monitoring
O&M	Operation & maintenance
OEE	Overall equipment efficiency
OPC-UA	Open Platform Communications—unified architecture
PC	Personal computer
PHM	Prognostics and health management
PLC	Programmable logic controller
RMS	Root mean square
RUL	Remaining useful life
SCADA	Supervisory control and data acquisition
SMS	Short message service
SOA	Service-oriented architecture
SoU	Scenario of Use
SRM	Stability roadmap
STL	Standard triangle language
TCP	Transmission Control Protocol
TWE	Tool–workpiece engagement
VMT	Virtual machine tool

Introduction

This book presents developments, research results and industrial applications that were achieved in the European Twin-Control project. This book serves as the public report of the project and lies within the dissemination activities that have been carried out by project partners in the last three years.

Twin-Control project has developed ICT applications in the field of machine tool industry. Project developments have been split into two main workflows. Firstly, different simulation models were developed with the aim to create a digital twin of the machine tool. Secondly, a data monitoring and management infrastructure were defined and implemented in several use cases (industrial and research environments). These two workflows have, then, been combined to implement model-based control features in the form of cyber-physical systems. One of the highlights of Twin-Control project is the complete industrial validation stage, consisting in two scenarios from the most demanding industrials sectors: aerospace and automotive.

The structure of this book is based on the one applied in Twin-Control project. The book is separated into five main parts that are composed of several chapters. Each chapter deals with an independent feature developed in the project and begins with an abstract which briefly describes its contents. At the end of each chapter, the conclusions and future steps related to the presented feature are presented. Finally, related references are presented to allow further study of the subjects.

Part I provides a technical introduction to the project contents. Firstly, a state-of-the-art related to ICT applications in machine tool industry is presented. Secondly, the general approach followed in Twin-Control project is presented, including the defined architecture and basic features.

Part II deals with different simulation models developed in the project towards creation of a complete digital twin of a machine tool. Different chapters describe models linked with machine tool dynamics, machining process models, energy efficiency and end of life of critical components.

Part III presents the activities done in the field of machine tool and process monitoring and the management of this data. Firstly, the monitoring infrastructure designed and implemented in a total of 12 machine use cases is presented. This

infrastructure basically consists of a local monitoring system that uploads data to a cloud-based data management platform where data is managed at fleet level. Secondly, two different chapters dealing with the application of energy monitoring capabilities are presented.

Part IV deals with the integration of different features developed in the previous two parts. Firstly, a state-of-the-art model of the machine tool that integrates complete machine tool dynamics and machining process is presented. Secondly, different model-based control actions developed in the project with the aim of improving the control of the machining processes are presented. This model-based control features include process monitoring, energy monitoring, collision avoidance. The third chapter presents the fleet-wide proactive maintenance platform developed in Twin-Control. The part is closed with the presentation of machining process-related visualization features to enhance users experience.

Part V presents the implementation and validation of the different Twin-Control developments in two industrial scenarios. In the first one which is from aerospace sector, three Gepro machines located at MASA (Logroño, Spain) have been selected. In the second one which is from the automotive industry, three Comau machines located at Renault plant in Cleon (France) have been used. Most of the features have been successfully applied in both use cases, although, due to different impacts in each use case, some activities have been focused in one of them. This part presents the functional evaluation of Twin-Control project features, as well as the impact caused by their application in the industrial end users. To improve this analysis, the evaluation of Twin-Control has been separated in five Scenarios of Use (SoU)

- Scenario of Use 1: Machine tool design
- Scenario of Use 2: Machining process design
- Scenario of Use 3: Process control
- Scenario of Use 4: Maintenance
- Scenario of Use 5: Quality

After the five main parts are presented, the book is closed with the general conclusions and next steps.

Mikel Armendia
Mani Ghassempouri
Erdem Ozturk
Flavien Peysson

Part I
Introduction

Chapter 1
Machine Tool: From the Digital Twin to the Cyber-Physical Systems

Mikel Armendia, Aitor Alzaga, Flavien Peysson, Tobias Fuertjes, Frédéric Cugnon, Erdem Ozturk and Dominik Flum

1.1 Introduction

Europe is the world's largest manufacturer of machine tools, but this position is threatened by the emergence of Asian countries. However, Europe has world-class capabilities in the manufacture of high-value parts for such competitive sectors like aerospace and automotive , and this has led to the creation of a high-technology, and

M. Armendia (✉) · A. Alzaga
IK4-Tekniker, C/Iñaki Goenaga, 5, 20600 Eibar, Gipuzkoa, Spain
e-mail: mikel.armendia@tekniker.es

A. Alzaga
e-mail: aitor.alzaga@tekniker.es

F. Peysson
PREDICT, Vandoeuvre-lès-Nancy, France
e-mail: flavien.peysson@predict.fr

T. Fuertjes
MARPOSS Monitoring Solutions GmbH, Egestorf, Germany
e-mail: tobias.fuertjes@mms.marposs.com

F. Cugnon
Samtech s.a., a Siemens Company, Liège, Belgium
e-mail: frederic.cugnon@siemens.com

E. Ozturk
AMRC with Boeing, The University of Sheffield, Wallis Way, Catcliffe, Rotherham S60 5TZ, UK
e-mail: e.ozturk@sheffield.ac.uk

D. Flum
PTW TU, Darmstadt, Germany
e-mail: d.flum@ptw.tu-darmstadt.de

M. Armendia et al. (eds.), *Twin-Control*,
https://doi.org/10.1007/978-3-030-02203-7_1

high-skill industry. European machine tool builders, part manufacturers and other agents must work together to increase the competitiveness of European manufacturing industry.

To fulfil this objective, machine tool industry needs to meet current trends in manufacturing industry, linked to initiatives like Industry 4.0 and englobing ICT advances such as cyber-physical systems (CPS) [1], Internet of things (IoT) [2] and cloud computing [3]. In this line, Liu and Xu [4] propose a new generation of machine tools, cyber-physical machine tools that, apart from the CNC machine tool, englobes data acquisition devices, smart human–machine interfaces and a cyber twin of the machine tool.

This cyber twin, better known as digital twin, is a digitalization of the machine tool. Some partial versions of this virtual representation of the machine are currently well known by machine tool builders, like computer-aided design (CAD), computer-aided manufacturing (CAM) and finite element modelling (FEM). These tools are very useful to optimize machine tool designs and reduce design and mechanical set-up stages. However, most available software packages deal with isolated features of the machine tools and/or manufacturing processes, and a lack of integration of the different key features exists [5]. In the last years, a new application of the digital twin has been spreading, called "virtual commissioning" [6, 7]. In this case, a virtual representation of the machine is used to design, program and validate the controller.

Another key principle of Industry 4.0 is to increase the knowledge of the process obtained through monitoring [8]. This knowledge can be applied, for example, for process control [9], maintenance actions optimization [10] and even to create digital twins. The combination of models and process monitoring will be useful not only in the development and design stages, but mainly during the production stage to check that production is running smoothly, detect wear and tear without needing to halt production or predict component failure and other disruptions.

Combining these new features, the overall equipment efficiency (OEE) [11] can be increased by affecting the different stages of the life cycle of the machine and process (Fig. 1.1): (1) accelerating the ramp-up process with a time reduction of the machine and/or process set-up; (2) optimized productivity, for example predicting and avoiding quality problems; (3) unavailability reduction thanks to the faster new process set-up and a proactive maintenance strategy, driven by root cause analysis and "predict and prevent" policies; (4) increase the production system life-time base on the reuse and refurbishment of machines and components.

This first chapter of the book presents the current state of the art regarding ICT-related technologies applied in machine tool industry. After this introduction, the concept of machine tool digital twin and its application in different stages of machine tool and process design and set-up is presented. Next, the monitoring and management of data, from local monitoring to cloud-based fleet level data management, is reviewed. In the following section, the concept of cyber-physical system for Machine Tools is defined, and some examples used to improve the adaptability and productivity of machine tools are presented. Finally, the conclusions and the future steps are presented.

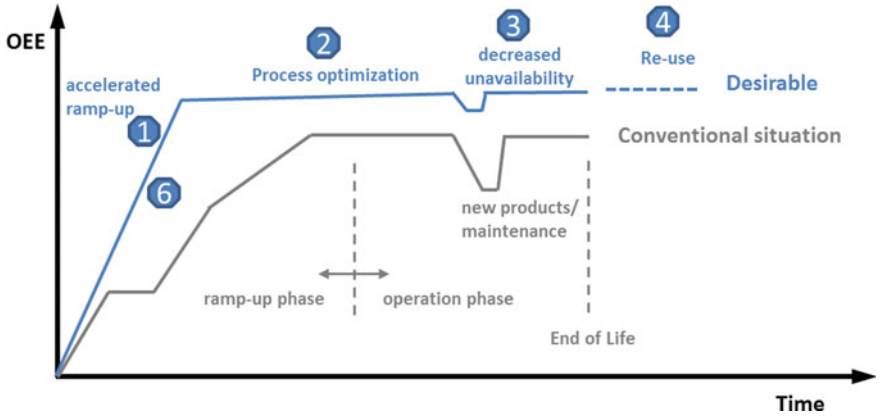

Fig. 1.1 Increase of the overall equipment efficiency (OEE) in the different stages of the life cycle of a process

1.2 Machine Tool Digital Twin

Simulation tools are currently a key complement to European machine tool industry expertise to increase competitiveness. In fact, according to Industry 4.0 [3], modelling plays a key role in managing the increasing complexity of technological systems. A holistic engineering approach is required that spans different technical disciplines and providing an end-to-end engineering across the entire value chain. In addition, more and more important life cycle concepts like energy consumption and component end-life and degradation are not always present in machine tool builders and part manufacturer's calculations.

The digital twin concept covers this holistic approach for machine tool and machining process modelling. Apart from that the digital twin provides the possibility to interact with the real representation of the machine [12]. The possibility to combine the real data with the simulation models provides a new range of applications with clear benefits:

- Digital twins can be evaluated with real data by feeding monitored inputs as in the real representation of the machine. This way, models can be tuned to improve their performance [13].
- Simulation models can be used for the so-called virtual commissioning [7, 14] which consists in the usage of the digital twin of a physical system to set-up the controller even before the physical system is ready for that. Inputs and outputs of the controller are connected to the digital twin as they would be connected to the real twin. This feature allows the reduction of the overall production stage of a product.
- Digital twins can be also used to improve health monitoring capacities. Simulation models can be used to determine nominal conditions of the studied systems and, hence, improve the detection of anomalous performance [15].

– Models can be used to be integrated in controller systems and optimize their performance [16].

Next, an overview of different types of digital twin for machine tool and machining process is presented. As mentioned, there is a lack of simulation environments that provide integrated features [5] and, hence, independent functionalities are presented.

1.2.1 Virtual Machining

The state of the art in virtual machining is presented in a recent keynote paper by Altintas [17]. It summarizes the research outputs on prediction of cutting forces, torque, power, stability and vibrations. Although there are many important results in this paper, there is not one system that can integrate all the solutions proposed. For example, for milling and turning processes, surface roughness, dynamic tool position and inclusion of the spindle dynamics nonlinearities in predictions are not available in existing tool path simulation capabilities.

For surface roughness prediction, Biermann [18] and Breitensprecher [19] presented surface texture predictions using time domain models which correlate well with experimental measurements for specific processes. Altintas et al. [17] highlighted the importance of tool/workpiece engagement evaluation along the tool path. This can be done by using various approaches (voxel, dexel, CSG, B-rep geometries, etc.).

The accuracy of virtual machining is directly related to the identification of the engagement conditions. However, there must be a trade-off between accuracy of engagement predictions and simulation times that is acceptable by the industry. Further research is needed to improve both the accuracy and computational efficiency of tool/workpiece engagement conditions.

There are two types of tool path simulation software available in the market for machining. Geometry-based simulation tools (Volumill [20] and Vericut Optipath [21]) can only calculate material removal rate and uncut chip thickness variation along a given tool path, but they cannot simulate process mechanics and dynamics, and hence, they cannot predict problems such as tool breakages due to high cutting forces, form errors and vibrations. The second type includes process physics into the simulations. Vericut provides the so-called force module that includes cutting force for the tool path optimization procedure. In this line, Machpro [22] can let the user about stability issues in addition to simulation of cutting forces, allowing an optimization of the machining process. However, no software can predict the surface roughness and thermal errors.

For simulation of effect of certain process parameters, there are analytical and FEA analysis-based simulation software available on the market. Cutpro [23] software runs analytical model for calculation of cutting forces and stability for a given set of parameters. Deform [24] and Advantedge [25] are FEA packages for simulation of

cutting forces and temperatures in machining. These software packages cannot be used in simulation of the complete tool path for a given part.

Depending on the spindle used in the machine tool, nonlinear behaviour of the spindle may lead to inaccuracies in stability predictions. For example, Ozturk et al. [26] demonstrated the effect of including the effect variable preload in stability of a milling operation. Hence, such potential effects need to be included in stability predictions for improved accuracy.

1.2.2 Virtual Machine Tool

In 2005, Altintas summarized the research performed on virtual machine tool technology [27]. Main developments in the field consist of machine tool structure kinematic (rigid body) [28] and dynamic (FEM) [29] analysis. For geometric error modelling, data-driven models have been used [30]. The different software packages available to analyse machine tool or machining performance are focused in a single feature.

Commercial simulation packages used for machine tool structural analysis can be classified into two categories. Rigid-body simulation software (MSC ADAMS [31], LMS Virtual.Lab [32]) is fast but does not consider all the deformation and vibrational characteristics of the structural parts of complex machines. This approach is not valid for lightweight modern machine tools with higher dynamics requirements. The finite element method packages (MSC Nastran [33], ABAQUS [34], SAMCEF [35]) are more appropriate to analyse complex compliant systems. The drawback of this approach is that simulations are time prohibitive.

For the coupling of structural dynamics and control loops, there are two main approaches (Fig. 1.2): replacing models, where simplified structure models are included in the control loop simulation [36]; and co-simulation, where two simulation environments are coupled via interfaces [37].

Nowadays, both rigid-body tools and FEA packages are combined to simulate complex mechatronic systems like machine tools. As those codes are usually well interfaced to block simulation tools as MATLAB Simulink [38], Dymola [39] or Simcenter Amesim [40] mechatronic models of machine tools can be achieved. The weak point of such approach is that it does not allow accounting properly for distributed flexibility in the couplings. The alternative is to use FEA solvers that have implemented joint capabilities as ANSYS, ABAQUS or SAMCEF Mecano. However, many FEA packages have only weak capabilities to integrate digital blocks to simulate control loops. During the two last decades, SAMCEF Mecano [41] has been successfully used to model flexible multi-body systems with detailed local nonlinear FE models of critical components for many applications in space, aeronautic and automotive domains. In addition, SAMCEF Mecano is well positioned as it can be interfaced with codes like MATLAB Simulink and Imagine Lab. There is no commercial package in which machining process is integrated with machine tool structure. Abdul-Kadir et al. [5] presented an extensive state of the art about virtual manufacturing. They group the different virtual models in two main groups:

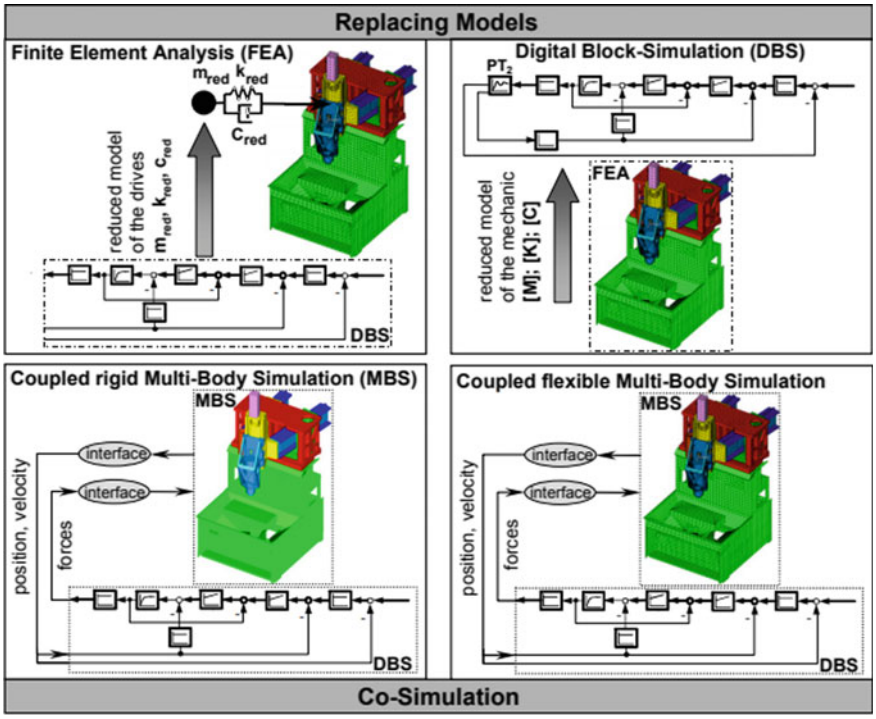

Fig. 1.2 Virtual machine tool: coupling alternatives for machine structure and control [27]

virtual machine tool and virtual machining. They also call virtual manufacturing to the combination of the previous and more. They concluded that there are lots of tools analysing different aspects of machine tools and machining, but they felt a lack of integration, "The developed tools are still not capable of supporting an inclusive simulation package".

According to process integration in virtual machine tool, most NC tool path and machining simulation systems consider only the rigid-body kinematics of the machine tool. Altintas et al. [27] proposed a possible architecture for the coupled simulation of cutting process (Fig. 1.3). Brecher and Witt [41] presented an approach to simulate a machining process, including interactions between a machine tool and a cutting process. They argued in favour of better quality predictions relating to process forces and stability boundaries. Bartelt et al. [42] developed a new software architecture to synchronize concurrent simulations performed in different environments. Though it is a flexible approach, it is not the most efficient with respect to calculation time and industrial application.

In the last years, so-called virtual machine tool packages have appeared that offer similar solutions based on the interpretation of G-code to check machine tool movements according to the programmed tool path and kinematics with the purposes

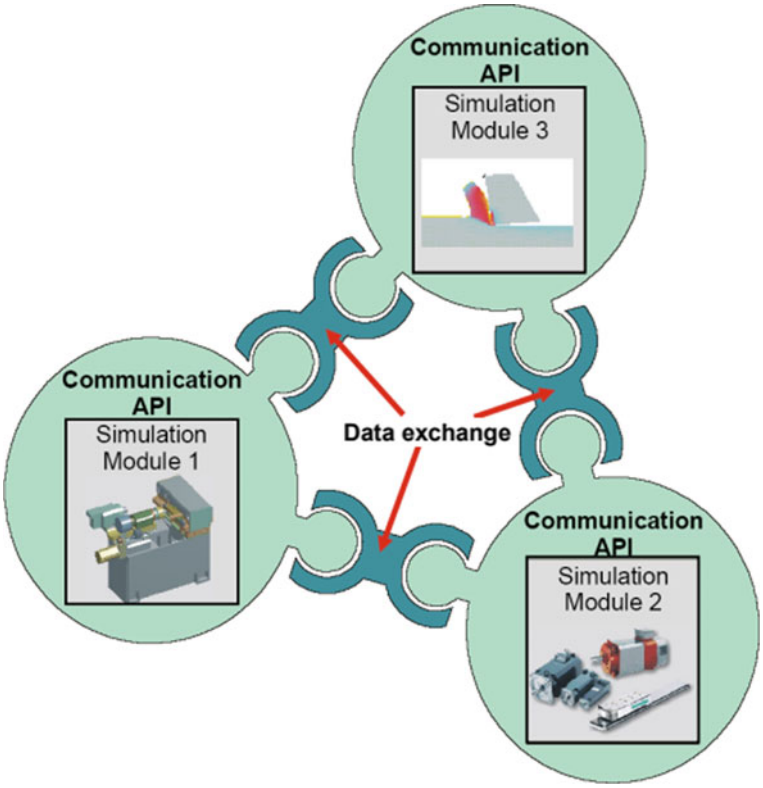

Fig. 1.3 Environment for the coupled simulation of machine tool and process [27]

of training and process checking, including collision avoidance [43, 44]. However, none of these packages deals with aspects like dynamics, machining processes or life cycle estimation.

1.2.3 Life Cycle Features

1.2.3.1 Energy Consumption

Even though simple energy optimization measures of machines tool are usually profitable within a time period of two years [45], energy efficiency in investment decisions usually attracts minor interest due to a multitude of reasons. In the car manufacturing industry, some companies (BMW, Daimler) included energy efficiency criteria in the machine tool specification sheet during machine acquisition but, based on a

deducted expert consultation, not often are rechecked after the machine is set up at the car manufacturers' site. Simulation tools can help to evaluate energy efficiency measures on machine tools, but no industrial software solutions do exist for doing it so far.

Dietmair [46] developed an empirical model to predict the energy consumption of machine tools. Every machine component is linked to a certain electric power demand corresponding to the actual machine mode. By providing a temporal sequence of machine modes, the energy demand of each component, as well as the entire machine, can be evaluated. Based on the research of Dietmair [46], Bittencourt [47] enlarges the existing model by connecting trajectories between different machine modes to a certain power and time demand. Both models' common point is that dynamic effects are neglected. Each machine mode is associated to a single power demand. Using empirical data gained from datasheet information in combination with mathematical models, Eisele [48] developed a simulation library within the simulation environment MATLAB Simulink/SimScape®. The library enables the user to build machine tool models for estimating the energy demand using the actual NC program as input. In addition, Heinemann et al. [49] included a basic cutting force model based on Kienzle [50] to calculate torque and forces on the spindle and feed drives. Following a similar approach, Schrems [51] developed a dynamic simulation approach to assess the energy demand of process chains within the widely used spreadsheet application Microsoft Excel®. Within the research project ECOMATION, simulation models are developed to calculate the electric power demand of machine tools on component level. The focus lies especially on real-time capable models for monitoring application. Besides electric energy, no further energy is regarded [52]. Within the research project "ESTOMAD—Energy Software Tools for Sustainable Machine Design" funded under European Union Seventh Framework Programme (FP7/2007-2013) software tool was developed using the commercial simulation software AMESim to model, simulate and analyse the energy flow in machines [53].

1.2.3.2 Component End of Life

For end-of-life estimation of the components, machine tool builders use a calculation procedure defined in component technical brochures or directly apply estimations from their suppliers. Generally, these procedures are based in a rough estimation of machine tool component loads. Due to the common ignorance of load of components through machine tool life, very conservative estimations are obtained resulting in inaccurate (low) estimations of component life.

Numerous methods and tools can be used to predict the end of life of machine tool components [54]. These methods can be classified into two principal approaches: model-based prognostics (also called physics of failure prognostics) and data-driven prognostics. Model-based prognostics [55] deals with the prediction of the end of life of critical physical components by using mathematical or physical models of the degradation phenomenon (crack by fatigue, wear, corrosion, etc.). The main advantage of model-based approaches is their ability to incorporate physical understand-

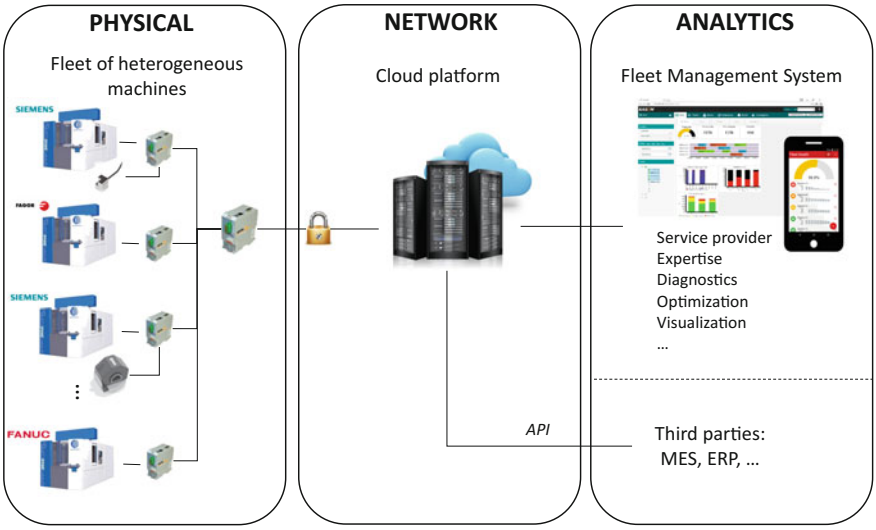

Fig. 1.4 Overview of a typical data monitoring and management architecture

ing of the monitored system [56]. However, this approach supposes a very complex modelling activity, and it can be difficult, if not impossible, to catch the system's behaviour. Component users do not trust in this approach to estimate component end life. The data-driven prognostics [55] is currently receiving extensive research and aims at transforming the data provided by the sensors into relevant models (which can be parametric or nonparametric) of the degradation's behaviour. Since they are based on real monitored data, current component degradation condition can be estimated. In practice, however, it is not easy to apply data-driven techniques due to the lack of efficient procedures to obtain training data and specific knowledge [56].

1.3 Monitoring and Data Management

Figure 1.4 shows a schema of a typical architecture for monitoring and data management for manufacturing. Three main sections are observed: (1) the local monitoring of the physical systems (machines and process); (2) the platform (normally cloud-based) where the data will be managed; (3) the network through which the information will be collected and transferred between the previous systems.

1.3.1 Local Monitoring and Data Management

Machine tool and process monitoring systems in general must deal with the two fields of data acquisition and data processing. The selection of the sensors for data acquisition is dependent on the type of machine tool, mounting options, process influences, signal amplitudes and process disturbances. They can be classified into three types:

- Internal sensors: they are already available in the machine tool. The data of the internal sensors, like axis position or motor consumption, is normally retrieved via a field-bus like PROFIBUS from the machine control (PLC and/or CNC). CNC manufacturers are providing more and more tools to share this internal data with third-party applications [57]. This approach is fast to install and fail-safe, but they cannot be used in every field of application [58, 59].
- External sensors: they are used to obtain further information of the process and high-frequency information. Typical examples are accelerometers (for process control [60] and condition monitoring [61]) and force sensors embedded in tool holders [62]. Transferring all the high-frequency data generated by these sensors would be a non-sense, so local processing is performed to generate indicators. The drawback of this approach is that additional hardware (sensor and processing hardware) must still be installed.
- Virtual sensors: it consists in an indirect measurement of some feature. For example, tool wear is a very difficult feature to be measured in process. To solve this problem, spindle power consumption is used to qualitatively estimate the tool wear [63, 64].

There exists a wide variety of monitoring hardware to collect this data. This hardware provides high connectivity features (Ethernet, CANOpen, Profibus, etc.) and, in some cases, the integration of some intelligence in the system and even the feedback to the machine controller.

Kaever [65] classified the state of the art of local process monitoring strategies into two categories. The strategies of the first category rely on a teach-in phase in which tolerances or characteristic values for the individual process are determined. The strategies of the second category do not have the possibility to access to teach-in data which is the case of single-piece production. Current research trends in the context of process monitoring focus on the integration of machine positions into the monitoring or even to use process simulation approaches. In [66], Klocke, Kratz and Veselovac presented a position-oriented monitoring by utilising all position encoder signals from a 5-axis milling machine for an in-depth analysis of a freeform milling operation. In [59], Yohannes presented a monitoring strategy based on a material removal simulation. By integrating a simulation into the monitoring, the teach-in phase can be eliminated.

1.3.2 Network

About the data collection and communication, there are two relevant issues to be considered, the communication protocol and security aspects.

OPC UA is a machine to machine communication protocol developed by the OPC Foundation. It has been standardized by the International Electrotechnical Commission as the IEC 62541 standard [67]. Its goal is to allow communicating with machines from different vendors without having to buy specific hardware or software. Contrarily to its ancestor OPC DA, it is based on standard Internet protocols and is not tied to a specific platform or operating system. Therefore, it is well suited for complex network infrastructure and can be easily processed by firewalls.

Several services are defined in the specification. The main service is data access that describes data flow of values such as sensor signals. There are also services transmitting alarms, history data, aggregates or programs. All these services are using a structured information model that can be expanded to describe complex data.

Transport can be made using binary streams or HTTP requests. Security uses standard TLS protocol, using public key infrastructure (PKI) with certificates, for signature and encryption and authentication.

There are several implementations of OPC UA. The OPC Foundation provides a C# full implementation and a C++ stack. Several vendors provide other languages implementation and embedded software. Currently, most CNC/PLC manufacturers provide data access through OPC as standard or complimentary functionality.

MTConnect is a manufacturing technical standard to retrieve process information from numerically controlled machine tools. The MTConnect standard offers a semantic vocabulary for manufacturing equipment to provide structured, contextualized data with no proprietary format [68]. In contrast, MTConnect requires someone to develop the MTConnect adapter, which is the software that collects the data from the machine and formats it for the MTConnect agent. Recently, in order to compete to the MTConnect standard, the OPC Foundation, in collaboration with the German Association of Machine Tool builders, is working in an OPC UA Information Model for CNC Systems [69].

Cyber security is an important part of a modern IT architecture design. Several rules can strengthen the resistance to cyber-attacks. Firstly, the principle of least privilege that describes that every part of an architecture must only be able to access resources needed for legitimate purpose. Secondly, defence in-depth principle builds several layers against attacks, so an attack compromising one layer would not compromise the others. Finally, intrusion detection systems and audit trails can detect intrusion attempts and warn administrators.

One of the most important aspects in cyber-security is encryption. By using secure protocols, full disc encryption and public key infrastructure (PKI), data encryption can be used on the whole data life cycle. Moreover, modern microprocessors have built-in hardware encryption and the performance penalty of using encrypted data is negligible even for hardware embedded inside machine tools.

1.3.3 Data Analytics

Big data is defined as data where one or more of the following characteristics are high: volume, velocity, variety. Machine tool industry encounters big data in the following sense: firstly, machine tools produce data of high rate such as axes movements that must be acquired with millisecond precision. Secondly, machine tools related data has a variety of types, such as time series, spectral data, production data, and quality control data. Finally, data volume generated by a machine tool has a considerable daily volume. Each machine can generate several gigabytes of data per day.

Traditional software is not designed to handle this massive amount of data. New technologies based on distributed computing are now developed, such as NoSQL databases. These solutions use horizontal scalability: extending storage and computation capabilities by adding new nodes to the system, based on commodity hardware. With algorithms such as MapReduce, a computing problem can be split across several machines running in parallel, and then aggregated in a single result.

In addition to big data technology, virtualization (running several environments on a physical machine), containerization (a lightweight version of virtualization for stateless computing jobs) and software-defined networking (changing network configuration without using dedicated appliances) allow rapid deployment of solutions without dedicated hardware management. These technologies serve as the basis for cloud-oriented architecture.

Cloud offerings ranges from infrastructure as a service, to software as a service. Infrastructure as a service (IaaS) provides vendor-managed networking, storage and servers. Platform as a service (PaaS) adds API, middleware and managed services. Software as a service (SaaS) is a completely managed environment.

The combination of cloud-based environments and big data software enables the development of new kind of monitoring algorithms targeting fleets of machine tools. A fleet can be viewed as a population consisting of a finite set of units (individuals). Fleet's units must share some characteristics that enable to group them together according to a specific purpose. By considering domain-specific attributes, fleet-wide approach of data management allows to analyse data and information through comparison according to different point of view of heterogeneous units (e.g. compare condition index of similar equipment in the different location, compare different system health trend for the same operation). Fleet-wide approach provides a consistent framework that enables coupling data and models to support diagnosis, prognostics and expertise through a global and structured view of the system and enhances understanding of abnormal situations. Fleet-management raises issues such as how to process large amount of heterogeneous monitored data (i.e. interpretable health indicator assessment), how to facilitate diagnostics and prognostics of heterogeneous fleet of equipment (i.e. several technologies and usage) or how to provide key users with an efficient support to decision-making throughout the whole asset life cycle. Towards this end, a complete guide (model, method and tool) is needed to support such processes (i.e. monitoring, diagnostics, prognostics) at the scale of the fleet.

Fleet-wide diagnosis, prognostic and knowledge management has gained significant interest across different industries and is at different maturity level depending on the industry. Sensory data is becoming more and more accessible from supervisory control and/or low-cost embedded acquisition system that drives the need of more advanced, structured data management strategy [70]. As a result, several fleet-management systems have been developed in military, energy and mining sectors. In most of those systems, the fleet concept mainly addresses only centralized and remote access to "n" system (individually). Even if a large amount of data can be managed, they are lacking enough structuring in order to benefit from the knowledge arising from the fleet dimension. Moreover, the data processing in such system is rather limited where aggregated synthesis and comparison of "n" systems is not addressed.

From the previous industrial statement, further research is actively conducted to overcome these limitations. In machine tool domain, one can refer to [71] where the fleet dimension aims at providing indicators on the state of a machine or of a fleet (of machines or components). Moreover, data can be stored and comparisons about the evolution of indicators along the time could be also performed. In addition, some recent research intends to work on knowledge formalization in order to better manage heterogeneous data and information in order to take into account system and process, technical and operational specificities and working conditions [72, 73].

The knowledge of machines fleet state is a high value-added information for both maintenance and production managers to optimize their planning activities by considering real machine's health estimation.

From maintenance point of view, intervention dates can be adjusted and anticipated according to the evolution of machine's health and so machine production stops to perform the preventive actions only when it is necessary. Control of the risks failures allows a better management of the spare part stock, the reduction of the number of available spare parts while supplying the right parts at the right time.

From production point of view, there is almost no more unexpected production stop and machine's availability is increased. Part production repartition over machines can be adjusted according to part quality specifications and machine's health.

1.4 Cyber-Physical Systems in Machine Tools

Cyber-physical system (CPS) is a term supported by important initiatives, like industry 4.0 [3], that is gaining relevance in the manufacturing community. Although several interpretations of CPSs exist, they can be defined as physical and engineered systems whose operations are monitored, coordinated, controlled and integrated by a computing and communication core [1]. Cyber-physical systems are considered as one of the main enablers for flexibility and productivity in manufacturing processes in the future [74].

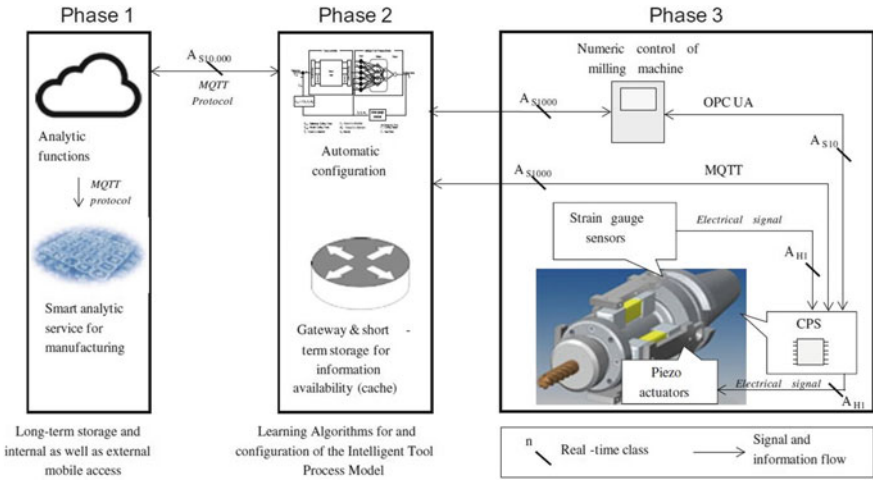

Fig. 1.5 Communication architecture of the intelligent milling machine [75]

Berger et al. [75] presented an overview about the application of CPSs in machine tools. In this work, CPSs are observed as smart device that interacts with the machine (through sensors and actuators) to increase its performance. Berger et al. present examples like an intelligent chuck for a turning machine that controls and regulates the clamping force based on sensor data [76] and an intelligent milling tool with integrated chatter compensation and adaptive control system (Fig. 1.5).

EU-funded MC-Suite project presents relevant developments in the field of CPS application in Machine Tools. Mancisidor et al. [77] present an active damper system to suppress chatter effects during machining. In addition, Beudaert et al. [78] developed a chip breaking system to control chip length and, hence, make the automation of the processes possible.

Another example of the application of CPSs in machine tools is the intelligent fixtures. Möhring et al. [79] present an overview of the work done in this field within the EU project INTEFIX. Fixtures provided by sensors and actuators that were able to adapt to the workpieces and process have been developed in this project. For example, Gonzalo et al. [80] presented an intelligent fixture for turning low pressure turbine castings. This fixture was provided with special actuators which apply forces in specific areas of the workpiece to modify its dynamic behaviour to reduce vibrations.

The CNC of the machine can also be regarded as a CPS. It has a powerful processing power and the possibility to use actuators and sensors of the machine. In this line, new CNC models present a wide variety of compensation tools (thermal [81] and geometric [82]). There are many researchers following this approach. Indeed, Liu and Xu [4] present the expression cyber-physical machine tool (CPMT). For the authors the CPMT is the integration of machine tool, machining processes, computation and networking, where embedded computers and networks can monitor and

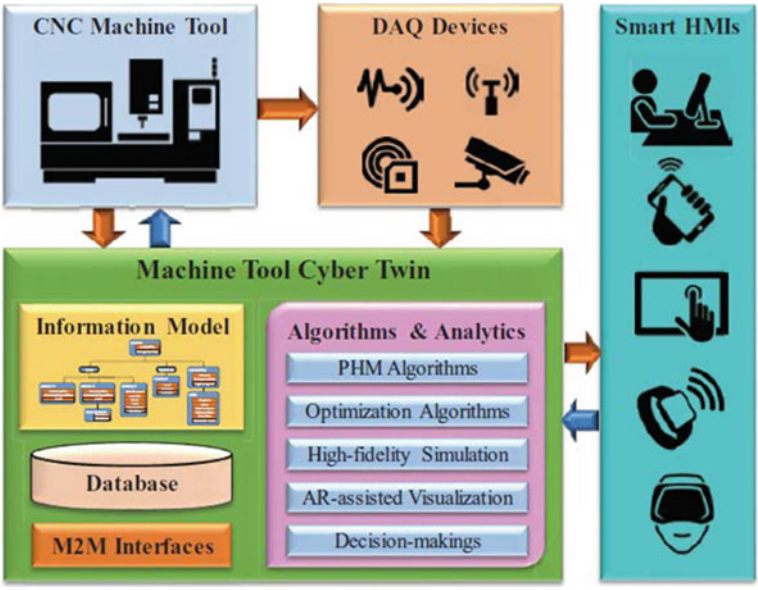

Fig. 1.6 Cyber-physical machine tool concept as defined by Liu and Xu [4]

control the machining processes, with feedback loops in which machining processes can affect computations and vice versa (Fig. 1.6).

1.5 Conclusions

This chapter presents an overview of the possibilities that ICT provide to increase the performance of machine tools. This overview covers features like digital twins of machine tools, monitoring and data management and the concept of CPS to improve machine's performance. Some of these technologies are currently applied, and others need further development to be used in industrial environment. Indeed, currently, the main problem of this technology is that it is applied in controlled environment, for research purposes. Further efforts are needed to take all this technology to the industry.

One of the main objectives of twin control project is to develop this type of technologies for machine tools and make them a scalable, easy to apply and use in an industrial environment. To do that different activities have been carried out by developing a state-of-the-art digital twin for machine tools; that integrates most relevant features to simulate machining processes; a CPS based on a monitoring device that includes simulation models to optimize process control and a machine tool specific fleet knowledge system.

References

1. Rajkumar, R., Lee, I., Sha, L., Stankovic, J.: Cyber-physical systems: the next computing revolution. In: 47th ACM/IEEE, Design Automation Conference (DAC), Anaheim, CA, USA (2010)
2. Dervojeda, K., Rouwmaat, E., Probst, L., Frideres, L.: Internet of Things: Smart machines and tools. Report of the Business Innovation Observatory for the European Commission
3. Kagermann, H., Wahlster, W.: Recommendations for Implementing the strategic initiative INDUSTRIE 4.0. Final Report of the Industrie 4.0 Working Group
4. Liu, C., Xu, X.: Cyber-physical machine tool—the Era of Machine Tool 4.0. In: The 50th CIRP Conference on Manufacturing Systems. Taichung, Taiwan (2017)
5. Abdul-Kadir, A., Xu, X., Hämmerle, E.: Virtual machine tools and virtual machining—a technological review. Robot. Comput.-Integr. Manuf. **27**, 494–508 (2011)
6. Hoffmann, P., Maksoud, T. M. A.: Virtual commissioning of manufacturing systems: a review and new approaches for simplification. In: Proceedings 24th European Conference on Modelling and Simulation; Kuala Lumpur, Malaysia (2010)
7. Lee, C.G., Park, S.C.: Survey on the virtual commissioning of manufacturing systems. J. Comput. Des. Eng. **1**(3), 213–222 (2014)
8. Lee, J., Bagheri, B., Kao, H.-A.: A cyber-physical systems architecture for industry 4.0-based manufacturing systems. Manuf. Lett. **3**, 18–23 (2015)
9. Denkena, B., Fischer, R., Euhus, D., Neff, T.: Simulation based process monitoring for single item production without machine external sensors. In: 2nd International Conference on System-Integrated Intelligence: Challenges for Product and Production Engineering, Procedia Technology, vol. 15, pp. 341–348 (2014)
10. Alzaga, A., Konde, E., Bravo, I., Arana, R., Prado, A., Yurre, C., Monnin, M., Medina-Oliva, G.: New technologies to optimize reliability, operation and maintenance in the use of machine tools. In: Euro-Maintenance Conference, Helsinki, Finland, 5–8 May 2014
11. Mahmood, K., Otto, T., Shevtshenko, E., Karaulova, T.: Performance evaluation by using overall equipment effectiveness (OEE): an analyzing tool. In: International Conference on Innovative Technologies 2016, Prague
12. Vergniaud, M.: Exemples de Jumeaux Numeriques, Report from the Centre technique des industries mécaniques (CETIM) (2018)
13. Jerard, R., Fussell, B., Xu, M., & Schuyler, C.: A Testbed for research on smart machine tools. In International Conference on Smart Machining Systems (2007)
14. Hoffmann, P., Schumann, R., Maksoud, T.M.A., Premier, G.C.: Virtual commissioning of manufacturing systems—a review and new approaches for simplification. In: Proceedings of the 24th European Conference on Modelling and Simulation (ECMS 2010), pp. 175–181. Kuala Lumpur, Malaysia
15. Magargle, R., Johnson, L., Mandloi, P., Davoudabadi, P., Kesarkar, O., Krishnaswamy, S., Batteh, J., Pitchaikani, A.: A simulation-based digital twin for model-driven health monitoring and predictive maintenance of an automotive braking system. In: Proceedings of the 12th International Modelica Conference, Prague, Czech Republic, May 15–17, 2017, Issue No. 132, pp. 35–46, 4 July 2017
16. Elfizy, A.T., Bone, G.M., Elbestawi, M.A.: Model-based controller design for machine tool direct feed drives. Int. J. Mach. Tools Manuf. **44**(5) (2004)
17. Altintas, Y., Kersting, P., Biermann, D., Budak, E., Denkana, B., Lazoglu, I.: Virtual process systems for part machining operations. CIRP Ann. **63**(2), 585–605 (2014)
18. Biermann, D., Kersting, P., Surmann, T.: A general approach to simulating workpiece vibrations during five-axis milling of turbine blades. CIRP Ann. **59**(1), 125–128T (2010)
19. Breitensprecher, T., Hense, R., Hauer, F., Wartzack, S., Biermann, D., Willner, K.: Acquisition of heuristic knowledge for the prediction of the frictional behavior of surface structures created by self-excited tool vibrations. Key Eng. Mater. **504–506**, 963–968 (2012)
20. http://www.volumill.com/

21. https://www.cgtech.com/products/about-vericut/optipath/
22. https://www.malinc.com/products/machpro/
23. https://www.malinc.com/products/cutpro/
24. https://www.deform.com/products/deformd-machinin/
25. https://www.thirdwavesys.com/advantedge/
26. Ozturk, E., Kumar, U., Turner, S., Schmitz, T.: Investigation of Spindle bearing preload on dynamics and stability limit in milling. CIRP Ann. Manuf. Technol. **61**(1), 343–346 (2012)
27. Altintas, Y., Brecher, C., Weck, M., Witt, S.: Virtual machine tool. CIRP Ann. Manuf. Technol. **54**(2), 115–138 (2005)
28. Weule, H., Albers, A., Haberkern, A., Neithardt, W., Emmrich, D.: Computer aided optimisation of the static and dynamic properties of parallel kinematics. In: Proceedings of the 3rd Chemnitz Parallel Kinematic Seminar, pp. 527–546 (2002)
29. Weule, H., Fleischer, J., Neithardt, W., Emmrich, D., Just, D.: Structural optimization of machine tools including the static and dynamic workspace behavior. In: Proceedings of the 36th CIRP International Seminar on Manufacturing Systems, Saarbrücken, pp. 269–272 (2003)
30. Fesperman, R.R., Moylanb, S.S., Vogl, G.W., Alkan Donmez, M.: Reconfigurable data driven virtual machine tool: geometric error modeling and evaluation. CIRP J. Manufact. Sci. Technol. **10**, 120–130 (2015)
31. http://www.mscsoftware.com/product/adams
32. https://www.plm.automation.siemens.com/es/products/lms/virtual-lab/
33. http://www.mscsoftware.com/product/msc-nastran
34. https://www.3ds.com/products-services/simulia/products/abaqus/
35. https://www.plm.automation.siemens.com/es/products/lms/samtech/samcef-solver-suite/
36. Großmann, K.: Die digitale Simulation für den Entwurf der Werkzeugmaschine, pp. 459–472. Autonome Produktion, Springer, Berlin (2003)
37. Denkena, B., Tracht, K., Rehling, S.: Simulationsmodul für Maschinendynamik im Rahmen eines Fertigungssimulationssystems, WT Werkstattstechnik online, vol. 92, pp. 223–225. Springer-VDI-Verlag, Düsseldorf (2002)
38. https://www.mathworks.com/
39. https://www.3ds.com/products-services/catia/products/dymola/
40. https://www.plm.automation.siemens.com/global/en/products/simcenter/simcenter-amesim.html
41. Brecher, C., Witt, S.: Simulation of machine process interaction with flexible multi-body simulation. In: Proceedings of the 9th CIRP International Workshop on Modeling of Machining Operations, Bled, Slovenia (2006)
42. Bartelt, C., Böß, V., Brüning, J., Denkena, B., Rausch, A., Tatou, J-P.: A software architecture to synchronize interactivity of concurrent simulations in systems engineering. In: 20th ISPE International Conference on Concurrent Engineering, Melbourne (2013)
43. Li, X., Zhan, X.: Modeling and simulation of five-axis virtual machine based on NX. In: AIP Conference Proceedings, vol. 1955, p. 030044 (2018)
44. Sanchez, C.A., Arroyo, J.M., Gil, L.; Building a virtual machine tool in a standard PLM platform. Int. . Interact. Des. Manuf. (IJIDeM) **11**(2) (2016)
45. Abele, E., Sielaff, T., Beck, M.: Konfiguration energieeffizienter Werkzeugmaschinen. In: Werkstattstechnik online: wt, vol. 102, Issue No. 5, pp. 292–298. Springer VDI Verlag, Düsseldorf (2012)
46. Dietmair, A., Verl, A.: Energy consumption assessment and optimisation in the design and use phase of machine tools. In: 17th CIRP International Conference on Life Cycle Engineering (LCE 2010), pp. 116–121. University of Technology Press, Hefei (2010)
47. Bittencourt, J.L.: Selbstoptimierende und bedarfsgerechte Steuerungsstrategien für Werkzeugmaschinen zur Steigerung der Energieeffizienz, 1st edn. Apprimus-Verl, Aachen (2013)
48. Eisele, C.: Simulationsgestützte Optimierung des elektrischen Energiebedarfs spanender Werkzeugmaschinen: [Dissertation] (2015)

49. Heinemann, T., Schraml, P., Thiede, S., Eisele, C., Herrmann, C., Abele, E.: Hierarchical evaluation of environmental impacts from manufacturing system and machine perspective. In: 21st CIRP Conference on Life Cycle Engineering in Trondheim, pp. 141–146. Norway, 18–20 June 2014
50. Kienzle, O., Victor, H.: Spezifische Schnittkräfte bei der Metallbearbeitung. Werkstofftechnik und Maschinenbau **47**(H5), 224–225 (1957)
51. Schrems, S.: Methode zur modellbasierten Integration des maschinenbezogenen Energiebedarfs in die Produktionsplanung: [Dissertation] (2014)
52. Abele, E., Eberspächer, P., Schraml, P., Schlechtendahl, J., Verl, A.: A model- and signal-based power consumption monitoring concept for energetic optimization of machine tools. in: 21st CIRP Conference on Life Cycle Engineering in Trondheim, pp. 44–49. Norway, 18–20 June 2014
53. Iqbal, S., Croes, J., Al-Bender, F., Pluymers, B., Desmet, W.: Frictional power loss in solid grease lubricated needle roller bearing. Lubr. Sci. (2012). https://doi.org/10.1002/ls.1195
54. Medjaher, K., Tobon-Mejia, D., Zerhouni, N.: Remaining useful life estimation of critical components with application to bearings. IEEE Trans. Reliab. Inst. Electr. Electron. Eng. (IEEE) **61**(2), pp. 292–302 (2012)
55. Heng, A., Tan, A.C., Mathew, J., Montgomery, N., Banjevic, D., Jardine, A.K.: Intelligent condition-based prediction of machinery reliability. Mech. Syst. Signal Process. **23**(5), 1600–1614 (2009)
56. Dragomir, O.E., Gouriveau, R., Dragomir, F., Minca, E., Zerhouni, N.: Review of prognostic problem in condition-based maintenance. In: IFAC and in Collaboration with the IEEE Control Systems Society. European Control Conference, ECC'09, 2009. Budapest, Hungary
57. Zheng, B., Xu, J., Li, H., Xing, J., Zhao, H., Liu, G.: Development of remotely monitoring and control system for siemens 840D sl NC machine tool using Snap 7 codes. In: 2nd International Conference on Electrical, Automation and Mechanical Engineering (EAME 2017)
58. Weck, M., Brecher, C.: Werkzeugmaschinen 3 - Mechatronische Systeme, Vorschubantriebe, Prozessdiagnose. Springer, Berlin (2006)
59. Yohannes, B.: Industrielle Prozessüberwachung für die Kleinserienfertigung. Dr. -Ing. Diss., Leibniz Universität Hannover, Berichte aus dem IFW, TEWISS (2013)
60. Chen, J.C., Chen, W.L.: A tool breakage detection system using an accelerometer sensor. J. Intell. Manuf. **10**(2), 187–197 (1999)
61. Esu, O.O., Flint, J.A., Watson, S.J.: Condition monitoring of wind turbine blades using MEMS accelerometers. Renew. Energy World Europe (REWE) 12 (2013)
62. Reyes-Uquillas, D.A, Yeh, S.S.: Tool holder sensor design for measuring the cutting force in CNC turning machines. In: 2015 IEEE International Conference on Advanced Intelligent Mechatronics (AIM), , pp. 1218–1223, Busan (2015)
63. Cuppini, D., D'errico, G., Rutelli, G.: Tool wear monitoring based on cutting power measurement. Wear **139**(2) (1990)
64. Axinte, D., Gindy, N.: Assessment of the effectiveness of a spindle power signal for tool condition monitoring in machining processes. Int. J. Prod. Res. **42**(13), 2679–2691 (2007)
65. Kaever, M.: Steuerungsintegrierte Fertigungsprozessüberwachung bei spanender Bearbeitung. Dr. -Ing. Diss., RWTH Aachen, Fakultät für Maschinenwesen, 2004
66. Klocke, F., Kratz, F., Veselovac, D.: Position-oriented process monitoring in freeform milling. CIRP J. Manuf. Sci. Technol. (2008)
67. https://opcfoundation.org/about/opc-technologies/opc-ua/
68. http://www.mtconnect.org/
69. German Machin Tool builder Association, OPC-UA Information Model for CNC Systems, Report, 2015
70. Johnson, P.: Fleet-wide asset monitoring: sensory data to signal processing to prognostics. In: Proceedings of the Annual Conference of the Prognostics and Health Management Society, Minneapolis, 23–27 September 2012
71. Prado, A., Alzaga, A., Konde, E., Medina-Oliva, G., Monnin, M., Johansson, C-A., Galar, D., Euhus, D., Burrows, M., Yurre, C.: Health and performances machine tool monitoring architecture. E-maintenance Conference from 17th to 18th of June 2014, Luleå, Sweden

72. Voisin, A., Medina-Oliva, G., Monnin, M., Leger, J-B., Iung, B.: Fleet-wide diagnostic and prognostic assessment. In: Annual Conference of the Prognostics and Health Management Society (2013)
73. Medina-Oliva, G., Voisin, A., Monnin, M., Leger, J.-B.: Predictive diagnosis based on a fleet-wide ontology approach. Knowl.-Based Syst. **68**, 40–57 (2014)
74. Medina-Oliva, G., Voisin, A., Monnin, M., Leger, J-B., Iung, B.: Key factor identification for energy consumption analysis. In: 2nd European Conference of the Prognostics and Health Management Society, PHME (2014)
75. Johansson, C-A., Galar, D., Villarejo, R., Monnin, M., Green condition based maintenance-an integrated system approach for health assessment and energy optimization of manufacturing machines. In: International Conference on Condition Monitoring and Machinery Failure Prevention Technologies (2013)
76. Reinhart, G., Wittenstein, M., Scholz-Reiter, B., et al. (eds.): Intelligente vernetzung in der fabrik: industrie 4.0 umsetzungsbeispiele für die Praxis. Fraunhofer, Stuttgart (2015)
77. Mancisidor, I., Laka, I., Beudaert, X., Munoa, J.: Design and Validation of an active damping device for chatter suppression on flexible workpieces. In: 5th International Conference on Virtual Machining Process Technology (VMPT 2016) (2016)
78. Beudaert, X., Bediaga, I., Argandoña, J., Loc'h, J., Muñoa, J.: Effects of a chip breaking system using machine drive oscillations. In: IVth International Conference on High Speed Machining—17–18 April 2018, Donostia/San Sebastian-Spain
79. Möhring, H.-C., Wiederkehr, P., Gonzalo, O., Kolar, P.: Intelligent Fixtures for the Manufacturing of Low Rigidity Components. Lecture Notes in Production Engineering. Springer, Berlin (2018)
80. Gonzalo, O., Olabarrieta, E., Seara, J.M., Esparta, M., Zamakona, I., Gómez-Korraletxe, M.: Conceptos de Utillaje para la Mejora del Mecanizado de Componentes Aeronáuticos de Baja Rigidez. 20 Congreso de Máquinas-Herramienta y Tecnologías de Fabricación 2015, San sebastian, Spain
81. Chen, T.C., Chang, C.J., Hung, J.P., Lee, R.M., Wang, C.C.: Real-time compensation for thermal errors of the milling machine. Appl. Sci. 6 (2016)
82. Holub, M., Blecha, P., Bradac, F., Marek, T., Zak, Z.: Geometric errors compensation of CNC machine tool. MM Sci. J. (2016)

Chapter 2
Twin-Control Approach

Mikel Armendia, Aitor Alzaga, Flavien Peysson and Dirk Euhus

2.1 Introduction

Twin-Control (http://twincontrol.eu/) is a novel concept for machine tool and machining process performance optimization. It combines several features in the field of ICTs in manufacturing towards a better performance of machine tools [1]. A holistic simulation model, a so-called Digital Twin [2] of the machine tool, integrating most important features of machine tools and machining process, is combined with monitoring and data management capabilities.

Twin-Control will use a Digital Twin concept for the development of the simulation tool (Fig. 2.1). The Digital Twin is based on a combined application of the Cyber and Physical worlds, following the cyber-physical system (CPS) concept. The Cyber world consists in the computation, communication and control systems. The Physical world is composed by the natural and human-made systems governed by the laws of physics.

A Digital Twin of the machine tool resulting from the combination of the different theoretical models that cover different aspects of the manufacturing process corresponds to the Cyber world, together with the cloud-based data management part,

M. Armendia (✉) · A. Alzaga
IK4-Tekniker, C/Iñaki Goenaga, 5, 20600 Eibar, Gipuzkoa, Spain
e-mail: mikel.armendia@tekniker.es

A. Alzaga
e-mail: aitor.alzaga@tekniker.es

F. Peysson
PREDICT, Vandoeuvre-lès-Nancy, France
e-mail: flavien.peysson@predict.fr

D. Euhus
MARPOSS Monitoring Solutions GmbH, Egestorf, Germany
e-mail: dirk.euhus@mms.marposs.com

M. Armendia et al. (eds.), *Twin-Control*,
https://doi.org/10.1007/978-3-030-02203-7_2

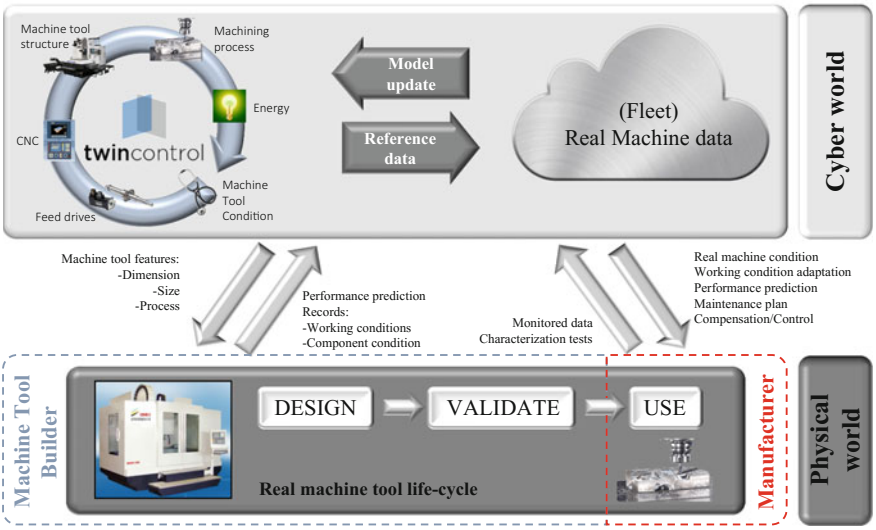

Fig. 2.1 Twin-Control concept

where machine fleet data is managed. The Physical world corresponds to the real machine that performs the real manufacturing process.

Both Physical and Cyber worlds will be interconnected. The Cyber world will make use of real machine tool and process data through all its life cycle. The Digital Twin of the manufacturing system has been created by combining the correspondent theoretical models according to machine tool design and process specifications. During part manufacturing, the holistic simulation model can be updated according to machine tool real condition using data obtained through monitoring and additional characterization tests designed for this purpose. This way, the virtual manufacturing system will be able to predict current machine/process performance in an accurate way.

In the same way, the simulation outputs obtained with the new Twin-Control tool will be useful through all machine tool life cycle. In the machine tool design stage, Twin-Control will be an extraordinary tool to predict the performance of projected machine tools. The same occurs with the process design, providing accurate estimation of cycle times and resultant part accuracy allowing a quick optimization procedure. By applying Twin-Control, machine tool and machining process set-up stage will be considerably reduced.

Finally, during machine tool usage period, process will be under control by the monitoring of the most important variables and the possibility to include simplified versions of the Digital Twin of the machine tool to perform model-based control actions [3]. According to machine tool health management, both local and fleet-level tasks will be implemented. On the one hand, variables like spindle temperature, power consumption and vibrations are monitored on machine level to control spindle's

condition. On the other hand, additional variables of the most important components of the machines will be also monitored and managed at fleet level.

The following pages provide an overview of the Twin-Control concept and its architecture and serve as introduction of the rest of the book, where developments are presented in detail. The first chapter introduces the Twin-Control concept. The second one presents an overview of the technical solution architecture of Twin-Control. Next, one of the highlights of the project, the industrial evaluation of Twin-Control is introduced. Finally, the conclusions are presented.

2.2 Twin-Control Architecture

Two separate application environments have been clearly defined: simulation, linked to a theoretical representation of the machine tool and the process; monitoring and control, linked to a real representation of the machine tool and the process. The fleet-based knowledge acts as a link between both representations by managing the real machine data (machine tool state, usage conditions, etc.) at a fleet level and using it to improve the accuracy of the simulation models. In the same way, simplified versions of the simulation part and results will be used in the real part to enhance monitoring and control activities (Fig. 2.2).

The results of the project have been grouped using the same structure. This way, three main results have been obtained.

2.2.1 Integrated Simulation Tool

The application of complex theoretical models leads to very accurate estimations of process performance, allowing its optimization. A holistic simulation tool has been

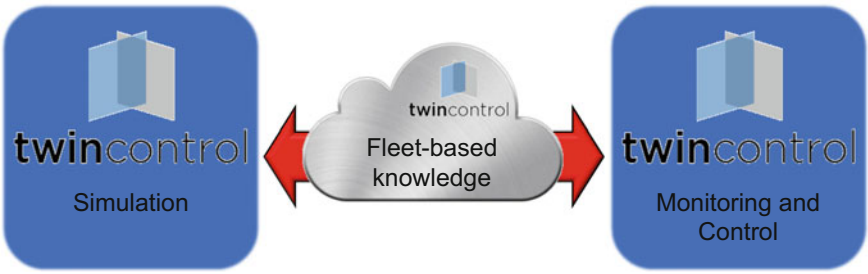

Fig. 2.2 Main application environments of Twin-Control

developed in the project to support machine tool and machining process design and optimization stages.

The core of the developed Digital Twin is a Virtual Machine Tool module based on SAMCEF Mecano [4] finite element (FE) software that is able to integrate the toolpath simulation and process effects (Fig. 2.3). This integration leads to a complete understanding of machine tool dynamic performance during real machining processes and will allow the prediction of the most important features like surface roughness and form errors. The integrated process models include features like cutting force estimation, stability analysis and even surface roughness estimation. The usage of ModuleWorks libraries provides advanced capabilities for tool-workpiece engagement calculation and also the possibility to visualize process results over workpiece geometry, improving user experience.

By using the results of this Virtual Machine Tool, some complementary features are studied through additional models. This way, energy efficiency of the simulated machine tool and/or process and end-of-life estimations of the most critical elements can be also provided by the developed Digital Twin.

End-of-Life module estimates the end-of-life of typically problematic machine tool components like bearings, linear guidelines and screw drivers. Based on the predictions of the integrated Virtual Machine Tool model, which will be able to estimate operating conditions of these elements, an accurate prediction of their end-of-life will be made based on the methods defined in the well-established standards defined by the International Standard Organization [5].

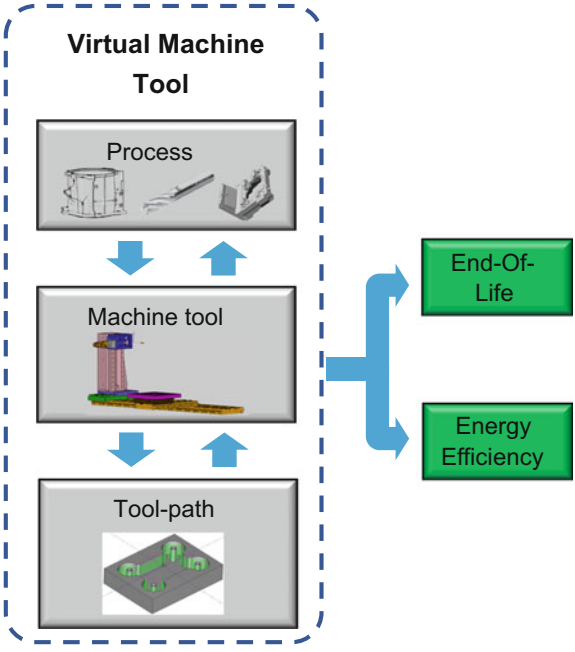

Fig. 2.3 General overview of the simulation operation mode architecture

The energy efficiency module provides the energy consumption of machine tools. To gain a most wide transparency, the energy consumption is observed on a component level. This leads to the possibility to design energy efficient machine tools and processes. The Simscape model library to be developed will be the basis for the configurator. The physical input parameters are obtained from data sheets: if detailed characteristic curves are available, they are directly used for simulation; if less information is available, the behaviour will be modelled.

The link with the real world is obtained, in one direction, by the usage of the fleet-level knowledge stored in the cloud for validation (inputs and outputs for the simulations) and, in the other direction, by uploading simplified models or simulated results and parameters to the cloud ("reference" machine values).

By using the estimations provided by its different modules, Twin-Control will provide the chance to optimize the process by adapting the toolpath and/or cutting conditions. In addition, the analysis of the results provided by Twin-Control could be used to make changes at machine tool level. In addition, simplified versions of this Digital Twin will be integrated in the real world to improve machine tool and process performance.

Due to computational costs, this operation mode is oriented to offline simulations executed in a conventional PC. In the project, a simplified version based on the process models module has been also developed. This alternative version provides limited results, since does not include machine tool kinematics and dynamics, but allows faster configuration and simulation. Depending on the application, one of the two alternatives could be used.

2.2.2 Local Monitoring and Control System

The most important variables of the machine tool and machining process performance will be monitored and managed at machine and fleet level. For monitoring purposes, ARTIS Genior Modular is installed in the machines. This device allows direct exchange of CNC data at high real-time rate. Depending on the CNC model installed in the machine, CANOpen or Profibus communication protocol can be applied.

Additionally, an ARTIS OPR unit—Offline Process Recorder—will be used and connected via Ethernet to the Genior Modular to store the real-time data capturing and also to receive OPC data in non-real-time as a second data source. The OPR will act as a gateway by pushing real-time and OPC data to the remote or local service hosting the fleet-based database, in this case, KASEM® (Fig. 2.4).

The real-time local data management does not only monitor data, it allows implementing some intelligence that can be used to detect anomalous performance or even directly act on the machine controller to optimize its behaviour. For example, ARTIS process monitoring capabilities are used to safeguard production [6]. Spindle torque monitoring on all machines will be used to detect abnormal behaviour during processing. This could be a sudden action in case of tool breakage, delayed stop in

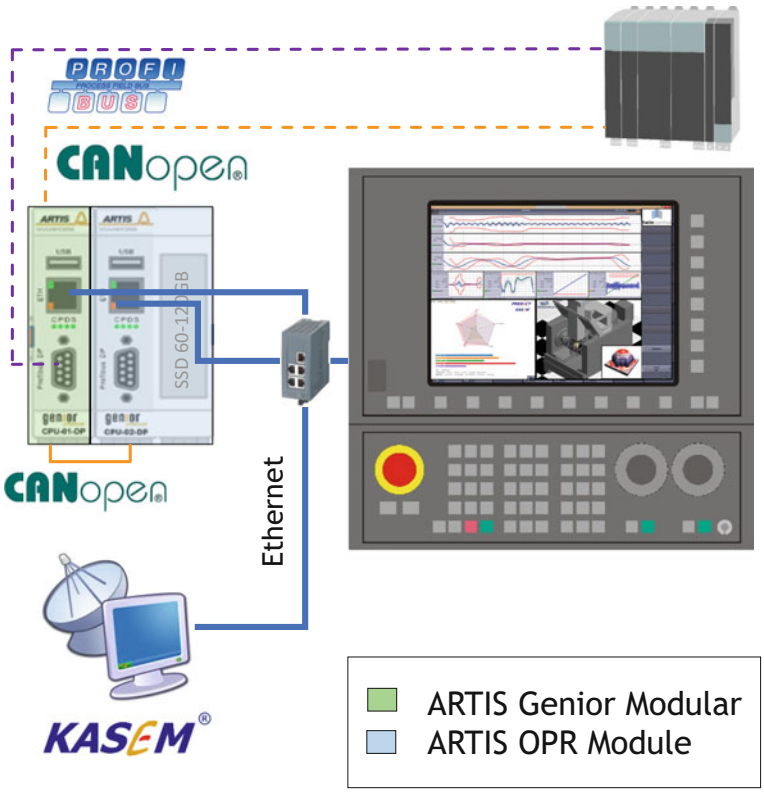

Fig. 2.4 Conceptual diagram of the monitoring architecture used in Twin-Control

the case of tool breakage during tapping operation or tool wear events. Currently, process monitoring is done based on a learning stage and, hence, can be only applied to medium-to-large batch sizes.

Within Twin-Control, the application of parts of the developed Digital Twin in the real world is proposed. The proposed monitoring hardware is the best environment to do this integration. For example, the integration of process models with real monitored data could be used for process monitoring [3], replacing the learning stage when it is not feasible, for example, in aerospace applications where batches are normally small.

A new energy monitoring system that avoids the extensive use of hardware (hall) sensors has been also implemented, leading to a drastic reduction in investment costs for an energy monitoring solution on component level. Using CNC and PLC data, the module will be able to determine energy consumption per component.

Other similar features like the integration of CNC simulation capabilities have been developed in the project and will be covered in specific chapters of this book.

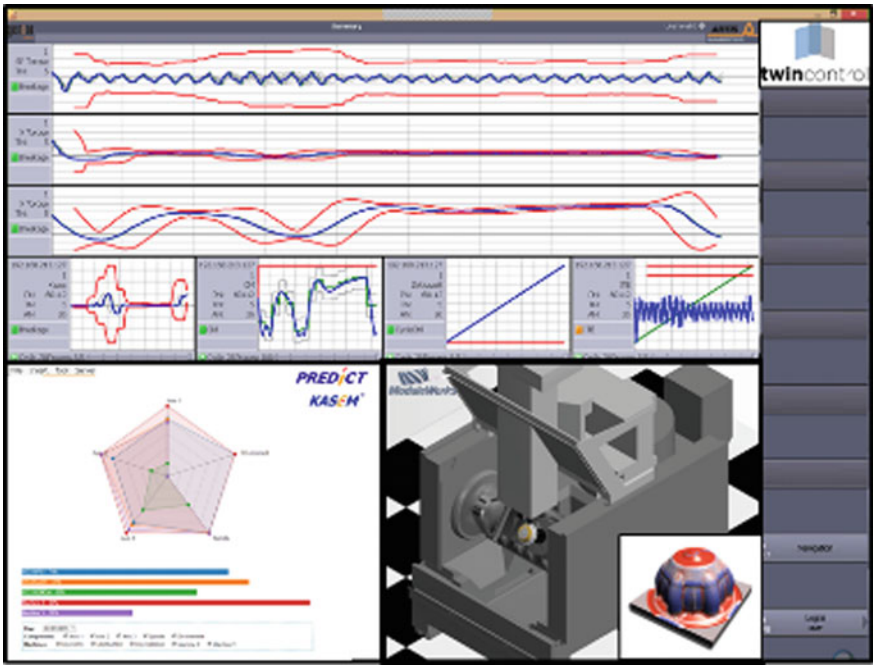

Fig. 2.5 Conceptual design of the ARTIS HMI including Twin-Control PlugIns

The different features are visualized in a central HMI solution (Fig. 2.5). HMI will be enhanced by including PlugIns of additional features like fleet-level knowledge reports or graphical representation of simulation results. This machine tool control-based HMI could be also made available on a tablet, external PC, or smartphone, since Genior HMI product is available as Windows DLL. This way, operators that are not in front of the machines can receive information, including alarm signals.

2.2.3 Fleet-Based Knowledge System

From Twin-Control point of view, fleet refers to a set of machine tools of different owners and builders. In addition to individual modelling and health monitoring, it is necessary to provide fleet-wide facilities. Towards this end, the platform integrates semantic modelling that allows gathering and sharing data, models and expertise from the different systems and equipments, using a fleet-wide approach. The fleet-based data management, depicted in Fig. 2.6, is built around a global methodology that allows guiding the proactive strategy definition all along the asset life cycle. It provides a consistent framework that enables coupling data and models to support diagnostics, prognostics and expertise through a global and structured view of

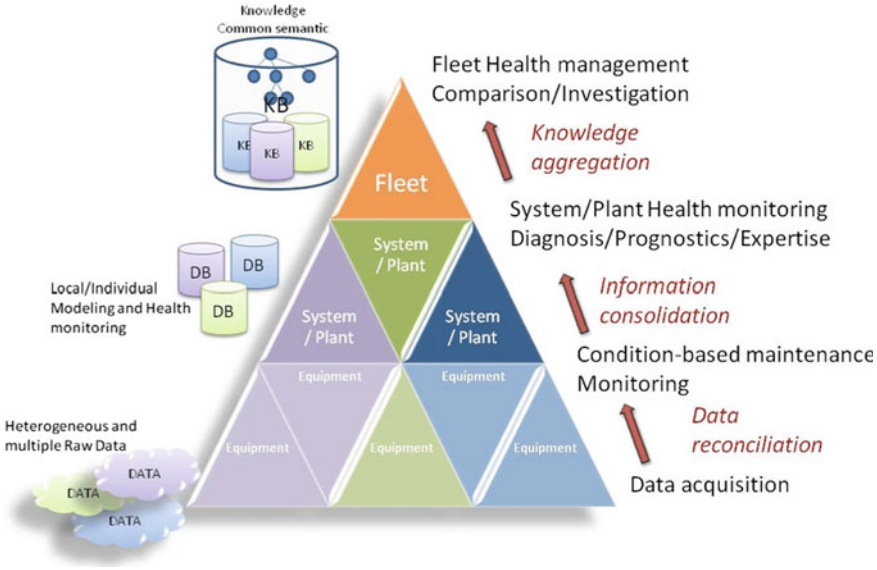

Fig. 2.6 Hierarchical approach of the proactive fleet management [7]

the system and enhances understanding of abnormal situation (i.e. system health monitoring level).

Starting from the definition of the system functioning in relation to its environment, the formalization of the system malfunctioning analysis is then considered. The corresponding knowledge (i.e. functioning and malfunctioning models) is incrementally built within a knowledge-based system that supports a structured and hierarchical description of the fleet. This formalization enables to reduce the effort for data consolidation within system health management as well as for knowledge aggregation within fleet health management, since it enhances understanding of the impacts between and within levels.

The fleet-level data management platform proposed for the Twin-Control project is based on KASEM® (Knowledge and Advanced Service for E-Maintenance) [8]. It is a collaborative e-maintenance platform, integrating engineering, proactive maintenance, decision-making and expertise tools [9] and used in former Power-OM project [10].

2.2.3.1 Data Exchanges with Machine Tools

Twin-Control's fleet platform is in the "cloud", i.e. on the Internet, and hosted to a predict secure server. Machine tools push data to the server to feed the knowledge base. Details of the proposed monitoring and data management architecture are presented in Sect. 3.1 of this book.

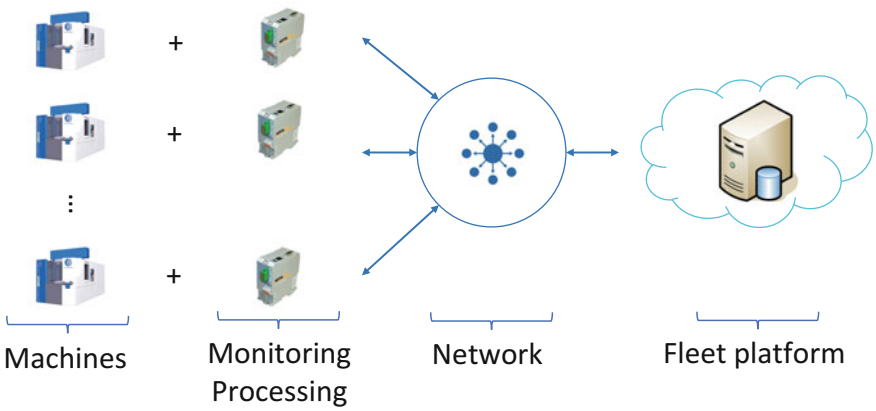

Fig. 2.7 Fleet data management approach used in Twin-Control

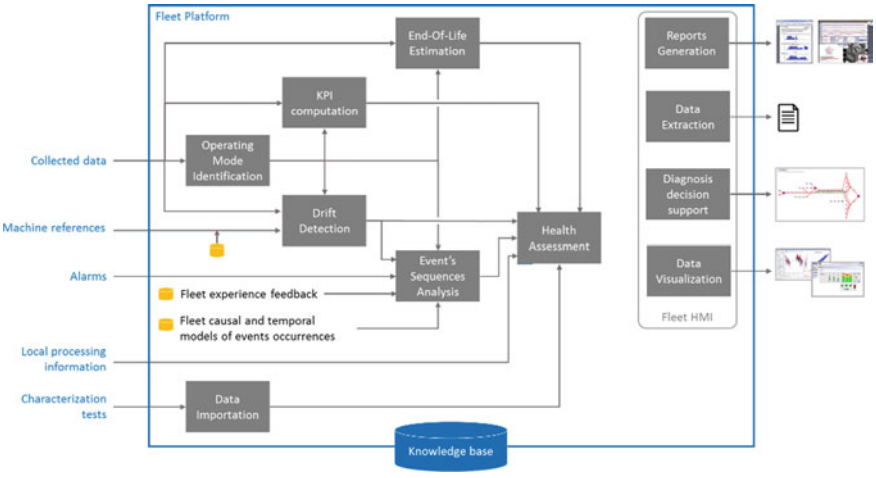

Fig. 2.8 Architecture of Twin-Control fleet data management

The concept of fleet data management is presented in Fig. 2.7. The different machines are monitored using the correspondent. A detailed architecture for each of the use cases of the project will be presented in Sect. 3.1.

Figure 2.8 summarizes presents the architecture proposed for Twin-Control fleet data management. All collected, computed and extracted information by the platform will be stored in the knowledge base. For each machine tool, expected inputs of the fleet platform can be classified in two groups:

– Automatic inputs that are regularly pushed to the fleet platform. The automatic inputs are:

- Collected data: raw data acquired directly from the machine tools with high and low sampling rate according to data dynamics.
- Local processing information: locally computed information (in ARTIS), such as energy monitoring information.
- Alarms: warnings generated by both CNC of the machines tools and monitoring hardware.

– Manual inputs that are entered or uploaded by users. The manual inputs are:

- Characterization tests: test results file and/or additional collected data from mobile equipment can be uploaded on the platform via a specific HMI represented by the bloc "Data importation".
- Machine references: To detect behavioural drifts, it is necessary to have reference behaviours, the fleet platform can learn references but also to use references extracted from the simulation environment.

Fleet platform will be powered by the KASEM® platform of predict. KASEM® will also provide generic and standard HMI that could be updated to fit project requirements. KASEM® is a Web platform with a service-oriented architecture (SOA). Following sub-sections explain main functions deployed in the fleet platform once machine tools knowledge will be formalized.

2.2.3.2 Health Assessment

Health assessment functionality consists of the correlation of various information computed by the fleet platform to evaluate the health status of one machine and health status of machines set. Health assessment is mainly based on a rating principle of different features:

- Key performance indicators (KPIs): These indicators allow users to have a synthetic view of an equipment, a machine or a fleet of machines. They are computed at the equipment, and then they are aggregated to build higher-level indicators. Aggregation of equipment KPI gives machine KPI, and aggregation of machine KPI gives the fleet KPI.
- Drift detection: this functionality is necessary to have early detections of machine non-nominal behaviours. Early detection is based on residual analysis of the difference between observed behaviour and reference behaviour. Early detection allows generating proactive alerts to anticipate fault occurrences and then to avoid machine tool down-time. Detection can be done on operating points but also on transient behaviours. Figure 2.9 depicts an early detection of a temperature transient drift according to spindle speed level. In this case, detection is based on a thermal model learned by the fleet platform.
- Machine references: To detect behaviour drifts, it is necessary to have some reference behaviours. The fleet platform can learn references from the monitored data, but can also use simulation models to create these references. In this line,

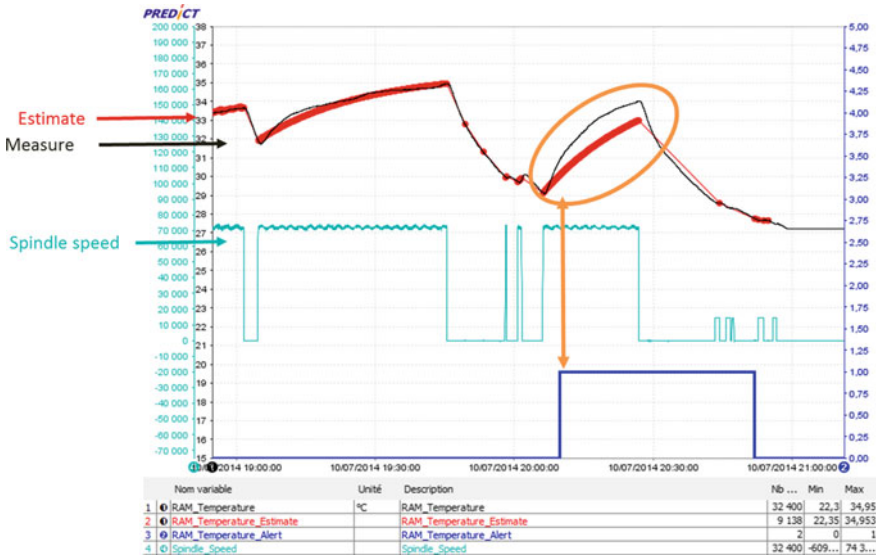

Fig. 2.9 Example of drift detection on temperature measurement

the fleet platform will take advantage of the simulation models developed within Twin-Control project.

- Machine tool characterization tests: The periodic execution of the test procedure will allow obtaining a good source of information that reflects the condition of the different components of the machine tool without process effects.

A score is assigned to each component of the health status, and then scores are merged to compute the health status. This principle allows a graphical representation of machine's health status on radar plot. Several machines can be overlaid to make a fleet comparison as depicted in Fig. 2.10.

2.2.3.3 Event's Sequence Analysis

Events include both alarms from local monitoring and alerts from fleet drift detection. This module will oversee the interpretation of event sequences, i.e. the interpretation of frequency and order of the events. Information about event types and the time stamps of their occurrence will be used to analyse the time series data and thus finding dependencies between different alarms. Generic causal models, i.e. models shared by all machines of the fleet, will be used during the analysis. A causal model represents the relationship between the different event types. These causal relationships can be used to recognize an event sequence on a given period. Once the sequence is identified, causal models allow to identify the sequence root cause (diagnosis) but also to know what could be the next event (prognostic) of the sequence.

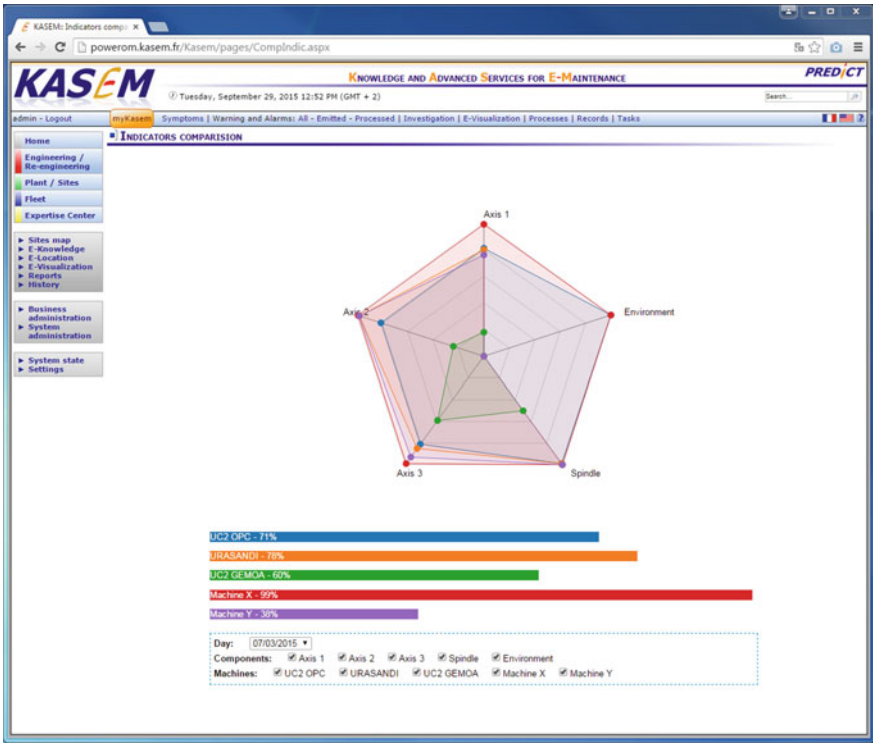

Fig. 2.10 Graphical representation of machine health status in KASEM®

This module will use event sequences as signatures of machine situations. For each machine, past situations will be stored in the knowledge base with generic label to build the fleet experience feedback and thus to improve event's sequence analysis.

2.2.3.4 Platform Portal and Outputs

For accessibility, all the functions of the platform are available through a Web portal. Results can also be made available directly on site by means of report, for instance, that can be sent (e.g. by mail) to the users and/or displayed on machine local HMI through ARTIS PlugIn. The platform Web portal will provide HMI to support decision-making for diagnosis activities, to visualize knowledge-based information with dynamics dashboards and static reports.

In addition, a functionality of data and knowledge extraction will be developed for both manually and automatically download information from platform to simulation environment and local monitoring environment.

2.3 Twin-Control Validation and Evaluation

The different Twin-Control features have been tested, first, at laboratory level, allowing a proper tuning, when needed, and validating their functionalities. Apart from that, one of the highlights of the project has been the evaluation of Twin-Control in industrial environment.

Different demonstrator scenarios have been implemented in two of the key industries for European economy: automotive and aerospace. These two sectors are very dependent on machine tool industry but show several differences with respect to the process types and requirements. Automotive sector typically deals with large batches of moderate cycle-time parts. Current major concerns are (1) to ensure part quality over time, (2) reduction of breakdowns and (3) energy efficiency. In aerospace, smaller batches are usually manufactured, but parts are normally bigger and with a complex geometry. There, new process set-up times and quality requirements are most important concerns.

The different requirements of such important industries have been taken as a reference to determine the Twin-Control concept and architecture. Apart from that, both use cases will be used for the evaluation of the different features of Twin-Control, not only at technical level, but also by studying the impact caused by the features in the end-users. For each automotive and aerospace sector, a tandem of end-users composed by a part manufacturer and one of its machine tool providers will be involved in this industrial validation (Fig. 2.11). Three machines will be monitored on each end-user installation to apply fleet-based knowledge management.

- For aerospace, Twin-Control will be implemented in several Gepro system machines in MASA Aerospace installations, in Logroño (Spain). Gepro system develops big-sized gantry type multi-spindle machine tools with which MASA aerospace machines medium-to-big size aircraft parts.
- For automotive, Twin-Control will be implemented in several COMAU machine tools located in Renault plant at Cleon (France). In the manufacturing line selected for the automotive demonstration scenario, COMAU machine tools (medium-sized high-speed machining centres) are applied by Renault to machine housings of gearboxes.

The three main results of the project, presented in this chapter, have been evaluated in both validation scenarios, following a specific approach defined for Twin-Control project. Different Scenarios of Use have been defined by end-users, and the different functionalities that affect each scenario are independently evaluated. For each scenario, key performance indicators (KPIs) are defined to evaluate the impact of each Twin-Control feature implementation. The proposed scenarios are:

– Scenario of Use 1: Machine tool design. The simulation capabilities developed in Twin-Control can improve the product development process of machine tool builders.
– Scenario of Use 2: Machining process design. Twin-Control process simulation feature provides the chance to optimize process definitions of part manufacturers

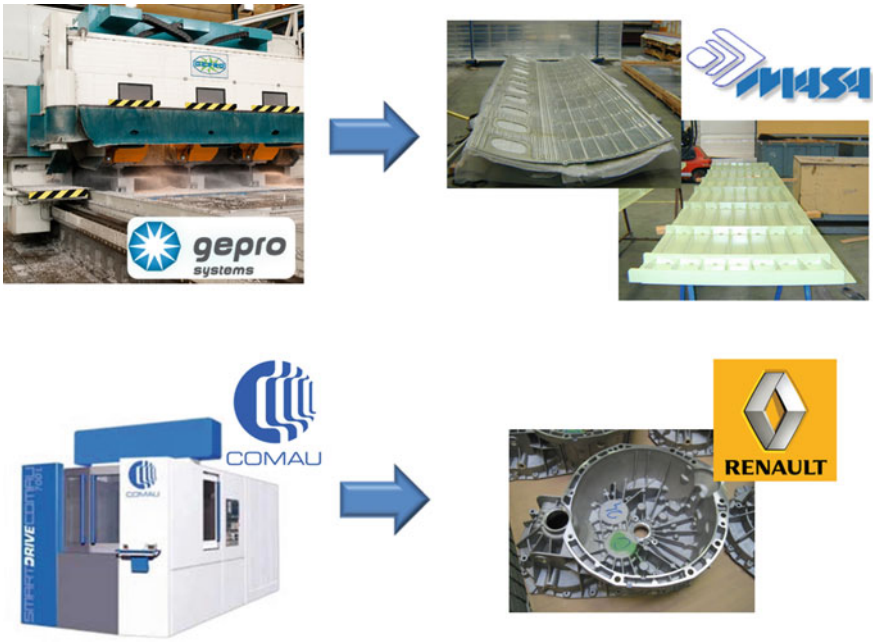

Fig. 2.11 Industrial validation and demonstration in two industries: aerospace and automotive

at design stage and, hence, minimize set-up times and reduce scrap parts in this process.

- Scenario of Use 3: Process control. Suited for operator level in part manufacturer's workshop, the Twin-Control monitoring and control device enhanced by embedded simulation models allow a better control of the manufacturing process.
- Scenario of Use 4: Maintenance. Fleet knowledge system developed in Twin-Control will lead to a better maintenance strategy for end-users.
- Scenario of Use 5: Quality. The combination of process and quality monitoring leads to a better control of part quality by reducing the amount of time spent in measurements.

Apart from that, three additional use cases have been defined this time for dissemination purposes. Twin-Control has been implemented in three pilot lines at reference-manufacturing research locations: The Advance Manufacturing Research Centre with Boing (AMRC) at Sheffield, United Kingdom, The Eta-Factory at Darmstadt, Germany, and the CFAA at Bilbao, Spain. Twin-Control can be presented to industrial partners in these relevant environments. Indeed, during the project, workshops have been organized at each pilot line (Fig. 2.12).

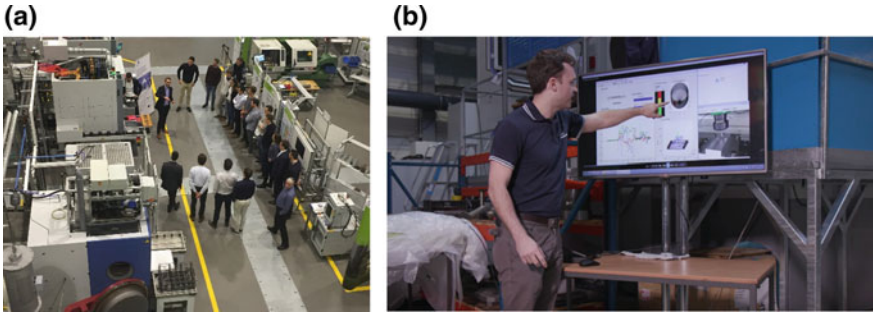

Fig. 2.12 Twin-Control dissemination activities in relevant pilot lines: **a** Johannes Sossenhiemer (Technical University of Darmstadt) presents Twin-Control features linked with energy efficiency at the ETA-Factory (Darmstadt, Germany). **b** Luke Berglind (University of Sheffield) presents a demonstration of the integration of process models with monitored data at the Advanced Manufacturing Research Centre with Boing (Sheffield, UK)

2.4 Conclusions

Twin-Control (http://twincontrol.eu/) is a new concept for machining process performance optimization, covering ICT-related features like Digital Twin, condition monitoring, fleet data management and model-based control. This section presents the concept behind Twin-Control and the proposed architecture, defined after gathering requirements from end-users involved in the project. In addition, the industrial evaluation approach is also introduced. In the next chapters of the book, the presented features will be defined in detail.

References

1. Kagermann, H., Wahlster, W.: Recommendations for implementing the strategic initiative INDUSTRIE 4.0. Final report of the Industrie 4.0 Working Group
2. Boschert, S., Rosen, R.: Digital twin—the simulation aspect. In: Hehenberger, P., Bradley, D. (eds.) Mechatronic Futures. Springer, Cham (2016)
3. Denkena, B., Fischer, R., Euhus, D., Neff, T.: Simulation based process monitoring for single item production without machine external sensors. In: 2nd International Conference on System-Integrated Intelligence: Challenges for Product and Production Engineering. Procedia Technology, vol. 15, pp. 341–348 (2014)
4. Maj, R., Bianchi, G.: Machine tools mechatronic analysis. In: Proceedings of the Institution of Mechanical Engineers Part B Journal of Engineering Manufacture 220 (2016)
5. ISO 281:2007: Rolling Bearings—Dynamic Load Ratings and Rating Life
6. http://www.artis.de/en/technology/products/process-monitoring/
7. Monnin, M., Leger, J-B., Morel, D.: Proactive facility fleet/plant monitoring and management. In: Proceedings of 24th International Congress on Condition Monitoring and Diagnostics Engineering Management, 29th May–1st June, Stavanger, Norway (2011)

8. Léger, J-B.: A case study of remote diagnosis and emaintenance information system. Keynote speech of IMS'2004. In: International Conference on Intelligent Maintenance Systems, Arles, France (2004)
9. Prado, A., Alzaga, A., Konde, E., Medina-Oliva, G., Monnin, M., Johansson, C-A., Galar, D., Euhus, D., Burrows, M., Yurre, C.: Health and performances machine tool monitoring architecture. E-maintenance Conference from 17th to 18th of June 2014, Luleå, Sweden
10. http://power-om.eu/

Part II
Virtual Representation of the Machine Tool and Machining Processes

Chapter 3
Virtualization of Machine Tools

Frédéric Cugnon, Mani Ghassempouri and Patxi Etxeberria

3.1 Introduction

The virtual prototype of a machine tool is a computer simulation model of the physical product that can be presented, analysed and tested like a real machine. The technology included in such a virtual prototype covers several engineering fields and tools depending on the stage of the design process or the studied manufacturing process. A complete review of Virtual Machine Tool technology is available in [1].

Modern machine tools are very complex mechatronic systems. The capability and efficiency of a machine tool are mainly determined by its kinematics, structural dynamics, computer numerical control system and the machining process. The kinematics is usually analysed by means of rigid multibody simulation tools (MBS) based on a 3D CAD model of the machine [2]. The finite element analysis (FEA) is used to calculate static stiffness or dynamic characteristics of the machine tool, e.g. natural frequencies and mode shapes [3]. 1D-CAE functional tools are efficiently used for computer numerical control systems [4] and actuation, while very dedicated commercial and research tools are used for cutting processes [5].

New highly dynamic machine requires high static and dynamic stiffness to ensure machining accuracy and high dynamic properties of the feed drive to decrease the manufacturing time. This is achieved by employing small moving masses with suffi-

F. Cugnon (✉)
Samtech s.a, a Siemens Company, Liège, Belgium
e-mail: frederic.cugnon@siemens.com

M. Ghassempouri
COMAU France, Castres, France
e-mail: mani.ghassempouri@comau.com

P. Etxeberria
GEPRO Systems, Durango, Spain
e-mail: petxebarria@geprosystems.com

M. Armendia et al. (eds.), *Twin-Control*,
https://doi.org/10.1007/978-3-030-02203-7_3

cient stiffness of the structural parts and high adjustable controller parameters of the drives. This leads to interactions between structural dynamics and feed drive controls, which have to be considered in the simulations [6, 7]. Natural frequencies of the feed drives are coupled with lower natural frequencies of the machine structure. To avoid instabilities, the control parameters have to be reduced, which leads to a limitation of the productivity of the machine tool.

The methodology proposed in Twin-Control is considering these interactions from the early design stage of the machine to the virtual prototyping verifications. The best method to couple structural dynamic and control loops is the flexible multibody approach. In this case, the components of the machine tool can represent the static as well as the dynamic behaviour. Those flexible components are introduced in flexible multibody system (MBS) simulation tool as super-elements created by modal reduction of detailed FEA models. The different elements which are used to connect the structural components, such as guiding systems, mounting devices or ball screw drives, are modelled as a combination of flexible connectors and flexible joints depending on the specific configuration.

The coupling with the control loops is achieved by co-simulation with 1D-CAE functional models. Most of 1D-CAE tools offer the possibility to embed the model of the control loop in some dynamic libraries (DLL). On the other side, MBS tools have interfaces or special elements that can use such DLL as a slave process and close the control loop providing velocities and displacements of the axes and receiving driving forces.

In the Twin-Control system, all this is achieved using the SAMCEF Mecano solver coupled with MATLAB/Simulink. As SAMCEF Mecano [8] is an implicit nonlinear FEA solver with MBS capabilities [9], this solution can be used from early concept design (machine kinematic) to virtual prototyping, including all FEA analyses made for components design and verification. Moreover, the finite element approach of MBS simulation is more efficient when many flexible components are considered within a large frequency range. In this case, because of extensive use of super-elements, the flexible MBS system can become unusually large for MBS solvers, but are still quite small for a FEA solver.

3.2 The Virtual Machine Tool Concept

Within the scope of the Twin-Control project, the VMT concept was used to model two machines, a high-speed 4 axes box-in-box machine from Comau and a large 3 spindles five axes machine from Gepro (Fig. 3.1).

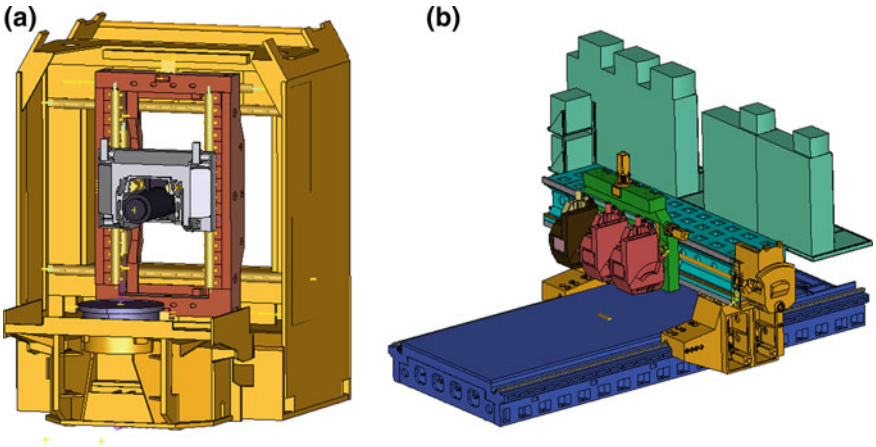

Fig. 3.1 Virtual machine tool models developed in Twin-Control project: **a** Comau Urane 25V3 machine, **b** Gepro 502 machine

3.2.1 Structural Model

To fully model the dynamic behaviour of a machine tool when operating, the following objectives are followed:

- Fully account for the flexibility of all structural components, connections and feed drive to obtain a model that can represent vibrations inside the machine.
- Limit the number of degrees of freedom to as few as possible to allow for efficient time domain simulation (small time step imposed mainly by the machining simulation module and the controller model).

Usually, a machine is made of several main structural frames, which are modelled using the super-element technique. The selected modal contains of the super-elements allow considering vibrations up to a desired frequency range. Non-structural masses are added to the moving frames to properly account for all moving components as motors, lubrication and cooling systems, etc., which are not considered in the mechanical model. Figure 3.2 shows the mesh used to create the super-element corresponding to one of the "support leg" of the Gepro machine. Ones can see the spider connections that link the retained nodes to the structure.

The guiding system for translational motion between two frames is based on sliders. Modelling such devices requires a flexible slider element, which constrains a node to move along a deformable trajectory represented by a beam element. As the track is part of the structural frame model, fictive beams are used to connect the slider nodes to the retained node of the super-element, considering its stiffness inside the slider element. The skates are idealized by the sliding node and an associated bushing that characterizes its stiffness and damping.

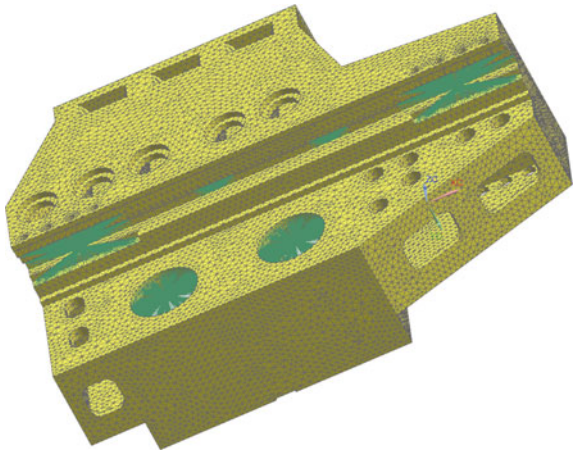

Fig. 3.2 FE model for super-element creation (leg of the Gepro machine)

3.2.2 Drive Train

If the machine is driven by pairs of linear motors as in the case of Comau machine, it is modelled by pairs of flexible sliders defined from the frame super-elements retained nodes. As the role of those sliders is to transfer axial forces, and not to contribute to the guiding function, the bushing associated with the sliding node has only axial stiffness. For those sliders, the sliding DOF can be force-driven by the controller model.

For drive systems including conventional motors, screw, rack–pinions, or other transmission systems, like in the Gepro machine, a library of simplified components models is used. An example is given for the driving system of the X-axis of Gepro's machine (highlighted in Fig. 3.1), which is made of four rack–pinion connections individually driven by a rotational motor and a gearbox.

Figure 3.3 shows a schematic view of this model, where blue nodes are structural components, green arrows kinematical dofs, orange cylinders represents masses and inertia, CNLI boxes are kinematical constraints, K boxes local stiffness, and red points belongs to the table (slider).

The green box is the motor model, it is a "scalar model" with only one rotation dof per node; flexible coupling is considered as part of the motor. The torsional stiffness K1 is introduced between input and output nodes, while all rotating inertias associated with the motor shaft are applied on the output node. The motor mass is reported to a structural node of the gearbox model. The red box represents the gearbox. The CNLI constraint account for the reduction factor, it relates the motor shaft dof to the output shaft of the gearbox. The gearbox output shaft is modelled by two coincident nodes connected to the "leg" structure by two hinge joints of y-axis. Those two nodes are also linked by the K2 torsional stiffness of the gearbox with respect to the output shaft. The torsional inertia associated with the output shaft of the gearbox is defined in the mass and inertia element associated with node named

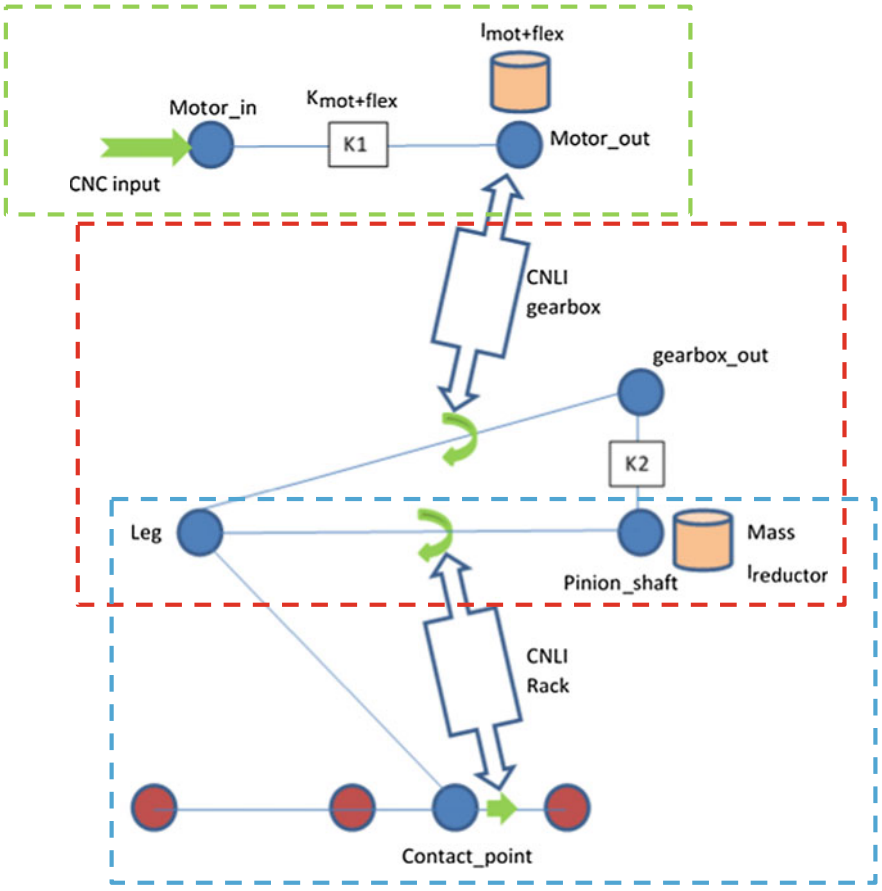

Fig. 3.3 Schematic view of the feed drive model (X-axis of the Gepro machine)

"Pinion shaft", which also include the mass of the whole system. The rotational dof of the gearbox output shaft is driven from the linear constraint (CNLI box) that imposes the reduction factor, while pinion rotational dof is used to constraint the sliding dof on the rack (red nodes) with the second linear constraint. This is done in the blue box that manages the rack–pinion interaction. The coefficient of the linear constraint is the primitive radius of the pinion. This model is repeated for each of the four motors associated with this X-axis.

3.2.3 *Spindle Model*

The spindle is a crucial component of the machine, which should be accounted in the mechanical model. From the structural point of view, it is made of housing, a shaft and a set of bearings (see Fig. 3.4).

In the VMT approach, the shaft is not rotating, and tool spinning is considered in the machining module. In our models, the spindle rotor is idealized by a set of beam elements. Those are connected to the structure (super-element) by a set of bearing elements. The integrated model is shown in Fig. 3.5.

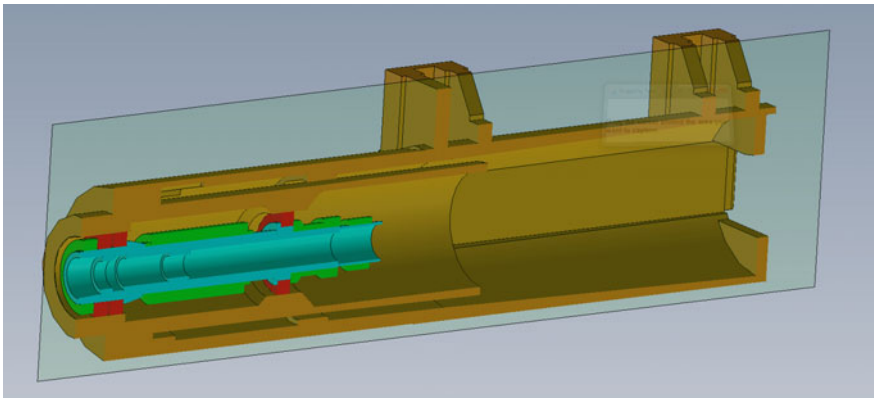

Fig. 3.4 Spindle CAD model

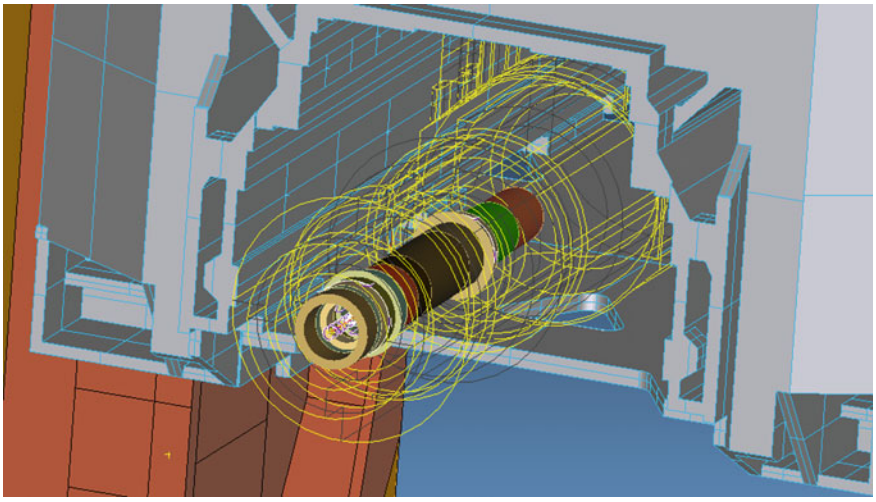

Fig. 3.5 Spindle beam model in the Comau machine

3.2.4 Modelling Principle

To summarize, the modelling process based on the CAD model of the machine is the following:

- Create/import the CAD model of the machine in the modelling environment (Simcenter).
- Create FE models of the structural components.
- Create super-elements from those models retaining the nodes needed for the connections.
- Import super-elements in the simulation environment (SAMCEF Mecano used as MBS solver) as shown in Fig. 3.6. If CAD models of the components are extracted from the global CAD model of the machine, the super-element created from those are at correct positions.
- Connect the structural components with flexible joints.
- Model drive trains, sensing systems, motors, etc.
- Include CNC model (Simulink model imported as a DLL in the mechanical model), and link to the CNC the axes position set point, which are the boundary conditions of the model.
- Use the dedicated TOOL element of Mecano to couple the VMT with the machining force module.

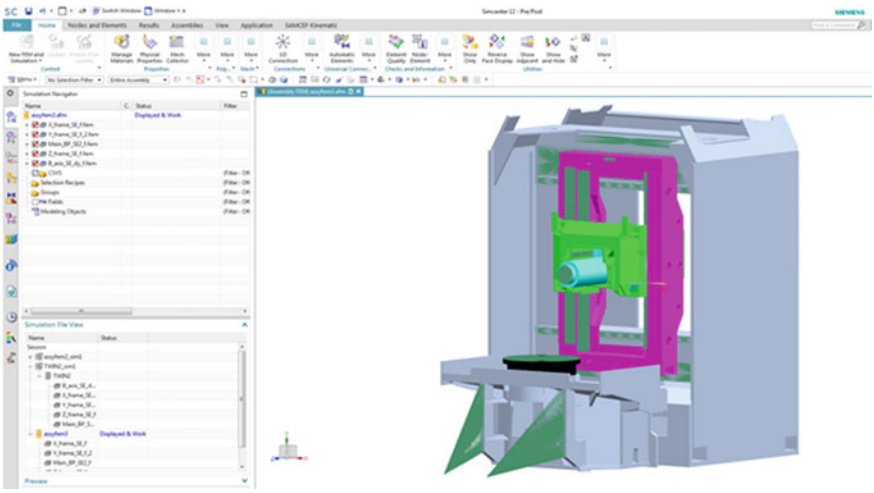

Fig. 3.6 Definition of a machine tool in Simcenter for Samcef

3.2.5 Control

For each axis, there are one or two rulers measuring the relative motion between two successive frames. These measurements are used as inputs to the controller and to compare against nominal axis motions. The rulers are represented in the model by sensor elements that associate measures in the model to some nodal DOF that can be connected to the controller model.

Most of CNC (Siemens 840D for the Comau machine and Fagor 8070 for the Gepro machine) have a similar architecture, and the main components of controller model are:

- Position, velocity and current feedback control loops;
- Velocity and acceleration feedforward;
- Power stage and motor models;
- Filters;
- Current set-point filters.

A simplified version of the control model was developed [10], disregarding the effect of current control loop and filters. Proper inputs and outputs are added to connect the mechanical model. Also, specific systems such as the pre-load loop are integrated to adapt to specific machine axes. This adapted Simulink model (see Fig. 3.7) is translated into a dynamic library and associated with a specific control element of SAMCEF Mecano that is used to manage the coupling between 1D model (control) and the full flexible 3D model (machine).

3.3 Validation of the VMT

The validation test procedure is presented focusing on the Comau machine. Models are validated considering two types of tests. First, hammer tests are done in six machine configurations (see Fig. 3.8). Obtained frequency response function (FRF) at the spindle tip position in the three main directions is checked to verify modal frequencies of the structure and to tune the structural damping. Secondly, the model driven by its controller is used to impose quick uniaxial motion. Model results are compared with experimental data obtained in real machines from the CNC monitoring. Some validation examples are shown in the next section for the Comau box-in-box machine.

3.3.1 Hammer Test (Comau Machine)

Most of the tests are done hitting the extremity of the spindle frame, having the accelerometer at the same localization. For some configurations, tests have been performed hitting also on a tool holder, while measuring acceleration on it. This allows

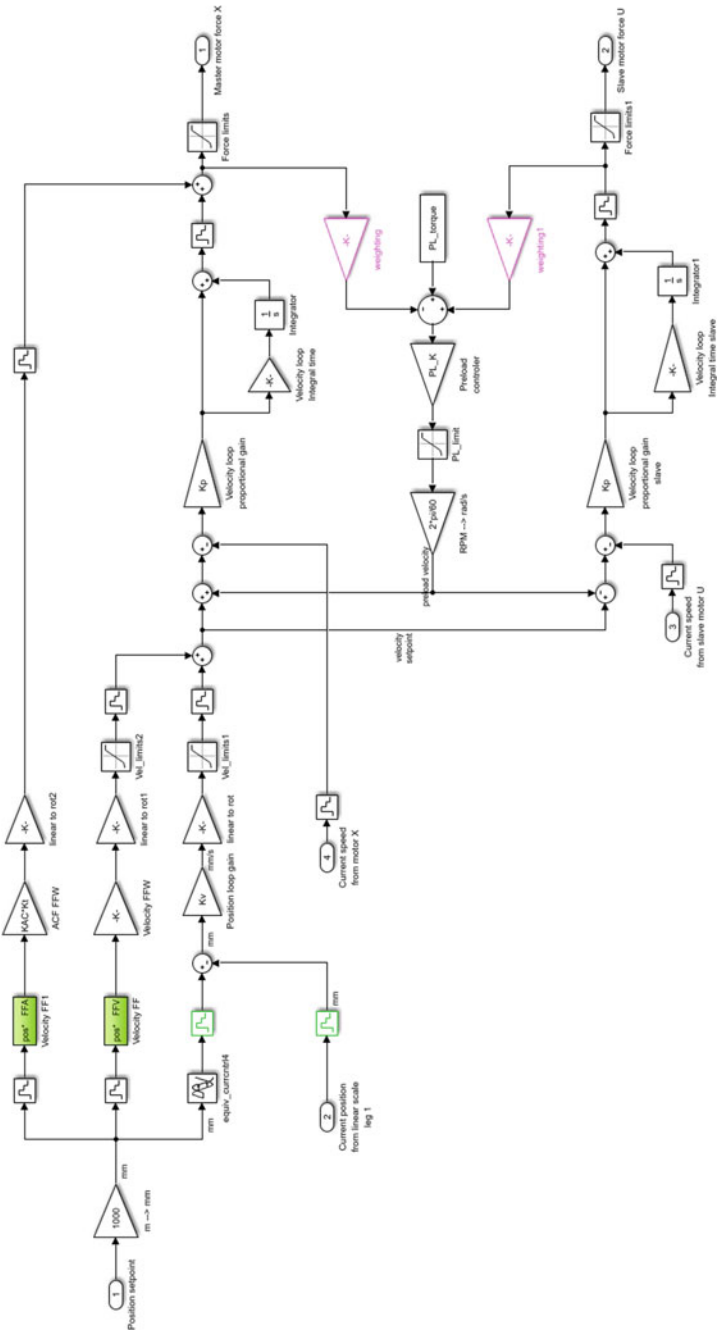

Fig. 3.7 CNC model for rack drive with 2 motors (X-axis of Gepro 502 machine)

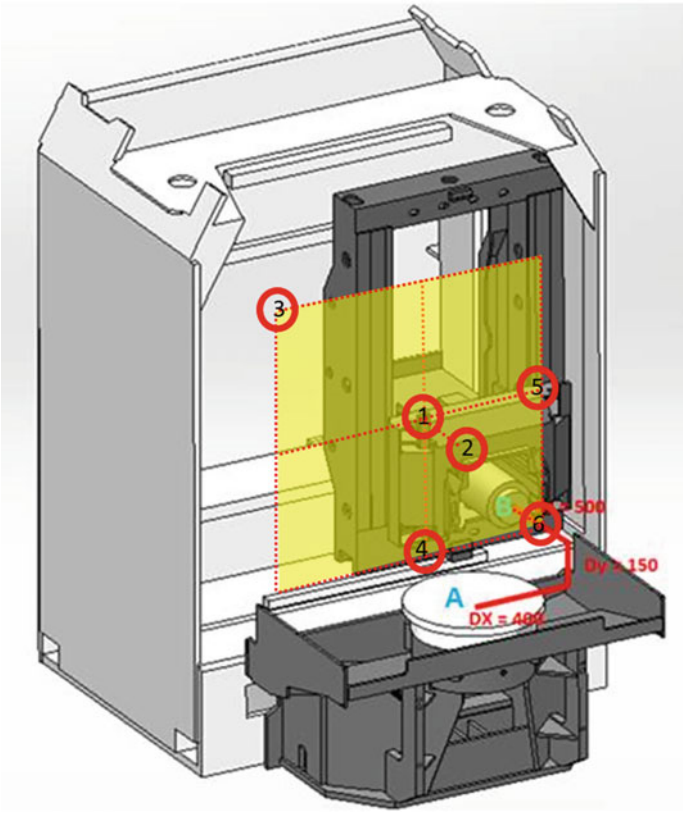

Fig. 3.8 Machine configurations

exciting not only the structure modes, but also the spindle modes. In the models, excited nodes are located either on the frame super-element or at the extremity of the spindle beam (see Figs. 3.5 and 3.9).

The modelling of a hammer test can be performed either in the frequency or the time domain. In the first approach, the flexible MBS model is used to position the machine in the desired configuration, and the solver exports its linearized matrices that are used to perform a harmonic response on the frequency range of interest. For this analysis, a unitary force is applied on the hammer impact position, resulting acceleration at the measurement point is monitored to obtain the desired FRF function. Modal damping is introduced to tune the magnitude of the excited modes. For the time domain simulation, the machine is positioned in the test configuration, and a constant force impact is applied during 1 ms. The one-second interval after the impact is simulated, and the acceleration signal is stored. The FRF is then obtained by dividing the fast Fourier transform (FFT) of the measured acceleration by the FFT

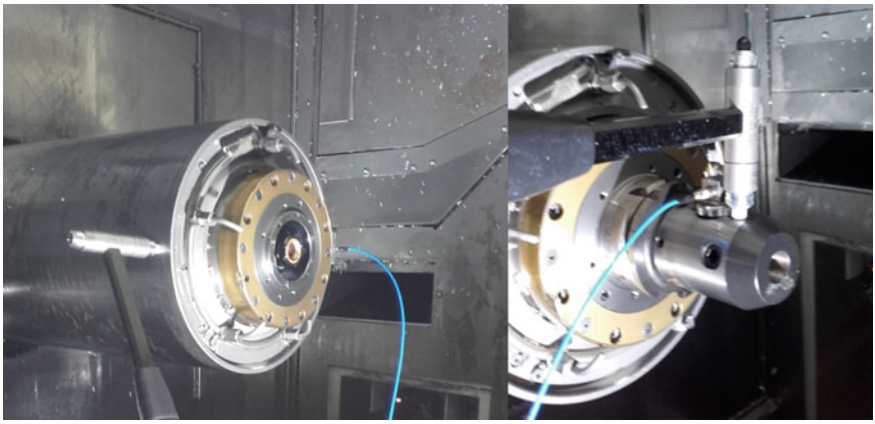

Fig. 3.9 Hammer test on z-frame and tool (spindle tip)

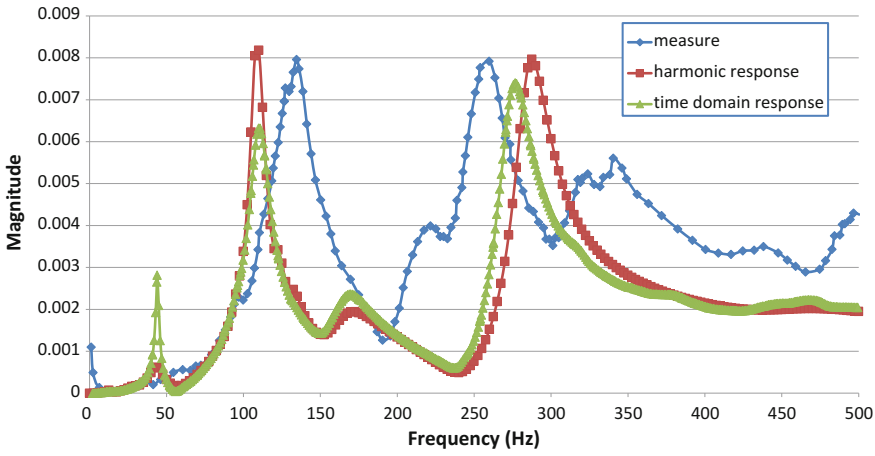

Fig. 3.10 FRF (X-direction magnitude in g/N) computed by harmonic response, by time domain simulation and measured values

of the applied force. Some simulation results are compared to the test measurements for configuration 1, which is representative of all other configurations (Fig. 3.10).

Both numerical models exhibit two main peaks close to 110 and 260 Hz that corresponds to the measurement within a 10% error margin. Frequency and time domain responses show small discrepancies in resonance locations because of different representations of the CNC, damping models are also different in both modelling approaches. The experimental curve presents "noise" in the frequency range above 300 Hz, and this behaviour is approached by the model. For harmonic response, the magnitudes at the resonances are easily tuned from the definition of modal damping. The management of damping in time domain simulation is less flexible. However, it

Table 3.1 Validation of the spindle model

	Model		Test measures	
	Frequency (kHz)	Magnitude (g/N)	Frequency (kHz)	Magnitude (g/N)
Mode 1 (x_test)	0.8	0.05	0.85	0.18
Mode 1 (y_test)	0.8	0.05	0.85	0.27
Mode 2 (x_test)	1.3	0.17	1.4	0.48
Mode 2 (y_test)	1.3	0.17	1.42	0.37
Mode 1 (z_test)	0.65	0.11	0.65–0.8	0.027

was possible to approach resonance magnitudes by adjusting structural damping in the super-elements and inside the ground fixations.

Higher natural frequencies related to the spindle dynamics are observed depending on the direction of the impact and the measure. Results from the model are compared to the validation test data in Table 3.1.

The simulated frequencies match quite well the experimental results. Resonance magnitudes show less agreement, probably due to the FRF computation process and a lack of damping characterization in the spindle model. Notice that modes simulated for the test in the transverse directions (x and y) are perfectly symmetric, which is not in the case in real machine.

3.3.2 Fast 1 Axis Motion (Comau Machine)

The purpose of this second type of test is to validate the simulation while the machine and its controller interact. Considering real machine dynamic restrictions (maximum jerk, acceleration and velocity), the quickest 100 mm displacement along the Y-axis is generated and fed as a time function to the controller model, which also gets from the machine model the position and velocity along the ruler of the considered machine axis. The controller model of Fig. 3.7 is, then, able to impose forces on the dof of the sliders representing the two linear motors driven by this control loop. CNC model provides also positioning and velocity errors.

Figures 3.11 and 3.12 show axis motion (position, velocity and positioning error) resulting from the force applied by the linear motors. The machine is almost perfectly driven by the CNC, with maximal positioning error limited to 28 microns during acceleration phases. This is the same as the data recorded by the physical CNC during the manoeuver (Fig. 3.13). Computed axis velocity is also in close agreement

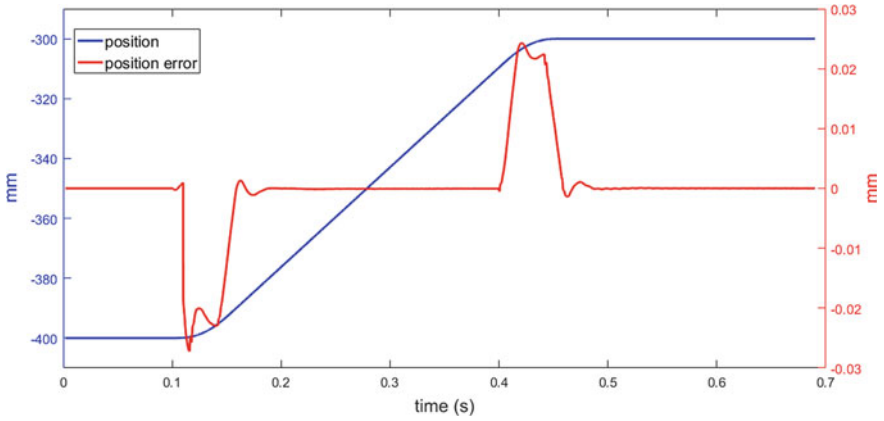

Fig. 3.11 Y-axis position and positioning error during simulation of the positioning test

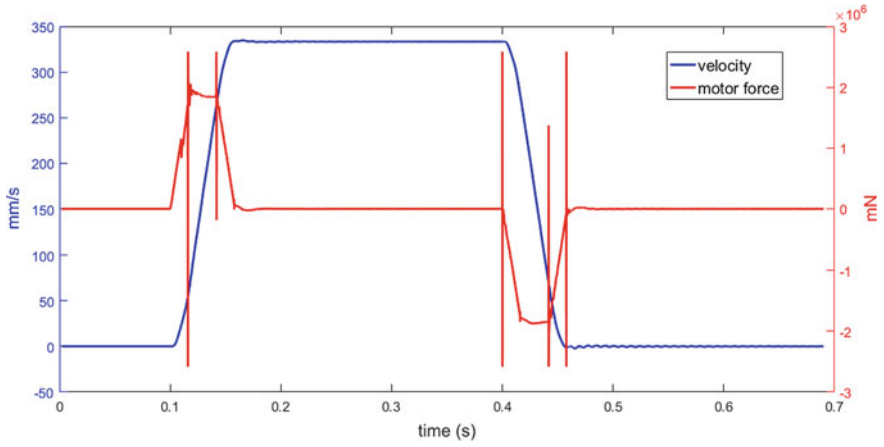

Fig. 3.12 Y-axis velocity and motor force during simulation of the positioning test

with experimental measures. Because the simplified CNC model does not include the current loop, current is not available from the model. However, the force applied in the linear motor has the same shape as the current curve of Fig. 3.13.

The upper graph recorded by the CNC (Fig. 3.13) presents the requested position and the associated positioning error. The bottom graph presents the velocity and applied current inside the linear motor, which is proportional to the generated force.

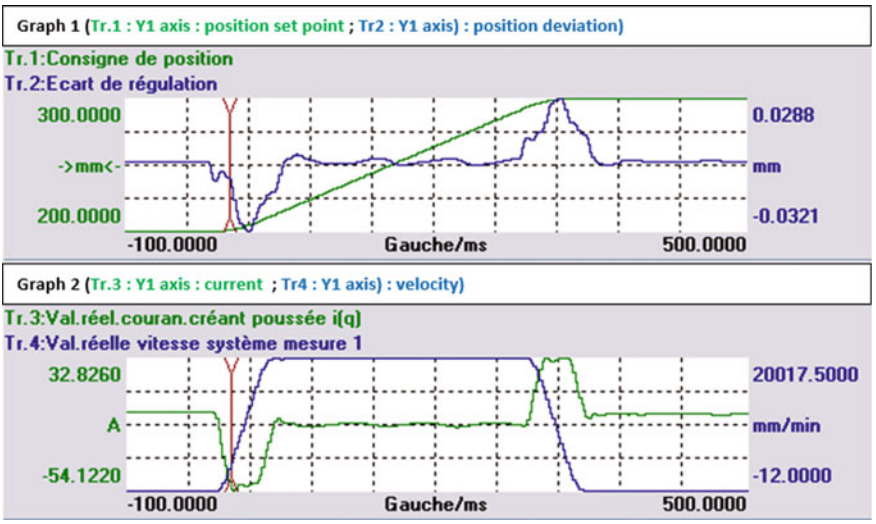

Fig. 3.13 Record of the CNC during real positioning test

3.4 Conclusions

In this section, a methodology for virtual prototyping of machine tool is presented. The proposed technology has been applied to build mechatronic flexible multibody models of several machines. The virtual machine tool can be coupled to a cutting force module. This modelling approach is of key importance to provide comprehensive simulations capabilities for virtual machine tool prototyping in working conditions. The resulting Twin-Control simulation package, which includes the VMT concept, is intended for both machine tool builders for design activities and machine tool users to improve their processes. In both cases, this virtual model can be used to avoid performing costly physical tests.

References

1. Altintas, Y., Brecher, C., Weck, M., Witt, S.: Virtual machine tool. CIRP Ann.—Manufact. Technol. (2005)
2. Weule, H., Albers, A.., Haberkern, A., Neithardt, W., Emmrich, D.: Computer aided optimisation of the static and dynamic properties of parallel kinematics. In: Proceedings of the 3rd Chemnitz Parallel Kinematic Seminar, pp. 527–546 (2002)
3. Cook, R., Malkus, D., Plesha, M.: Concepts and Applications of Finite Element Analysis, 3rd edn. Wiley, Madison (1988)
4. Prévost, D., Lavernhe, S., Lartigue, C.: Feed drive simulation for the prediction of the tool path follow up in high speed machining. J. Mach. Eng. High Perform. Manuf.—Mach. **8**(4), 32–42 (2008)

5. Schmidt, J., Söhner, J.: Use of FEM simulation in manufacturing technology. In: ABAQUS Users' Conference, Newport, RI, USA, 29–31 May 2002
6. Ghassempouri, M., Vareilles, E., Fioroni, C.: Modelling and simulating the dynamic behavior of a high speed machine tool. In: Samtech Users Conference (2003)
7. Morelle, P., Granville, D., Goffart, M.: SAMCEF for Machine Tools resulting from the EU MECOMAT project. In: NAFEMS Seminar—Mechatronics in Structural Analysis, Wiesbaden, Germany, May 2004
8. Samtech: SAMCEF V18.1 User Manual (2017)
9. Géradin, M., Cardona, A.: Flexible Multi-body Dynamics: A Finite Element Approach. Willey, New York (2001)
10. Cugnon, F., Ghassempouri, M., Armendia, M.: Machine tools mechatronic analysis in the scope of EU Twin-Control project. In: Nafems World Conference, Stockholm, Sweden, June 2017

Chapter 4
Modelling of Machining Processes

Luke Berglind and Erdem Ozturk

4.1 Introduction

Interactions between cutting tool and workpiece are critical in any machining operation. As the tool moves through a workpiece, cutting process induces forces on both the tool and the workpiece. These forces in turn have an effect on the process and can have a detrimental effect on the machine, tool and resulting part under certain conditions. It is critical then to understand these interactions before a part is machined to avoid scrapped parts or damage to the tool or machine. This chapter first covers the development of process models used to predict cutting forces for specific part programs. The cutting force model is then used for dynamic analysis to determine the effects of tool vibration on the final part outcome.

4.2 Discrete Cutting Force Model

The 5-axis machining operations bring new challenges for predicting cutting forces, where complex tool-workpiece engagements and tool orientations make it difficult to adapt 3-axis process models for 5-axis operations. A model is developed here to predict cutting forces with arbitrary tool/workpiece engagement and tool feed direction. A discrete force model is used, in which the tool is composed of multiple cutting elements. Each element is processed to determine its effect on cutting forces, and global forces are determined by combining the effects of multiple engaged elements. The

L. Berglind (✉) · E. Ozturk
The Advanced Manufacturing Research Centre (AMRC) with Boeing, University of Sheffield, Sheffield, UK
e-mail: l.berglind@amrc.co.uk

E. Ozturk
e-mail: e.ozturk@sheffield.ac.uk

M. Armendia et al. (eds.), *Twin-Control*,
https://doi.org/10.1007/978-3-030-02203-7_4

cutting force model is combined with ModuleWorks software which predicts tool-workpiece engagement regions (TWE) based on tool motion through the workpiece geometry. Cutting forces are predicted throughout complex operations by applying TWE data to the elements of the force model. The force model is validated through cutting trials in which the measured forces are compared with predicted forces during 5-axis milling.

4.2.1 Introduction

Cutting forces depend on the tool and workpiece material, cutting tool geometry and cutting conditions. In 5-axis milling, cutting conditions can vary considerably in process, and the varying cutting conditions can result in complex tool-workpiece engagements (TWE). Ozturk and Budak calculated TWE analytically for 5-axis ball end milling [1] and simulated cutting forces throughout a toolpath after calculating the cutting parameters at discrete intervals [2]. Although this method gives accurate results for smooth machining operations, the analytical engagement model loses accuracy when the uncut surface is more complex.

More detailed engagement calculation methods have been developed to better simulate more complex machining operations. These models operate by creating a virtual workpiece and removing any material that interferes with the geometry of a tool moved along a path. For each tool motion, the surface patches of the tool that remove material are the TWE region. In the solid model-based material removal simulation, the engagement area is derived from finding intersections between the solid models of both the tool and the workpiece [3–5]. Taner et al. used a planar projection strategy to determine TWE for constant feed and constant lead and tilt operations [6]. Others have represented the workpiece as a Z-map, also known as height map, a matrix/manifold of lines which are virtually cut when they interfere with the tool mesh [7]. A more advanced version of Z-map is the dexel approach [8] that can model overhangs in the geometry, thus supporting 5-axis milling. The dexel approach may be improved to so-called tri-dexel model by introducing virtual grid lines in three directions to reduce dependence on grid directionality in the geometry accuracy for any cut direction [8–10].

In the current model, ModuleWorks software which applies the tri-dexel model is used to determine TWE data for every cutter location (CL) point of a part program (see Fig. 4.1a). This TWE data determines which elements of a discretized tool mesh are engaged in the cut during that move. The cutting force contribution of each engaged element is then combined to determine the global cutting force for that move.

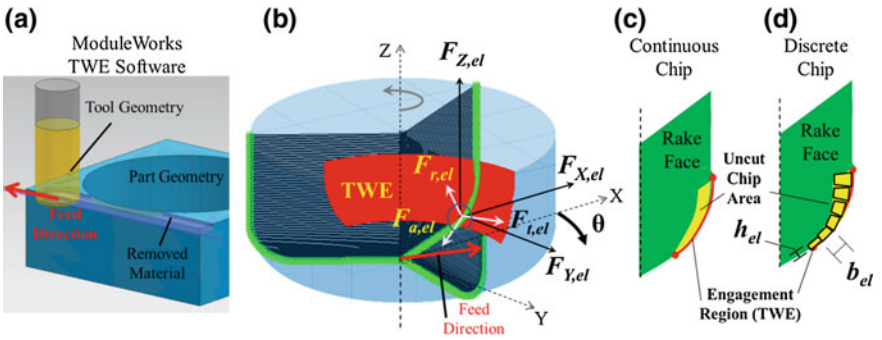

Fig. 4.1 **a** Illustration of TWE calculation from ModuleWorks software, **b** the resulting TWE data shown on the tool geometry, with element forces and tool forces shown, and **c**, **d** illustration of the true chip area and the discrete approximation of chip area used by the current cutting force model

4.2.2 Discretized Force Model

In order to predict cutting forces for arbitrary feed direction with arbitrary TWE, a discrete cutting force model is used. The model concept is shown in Fig. 4.1b, where cutting forces on a bull nose end mill act in different directions based on the cutter position and orientation. An example of the local cutting forces is shown at one section of the cutting edge, where the local radial force F_r, acts inward, normal to the cut surface, the tangent force, F_t, acts in the opposite direction of the cutter motion, and the axial force, F_a, acts tangent to the cut surface along to the tool profile.

The complex cut area from Fig. 4.1c is discretized into multiple elements in Fig. 4.1d. Each element has an effective cut width, b_{el}, along the tool profile, and thickness, h_{el}, normal to the tool profile. The global tool force is determined by combining the effects of all active cutting elements.

This section outlines the processes to determine the effects each tool element have on global cutting force.

4.2.2.1 Tool Discretization

The tool is discretized circumferentially into elements, $\mathrm{d}\theta$, and along the tool profile, L, into elements b_{el}. Discretization along the tool profile and circumferentially allows the TWE of the tool to be defined by a single 2D matrix. Elements along L are created with equal length, b_{el}, regardless of the orientation of the elements, and the element size circumferentially is dependent on the radial position of the element, r_{el}. An example mesh for a bullnose end mill with diameter, D, corner radius, R_c, and a maximum axial length of $Z_{\max}$, is shown in Fig. 4.2a. The mesh is created to follow the helical curve to match the shape of the cutting edge, as shown in Fig. 4.2b for zero helix angle and 30° helix tools.

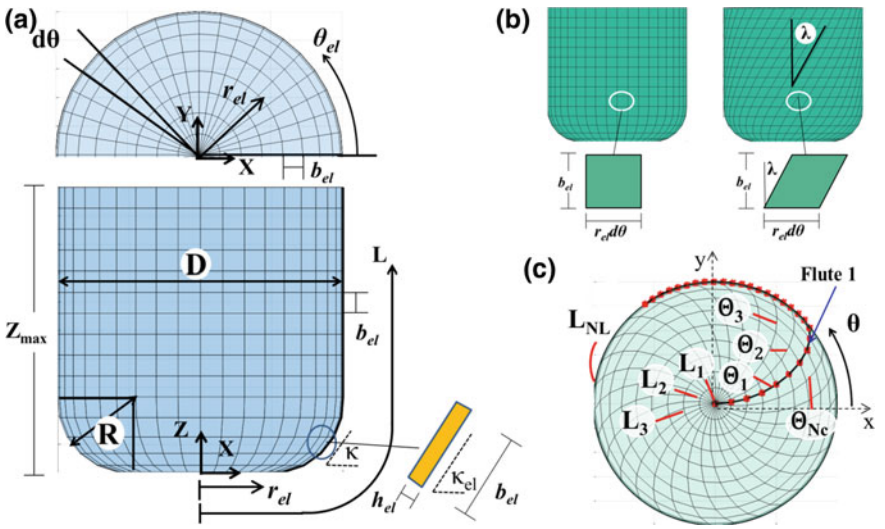

Fig. 4.2 Tool discretization along the tool profile, L, with increments, b_{el}, at angle, θ, in increments of $\mathrm{d}\theta$

The tool is discretized along the tool profile, L, into N_L elements, and circumferentially into N_c. The mesh structure is shown in Fig. 4.2c, with L mesh indices representing concentric circles radiating from the tooltip center and extending up the side of the tool. The element cut width, b_{el}, is the distance between two adjacent L elements. The Θ indices indicate the circumferential position of the elements. The elements are positioned with lag angles to follow the helical curve of the cutting edge, as shown in Fig. 4.2c. By creating the mesh along the helical curve, the indices of the TWE map always correspond directly to the cutting edge, and each Θ index corresponds to the elements of one flute at one rotational position.

Each element of the mesh has the indices, $el(\Theta, L)$, and is defined by a set of position coordinates in Cartesian (X_{el}, Y_{el}, Z_{el}) and polar (r_{el}, θ_{el}, Z_{el}) coordinates and by an orientation angle, κ_{el} (see Fig. 4.2a).

4.2.2.2 Tool Coordinate Systems

Three coordinate systems (CS) are used in the cutting force analysis for each element of the cutting edge; {rta}, $\{RTA\}$ and {XYZ}. {XYZ} is the tool global CS, in which tool motions and cutting forces are determined. $\{RTA\}$ is the tool global polar CS, describing radial, tangent, and axial directions. {rta} is the local element CS and is used to account for the orientation of the cutting elements. The rta directions correspond to the force directions associated with the cutting force coefficients (CFCs), $K_{e,rta}$ and $K_{c,rta}$, which are fixed relative to the orientation of the cutting element, but

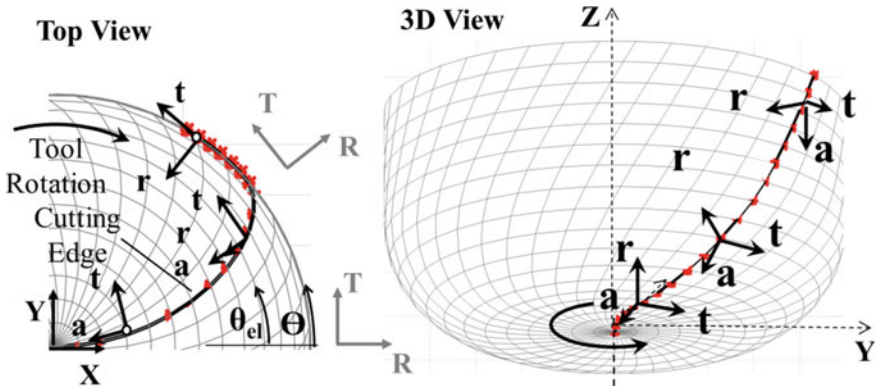

Fig. 4.3 Local and global coordinate systems

change direction based on the element orientation along a cutting edge (i.e., side or bottom of the tool profile).

Forces in these three coordinate systems are shown for a single element in Fig. 4.5. Ultimately, forces in the XYZ direction are required based on tool feed in the XYZ direction, but the cutting forces must first be determined in {rta} in which the CFCs are defined. Operations required to transform forces from {rta} to {XYZ}, as shown in Fig. 4.3, are discussed in this section.

4.2.2.3 Element Cutting Forces

Each tool element will contribute to the global cutting force if it is engaged in the cut. In this section, the element cutting forces are first calculated in the local {rta} CS and then transformed to the global tool {XYZ} CS.

4.2.2.4 Element Local Cutting Force

Element cutting forces are calculated in {rta} using Eq. (4.1). To determine these element forces for any feed direction, chip thickness, h_{el}, in Eq. (4.1) is defined based on the relative feed of that element in the local rta directions, f_{rta} (feed per tooth vector in the rta directions). By defining the element uncut chip thickness, h_{el}, as a function of the feed vector, it is possible to calculate element forces for any feed direction from a single cutting force matrix for that element. This feature is especially convenient in 5-axis machining where the tool continually changes feed direction.

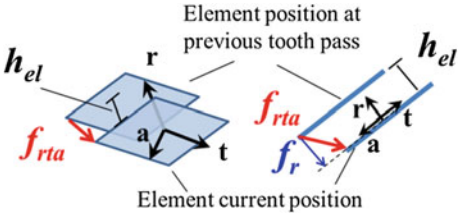

Fig. 4.4 Uncut chip thickness, h_{el}, for a tool element based on the tool feed, f_{rta}, relative to the prior tooth pass

$$\begin{Bmatrix} F_{r,el} \\ F_{t,el} \\ F_{a,el} \end{Bmatrix} = \begin{Bmatrix} K_{e,r} \\ K_{e,t} \\ K_{e,a} \end{Bmatrix} b_{el} + \begin{Bmatrix} K_{c,r} \\ K_{c,t} \\ K_{c,a} \end{Bmatrix} h_{el} b_{el} \tag{4.1}$$

The relationship between the uncut chip thickness and the relative feed of the element, f_{rta}, is illustrated in Fig. 4.4, where h_{el} is equal to the distance that the element is fed in the negative r-direction, f_r (the local **r**-direction vector always points inward, normal to the cut surface). Defining the uncut chip thickness for each element in Eq. (4.2) and combining with Eq. (4.1), the resulting expression for the cutting force for each element is given in Eq. (4.3).

$$h_{el} = \begin{Bmatrix} -1 & 0 & 0 \end{Bmatrix} \begin{Bmatrix} f_r \\ f_t \\ f_a \end{Bmatrix} \tag{4.2}$$

$$\begin{Bmatrix} F_{r,el} \\ F_{t,el} \\ F_{a,el} \end{Bmatrix} = \begin{Bmatrix} K_{e,r} b_{el} \\ K_{e,t} b_{el} \\ K_{e,a} b_{el} \end{Bmatrix} + \begin{bmatrix} -K_{c,r} b_{el} & 0 & 0 \\ -K_{c,t} b_{el} & 0 & 0 \\ -K_{c,a} b_{el} & 0 & 0 \end{bmatrix} \begin{Bmatrix} f_r \\ f_t \\ f_a \end{Bmatrix}$$

$$\begin{Bmatrix} F_{r,el} \\ F_{t,el} \\ F_{a,el} \end{Bmatrix} = \begin{Bmatrix} F_{e,r,el} \\ F_{e,t,el} \\ F_{e,a,el} \end{Bmatrix} + \begin{bmatrix} \frac{F_{c,r,el}}{f_r} & \frac{F_{c,r,el}}{f_t} & \frac{F_{c,r,el}}{f_a} \\ \frac{F_{c,t,el}}{f_r} & \frac{F_{c,t,el}}{f_t} & \frac{F_{c,t,el}}{f_a} \\ \frac{F_{c,a,el}}{f_r} & \frac{F_{c,a,el}}{f_t} & \frac{F_{c,a,el}}{f_a} \end{bmatrix} \begin{Bmatrix} f_r \\ f_t \\ f_a \end{Bmatrix}$$

$$\{F_{rta,el}\} = \{F_{e,rta,el}\} + [Q_{rta,el}]\{f_{rta}\} \tag{4.3}$$

Equation (4.3) gives cutting forces in {rta} based on the element feed in the rta directions using the cutting force matrix, $F_{c,rta,el}/f_{rta}$, or $Q_{rta,el}$. The use of $Q_{rta,el}$ is not a significant improvement on Eq. (4.1) in {rta}, however, though transformation of $Q_{rta,el}$, the same force to feed relationship can be applied in any CS.

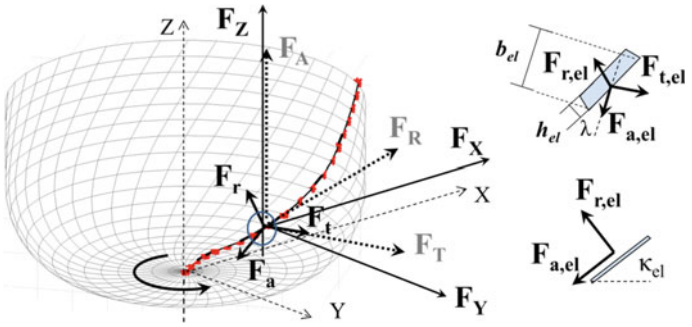

Fig. 4.5 Transformation of the cutting force directions for a single cutting edge element

4.2.2.5 Cutting Force Transformations

Cutting forces from Eq. (4.3) must be transformed from {rta} to {XYZ}, as shown in Fig. 4.5. Two coordinate transformations are required. The first transformation accounts for the local orientation of the cutting edge which is defined by the tool profile angle, κ_{el}. The transformation matrix, $T_{\kappa el}$, in Eq. (4.4) transforms from {rta} to the tool $\{R\,T\,A\}$.

$$\boldsymbol{T}_{\kappa_{el}} = \begin{bmatrix} -\sin\kappa_{el} & 0 & -\cos\kappa_{el} \\ 0 & 1 & 0 \\ \cos\kappa_{el} & 0 & -\sin\kappa_{el} \end{bmatrix} \tag{4.4}$$

The second transformation accounts for the angular position of the element around the tool. The transformation matrix, $T_{\theta el}$ in Eq. (4.5) transforms from $\{R\,T\,A\}$ to {XYZ}.

$$T_{\theta_{el}} = \begin{bmatrix} \cos\theta_{el} & -\sin\theta_{el} & 0 \\ \sin\theta_{el} & \cos\theta_{el} & 0 \\ 0 & 0 & 1 \end{bmatrix} \tag{4.5}$$

Combining (4.4) and (4.5), the transformation matrix to transform from {rta} to {XYZ} is shown in Eq. (4.6).

$$T_{el} = T_{\theta_{el}} T_{\kappa_{el}} \tag{4.6}$$

Forces in {XYZ} are found by performing a coordinate transformation to the edge force vector in (4.7), and the vector field rotation on the cutting force matrix in (4.8).

$$\left\{F_{e,XYZ,el}\right\} = T_{el}\left\{F_{e,rta,el}\right\} \tag{4.7}$$

$$\left[Q_{XYZ,el}\right] = T_{el}\left[Q_{rta,el}\right]T_{el}^{T} \tag{4.8}$$

The resulting element force vectors, $F_{e,XYZ,el}$, and matrices, $Q_{XYZ,el}$, can then be applied in Eq. (4.9) to determine element forces in XYZ based on feed in XYZ.

$$\left\{F_{e,XYZ,el}\right\} = \left\{F_{e,XYZ,el}\right\} + \left[Q_{XYZ,el}\right]\{f_{XYZ}\} \tag{4.9}$$

4.2.3 Tool Cutting Forces

After transforming in Eqs. (4.7) and (4.8), all of the element force vectors, $F_{e,XYZ,el}$, and matrices, $Q_{XYZ,el}$, share a common CS. Also, at any instant in time (or at any flute position, Θ), all elements of the tool share a common feed, f_{XYZ}. As a result, the global effect of a flute at each position, Θ, can be determined by combining $F_{e,XYZ,el}$ and $Q_{XYZ,el}$ of active elements at each Θ position. The total cutting force for each angular position is calculated in Eq. (4.10), where the outer inner summation considers all active cutting elements along a single cutting edge, and the outer summation combines the effects of multiple cutting flutes, where N_f is the total number of flutes, N_L is the number of elements along the tool profile, and N_c is the number or circumferential elements.

$$\begin{aligned} F_{e,XYZ}(\Theta) &= \sum_{j=0}^{N_f-1}\left(\sum_{L=1}^{N_L} g\left(\Theta + \frac{N_C j}{N_f}, L\right)\left[F_{e,XYZ,el\left(\Theta+\frac{N_C j}{N_f},L\right)}\right]\right) \\ \left[Q_{XYZ}(\Theta)\right] &= \sum_{j=0}^{N_f-1}\left(\sum_{L=1}^{N_L} g\left(\Theta + \frac{N_C j}{N_f}, L\right)\left[Q_{XYZ,el\left(\Theta+\frac{N_C j}{N_f},,L\right)}\right]\right) \end{aligned} \tag{4.10}$$

The term, $g(\Theta, L)$, in Eq. (4.10) is a matrix of ones and zeros defining which tool mesh elements along the tool profile, L, are engaged in the workpiece at each flute position, Θ. $g(\Theta, L)$ is illustrated in Fig. 4.6, for example, TWE for a 30° helix tool mesh with 30 angular positions, Θ, and 30 elements along the tool profile, L. As the tool rotates, the flute position shifts to different angular positions, and only the elements corresponding to those angular position are engaged at that time. For example, at position Θ_1 in Fig. 4.6 the flute is not in the cut, and $g(\Theta, L) = 0$ for all elements at that position. When the flute is at Θ_{26}, elements 10 through 20 are engaged and their effects are combined using Eq. (4.10).

The global cutting force on the tool for each flute position is determined using Eq. (4.11). Note if multiple flutes are engaged in the cut at once, the effects of all engaged flutes can also be combined.

$$\{F_{XYZ}(\Theta)\} = \left\{F_{e,XYZ}(\Theta)\right\} + \left[Q_{XYZ}(\Theta)\right]\{f_{XYZ}\} \tag{4.11}$$

Cutting forces are determined by evaluating Eq. (4.11) for each flute position. As the tool rotates through the different positions, the components of Eq. (4.11) change to reflect the engaged elements in that section.

The example in Fig. 4.7 shows the calculated cutting forces for a two-fluted, 12-mm-diameter ball end mill with full radial immersion at 10,000 RPM with a cutting depth of 3 mm. For this cut, the tool is fed in the negative Y-direction at a rate of 0.1 mm per tooth, so the feed vector is constant at $f_{XYZ} = \{0, -0.1, 0\}^{\mathrm{T}}$. Equation (4.11) is then evaluated at each position (only positions 1 through 7 are shown), to obtain the changing cutting forces as the tool rotates through the engagement region.

4.2.4 Part Cutting Forces

In 5-axis machining, the orientation of the tool can change continually with respect to the workpiece. So far cutting forces have been determined in the tool CS. However, cutting forces in the part CS, XYZ_P, based on tool feed in XYZ_P are often more convenient as tool motions are programed in the part CS. After transforming $F_{e,XYZ}(\Theta)$ and $Q_{XYZ}(\Theta)$ in Eq. (4.12) based on the coordinate transformation from the tool CS to the part CS, T_{T2P}, cutting forces are obtained in the part CS using Eq. (4.13).

$$\begin{aligned} \left\{F_{XYZ_P}(\Theta)\right\} &= T_{T2P}\left\{F_{e,XYZ}(\Theta)\right\} \\ \left[Q_{XYZ_P}(\Theta)\right] &= T_{T2P}\left[Q_{XYZ}(\Theta)\right]T_{T2P}^{T} \end{aligned} \tag{4.12}$$

$$\left\{F_{XYZ_P}(\Theta)\right\} = \left\{F_{e,XYZ_P}(\Theta)\right\} + \left[Q_{XYZ_P}(\Theta)\right]\left\{f_{XYZ_P}\right\} \tag{4.13}$$

4.2.5 Cutting Trials

Two cutting tests are performed to compare simulated and measured cutting forces. The tool for both tests is a 12-mm-diameter ball end mill with two flutes and helix

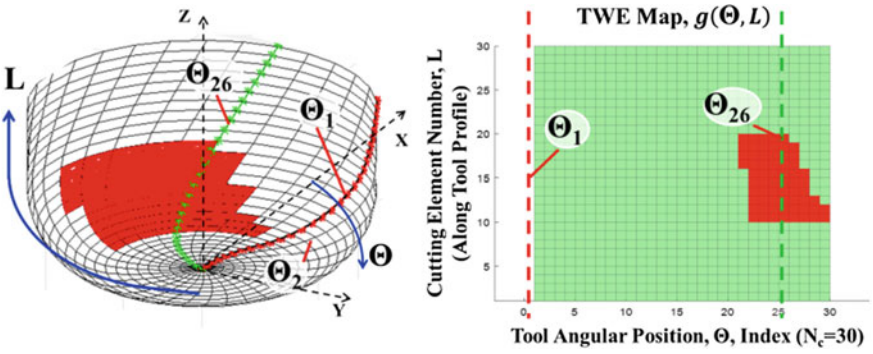

Fig. 4.6 Mesh and TWE indices for a 30° helix cutter

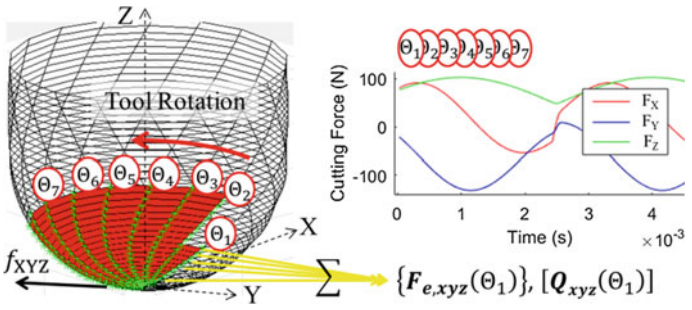

Fig. 4.7 Calculation of cutting forces with a single operation for each global rotation angle by combining all active cutting elements at that angle

angle of 30° (Sandvik R216.42-12030-AK22A H10F). The machine used for the tests is a MAG FTV5-2500, and force measurements are collected using a Kistler 9139AA dynamometer. The CFCs used for the AL7075-T6 workpiece are found experimentally using a ball end mill mechanistic model [11], to be: $K_{e,r} = 13.9$, $K_{e,t} = 7.1$, $K_{e,a} = -1.3$ N/mm, and $K_{c,r} = 619.9$, $K_{c,t} = 1014.2$, and $K_{c,a} = 58.2$ N/mm^2. Note that average CFC values identified experimentally are used for all elements regardless of local oblique and rake angles. A summary of CFCs for this set of trials ("M" machining tests) along with the CFCs for other trials in this chapter are provided in Table 4.1.

The first test is a stair step test where the axial depth increases from 1 to 3 mm in increments of 0.25 mm, with full radial immersion and zero lead and tilt. For this test, the spindle speed is 10,000 RPM with a feed rate of 0.1 mm per tooth in the $-X_P$ direction. The force measurements in the part CS, $F_{XYZ,P}$, are shown in Fig. 4.8, along with the maximum and minimum simulated forces. A detailed comparison of the simulated and measured cutting forces is also shown in Fig. 4.8 for the minimum depth of 1 mm and maximum depth of 3 mm. It can be seen from these results that the simulated results closely match the experiment for this simple operation.

The second test is on the "M" part shown in Fig. 4.9, which is machined at 12,250 RPM using approximately 2000 CL points. During this test, the A and C axes of the machine are fixed at 21.1° and −134°, respectively, resulting in a lead and tilt

Table 4.1 Summary of CFCs used during cutting trials throughout this chapter

Test	$K_{e,r}$ (N/mm)	$K_{e,t}$ (N/mm)	$K_{e,a}$ (N/mm)	$K_{c,r}$ (N/mm^2)	$K_{c,t}$ (N/mm^2)	$K_{c,a}$ (N/mm^2)
"M" machining tests	13.9	7.1	−1.3	619.9	1014.2	58.2
Corner cut test	9.3	0.4	0.6	452.4	955.9	235.7
SLE groove tests	7.4	−3	−2.7	128.4	965.5	85.34

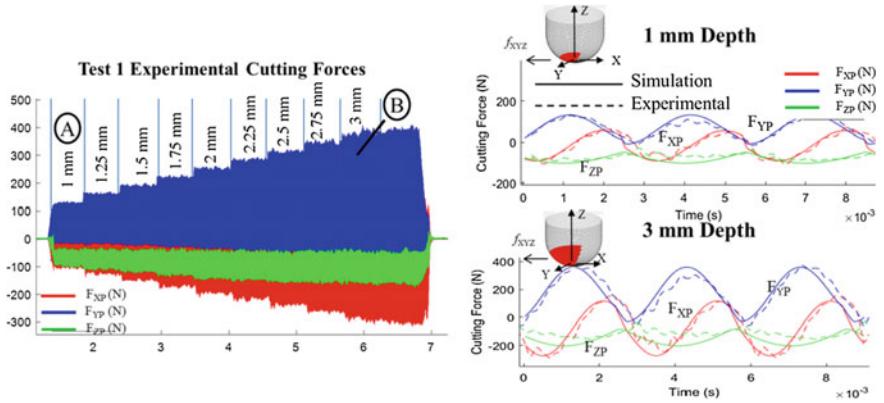

Fig. 4.8 Step cutting force test results for Test 1 (zero lead and tilt) showing detailed comparison of the simulated force results for (A) 1 mm depth and (B) 3 mm depth

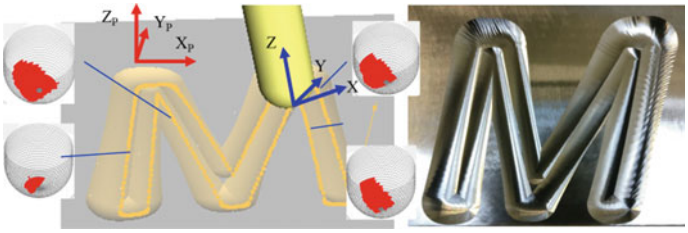

Fig. 4.9 Test cut "M" character with varying cut depth

of 15° when feeding in the $-X_P$ feed direction on the X_pY_P plane. The rotary axes are fixed to reduce tracking errors between the simulation and the true machine motions. This part is machined over a dome-shaped base which results in varying depth over the "M" profile. Further, the fixed tool orientation results in a fixed transformation, T_{T2P}, but variable lead and tilt angle as the tool changes direction.

Prior to the start of the simulation, the tool mesh is created, and $F_{e,XYZ,el}$ and $Q_{XYZ,el}$ are determined for each tool mesh element (these only need to be calculated once for a given tool mesh and fixed set of cutting force coefficients). Then, for each CL point, the TWE is obtained for that move using ModuleWorks Software. Figure 4.9 shows examples of how the TWE maps obtained change throughout the operation. The TWE data for each move is then applied to obtain $F_{e,XYZ}(\Theta)$ and $Q_{XYZ}(\Theta)$, and the cutting forces are calculated using Eq. (4.11) at each angular position.

Note that the transformation between the tool CS and part CS is dependent on how the tool CS is defined in the part CS. In the step example shown in Fig. 4.8, the tool CS is the same as the part CS, so no transformation is needed (except to reverse the sign of the forces to represent forces acting on the part, where forces are calculated as acting on the tool). The transformation, T_{T2P}, for the 5-axis example

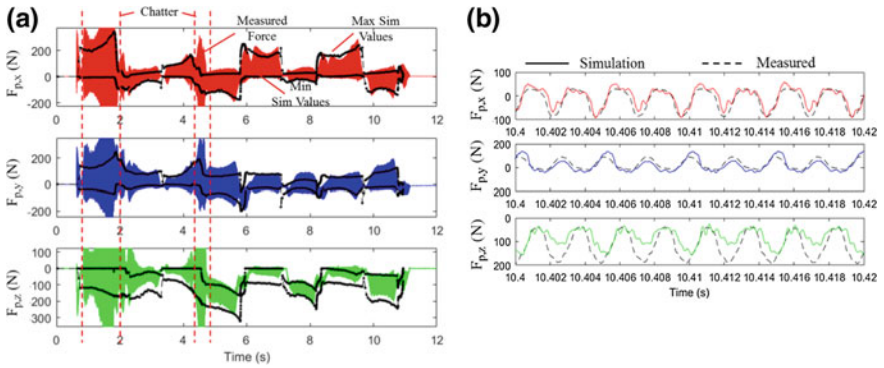

Fig. 4.10 **a** Measured forces in workpiece CS with maximum and minimum simulated force values at each corresponding location. **b** Comparison of simulated and measured force data at one location of the "M" part

in Fig. 4.9, is more complex because it is a function of both the tool orientation and the feed direction of the tool.

Due to tracking errors in the tool feed velocity (despite fixing the A and C axes), the total machining time is measured as approximately 20% longer than expected. To account for this in the simulation, the feed per tooth was reduced to 0.078 mm per tooth to match the actual and simulation machine time (this effectively reduced the simulated average tool feed speed, and hence feed per tooth).

The resulting forces are plotted in Fig. 4.10a along with the maximum and minimum simulated force values at those locations in time. The results show that the simulated maximum and minimum forces closely follow the force profile throughout the operation. Further, the simulated rotation dependent forces in Fig. 4.10b also closely match the measured forces. The only places where large deviations occur are in locations where chatter occurs. While the current force model does not predict forces during chatter, this model can be used to predict whether chatter will occur. This stability prediction approach is discussed in the following section.

4.2.6 Cutting Force Model Summary

The cutting force model developed here was created to predict forces for complex machining operations where the tool/workpiece engagement is complex and highly variable throughout. The key feature of this model is that it treats the elements of a discretized tool as individual entities which have predetermined force characteristics ($F_{e,XYZ,el}$ and $Q_{XYZ,el}$) which are independent of the feed rate and feed direction of the tool. When coupled with ModuleWorks TWE software to capture effect of changing cutting conditions on the TWE, it is possible to efficiently obtain complex cutting force predictions for 5-axis milling operations.

The experiments discussed here have shown that this model is capable of predicting cutting force for a ball end mill in 3- and 5-axis operations. The stair test resulted in accurate predictions of cutting force at varying cut depths. The "M" test demonstrated that this model is able to pair with Moduleworks TWE software and accounts for a high variation of cutting conditions effectively. The predictions from this test showed close agreement between simulated and measured forces.

4.3 Stability Roadmap

Chatter is one of the major limitations to machining processes that affects part quality and productivity. It has been extensively studied [12], and different approaches have been developed to predict and mitigate chatter. Several modelling techniques such as frequency domain solution [13], semi-discretization [14] and temporal finite element [15], and time domain solution [16] have been applied to predict stability in 3-axis milling operations. These methods are used to create stability lobe diagrams (SLDs) which show the stable and unstable depths of cut at different spindle speeds.

The frequency domain solutions for flat end mills were later extended to general milling tools [17] and 5-axis ball end milling operations [18]. Additional degrees of freedoms in 5-axis milling complicate the calculation of tool and workpiece engagement which is a required input in modelling the mechanics and dynamics of the process. Ozturk and Budak [18] simulated the stability of 5-axis ball end milling operation using both single and multifrequency solution. They used an analytical cutter workpiece engagement boundary definition [1]. In some complex toolpaths in 5-axis milling, the definition of tool and process parameters such as cutting depth, step over, lead and tilt angles may not be enough to define the tool and workpiece engagements. For such cases, numerical geometric engagement calculation methods are required [19]. Ozkirimli et al. [20] calculated the SLDs by using a numerical engagement method employing the frequency domain solution.

In order to simulate stability of a complex toolpath, Budak et al. simulated stability lobe diagrams for different points along the toolpath [21] and generated 3D stability lobe diagrams. This approach is applicable for parameter selection while designing toolpath. By looking to the 3D stability lobe diagram, the most conservative cutting depth and spindle speed can be selected for the process to have a chatter-free process. On the other hand, there are practical issues with using 3D stability lobe diagrams.

In complex cutting cases, definition of cutting depth can be vague. Even if the process planner has the 3D stability lobe diagram for a given process, it will be difficult for the process planner to identify whether the process is stable at a given point. First, they need to determine the cutting depths at each point in the toolpath and spindle speed and compare them with the 3D stability lobe diagram. Moreover, once the toolpath is generated it is not possible to change the cutting depth without generating the toolpath again. For these reasons stability lobe diagrams are less practical for the visualization of the stability and changing the cutting depth without changing the toolpath. In order to visualize the stability of a given process, the

stability roadmap (SRM) is proposed. It plots the stable speeds for a given part program considering the changing cutting conditions.

The purpose of the SRM is to efficiently obtain and represent stability information for complex 5-axis operations. Once a part program is created, the TWE is assumed to be fixed for each cutter location (CL) point of the program. Apart from regenerating the part program, the most effective way to reduce chatter is through spindle speed control. The SRM, thus, can be used by process planners to identify the best spindle speeds throughout the program.

The force and stability formulation required to generate SRMs are presented in this section, along with validation tests in which the model predictions are compared with measured results.

4.3.1 Dynamic Force Model

The cutting force matrices developed in Sect. 4.2.2 to predict cutting forces for any tool/workpiece engagement, and feed direction can also be applied to predict stability for the same operations. To simulate dynamic effects, Eq. (4.11) is modified by including dynamic effects in the tool displacement vector, Δ_{XYZ}. The dynamic feed vector is shown in (4.14), where f_{XYZ} is the nominal feed per tooth vector, and XYZ and XYZ_τ are tool displacements from the nominal position at the current time and at the previous tooth pass.

$$\{\Delta_{XYZ}\} = \{f_{XYZ} + XYZ - XYZ_\tau\} \tag{4.14}$$

The cutting force matrices, $Q_{xyz}(\Theta)$, are also applied for stability prediction using the zeroth order stability model developed in [13]. For the zeroth order linear milling stability formulation, the nonlinear relation between force and feed is not included in the model. The variable component of the cutting force is expressed in the frequency domain in Eq. (4.15) [13].

$$\{F_{XYZ}(\omega)\} = \left[Q_{XYZ}(\Theta)\right]\{\Delta_{XYZ}(\omega)\} \tag{4.15}$$

The dynamic force in Eq. (4.15) has time-varying coefficients due to the tool rotation angle dependence of $Q_{xyz}(\Theta)$ (each rotation angle can be expressed as a function of time as the tool rotates). Equation (4.15) is made time-invariant by approximating the time-varying term as an average value [12]. Averaging the $Q_{xyz}(\Theta)$ over the tooth passing period, or over the range of rotation angles, Θ, is analogous to the approximation of time-varying coefficients through the zeroth order Fourier series term in [12]. The average Q matrixes over one tool revolution, Q_0, are calculated in Eq. (4.16), where N_c is the total number of circumferential elements in the tool mesh.

After averaging to obtain Q_0 and defining $\Delta_{XYZ}(\omega)$ as a function of the frequency response function, FRF(ω), in Eq. (4.17), the resulting time-invariant dynamic force

equation is obtained as Eq. (4.18). Note here that Q_{xyz} and Q_0 are the force matrices in the tool CS, which should correspond to the FRF measurements taken at the tooltip.

$$[Q_0] = \frac{1}{N_c}\sum_{\Theta=1}^{N_c}[Q_{XYZ}(\Theta)] \tag{4.16}$$

$$\{\Delta_{XYZ}(\omega)\} = \left(1 - e^{-i\omega\tau}\right)[\mathrm{FRF}(\omega)]\{F_{XYZ}(\omega)\} \tag{4.17}$$

$$\{F_{XYZ}(\omega)\} = \left(1 - e^{-i\omega\tau}\right)[Q_0][\mathrm{FRF}(\omega)]\{F_{XYZ}(\omega)\} \tag{4.18}$$

The dynamic stability is determined through the determinant of the characteristic equation in Eq. (4.19), which defines the condition at the limit of stability [12].

$$\det\left([I] - \left(1 - e^{-i\omega\tau}\right)[[Q_0][FRF(\omega)]]\right) = 0 \tag{4.19}$$

For calculation, Eq. (4.19) is rearranged to the form used by the eig function in MATLAB in Eq. (4.20), as done in [22].

$$\det\left([Q_0][\mathrm{FRF}(\omega)] - \frac{1}{\left(1 - e^{-i\omega\tau}\right)}[I]\right) = 0;$$

$$\lambda = \mathrm{eig}\left([Q_0][\mathrm{FRF}(\omega)]\right) = \frac{1}{\left(1 - e^{-i\omega\tau}\right)} \tag{4.20}$$

Following the steps of reduction in [13, 22], the condition of Eq. (4.20) is satisfied in Eq. (4.21), when the real component of $\mathrm{eig}\left([Q_0][\mathrm{FRF}(\omega)]\right)$ is equal to 0.5.

$$0.5 = \frac{\left(\lambda_{\mathrm{Re}}^2(\omega) + \lambda_{\mathrm{Im}}^2(\omega)\right)}{\lambda_{\mathrm{Re}}(\omega)\left(1 + \lambda_{\mathrm{Im}}^2(\omega)/\lambda_{\mathrm{Re}}^2(\omega)\right)} = \lambda_{\mathrm{Re}}(\omega) \tag{4.21}$$

Equation (4.21) defines the conditions when the system is at the limit of stability. Because the current system is based on a discrete model, there is no additional variable which can be solved to satisfy Eqs. (4.20) and (4.21) (such as depth of cut in [13]). As a result, stability is predicted for each new Q_0 matrix, where Q_0 changes throughout a program based on changing TWE data. For each new Q_0 matrix, the eigenvalues are found over a range of frequencies using Eq. (4.20), and the conditions of Eq. (4.22) are used to determine at which frequencies the system is stable or unstable.

$$\lambda_{\max}(\omega) = \max(\lambda_{\mathrm{Re}}(\omega)) \begin{cases} > 0.5, \text{ Unstable} \\ = 0.5, \text{ Stabiltity Limit} \\ < 0.5, \text{ Stable} \end{cases} \tag{4.22}$$

$\lambda_{\max}(\omega)$ is the maximum real eigenvalue component in Eq. (4.20) for each frequency of [FRF(ω)] (there are multiple eigenvalues at each frequency). Any frequency, ω, at which $\lambda_{\max}(\omega) > 0.5$ is considered a chatter frequency, ω_c.

Equation (4.23) is then used to determine spindle speeds at which chatter will occur, Ω_c, based on the chatter frequencies. The chatter frequency is used to calculate unstable spindle speeds for multiple integers of the chatter frequency (similar to the multiple lobes of a stability lobe diagram) in Eq. (4.23). The following section describes this process in more detail.

$$\Omega_c = \frac{60\omega_c}{N_f\left(\epsilon(\omega_c) + 2\pi j\right)}; \epsilon(\omega_c) = \pi + 2\tan^{-1}\left(\frac{\lambda_{\mathrm{Im}}(\omega_c)}{\lambda_{\mathrm{Re}}(\omega_c)}\right) \tag{4.23}$$

4.3.2 Stability Roadmap Generation

The process used to produce a SRM from the system eigenvalues is shown for three example engagements in Fig. 4.11. For each engagement, the maximum real eigenvalues are identified over a range of frequencies, and values greater than 0.5 are considered chatter frequencies, ω_c, as indicated for the third engagement in Fig. 4.11a. The chatter frequencies correspond to spindle speeds, Ω_c, which repeat for each jth lobe, according to (4.23). Here, start and end chatter frequencies, $\omega_{c,(1,2)}$, are identified at location where the eigenvalues cross 0.5, and these values are used to calculate start and end chatter speeds, $\Omega_{c,(1,2)}$, for each jth lobe for each engagement, as shown in Eq. (4.24) and for the third engagement in Fig. 4.11b.

$$\Omega_{c,(1,2)} = \frac{60\omega_{c,(1,2)}}{N_f\left(\in\left(\omega_{c,(1,2)}\right) + 2\pi j\right)} \tag{4.24}$$

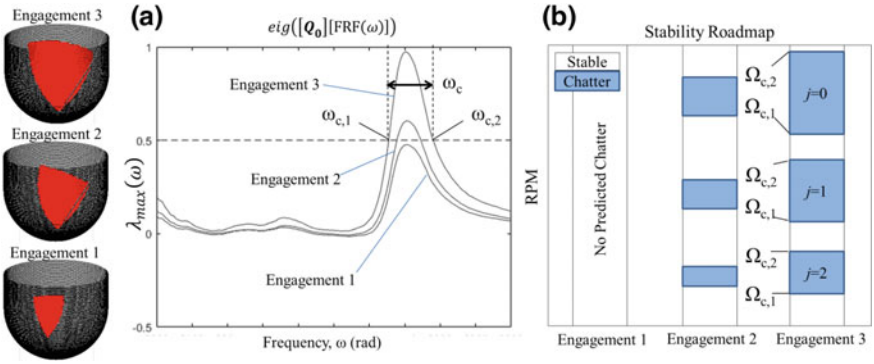

Fig. 4.11 Generation of stability roadmap from system eigenvalues

4.3.3 Stability Roadmap Trials

Stability roadmaps are generated for two example part programs and cutting trials are performed to compare the stability predictions with stability measurements. The first trial is a 5-axis ball end milling of a 3D "M" character in which the A and C axes are fixed, and the second is a continuously varying lead and tilt corner cut. The stability predictions from both examples are tested experimentally.

4.3.3.1 Stability Roadmap Trial 1

The "M" cutting trials used to test force predictions in Sect. 4.2.5 are also used here for stability prediction. The only new information required is the FRF data of the tool, which is plotted for the tool mounted on the FTV-5 in Fig. 4.12a. Figure 4.12a shows that this tool has significant dynamic asymmetry between X- and Y-directions, with significant magnitudes in the cross FRF measurements at the tooltip. As such, cross FRFs are considered in stability predictions. The resulting SRM for this operation, shown in Fig. 4.12b, is generated by following the steps shown in Fig. 4.11, using measured tool FRF data and the TWE data from each CL move.

Cutting trials are run at 12,250 and 10,850 RPM. After each test, a spectrogram of the microphone signal is generated to identify tooth passing and chatter frequencies throughout the cut. Dominant frequencies, excluding tooth passing harmonics, are considered to be a result of chatter.

The results of both tests are shown in Fig. 4.13. The SRM color map indicates the predicted chatter frequency at that location, where the chatter frequency with the highest real eigenvalue, λ_{max}, is represented for each spindle speed (there can be multiple chatter frequencies at the same speed). The results from the 12,250 RPM test (Fig. 4.13a) show that two frequencies are predicted to be dominant, at 1500 and 2300 Hz. The spectrogram results show high amplitudes at both frequencies when unstable during the first 850 CL points.

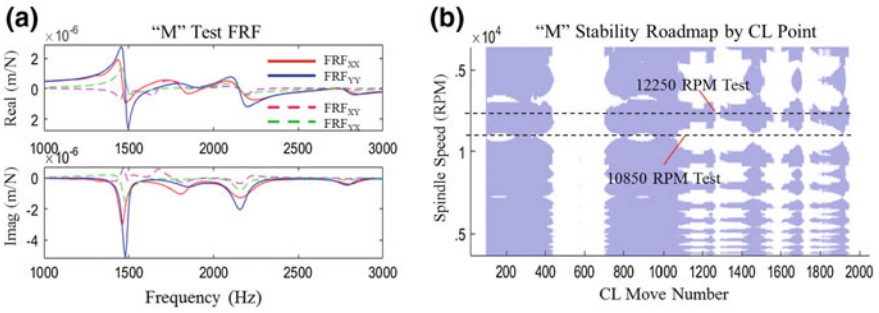

Fig. 4.12 Measured tool FRFs and resulting stability roadmap for "M" machining tests

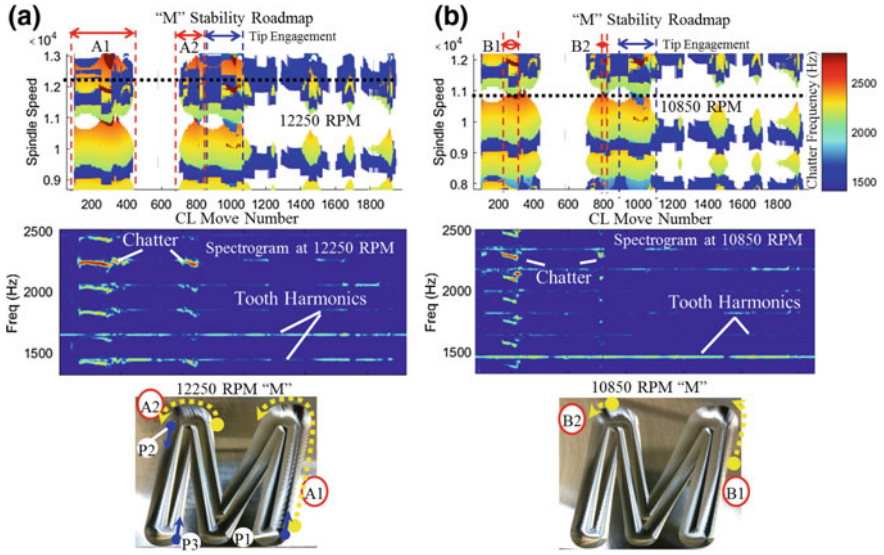

Fig. 4.13 "M" part stability roadmap, experimental sound spectrograms and part photos for 12,250 and 10,850 RPM

The 10,850 RPM test results (Fig. 4.13b) match the predicted chatter frequencies near 2300 Hz, and no chatter is observed near 1500 Hz. Predictions from the 10,850 rpm test are again most accurate for the first 850 CL points.

Both machined "M" parts are shown in Fig. 4.13 with locations of visible chatter on the part surface labelled. The CL points corresponding to the chatter locations are indicated both on the SRM and on the photos of the part for sections A1 and A2 at 12,250 RPM and B1 and B2 at 10,850 RPM. It can be seen that these chatter locations agree with the spectrogram measurements and SRM predictions for the first 850 points.

In both tests, the tool motion path begins at point P1 in Fig. 4.13 and follows the "M" path until it reaches point P2 (P2 corresponds the CL point 850). As the A and C axes positions are constant, the lead angle on the tool becomes negative from P2 to P3 and tip of the tool is engaged with the workpiece. One potential cause of chatter prediction errors starting at P2 is the indentation effects caused by tooltip engagement start at this point. This indentation effect, which results in underprediction of the stability, is not considered in this model.

4.3.3.2 Stability Roadmap Trial 2

The "M" stability trials presented some challenges for demonstrating the SRM concept, primarily due to tooltip engagement, and tracking errors in the feed speed of the machine tool which made it difficult to correlate simulated predictions to mea-

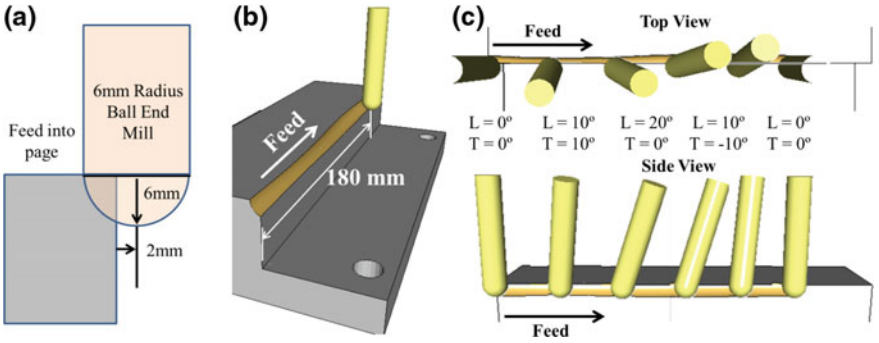

Fig. 4.14 Edge machining trial setup with no tip engagement, and continuously varying lead, tilt, and engagement

sured data. A second trial is designed in which a ball end mill machines the edge of the workpiece without engaging the tooltip, as shown Fig. 4.14a, b. As to the tool moves along the edge, the tool pivots about the tooltip, causing lead and tilt vary continuously (lead between 0° and 20°, tilt between −10° and 10°) as shown in Fig. 4.14c. The pivoting motion about the tooltip also creates continuous variation in the tool-workpiece engagement throughout the cut.

The second trial is conducted on a Starrag Ecospeed with data logging capability for the collection of true axis positions and spindle speeds throughout the cut. During the edge cutting trials, force measurements are collected using a Kistler 9139AA dynamometer. During the tests, the logged machine data and measured force data are synced so that force results can be tracked based on tool position. Further, the measured position data is applied directly to the stability model so that the stability predictions can be directly correlated to the measured force data. Note that the use of measured tool motion data does not change the SLM and is only used here to more easily compare simulation and measurement.

The CFCs used for the AL7075-T6 workpiece and the two-fluted 30° ball end mill with 6 mm radius (Sandvik R216.42-12030-AK22A H10F) are found experimentally to be: $K_{e,r} = 9.3$, $K_{e,t} = 0.4$, $K_{e,a} = 0.6$ N/mm, and $K_{c,r} = 452.4$, $K_{c,t} = 955.9$, and $K_{c,a} = 235.7$ N/mm^2 (also see "corner cut tests" in Table 4.1). Note that the CFC trials were repeated on the EcoSpeed with a new tool. Note that the tool used here is the same type but not the same tool used in the previous tests. New CFC tests are conducted with the current tool which better reflects the region of the tool used in the edge cutting trials, resulting in values which differ from the prior CFC tests.

Tool FRF measurements on the EcoSpeed showed symmetric dynamic behavior at the tooltip, with negligible cross FRFs at the tip compared with the same tool mounted to the FTV5 spindle. As such, only direct FRF measurements are used for stability prediction. However, some variation is observed in the FRF measurements before machining (but after spindle warm-up cycle) and after machining, as shown

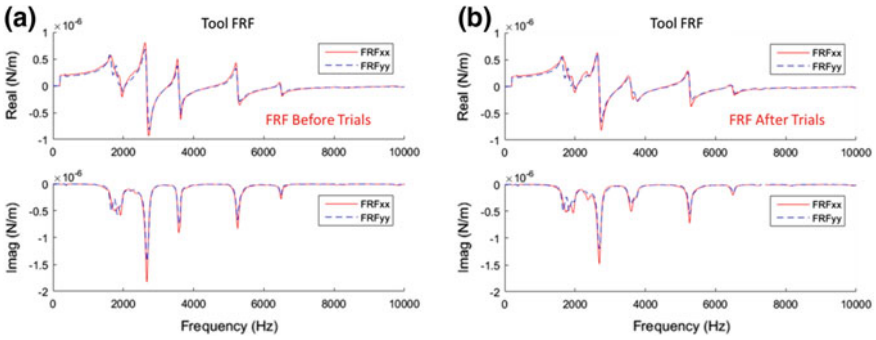

Fig. 4.15 Tool FRF measurements take **a** before the trials and **b** after the trials

in Fig. 4.15. These measurements were taken on the same day, with the same equipment and setup, but several hours apart. The primary difference is the reduction in amplitude of the 2700 Hz mode by approximately 20% in the post machining measurement. A result of this reduction is that the SRM predictions will change depending on which FRF is used. To account for this variability, SRMs are created using both FRFs and compared with the stability trial results.

During the trials, the edge machining operation is repeated 26 times at different spindle speeds. For each test, machine axis positions, spindle speeds, and measured force data are collected throughout the operation. The measured machine data is then applied directly to the simulation model to simulate the average forces and stability at each measurement step. The measured force data is used to verify the simulated average force data, as seen in Fig. 4.16a, and to determine the regions of chatter. A spectrogram of the Z-force data is used to determine stability, where peak amplitudes at the chatter frequency are compared with peak amplitudes of the tooth passing frequency. As shown in Fig. 4.16b, the system is considered unstable whenever the chatter frequency amplitude is greater than the tooth passing frequency amplitude, and stable otherwise. Note that Z-force data is used here because it has the smallest tooth passing frequency amplitude throughout the operation, making the distinction between chatter and stability more easily recognized using the current approach.

The process for determining stability in Fig. 4.16 is repeated for all machining trials, and the results are shown in Fig. 4.17 along with the predicted SRM using both sets of FRF measurements. The predicted and measured stability results are plotted based on the position of the tool. Tool position is used here because the cycle time of each test varies due to variations in feed rate to maintain a constant feed per tooth.

The results from Fig. 4.17 show that the stability regions do not line up exactly, as there is a shift in RPM between the predicted and measured stability regions. The cause of this shift is not known for certain; however, it is possible that this shift is a result of changes in the spindle dynamic parameters as a result of spindle speed. Despite these differences and the highly transient nature of this operation, the measured regions of stability of the corner machining example closely follow

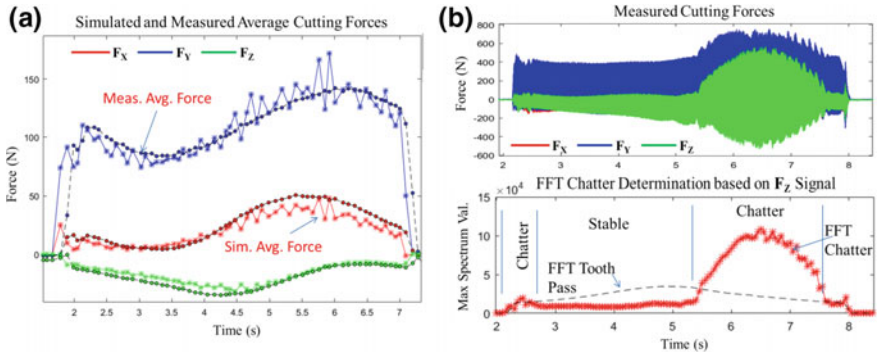

Fig. 4.16 Edge machining trial results: **a** simulated and measured average cutting forces throughout the operation and **b** use of force data to determine regions of chatter along the cut

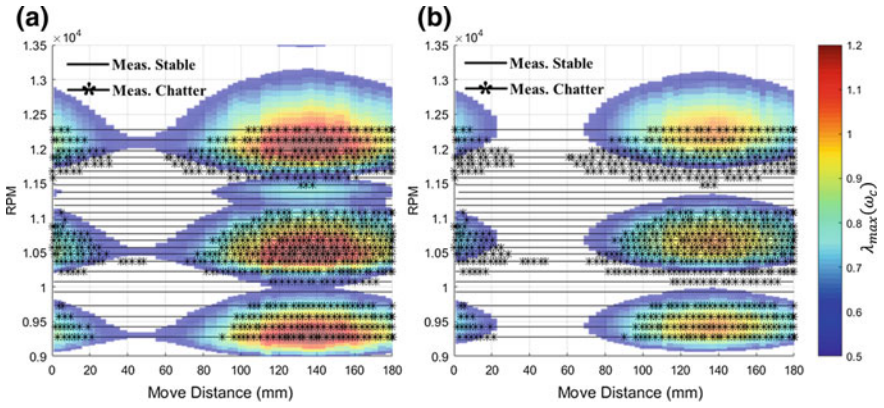

Fig. 4.17 SRM showing measured and simulated stability regions **a** using FRF measurements before the trials and **b** FRF measurements after the trials

the stability roadmap, and the chatter vibration amplitudes follow the qualitative predictions of the system eigenvalues.

Whereas the SRM was colored to represent predicted chatter frequency in the previous example, here, the SRM colors show the predicted maximum real eigenvalues of the system, $\lambda_{\max}(\omega)$. The use of $\lambda_{\max}(\omega)$ is useful for showing the predicted severity of the chatter. This is seen in Fig. 4.18 where the experimental chatter data is plotted with a third dimension, showing the ratio of the measured maximum chatter frequency amplitude, $\max(\text{Amp}(\omega_c))$, to the tooth pass frequency amplitude, $\max(\text{Amp}(\omega_t))$. It can be seen that the amplitudes of the chatter vibrations qualitatively follow the form of the eigenvalues, $\lambda_{\max}(\omega)$.

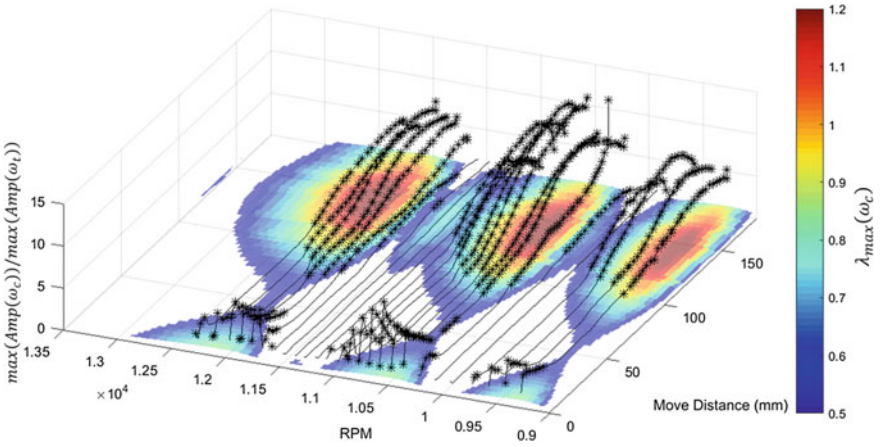

Fig. 4.18 Use of maximum eigenvalues, $\lambda_{\max}(\omega)$, to represent chatter severity compared with the measured tooth passing and chatter frequency ratios

4.3.4 Stability Roadmap Summary

The SRM provides an effective means of representing stability information for complex machining operations. Application of the zero-order approximation method to a discretized cutting force model allows for efficient stability prediction regardless of the engagement or the tool feed direction. When coupled with TWE simulation software, this approach can be used to represent the entire process virtually for a specific part program with a specific tool.

The experiments from this paper show that the SRM can accurately predict chatter locations, even with a tool with nonsymmetric direct FRFs and significant cross FRFs. However, the experimental results have shown that the current model is only effective when the tooltip center is not engaged in the cut.

Moving forward, the current SRM model can be expanded to include additional machining considerations, such as surface finish, surface location error, and workpiece dynamics.

4.4 Surface Location Error Model

During machining processes, cutting forces cause the tool to displace relative to the workpiece due to flexibility in the tool and/or workpiece. These relative displacements result in form errors in the part geometry, known as surface location errors (SLE). SLEs differ from chatter in that they are a result of periodic cutting forces (the forces calculated in the static cutting force module) and not regenerative effects. As such, SLEs are prevalent for both stable and unstable cutting conditions.

The prediction of surface location error has been made using various techniques in prior research. In these works, the motion of the tool in response to the cutting force is predicted, and this motion is imposed onto the rotating cutting edge to predict the true surface left behind. A closed form solution to predict SLE as a function of the tool FRF and forcing function is developed in [23]. Time domain simulations have also been used to predict tool motions in more complex cases, such as run-out [24], or 2-DOF milling dynamics [25]. Others used a truncated Fourier solution to determine tool motions based on modal parameters [26]. They then simulated the full 3D "morphed" cutting edge path, which then used to model the final machined surface.

Ozturk et al. [1] developed an approach for predicting form error for 5-axis ball end milling operations. Their approach predicts form error based simulation of static tool deflections, and these predictions were shown to closely agree with single point measurements in machining trials.

In this section, the strategy used to approximate SLE based on the discrete tool model is developed. This model is able to predict 5-axis SLE for complex tool geometries, tool/workpiece engagements, based on dynamic displacement and rotation of the tool. Cutting trials are conducted to compare predicted and measure SLE for a 5-axis ball end mill operation.

4.4.1 Form Error Prediction

Surface location error is predicted by first simulating tool displacements based on the cutting force profile and the system dynamic parameters. These displacements are combined with the rotary motion of the tool to model the true path of the cutting edge (helical or straight). The true cutting edge locations are compared with nominal (with no relative displacement) edge locations to determine the edge position error at each location of the tool.

These steps are shown in Fig. 4.19 for an example case. In Fig. 4.19a, the simulated tool displacements are shown which is based on the cutting force for the current operation and the frequency response function (FRF) of the tooltip.

Once the tool displacements are known, they are combined with the rotary motion of the cutting edge, as shown in Fig. 4.19b. With no tool displacements, the helical cutting edges nominally follow a path that forms a cylindrical shape. The addition of the tool vibrations causes the helical cutting edges to form a new shape, which represents the actual profile of the tool. By following the shape traced by the cutting edges, which is plotted with green points, the deviation of each point can be determined and the surface location error identified at each point of the tool. In the example in Fig. 4.19b right, the tool edge trace is oriented so that the tool is feeding out of the page, and the machined surface left behind is the leftmost side of the tool profile. Nominally, the tool removes material along the cylindrical shape, leaving behind the straight, blue edge. When vibrations are included, the resulting machined

surface is curved, resulting in overcut along the upper surface, and undercut at the lower surface.

In the current model, dynamic displacements are derived using a frequency domain solution. Compared with time domain simulation, the frequency domain approach is intended to be more efficient and robust. Further, this approach can be applied using system FRFs directly without the need to identify modal parameters, which is a requirement for time domain models. The frequency domain solution does not account for regenerative force effects which lead to chatter, so it is run under the assumption of stability (chatter is considered using a Stability Roadmap).

The process of determining the frequency domain solution is shown in Eqs. (4.25) through (4.27). The predicted force signal ($F(t)$ in Fig. 4.19) is first transformed to the frequency domain using the fast Fourier transform (fft in MATLAB) as shown in (4.25).

$$\begin{Bmatrix} F_x(\omega) \\ F_y(\omega) \\ F_z(\omega) \end{Bmatrix} = \text{FFT} \begin{Bmatrix} F_x(t) \\ F_y(t) \\ F_z(t) \end{Bmatrix} \tag{4.25}$$

Equation (4.26) is then used to solve for position in the frequency domain using the tool dynamic data (FRF(ω) in Fig. 4.19). The 3×3 FRF matrix in (4.26) allows for all direct and cross FRFs to be used when determining the tool response, although, typically only the diagonal, direct FRFs are nonzero. However, cross FRFs were used in the validation tests presented here due to their significant magnitudes.

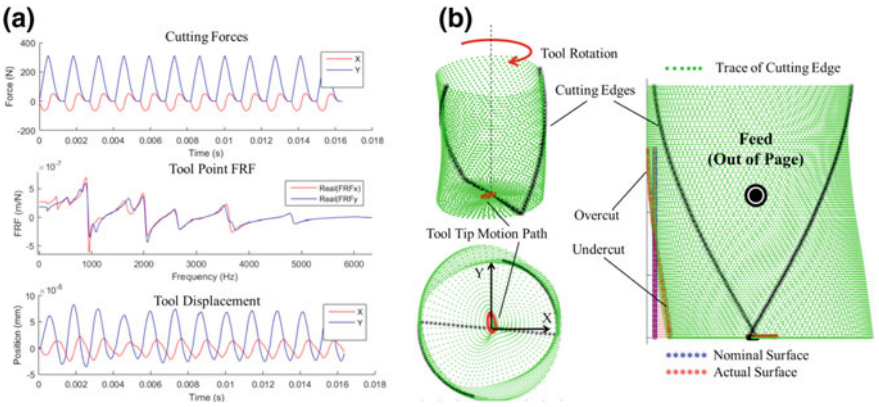

Fig. 4.19 **a** Cutting forces, tooltip FRFs, and resulting simulated tool displacements and **b** exaggerated depiction of surface location error prediction through cutting edge trace with superimposed rotation and vibration

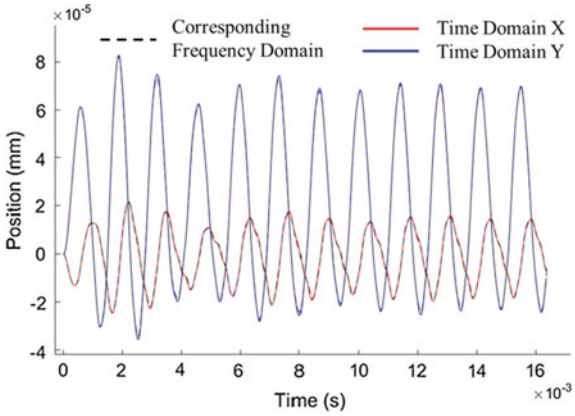

Fig. 4.20 Comparison of tool position prediction using both time domain simulation and frequency domain solution

$$\begin{Bmatrix} X(\omega) \\ Y(\omega) \\ Z(\omega) \end{Bmatrix} = \begin{bmatrix} \mathrm{FRF}_{xx}(\omega) & \mathrm{FRF}_{xy}(\omega) & \mathrm{FRF}_{xz}(\omega) \\ \mathrm{FRF}_{yx}(\omega) & \mathrm{FRF}_{yy}(\omega) & \mathrm{FRF}_{yz}(\omega) \\ \mathrm{FRF}_{zx}(\omega) & \mathrm{FRF}_{zy}(\omega) & \mathrm{FRF}_{zz}(\omega) \end{bmatrix} \begin{Bmatrix} F_x(\omega) \\ F_y(\omega) \\ F_z(\omega) \end{Bmatrix} \tag{4.26}$$

Finally, the resulting time response of the tool is obtained in (4.27) using the inverse fast Fourier transform (IFFT in MATLAB).

$$\begin{Bmatrix} X(t) \\ Y(t) \\ Z(t) \end{Bmatrix} = \mathrm{IFFT} \begin{Bmatrix} X(\omega) \\ Y(\omega) \\ Z(\omega) \end{Bmatrix} \tag{4.27}$$

The resulting time response obtained using the frequency solution is compared with time domain simulation results in Fig. 4.20. It can be seen that even though regenerative effects are ignored, the results are nearly identical using either method. The advantage of the frequency domain solution is that solutions are obtained more quickly, and determination of modal parameters it is not required. Note that this process is only valid for stable cutting conditions, and the results will differ if unstable. As such, this approach should be used in combination with the stability roadmap to ensure that the process is stable.

4.4.2 Surface Location Error Calculation

The tool position response is simulated over multiple cycles to increase the likelihood that the vibrations are in steady state. Once in steady state, the motions from a single tooth passing period are needed to model the tool motion. At each step of the tooth period, the instantaneous displacement of the tool is used to determine the

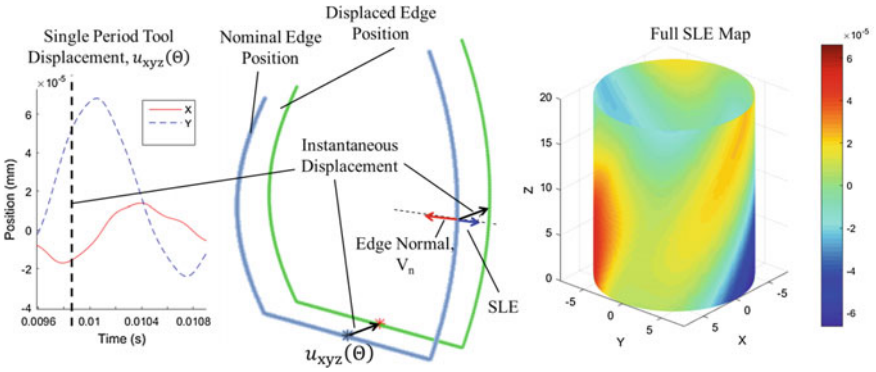

Fig. 4.21 Process of calculating SLE from tool displacements

error at the cutting edge location at that rotation angle. The process is illustrated in Fig. 4.21, starting with a single period of the tool motion. Each point in time of the tools' motion corresponds to a tool rotation position, and this displacement is applied to the cutting edge at that angle. As SLE is measured from the normal of the part surface, the SLE of each element along the cutting edge is determined by projecting the displacement vector, u_{XYZ}, onto an edge normal vector, V_n, as shown in Eq. (4.28). The resulting SLE is then recorded for that element on the cutting edge in that rotational position. This process is then repeated for each point of the tool rotation cycle. Once completed, the SLE data is represented tool mesh element using a color scale, as shown in Fig. 4.21.

$$\text{SLE}_{el(\Theta,L)} = V_{n,el(\Theta,L)} \cdot u_{xyz}(\Theta) \tag{4.28}$$

The full SLE map in Fig. 4.21 shows the SLE of each element of the tool mesh; however, we are only concerned with tool elements which are both engaged in the workpiece and are also located along the section of the tool which leaves behind a machined surface. These requirements are shown in Eq. (4.29), where engagement is determined with $g(\Theta, L)$, and "surface forming" elements are identified by projecting the feed vector, f_{XYZ}, onto the surface normal vector. This projection gives a value proportional to the chip thickness, and it is assumed that engaged elements which have zero chip thickness are machining at locations where a machined surface is left behind. Since the tool mesh is discrete, it is unlikely to find a calculated chip thickness of exactly zero, so a minimum value is set to identify elements close to the surface formation region. A summary of the process used to identify surface forming elements for predicting SLE of the machined surface is shown in Fig. 4.22.

$$\text{Surface Element if: } g(\Theta, L) = 1 \;\&\; V_{n,el(\Theta,L)} \cdot f_{xyz} < \text{MinVal} \tag{4.29}$$

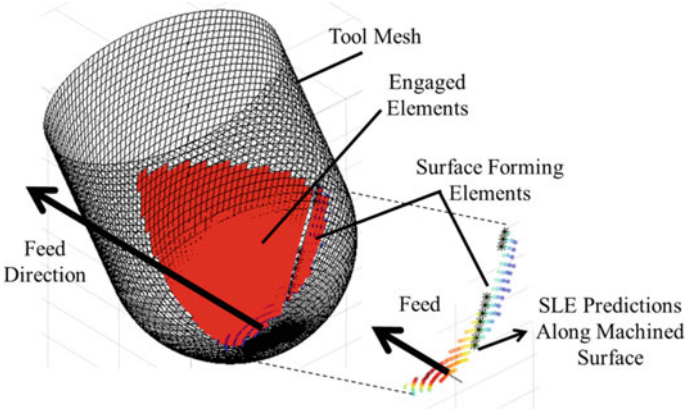

Fig. 4.22 Process of identifying surface forming elements of the tool mesh used to predict SLE on the machined surface

4.4.3 Surface Location Error Trials

The SLE model is tested using a grooving operation with a ball end mill with a constant lead and tilt. The trials are run at different spindle speeds and depths of cut, and the resulting measured groove surfaces are compared with simulated surface shapes. For each set of cutting conditions, the machined surface is simulated by predicting the path of the tool cutting edges as they rotate and vibrate simultaneously, as shown in Fig. 4.23a. Note that only elements that are both engaged in the cut, and are on the edge of the tool profile when looked at in the feed direction, are used to predict the surface left behind (see elements indicated in Fig. 4.23a).

Figure 4.23b shows both the nominal surface (with no vibrations) and the simulated surface with vibrations. From this view, the simulated surface is offset from the nominal surface by the surface location error (SLE) values which are predicted for each element based on the cutting edge trace.

Since we are comparing error results at many points along the simulated part surface, a best fit error approach is used to characterize surface errors. As the nominal shape of the ball end mill machined grooves is circular, circular fit errors are used.

Once a simulated surface is obtained, a circle is fitted to the simulated surface points (see best fit circle in Fig. 4.23b), and best fit errors are determined for each point (see in Fig. 4.23c). Even though SLE errors from the nominal surface are simulated directly, the best fit error approach allows for the simulated surface shape to be evaluated independently of a known reference (i.e., the nominal surface). This is useful for comparing simulated surface errors to the measured surface errors, which do not have an easily obtainable absolute reference. Both the simulated and experimental surfaces are evaluated using the same process based on a best fit circle.

A 12-mm-diameter ball end mill with two flutes and helix angle of 30° (Sandvik R216.42-12030-AK22A H10F) is used for this trial. The tool is mounted using a

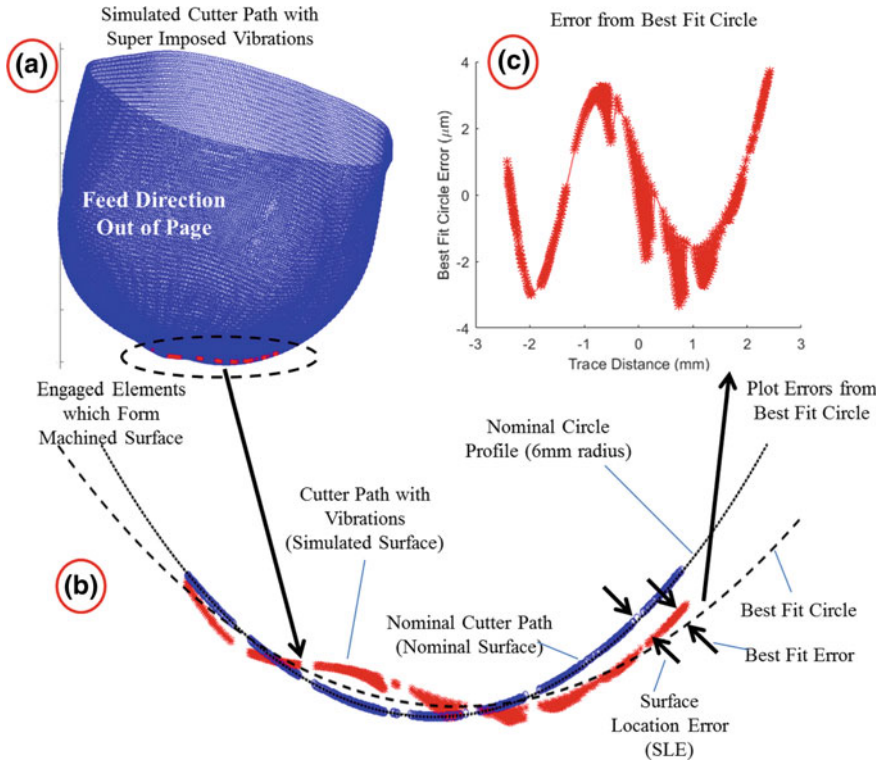

Fig. 4.23 Process used to measure simulated surface errors with tool vibrations

Bilz ThermoGrip T1200/HSKA63 tool holder with a tool overhang of 67.2 mm. The machine used for the tests is a MAG FTV5-2500, and force measurements are collected using a Kistler 9139AA dynamometer. The workpiece material is AL 7075 T6 and PTFE nylon. The CFCs used for the AL7075-T6 workpiece are found experimentally using a ball end mill mechanistic model [11], to be: $K_{e,r} = 7.43$, $K_{e,t} = -2.98$, $K_{e,a} = -2.7$ N/mm, and $K_{c,r} = 128.35$, $K_{c,t} = 965.49$, and $K_{c,a} = 85.34$ N/mm^2 (also see "corner cut tests" in Table 4.1). Note that average CFC values identified experimentally are used for all elements regardless of local oblique and rake angles.

During the trials, the ball end mill machines straight grooves on an aluminum and nylon workpiece. Two materials are used which have very different cutting force coefficient (CFC) values so that the resulting surface can be compared with equal cutting conditions, but different forces. Each test cut is run with a fixed feed, spindle speed, lead, tilt, and cut depth. A summary of the test conditions is shown in Table 4.2, and an image of the test block is shown in Fig. 4.24a.

After the tests, an Alicona Infinite Focus G5 is used to measure the shape of the machined grooves. This machine and an example of a surface produced during the

Table 4.2 Summary of cutting conditions for SLE experiments

Test #	Feed/tooth (mm)	Spindle speed (RPM)	Lead (Degrees)	Tilt (Degrees)	Cut depth (mm)
1	0.15	13,050	15	15	0.5
2	0.1	13,050	15	15	0.5
3	0.15	20,800	15	15	0.5
4	0.1	20,800	15	15	0.5
5	0.15	13,050	15	−15	0.5
6	0.1	13,050	15	−15	0.5
7	0.15	20,800	15	−15	0.5
8	0.1	20,800	15	−15	0.5
9	0.15	13,050	15	15	1
10	0.1	13,050	15	15	1
11	0.15	20,800	15	15	1
12	0.1	20,800	15	15	1
13	0.15	13,050	15	−15	1
14	0.1	13,050	15	−15	1

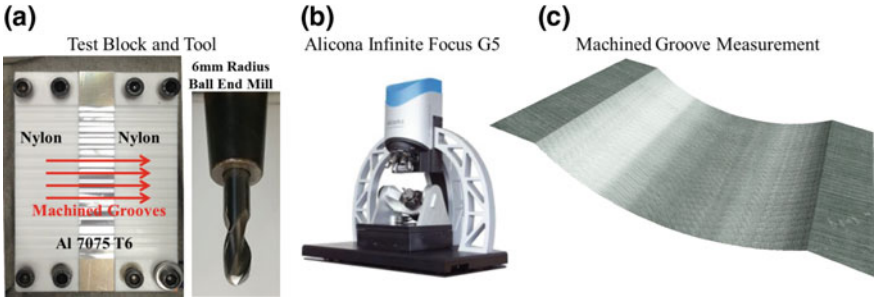

Fig. 4.24 Alicona Infinite Focus G5 and an example groove surface measurement

measurement are shown in Fig. 4.24b, c. Surface data generated in these measurements are used to characterize the true form of the grooves. As they are all machined with a 6 mm radius ball end mill, the nominal surface generated should also have a circular form with a radius of 6 mm.

To measure the true form, virtual traces are taken on the surface data measured on the Alicona. This process is shown in Fig. 4.25, where two traces are collected, providing the true form of the groove at two locations. The trace data is then compared with a simulated surface produced by simulating the tool vibrations as it cuts.

The measured and simulated surfaces are analyzed using the same process to determine the SLE in each. First, a circle is fitted to the measured and simulated surfaces, each circle having a best fit center point and radius. In Fig. 4.26, the resulting best fit radii are shown for the simulated and measured surfaces for all 14 tests. Note

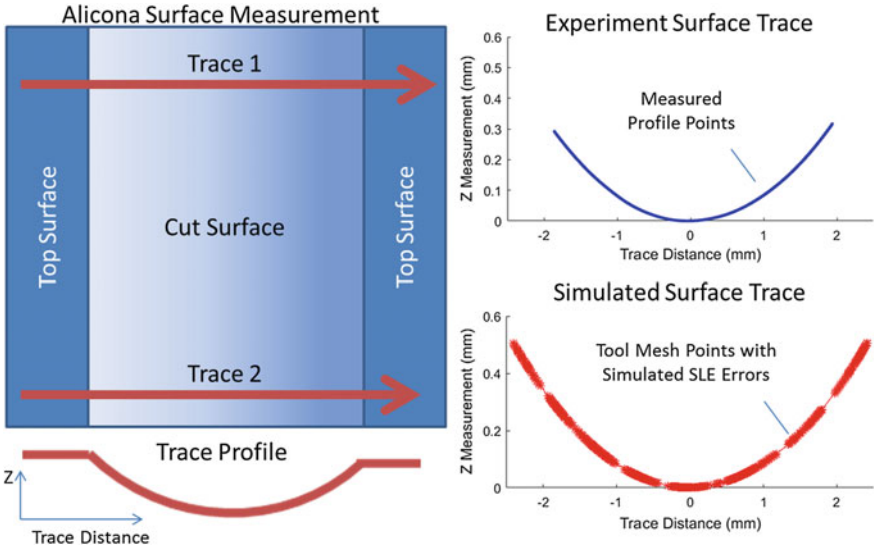

Fig. 4.25 Process of extracting surface profile traces from Alicona measurements, which are then compared with simulated surface traces

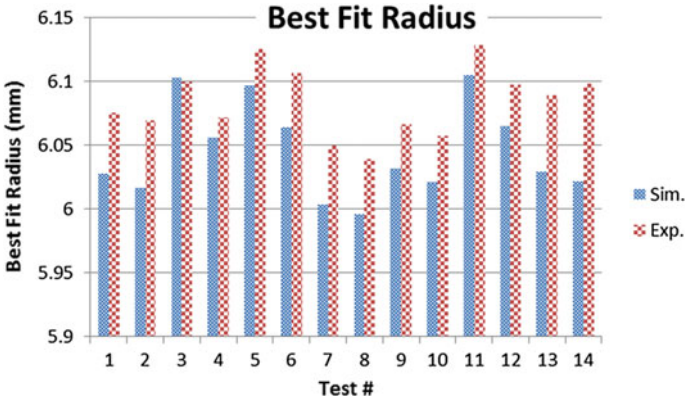

Fig. 4.26 Best fit radii of simulated and measured aluminum surfaces

that the fitting routine only considers points along machine groove, which represent only a small portion of the full 12 mm diameter circle, causing the best fit radii to be sensitive. Despite this, the resulting best fit radii closely follow the same trend for both the simulated and measured surfaces, although the measured surfaces appear to consistently have a larger radius, approximately 50 μm greater than the simulated surface. This difference may be due to errors in the actual tool geometry, such as run-out, errors in the measurement, part vibrations, or other machine errors which are out of scope of the current simulation model.

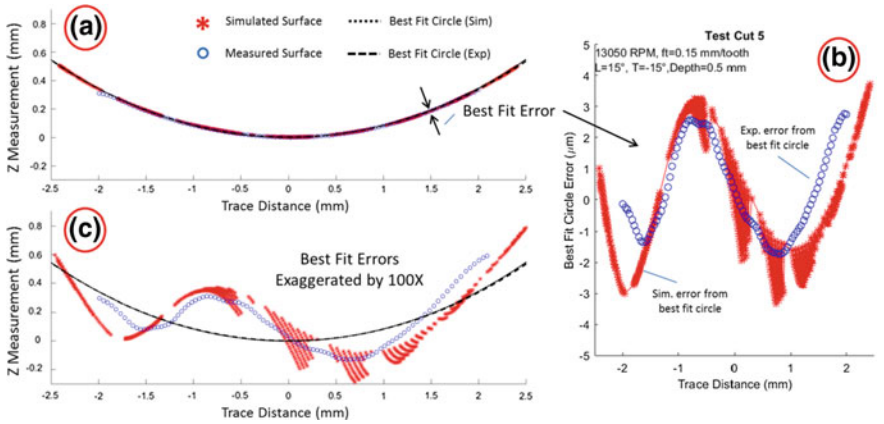

Fig. 4.27 Illustration of how profile errors are measured from a best fit circle for both the simulated and measured aluminum surfaces

One challenge for SLE experiments is determining an absolute reference from which to measure the errors in the true surface. For example, it is difficult to define the nominal center of the tool from which to compare the measured surfaces. For this reason, the best fit circles are used as a reference to measure errors for both simulated and measured surface data.

Once best fit circles are found for the simulated and measured surfaces, the deviation of each point along the surface from its respective best fit circle is set as the best fit error for that point. In Fig. 4.27a, the points of both surfaces are plotted along with the best fit circles. The errors are recorded along the trace direction, resulting in the best fit error plots shown in Fig. 4.27a. The best fit errors can then be exaggerated to represent the shape of the machined surfaces, as shown in Fig. 4.27c. It can be seen in this exaggerated view that both the simulated and measured surfaces deviate from the best fit circle in roughly the same general form for this current example.

This process is followed for each test, and the resulting errors are shown in Fig. 4.28. It can be seen that errors in the simulated surface closely trend with the errors on the measured surface, especially in the 13,050 RPM, 0.5 mm depth tests (Tests 1–5). Chatter also had an effect on the results (chatter is not considered in the simulated surfaces). When chatter is severe (Tests 9 and 10) the surface errors deviate greatly, however, for light chatter (Tests 11 through 14), the errors still trend closely, although there is additional waviness in the measured surface.

Both aluminum and nylon are machined during the tests. The purpose of this is to compare the surfaces when there is a significant difference in the cutting forces acting on the tool. For these tests, the mean forces acting on the tool are approximately 10 times greater during the aluminum sections. As a result, the steady-state vibration amplitudes which lead to SLE are expected to reduce by a factor of 10 while cutting nylon. Due to the inability to generate full measurements for the nylon surfaces (the Alicona could not measure the full sample due to surface lighting issues), we do not

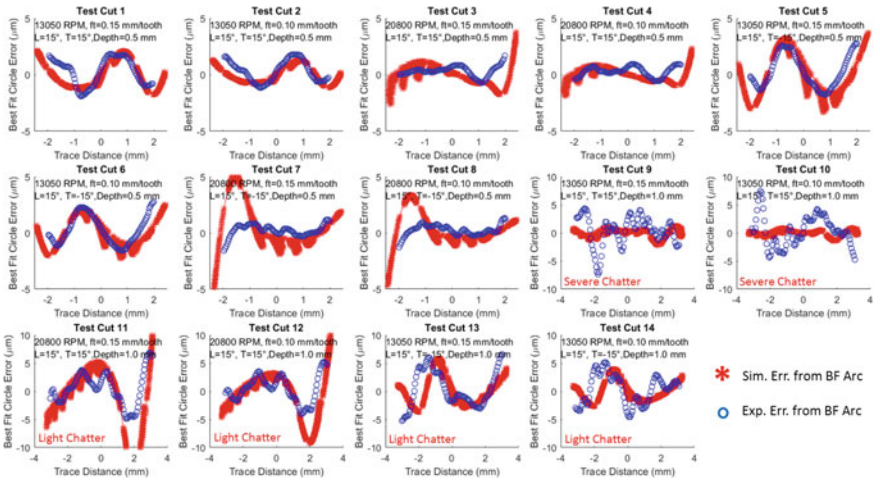

Fig. 4.28 Comparison between best form errors for measured and simulated surfaces

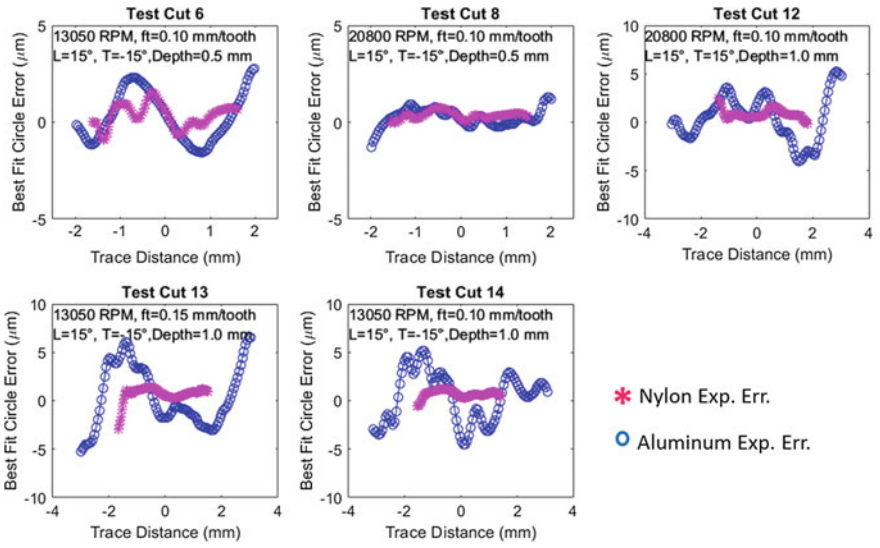

Fig. 4.29 Comparison of measured form errors for the aluminum and nylon sections

have analysis on all nylon surfaces yet. In Fig. 4.29, the partial data from the nylon samples is analyzed, and the errors are compared with the aluminum surface errors. These results indicate a significant decrease in error in the nylon surface, as would be expected with reduced cutting force. However, this result is only an indication, and data from more complete nylon measurements should be analyzed to fully validate this result.

The results from these tests show that the SLE model can provide a good indication of surface error for simple 5-axis operations using a ball end mill.

4.5 Process Model Simulation Interface

The process models discussed in this chapter have been developed in MATLAB. In order to make use of these models accessible to Twin-Control partners, a MATLAB graphical user interface (GUI) has been developed. The GUI contains all of the process models, and the interface allows users to execute any or all of the models from a single setup. This section describes the basic features of the Twin-Control process model GUI.

4.5.1 Process Model GUI Layout, Inputs and Options

An image of the process model GUI is shown in Fig. 4.30 with all of the key sections labelled. Upon launch, the user is first prompted to select a project folder which contains all of the process data for the current application. This project folder should contain the following items:

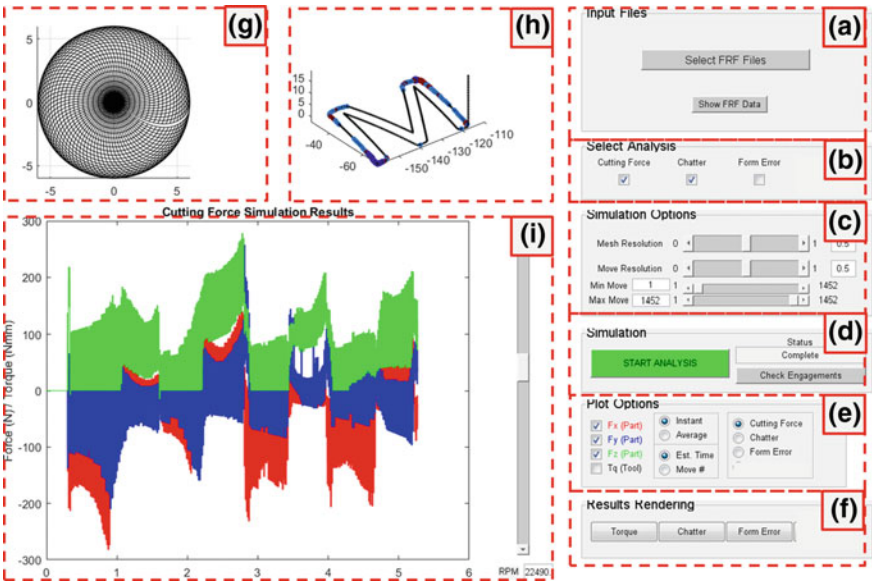

Fig. 4.30 Process model GUI developed to run process model code in MATLAB

- A database of tool geometries used (*.csv file),
- A database of cutting force coefficients used (*.csv file),
- An *.stl file of the stock part geometry (must be geometry before machining operation),
- A part program file containing tool motion and tool number data.

Once a project folder is selected, the data is processed and the tool geometry and programmed toolpath are shown in the GUI environment. At this point, the user has several options to control the simulation. The following lists show the function of each section of the GUI as labelled in

A. Users can select FRF files for up to ten tools used in the part program. The FRF data for all tools is plotted when the user selects "Show FRF Data".
B. The user selects which models to run during the simulation.
C. The user can control the resolution of the tool mesh and the tool path resolution at which all analysis is performed (analysis is performed at fixed distance points along the toolpath, and not an every CL point). The user can also select which section of the part program to analyze based on CL move number using Max/Min Move.
D. Once options are set, the user selects "Start Analysis" to start the simulation. During simulation, the status of the simulation is updated in the "Status" box. Once the simulation is complete, the user has the option to view all tool/workpiece engagements along the toolpath by selecting "Check Engagements".
E. After simulation, the results can be plotted based on the selections in the box. Forces and torques can be plotted as tool rotation angle dependent, or as average values over one revolution. They can be plotted against simulated time or against CL move number. Finally, the type of analysis results can be selected.
F. Selections in this box show the results rendered against the toolpath instead of time (see next section for examples).
G. Shows a plot of the tool mesh resolution and geometry.
H. Plot of simulation results against toolpath.
I. Main display window used during simulation setup and to show simulation results.

4.5.2 Process Model GUI Outputs

When the simulation analysis is completed, the results are stored in an output file for analysis. An example of the data stored and replotted for one simulation is shown in Fig. 4.31. The average forces and torques are first shown against the simulated time. The remaining results are plotted along the toolpath so that results correspond to specific locations on the part geometry. The average force magnitudes and torques are plotted first, where the color scales correspond to the simulated values. From this example, peak force and torque loads occur at the outer corners of the "M" structure. The results for chatter and SLE are also plotted along the toolpath. These

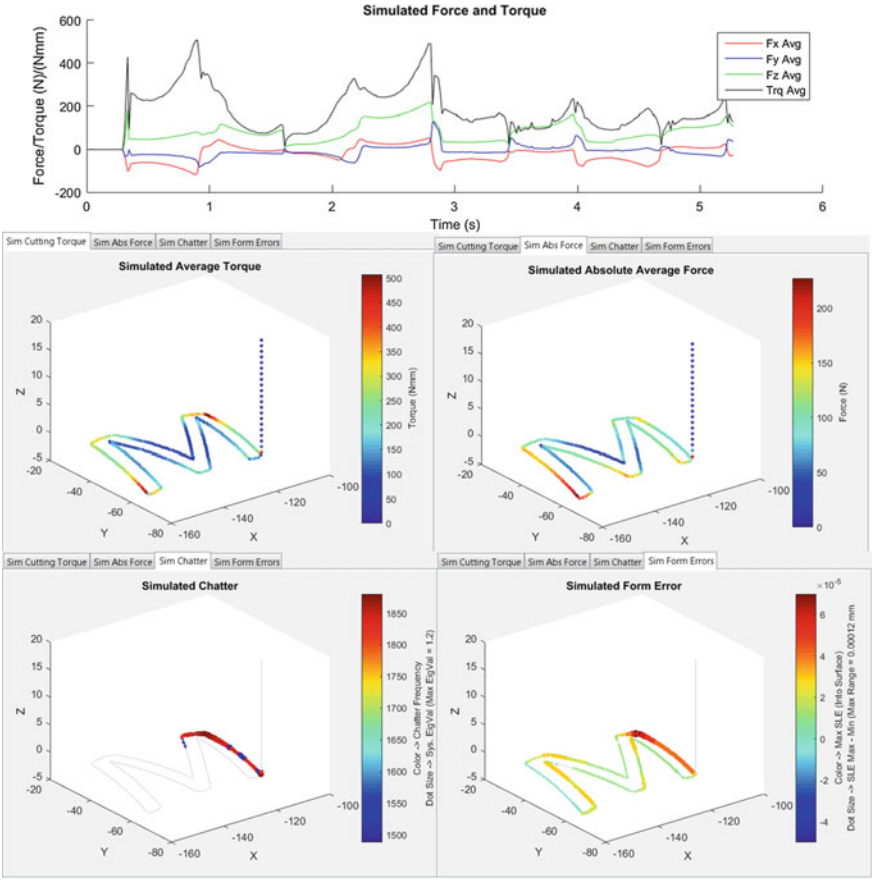

Fig. 4.31 Outputs of AMRC process model GUI, showing simulated force, torque, chatter, and surface location errors graphically on the part geometry

results are represented by both a color scale and dot size. For chatter results, the color indicates the predicted chatter frequency along the toolpath, and the dot size indicates the system eigenvalue along the toolpath, which correlates to the severity of chatter predicted (no dot indicates no predicted chatter). The color scale of the SLE data represents the maximum SLE value calculated within the surface generation section of the tool, and the dot size represents the range of SLE values over the surface generation section.

The method of display for the results in Fig. 4.31 is intended to allow process planners to quickly and easily interpret simulation data for a specific process. These results concisely show what issues may appear during the part program, and where they will occur on the part geometry.

4.6 Conclusions

The process models developed to model interactions between the tool, and the workpiece provide important predictions about the final outcome of an operation. The models developed here are all based on a discrete tool cutting force model which provides flexible and efficient solutions for complex machining operations. It has been shown through validation testing that these models are capable of predicting force and torque, as well as chatter and surface location error. By combining all of these separate model components into a single environment, we can efficiently simulate and view results for complex operations in a concise format. We will see in the following chapters how this system has been used to improve example machining operations from both the automotive and aerospace industries.

Acknowledgements This chapter is based on the publication at Procedia CIRP (Volume 58, 2017, Pages 445–450) of the work "Discrete Cutting Force Model for 5-Axis Milling with Arbitrary Engagement and Feed Direction" presented by Luke Berglind, Erdem Ozturk and Denys Plakhotnik at the 16th CIRP Conference on Modelling of Machining Operations (https://www.sciencedirect.com/science/article/pii/S221282711730433X).

References

1. Ozturk, E., Budak, E.: Modelling of 5-axis milling processes. Mach. Sci. Technol. **11**(3):287–311 (2007)
2. Budak, E., Ozturk, E., Tunc, L.T.: Modelling and simulation of 5-axis milling processes. Mach. Sci. Tech. (2007)
3. Lazoglu, I., Boz, Y., Erdim, H.: Five-axis milling mechanics for complex free from machining. CIRP Ann. Manuf. Technol. **60**, 117–120 (2011)
4. Boz, Y., Rdim, H., Lazoglu, I.: Modeling cutting forces for 5-axis machining of sculptured surfaces. In: 2nd International Conference, Process Machine Interactions (2010)
5. Layegh, S., Erdim, H., Lazoglu, I.: Offline force control and feedrate scheduling for complex free form surfaces in 5-axis milling. In: CIRP Conference on High Performance Cutting (2012)
6. Taner, T.L., Ömer, Ö., Erhan, B.: Generalized cutting force model in multi-axis milling using a new engagement boundary determination approach. Int. J. Adv. Manuf. Technol. **77**, 341–355 (2015)
7. Kim, G., Cho, P., Hu, C.: Cutting force prediction of sculptured surface ball-end milling using Z-map. Int. J. Mac. Tools Manuf. **40**, 277–291 (2000)
8. Boess, V., Ammermann, C., Niederwestberg, D., Denkena, B.: Contact zone analysis based on multidexel workpiece model and detailed tool geometry representation. In: 3rd CIRP Conference on Process Machine Interactions (2012)
9. Erkorkmaz, K., Hosseinkhani, A.K.Y., Plakhotnik, D., Stautner, M., Ismail, F.: Chip geometry and cutting forces in gear shaping. CIRP Ann. Manuf. Technol., 133–136 (2016)
10. Siebrecht, T., Kersting, P., Biermanna, D., Odendahla, S., Bergmann, J.: Modeling of surface location errors in a multi-scale milling simulation system using a tool model based on triangle meshes. In: CIRPe 2015—Understanding the Life Cycle Implications of Manufacturing (2015)
11. Gradisek, J., Kalveram, M., Weinert, K.: Mechanistic identification of specific force coefficients for a general end mill. Int. J. Mach. Tools Manuf. **44**, 401–414 (2004)
12. Altintas, Y., Weck, M.: Chatter stability of metal cutting and grinding. CIRP Ann. Manuf. Technol. **53**(2), 619–642 (2004)

13. Altintas, Y., Budak, E.: Analytical prediction of stability lobes in milling. CIRP Ann. Manuf. Technol. **44**(1), 357–362 (1995)
14. Insperger, T., Mann, B., Stépán, G., Bayly, P.: Stability of up-milling and down-milling, part 1: alternative analytical methods. Int. J. Mach. Tools Manuf. **43**(1), 25–34 (2003)
15. Mann, B., Bayly, P., Davies, M., Halley, J.E.: Limit cycles, bifurcations, and accuracy of the milling process. J. Sound Vib. **277**(1), 31–48 (2004)
16. Campomanes, M.L., Altintas, Y.: An improved time domain simulation for dynamic milling at small radial immersions. ASME J. Manuf. Sci. Eng. **125**, 416–422 (2003)
17. Altintas, Y., Engin, S.: Generalized modeling of mechanics and dynamics of milling cutters. CIRP Ann. Manuf. Technol. **50**(1), 25–30 (2001)
18. Ozturk, E., Budak, E.: Dynamics and stability of five-axis ball-end milling. J. Manuf. Sci. Eng. **132**, 1–13 (2010)
19. Gong, X., Feng, H.: Cutter-workpiece engagement determination for general milling using triangle mesh modeling. J. Computat. Des. Eng. **3**(2), 151–160 (2016)
20. Ozkirimli, O., Tunc, L., Budak, E.: Generalized model for dynamics and stability of multi-axis milling with complex tool geometries. J. Mater. Process. Technol. **238**, 446–458 (2016)
21. Budak, E., Tunc, L., Alan, S., Özgüven, H.: Prediction of workpiece dynamics and its effects on chatter stability in milling. CIRP Ann. Manuf. Technol. **61**(1), 339–342 (2012)
22. Schmitz, T.L., Smith, K.S.: Machining Dynamics, Frequency Response to Improved Productivity. Springer Science, New York, NY (2009)
23. Schmitz, T.L., Mann, B.P.: Closed-form solutions for surface location error in milling. Int. J. Mach. Tools Manuf. **46**, 1369–1377 (2006)
24. Schmitz, T.L., Couey, J., Marsh, E., Mauntler, N., Hughes, D.: Runout effects in milling: Surface finish, surface location error. Int. J. Mach. Tools Manuf. **47**, 841–851 (2007)
25. Insperger, T., Gradisek, J., Kalveram, M., Stepan, G., Winert, K., Govekar, E.: Machine tool chatter and surface location error in milling processes. J. Manuf. Sci. Eng. **128**, 913–920 (2006)
26. Bachrathy, D., Insperger, T., Stepan, G.: Surface properties of the machined workpiece. Mach. Sci. Technol. **13**, 227–245 (2009)

Chapter 5
Towards Energy-Efficient Machine Tools Through the Development of the Twin-Control Energy Efficiency Module

Dominik Flum, Johannes Sossenheimer, Christian Stück and Eberhard Abele

5.1 Introduction

Energy efficiency issues have played an increasingly important role in society, business and politics in recent years. Above all, noticeable environmental impacts are one reason for this. This increases customer awareness and introduces additional legal regulations. As a very large proportion of global primary energy demand is caused by the manufacturing industry, this represents a great lever for reducing energy demand and the associated emissions [1]. Furthermore, energy is an increasingly important cost factor. This results in high customer demand for energy-efficient machines.

Studies have shown that 26% of operating costs of a machine tool are caused by energy costs for machine tools—excluding labour, tooling and material costs [2]. As energy prices continue to rise in the foreseeable future, the importance of the energy efficiency factor will play a greater role alongside the classic dimensions of precision, performance and reliability [3, 4].

D. Flum (✉) · J. Sossenheimer · C. Stück · E. Abele
PTW TU Darmstadt, Darmstadt, Germany
e-mail: d.flum@ptw.tu-darmstadt.de

J. Sossenheimer
e-mail: j.sossenheimer@ptw.tu-darmstadt.de

C. Stück
e-mail: info@ptw.tu-darmstadt.de

E. Abele
e-mail: info@ptw.tu-darmstadt.de

M. Armendia et al. (eds.), *Twin-Control*,
https://doi.org/10.1007/978-3-030-02203-7_5

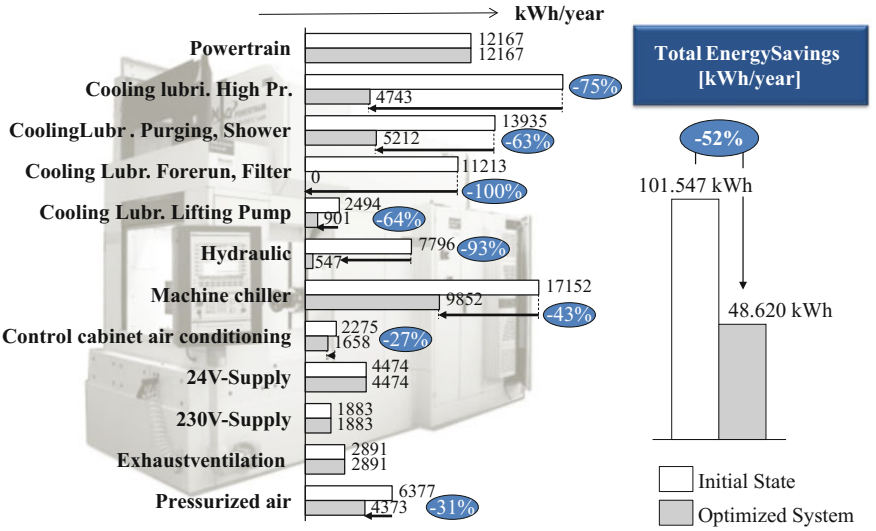

Fig. 5.1 Realized energy-saving measures on a machine tool of the type MAG XS211 [5]

5.1.1 Energy Efficiency of Production Machines

Many different approaches to increasing energy efficiency in production technology have already been investigated. One example of this is the research project "Maxiem—maximizing the energy efficiency of machine tools". The project results show the potential and possibilities with regard to energy efficiency optimization in machine tools. Various measures for component-oriented optimization and evaluation of energy efficiency were carried out using a MAG XS 211 four-axis machining centre as an example. By analysing the energy consumption of individual components, the actual delivery status of the machining centre was determined. Most of the energy was consumed by the machine cooling system, the cooling lubricant system and the hydraulic system. Based on the assumption of mass production with a three-shift operation and six working days per week, 50% of the energy could be saved through the use of an energy-optimized configuration (Fig. 5.1) [5].

5.1.2 Scope of Investigation

The measures to optimize the energy efficiency of metal-cutting machine tools are manifold. The optimization measures can generally be classified according to the overview in Fig. 5.2. According to this, an increase in the energy efficiency of machine tools can be achieved by [6]:

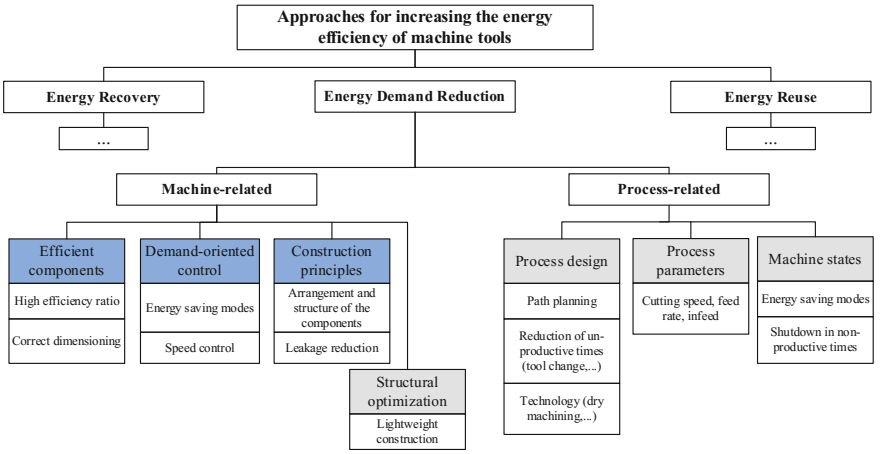

Fig. 5.2 Investigated approaches to increase energy efficiency (marked in blue) (see [3])

- Recovery of the energy used,
- Reuse of energy,
- Reduction of energy demand.

The research activities in the Twin-Control project focused on reducing the energy demand. This is basically the key step in optimizing energy efficiency, as it also reduces the energy loss such as waste heat. The measures used are not intended to influence the productivity of the machining process. Therefore, the optimization of the machine tool itself was investigated. Starting points in general are [6, 7]:

- Use of efficient components with higher efficiency,
- Implementation a demand-oriented control by (partially) switching off modules when not in use,
- Design of the machine modules by applying energy-efficient construction principles.

When considering the design of the assemblies, oversizing and "safety surcharges" that are frequently encountered, especially when designing pumps and motors, should be avoided. This results in the components no longer running at their optimum operating point, which in turn has a negative effect on energy efficiency [7].

Standby operation, which means switching off or activating an energy-saving mode for modules or components when they are not in use, also reduces the energy consumption of metal-cutting machine tools [8]. This is achieved, for example, by implementing energy management functions on the machine control whereby certain modules are switched off either after a time defined by the user or after completion of the part program [9].

Due to different operating states and varying process parameters, such as tool change, spindle speed and feed rate, different types and frequencies of loads act on the machine tool assemblies. The operation of the components can be adapted to the

different performance requirements by process-adapted and demand-oriented control of motors and pumps by means of speed control using a frequency converter. Often pumps in machine tools are operated at mostly constant speed whereby the flow rate is adapted to the current demand by a throttle or bypass control [7, 10]. In load cases where a component is operated at a constant operating point, speed control is energetically disadvantageous. The efficiency losses of the frequency inverter during speed control would lead to deterioration in energy efficiency [11]. A further optimization option is the use of efficient components with improved efficiency. Examples of components with high energy-saving potential are pumps, electric motors or cooling units [7].

5.2 Theoretical Background

Existing scientific approaches for both approximation and simulation of the energy requirements of machines and production processes are presented below.

5.2.1 Machine Simulation and Process Modelling

Reeber [12] developed an approach in the field of cutting machine tools that enables the calculation of the specific cutting energy. The basis is an empirical model of cutting force developed by [13]. This makes it possible to determine the cutting force depending on different material and process parameters [12, 13]. The calculations only take into account the energy required for the cutting process, not the total energy consumption of the machine [3].

Degner and Wolfram [14] presented an approach that complements the approach of [12] to the additional energy demand of the machine tool. For this purpose, electrical measurements of reactive power in the air cut formed the basis (all units enabled, no tool contact) [3, 14–18].

A first observation of the energy consumption of a machine tool in non-production times was made by [19]. His assumption was constant power consumption with stationary machine axes [19].

Another similar approach was developed by Gutowski et al. [20]. This is based on electrical power measurements on various machine tools. The energy demand of the process-specific component is calculated from a base load and the process load. The machining load was determined by various milling tests with different removal rates, while the base load is assumed to be constant [20, 21].

Draganescu et al. [22] evaluate the energy efficiency of machine tools by analysing the energy effectiveness, which is defined as the ratio of theoretical cutting energy to total energy demand. Using statistical methods and empirical data, a mathematical model was developed that maps the ratio of different operating parameters, such

as torque, feed rate and spindle speed in order to approximate the specific power consumption of a machine tool [22, 23].

Dietmair et al. [24] used an empirical model based on graph theory to predict the energy demand of cutting machine tools. A specific electrical power demand was set for each machine component according to the current machine mode. If the duration and the order of the individual machine modes are specified, the power consumption and the energy demand of the individual components can be determined. The result is the energy demand of the entire machine [3, 24–27].

The approach of [24] was extended by [28]. He assigned a certain power and time demand to the transition between different machine modes. However, both approaches neglect dynamic effects. Each machine mode is assigned to a single power consumption [28].

Schrems [29] developed an approach based on a dynamic simulation to predict the energy demand of various production processes and machines. For this purpose, production machines contained in a process chain are represented by generic models. Datasheet information is used to parameterizing the models that can be used to determine the energy demand of certain configurations. Eventually, the energy demand can be taken into account when planning process chains and selecting alternative production machines [29].

5.2.2 Energy Demand Approximation of Production Machines

Kuhrke [7] developed a methodology for a prospective assessment of the medium and energy demand that can already be used in the offer phase of machine tools. Therefore, a foundation for machine tool manufacturers, as well as for operators for a coherent evaluation of the energy and medium demand, is provided. The basis for this is the analysis of a sample machine, in which he developed calculation rules for each energy-relevant component. This was based on information from datasheets and data gained by measurements if the required information in the datasheets was insufficient. Finally, by aggregating the individual demands, the total energy consumption of the machine tool can be calculated [7].

Another approach emerges from Bittencourt [30]. He presented a prediction model for the energy demand of machine tools. Electrical power measurements on different modules under different operating conditions of the production machine serve as a basis. For modules with process-dependent power consumption, further test series were carried out under various load conditions. Subsequently, a characteristic curve model was developed using spline curves, which enables the calculation of energy consumption depending on the production task [30].

5.2.3 Summary

In contrast to many of the previous work, the approach presented below is not dependent on energy measurements on existing production machines. On the one hand, electrical power measurements are often unsuitable in a production environment because they are associated with increased effort and high costs, as the execution of the measurements is time-consuming, and production may have to be stopped. In addition, measurements cannot usually be used in the planning phase of a product or production due to a lack of physical components. The energy efficiency module of Twin-Control, however, supports the machine design by dimensioning and selecting components according to the prevailing needs using mainly datasheet information.

5.3 The Energy Efficiency Module

The energy efficiency module of Twin-Control aims to support machine tool builders within the machine design phase to choose an energetically optimal machine configuration. In addition, the simulation tool enables part manufacturers to guarantee an energy-efficient part production considering different NC Code alternatives. For establishing energy efficiency measures, a machine tool builder or user needs, in the first place, information about the possible energy efficiency measures. Secondly, a systematic and transparent decision-making process is necessary to evaluate several energy efficiency measures. These prerequisites will be accomplished by the energy efficiency module.

5.3.1 Framework

The energy efficiency module is intended to act as a platform between developers and users in order to promote the implementation of energy efficiency solutions through increased transparency of the energy demand.

The core of the energy efficiency module is the simulation models. Those models are established in the simulation software MATLAB/Simscape and will be discussed in Chap. 4. For parameterizing the simulation models, input from machine tool user and machine tool builder is employed. Hardware information needs to be provided, especially by the machine tool builder. This information is used to parameterize the developed component simulation models to a specific machine tool. The energy demand of a machine tool, however, is not only determined by its hardware but also by its production task. The production task can be divided into three dimensions (Fig. 5.3).

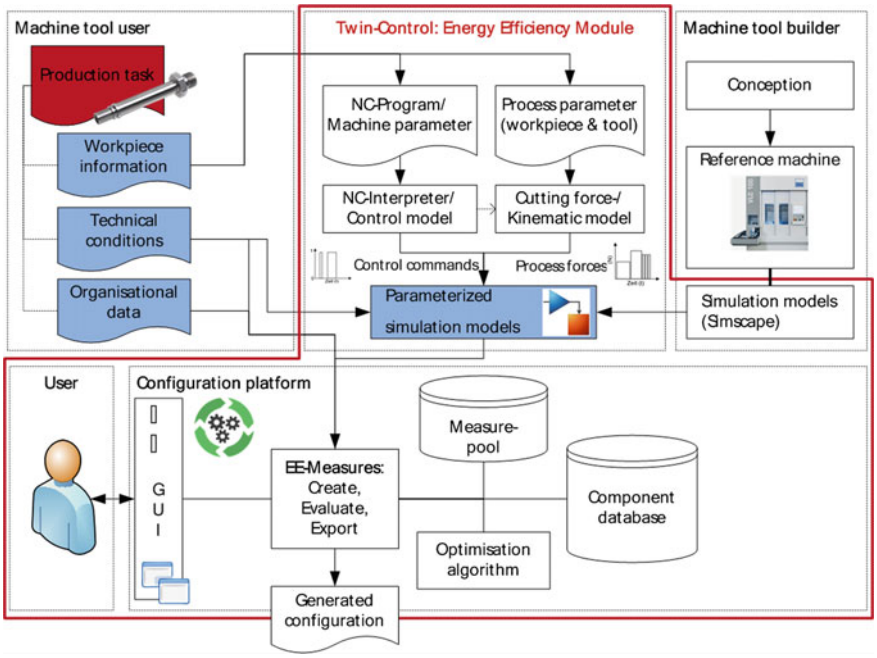

Fig. 5.3 Framework of the energy efficiency module

- Workpiece information: the component information includes the part to be produced, which is described by the NC program and related information, such as material and tool parameters.
- Technical conditions: this includes a variety of technical information.
  - Production environment: ambient conditions (temperature, vibration, etc.).
  - Technological requirements: required production processes, flexibility of machine, quality requirements.
  - Infrastructure: options to subscribe for compressed air, existing cooling/filtration systems, energy networks in buildings and other production machines and chip removal.
- Organizational data: The organizational data include company-specific information to the parent production environment, which go beyond the technical information. These include, inter alia, production hours per year, the price of electricity and the basic proportions of the machine conditions (production, standby, off). These data form the basis of the balance between energy efficiency and cost aspects.

The design of the energy efficiency module follows a tripartite model–view—controller (MVC) approach with the following features.

- Module database: the modules are held in the form of strategies for energy efficiency measures.

- Configuration algorithm: the algorithm creates configurations based on modules. The creation and review are automated.
- Input and output mask: visualization supports the configuration process.

5.3.2 Key Elements

The key elements of the energy efficiency module are briefly described below. Since the energy simulation models make up the essential part, they are discussed separately in this chapter.

- Energy efficiency measure pool: the basic approaches to energy efficiency improvements are collected in a measure pool. These approaches represent templates for energy efficiency measures that can be taken into account for the configuration.
- Measure creation: To apply an energy efficiency measure, it must first be created or configured. Since measures can only be performed on the basis of an existing basic configuration, it is important to create them if they do not exist as intended. During measure creation, the templates from the energy efficiency measure pool are linked to the conditions and requirements defined by the machine tool user. For individual measures, components are pre-selected from a database, which then represent configuration alternatives. This enables the optimization algorithm to perform an action automatically. If a measure is to be applied to several machine assemblies, it is created separately for each assembly. Assemblies that are not considered are initially treated as black boxes, which can be detailed by additional measures.
- Component database: the component database includes a plurality of components of different types. For each component, the required information such as datasheet specifications and list prices are stored. Since the creation of the database is associated with a comparatively high cost, it is created project and machine independent and is permanently available.
- Optimization algorithm: the optimization algorithm performs a measure by using mathematical optimization methods and a system of rules for an automated selection of a suitable configuration. An essential component is the quantitative review of alternatives as a guide for the selection. The alternative with the best value is then added to the project.
- Energy efficiency project: the project is a collection of already defined measures and thus shows the current configuration status. In order to offer the user control and modification possibilities of the optimization algorithm, there is a detailed view of existing measures.
- Configuration result: The generated configuration is a collection of measures. To make them available outside the platform, they must first be prepared. This includes, e.g. a collection of parts lists or datasheets based on the selected alter-

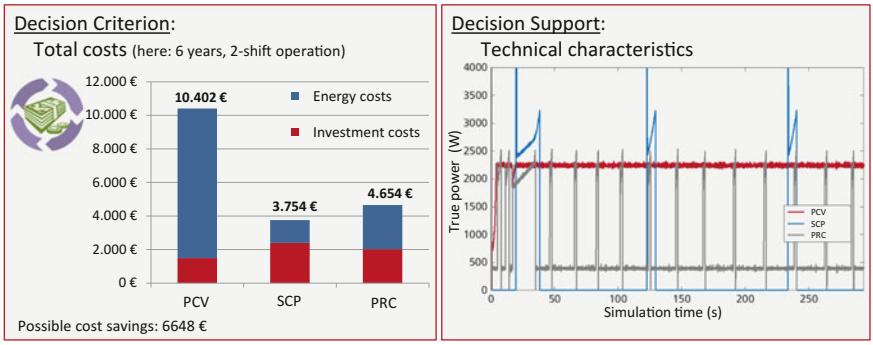

Fig. 5.4 Exemplary results of the configuration platform

natives. There should be an additional check of the configuration by an expert staff.

- Graphical user interface (GUI): a graphical user interface guides the operator in using the configuration platform. The elements, such as measure creation and solution selection are provided with dialogues, through which the user can perform inputs.

An exemplary application of the configuration platform is shown in Fig. 5.4, in which three different configuration options for a hydraulic system are compared. Basically, the three marketable variants are a pressure control valve (PCV), a speed controlled pump (SCP) and a pressure reduced circulation (PRC). Using an optimized configuration allows possible cost savings of up to 6648 € under the assumption of an investigation period of 6 years and a two-shift operation.

5.4 Energy Simulation of Machine Tools

A popular approach in order to predict the behaviour of production machines is the use of simulation models. According to [31], simulation can generally be applied for technical systems within every lifecycle phase: during product development, the predicted system behaviour can be verified; in the use phase, potential changes to the utilization profile or retrofit measures can be evaluated in advance [23, 31]. In order to forecast and simulate the energy consumption of machine tools, dynamic models of various components were set up. Those models represent the core of the configuration platform (Fig. 5.3). Through modelling all components relevant to the energy demand and the energetic interconnectivity, all functional modules of a production machine are set up. Besides electrical energy, all other energy types are taken into account influencing the electric behaviour (e.g. hydraulic and mechanical energy). The simulation model is implemented within the software environment MATLAB/Simscape.

5.4.1 Basic Principle

The presented simulation approach covers the relevant mechanisms for calculating the energy demand of production machines. In general, the simulation structure distinguishes between three model layers (compare to Fig. 5.5) [3]:

Process Layer (NC Code Interpreter)

Within the process layer, the interaction between the workpiece and the tool is mapped. Cutting force calculations, as well as tool engagement estimations, are performed in this part of the simulation model. Through transforming the calculated cutting forces into torque on the main spindle as well as forces on the feed drives, the load on the drive system of the production machine can be predicted.

Machine Layer (Machine Simulation)

Every functional module relevant to the energy demand of a production machine is mapped in the machine layer. Depending on the available datasheet information of the component manufacturer, physical/mathematical interrelationships and characteristic curves/maps are used for setting up the simulation models. Besides fixed component parameters, the model behaviour depends on dynamic interactions on functional module level, process-dependent loads from the process layer and control commands generated by the control layer.

Control Layer (Model Control)

The control layer represents the physical machine control of a production machine. Using input data of the process layer, speed for feed and spindle drives, as well as switching information of peripheral systems, are provided for the machine layer.

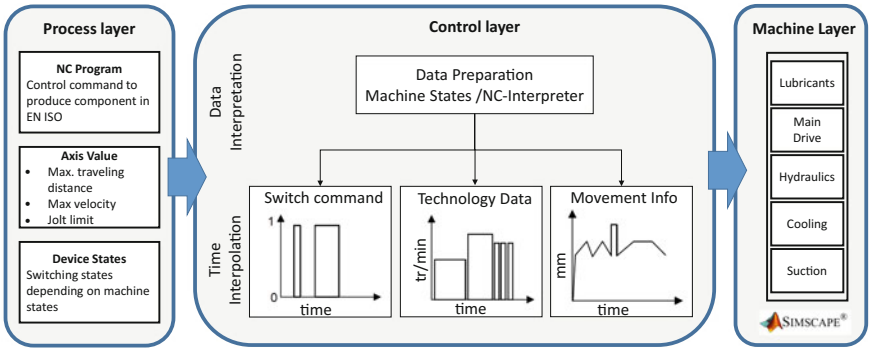

Fig. 5.5 Basic concept of the (physical) energy simulation models (see [3])

5.4.2 *Modelling the Machine Tool Components*

The simulation models are implemented within the software environment MATLAB/Simscape. It is an extension for Simulink, which makes an object-oriented modelling of physical systems possible. Unlike Simulink, physical components can be modelled using a Simscape-specific programming language. There are already some libraries of basic building blocks, such as electrical resistors. Since they can only be used to a limited extent for the purpose of the project, own components have been developed.

With the help of this library, machine assemblies can be easily mapped. Manufacturer information such as fluid or electrical plans is used for this purpose. The parameterization of the component models is carried out via datasheets. This results in a simple adaptability to different applications (Fig. 5.6).

A concrete model is built up from the individual components, which are taken from the Twin-Control library and then linked to each other. It is possible to orientate

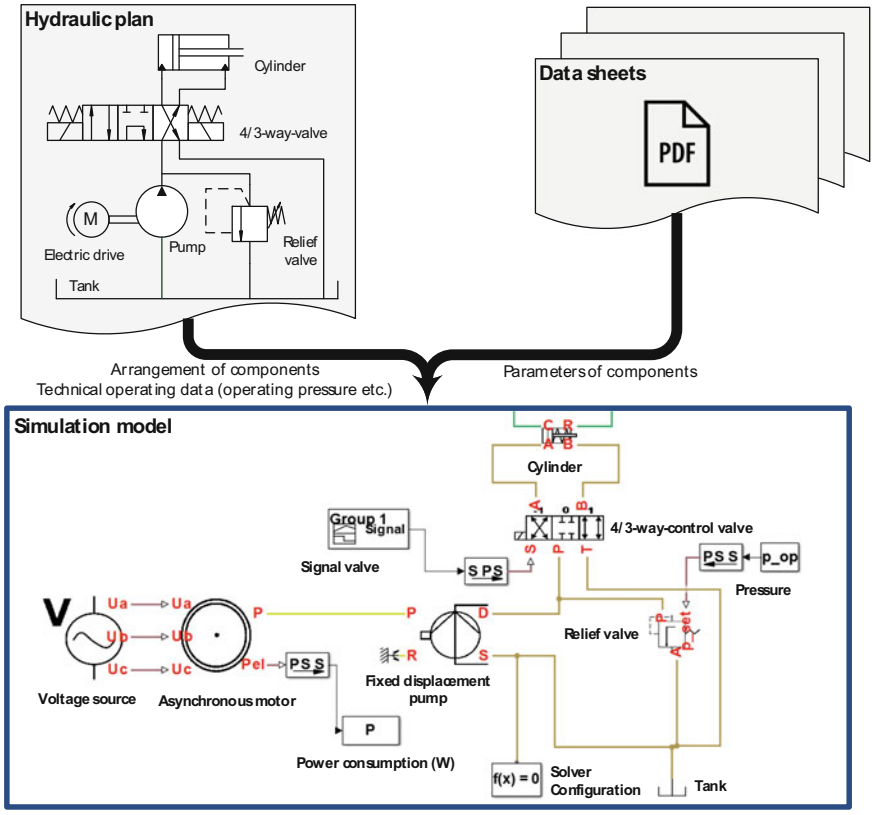

Fig. 5.6 Method of modelling using the example of a hydraulic system (schematic)

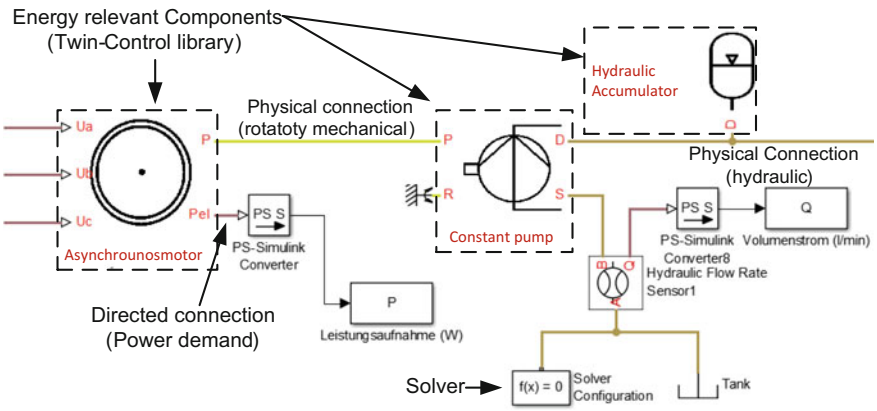

Fig. 5.7 Elements of a model with the methodology used by the example of a hydraulic system

oneself on the "real" machine, e.g. using the fluid diagram of the machine to be mapped. Generally, all required input data can be obtained from datasheets and the NC program. Measurements are not required.

The individual blocks are interconnected by means of non-directional physical connections to a network. The connections are in a physical domain (e.g. mechanics or hydraulics), which can also be recognized by the colour of the connection. In addition, there are directed physical connections (signals) which are used, for example, to reuse individual physical quantities outside the network. Each network also contains a solver block. In addition, all Simulink blocks can be used in the same model. For a connection with the Simscape blocks, their signal must be converted using a special "converter" block (Fig. 5.7).

Using this modelling approach, the level of detail is particularly high and allows the technical behaviour to be checked down to individual parts (valves, pumps, etc.). All energy-relevant assemblies can be modelled, including the drivetrain with dynamic effects.

5.5 Implementation on EMAG VLC100Y Turning Machine

As an exemplary application, the modelling and simulation of an EMAG VLC100Y turning machine are presented in this chapter. The machine is part of the Twin-Control pilot line ETA Factory. To validate the models, the electrical power consumption was measured and compared with the simulated values (Fig. 5.8).

For the measurements, a mobile measurement device was used. It consists of three measuring cases which are either connected via LAN or WiFi. With each case, it is possible to measure four consumers. The machining process of the use case consists

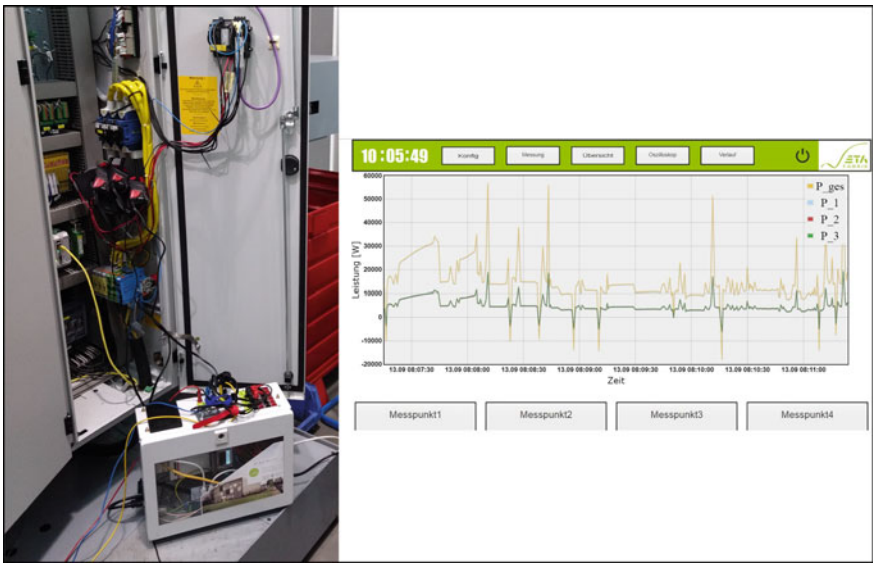

Fig. 5.8 Electric Power Measurement with mobile measurements device on the EMAG VLC 100Y turning machine

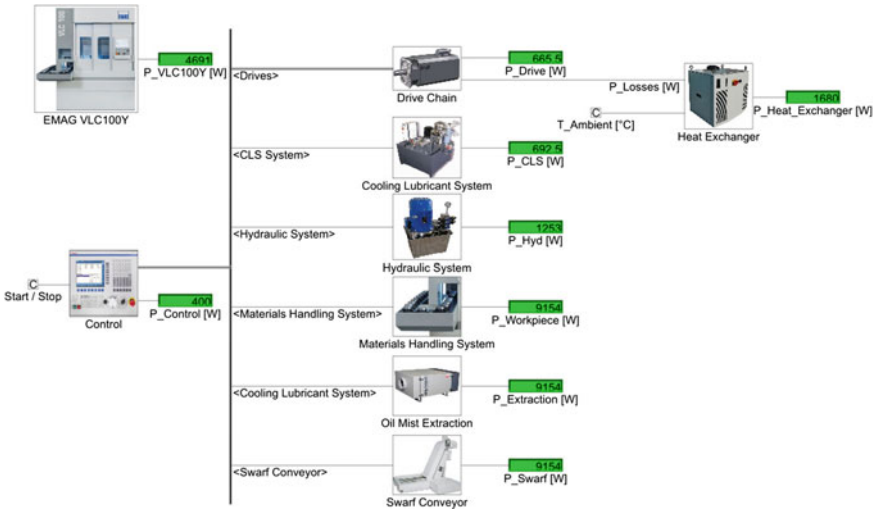

Fig. 5.9 Simulation models with energy-relevant subsystems of EMAG VLC100Y

of two sub-processes (OP10 and OP20). Further, the power consumption in standby and operational was considered (Fig. 5.9).

For a comparison of measurement and simulation data see Table 5.1. Here, the average power consumption in the different machine states is displayed. Especially

Table 5.1 Comparison of measurement and simulation data

	Standby measurement Ø [W]	Standby simulation Ø [W]	Ready measurement Ø [W]	Ready simulation Ø [W]	Work measurement Ø [W]	Work simulation Ø [W]
Main connection (machine)	443	438	3292	3283	6069	5911
Drive units	0	0	485	472	1669	1509
Cooling unit	0	0	1560	1405	1560	1405
Hydraulic pump	0	0	411	430	433	475
CL pump	0	0	0	0	1313	1461
Chip Conveyor	0	0	0	0	82	80
Suction	0	0	0	0	99	105
Others	443	438	836	876	913	876

for consumers with a more constant power consumption (e.g. chip conveyor and suction), the predicted values are quite close to the measurement data. For components with a more dynamic behaviour like the drive units, the deviation is a bit higher. However, the maximum deviation for the average power consumption is less than 10%. As a result, the applicability of the simulation models for predicting the energy consumption in planning phases could be demonstrated.

5.6 Conclusions

The energy demand of machine tools is largely determined in the development phase. This is why the largest levers for increasing energy efficiency are located here. The energy efficiency module of Twin-Control was developed as a planning tool for implementing energy-efficient machine tool configurations. The development of simulation models of all energy-relevant components creates the necessary transparency regarding the energy demand. By coupling with an optimization algorithm, the module automatically searches for the cost optimal configuration under the specified boundary conditions and restrictions. In addition to the investment costs of the components used, the energy costs for the prevailing electricity price are determined from the simulation. A graphical user interface ensures a high user friendliness by allowing user input to be made and results to be evaluated without having to go deeper into the simulation models.

The implementation of the simulation in the pilot line ETA Factory showed that a forecast of the energy demand is feasible with the presented approach.

References

1. IEA International Energy Agency: Worldwide Trends in Energy Use and Efficiency. IEA Publications, Paris (2008)
2. Abele, E., Dervisopoulos, M., Kuhrke, B.: Bedeutung und Anwendung von Lebenszyklusanalysen bei Werkzeugmaschinen. In: Schweiger, S. (ed.) Lebenszykluskosten optimieren. Gabler, Wiesbaden (2009)
3. Eisele, C.: Simulationsgestützte Optimierung des elektrischen Energiebedarfs spanender Werkzeugmaschinen. Shaker Verlag, Aachen (2014)
4. BDEW Bundesverband der Energie- und Wasserwirtschaft.: Energiewirtschaftliche Entwicklung in Deutschland. 1. Quartal 2013, Berlin (2013)
5. Abele, E., Sielaff, T., Beck, M.: Konfiguration energieeffizienter Werkzeugmaschinen. In: Werkstattstechnik online: wt, vol. 102, pp. 292–298 (2012)
6. Zein, A., Li, W., Kara, S.: Energy efficiency measures for the design and operation of machine tools: an axiomatic approach. In: Hesselbach, J. (ed.) Glocalized Solutions for Sustainability in Manufacturing. Proceedings of the 18th CIRP International Conference on Life Cycle Engineering, pp. 274–279 (2011)
7. Kuhrke, B.: Methode zur Energie- und Medienbedarfsbewertung spanender Werkzeugmaschinen. epubli, Berlin (2011)
8. Zäh, A., Niehuis, K.: Wieviel Energie verbraucht eine Werkzeugmaschine? In: fertigung. Das Fachmagazin für die Metallverarbeitung, pp. 30–32 (2009)
9. Denkena, B., Garber, B. (ed.).: NC-Plus. Prozess- und wertschöpfungsorientiert gesteuerte Werkzeugmaschine; Final report. PZH-Verl; TEWISS - Technik-und-Wissen-GmbH, Garbsen (2013)
10. Gontermann, D.: Drehzahlregelung reduziert Energiekosten und steigert die Betriebssicherheit. MM Maschinenmarkt 38–41 (2007)
11. de Keulenaer, H., et al.: Sparsame elektrische Antriebe (2004)
12. Reeber, R.: Der Energiebedarf bei trennenden Fertigungsverfahren. Werkstatt und Betrieb **113**, 109–113 (1980)
13. Kienzle, O., Victor, H.: Spezifische Schnittkräfte bei der Metallbearbeitung. Werkstofftechnik und Maschinenbau **47**, 224–225 (1957)
14. Degner, W., Wolfram, F.: Richtwerte und Regeln für den Energieaufwand bei spanender Fertigung. Fertigungstechnik und Betrieb **33**, 739–742 (1983)
15. Degner, W., Herfurth, K.: Energieaufwand bei spanender Teilefertigung. Fertigungstechnik und Betrieb **33**, 684–687 (1983)
16. Degner, W., Resch, R., Wolfram, F.: Energieaufwand spanender Fertigungsverfahren und das Prinzip der vergegenständlichten Energie in der Teilefertigung. Metallverarbeitung **83**, 132–134 (1984)
17. Wolfram, F.: Aspekte der energetischen Bewertung von Produkten und Prozessen der Abtrenntechnik nach dem Prinzip der vergegenständlichen Energie. Dissertation, Karl-Marx-Stadt (1986)
18. Wolfram, F.: Energetische produktbezogene Bewertung von Fertigungsprozessen. Dissertation, Chemnitz (1990)
19. Schiefer, E.: Ökologische Bilanzierung von Bauteilen für die Entwicklung umweltgerechter Produkte am Beispiel spanender Fertigungsverfahren. Darmstädter Forschungsberichte für Konstruktion und Fertigung (2001)
20. Gutowski, T., Dahmus, J., Thiriez, A.: Electrical energy requirements for manufacturing processes. In: The International Academy for Production Engineering (CIRP) (Hrsg.) Proceedings of the 13th CIRP International Conference on Life Cycle Engineering, pp. 623–627 (2006)
21. Gutowski, T., et al.: A thermodynamic characterization of manufacturing processes. In: International Association of electronics recyclers (Hrsg.) Proceedings of the 2007 IEEE International Symposium on Electronics & Environment, pp. 137–142 (2007)
22. Draganescu, F., Gheorghe, M., Doicin, C.: Models of machine tool efficiency and specific consumed energy. J. Mater. Proc. Technol. **141**, 9–15 (2003)

23. Abele, E., Braun, S., Schraml, P.: Holistic simulation environment for energy consumption prediction of machine tools. In: 22nd CIRP Conference on Life Cycle Engineering in Sydney, Australia, 7–9 April 2015
24. Dietmair, A.: Energy consumption assessment and optimisation in the design and use phase of machine tools. In: The International Academy for Production Engineering (CIRP) (ed.) Proceedings of the 17th CIRP International Conference on Life Cycle Engineering (2010)
25. Dietmair, A., Verl, A., Wosnik, M.: Zustandsbasierte Energieverbrauchsprofile – Eine Methode zur effizienten Erfassung des Energieverbrauchs von Produktionsmaschinen. In: wt Werkstattstechnik online, vol. 98, pp. 640–645 (2008)
26. Dietmair, A., Verl, A.: Energy consumption forecasting and optimisation for tool machines. Mod. Mach. (MM) Sci. J. 4 (2009)
27. Dietmair, A., Verl, A., Huf, A.: Automatisierung spart Energie – Direkte und indirekte Maßnahmen in der Gerätetechnik. In: Energy 2.0, p. 26 (2009)
28. Bittencourt, J.L.: Selbstoptimierende und bedarfsgerechte Steuerungsstrategien für Werkzeugmaschinen zur Steigerung der Energieeffizienz. Apprimus, Aachen (2013)
29. Schrems, S.: Methode zur modellbasierten Integration des maschinenbezogenen Energiebedarfs in die Produktionsplanung. Shaker Verlag, Aachen (2014)
30. Rief, M.: Vorhersagemodell für den Energiebedarf bei der spanenden Bearbeitung für eine energieeffiziente Prozessgestaltung. Shaker, Aachen (2012)
31. VDI Verein Deutscher Ingenieure: Simulation von Logistik-, Materialfluss- und Produktionssystemen(3633). Beuth Verlag GmbH, Berlin (2013)

Chapter 6
New Approach for Bearing Life Cycle Estimation and Control

Eneko Olabarrieta, Egoitz Konde, Enrique Guruceta and Mikel Armendia

6.1 Introduction

Machine tools are usually composed by several main elements with relative movements among them. In order to minimize friction losses, different types of bearing technologies have been applied: sliding contact, rolling, hydrostatic, aerostatic and magnetic. Among them, rolling technology has the leading position due to the best combination of performance, cost and reliability [1]. However, these elements are meant to be worn and, indeed, their failure is one of the most critical issues for machine tool reliability [2].

Rolling technology can be applied for both rotational (bearings) and linear (guideways) movements. It can be even applied to rotational-to-translational movement conversion elements like rolling screw drives. Since the first patent related to bearings was published in the eighteenth century, these mechanical components have been widely used in almost every engineering field and they continue being a proper mechanical solution to a vast variety of design challenges. Thus, the improvements in engineering theoretical and experimental tools and more efficient industry processes have led to the need to perform exhaustive research on bearing life prediction methodologies.

E. Olabarrieta (✉) · E. Konde · E. Guruceta · M. Armendia
IK4-Tekniker, C/ Iñaki Goenaga, 5, 20600 Eibar, Gipuzkoa, Spain
e-mail: eneko.olabarrieta@tekniker.es

E. Konde
e-mail: egoitz.konde@tekniker.es

E. Guruceta
e-mail: enrique.guruceta@tekniker.es

M. Armendia
e-mail: mikel.armendia@tekniker.es

M. Armendia et al. (eds.), *Twin-Control*,
https://doi.org/10.1007/978-3-030-02203-7_6

Bearing life estimation theories started on nineteenth century with the testing of rolling bearings performed by Stribeck [3]. Goodman [4] and Palmgren [5] continued the work on the twentieth century by introducing the important concept of fatigue limit in rolling bearing life. A new milestone was set by Weibull [6] with his statistical theory of the strength of materials and, in the 60s, Lundberg and Palmgren [7, 8] presented their life theory of rolling bearings. This was the basis for the current L10 formula [9] for the basic rating life of rolling bearing. Moreover, more accurate testing methods and complex analysis tools have let the researchers improve the rating life estimations, and the modified rating life [9] has become a powerful tool for better life predictions, taking into account aspects like oil condition or fatigue load.

Anyway, the deterministic prediction of the initiation of a failure in a specific bearing is impossible. For fatigue damages, bearing diagnostics is a powerful tool for avoiding undesired failures. Furthermore, if a bearing presents some evidence of wear instead of rolling contact fatigue, the lifetime cannot be mathematically predicted on a statistical basis [10].

The presented activity does not pretend the development of a new wear model that improves the performance of well-known references like the ones presented in the ISO 281 [9], but to present an approach that can facilitate the analysis to the end user and can be combined with other data sources to improve end-of-life estimations. The work is focused on bearings performance, but it can be easily extrapolated with other rolling-based elements like guideways and screw drives.

This work is composed of five sections. The first one presents the introduction and context of this research. The second one presents the background of the proposed approach. The third chapter introduces the developed calculation module and proposes a new approach for bearings lifecycle study. Next, a summary of the results obtained in experimental tests is provided. Finally, the conclusions are presented.

6.2 Theoretical Background

As mentioned, the aim of this work is not to determine a new model for bearing end-of-life calculation, but to use the existing theoretical standardized background [9] to implement it in a more efficient way. The objective is to avoid doing conservative estimations of the loads and replace them by more accurate estimations based on the results provided by a powerful simulation tool [11].

When a specific bearing (or bearing combination) is selected for an application, life must be estimated in order to analyze its suitability regarding the load characteristics of the whole system. Thus, preliminarily, the basic rating life (L_{10h}) is used. The following simple and well-known formula represents the life of the bearing in hours [9]:

$$L_{10h} = \frac{10^6}{60 \cdot n} \left(\frac{C}{P} \right)^p \tag{6.1}$$

where n is the rotating speed, C is the dynamic radial load capacity of the bearing with a 90% of reliability, P is the equivalent load and p is an exponent defined by the bearing type.

This simple operation gives to the designer a general idea of the performance of the bearing, but it has been shown that it is a quite conservative estimation. A more accurate estimation can be obtained by applying the modified life rating (L_{nmh}), which includes bearing operating conditions (lubrication, temperature, etc.) in the estimations.

$$L_{\text{nmh}} = a_1 \cdot a_{\text{ISO}} \cdot L_{10h} \tag{6.2}$$

where a_1 is the reliability factor and a_{ISO} is the life modification factor, which depend on the usage conditions (oil contamination level and viscosity) and the limit load regarding fatigue.

The load capacity C is determined both experimentally and analytically and is always provided by the manufacturer. However, the equivalent load P is more complex to calculate. The following basic formulation is used for that purpose in individual bearings:

$$P = X \cdot F_r + Y \cdot F_a \tag{6.3}$$

where X is the radial load factor, Y is the axial load factor and F_r and F_a are the average radial and axial loads actuating on the bearing. The factors are given by the bearing characteristics, and the average loads must be estimated from the correspondent application through calculations or measurements.

In most applications, load and speed conditions vary in time. To take into account, these time-dependent effects, equivalent rotating speed and loads must be considered. Thus, the equivalent values are computed as follows:

- Speed:

$$n_e = \sum_{1}^{N} n_i \cdot \frac{\Delta t_i}{100} \tag{6.4}$$

- Load:

$$F_{\text{re}}, F_{\text{ae}} = \sum_{1}^{N} F_i \cdot \frac{n_i}{n_e} \cdot \frac{\Delta t_i}{100} \tag{6.5}$$

where N is the number of samples of the vector, Δt_i the sampling rate, n_i and F_i the speed and load, respectively, at sample i, n_e the equivalent speed and F_{re} and F_{ae}, the equivalent radial and axial loads, respectively.

6.3 End-of-Life Calculation Module

Considering the previous formulation (Eqs. 6.1–6.5), a rating life calculation module has been set-up in MATLAB environment. Currently, the module calculates an end-of-life value based on bearing characteristics (type, load capacity and dimensions), applied loads and operating conditions (reliability, cleanliness, temperature and oil type). In order to facilitate the configuration to the end user, the module includes a bearing database. By selecting the bearing references, required bearing characteristics are automatically loaded in the module. With the defined inputs, the module provides both the basic rating life (in revolutions and hours) and the modified rating life (in hours) that considers the operating conditions. The proposed calculation module can enhance bearing analysis at two stages (Fig. 6.1).

In the machine tool design stage, the module can calculate end-of-life based on loads provided by a machine tool simulation module [11–13] that can provide very accurate component loads. The possibility to use an accurate input to the end-of-life module will, of course, enhance the life predictions and, hence, machine tool designers will be able to select more suitable bearing. Figure 6.2 presents the module integrated in the Twin-Control application, with two interfaces for the configuration and results visualization.

In the machine tool usage stage, thanks to the current NC monitoring capabilities, real component loads can be derived, without the need of expensive and complex bearing monitoring sensors. This allows the estimations of the remaining useful life of the studied component. In Twin-Control project, the end-of-life module has been integrated in KASEM, the fleet management system provided by PREDICT (Fig. 6.3). Remaining useful data is calculated periodically using real usage conditions monitored and uploaded thanks to the ARTIS hardware installed in the machine.

Equations defined in the ISO 281 standard [9] are based on ideal usage conditions, the ones used for the calculation. However, the real usage of a machine is not ideal and the results provided by the module may not be valid after certain uncontrolled events (e.g., collisions). Because of this, remaining useful life estimations should be combined with condition monitoring using vibration sensors to detect performance change in the bearings.

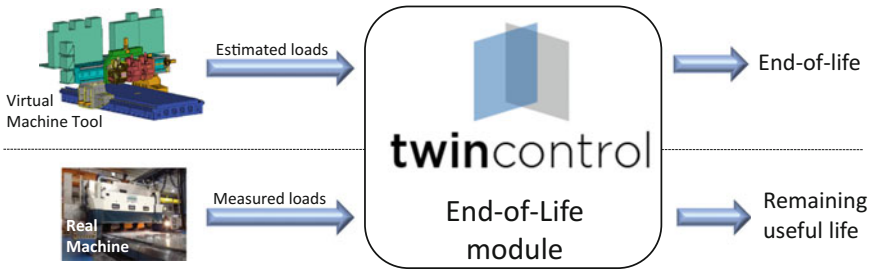

Fig. 6.1 Bearing lifecycle analysis approach

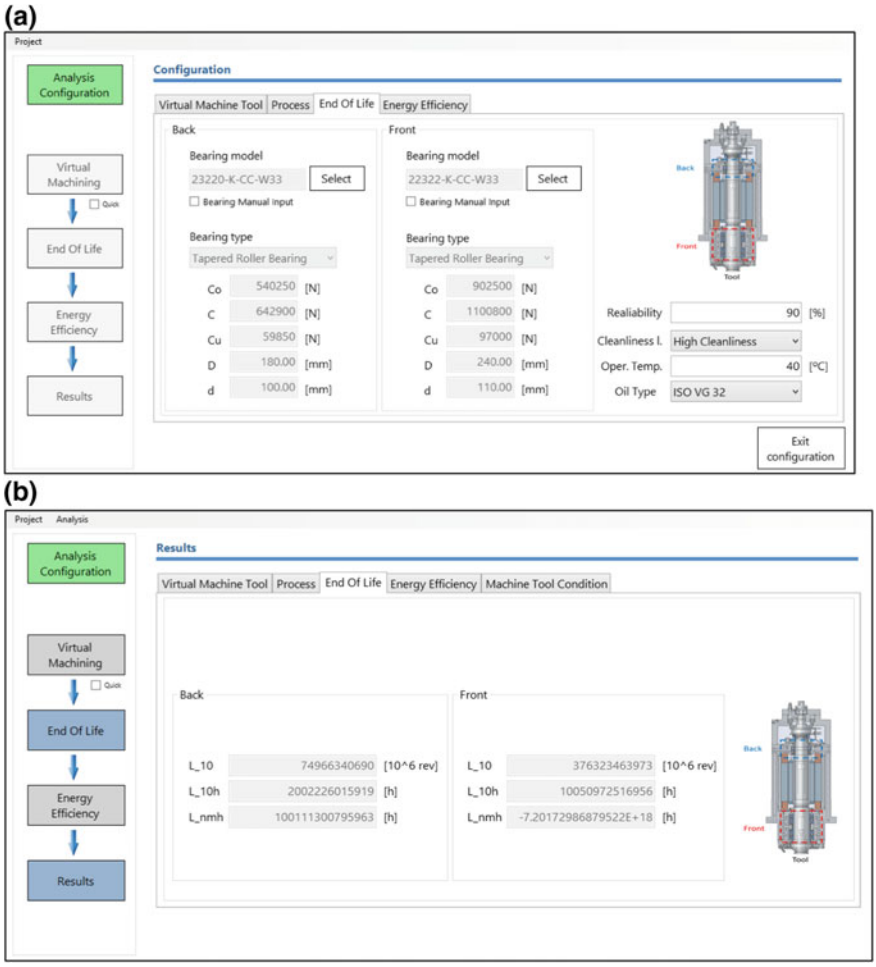

Fig. 6.2 Screenshots of the end-of-life module implemented in the main Twin-Control simulation application: **a** Configuration tab; **b** Results tab

6.4 Validation Tests

6.4.1 Experimental Set-up

For validation purposes, trials in a special test bench for testing rolling bearings that is available at IK4-TEKNIKER will be used (Fig. 6.4). This test bench provides the possibility to apply axial loads to the bearings while they are rolling at a certain speed.

Fig. 6.3 Remaining useful life module: **a** Approach followed in Twin-Control; **b** Example of results of the front spindle of a GEPRO 502 machine

The FALEX test bench has a complete monitoring infrastructure, including force, speed, temperature and vibration sensors and a National Instruments cDAQ acquisition system.

Bearing wear is normally a long duration phenomenon. To adapt test duration and be able to analyze results in an affordable period, accelerated wear tests have been performed by selecting a bearing that provides an end-of-life below 24 h with the loads that can be applied by the test bench (10 kN axial static force at 10,000 rpm).

A SKF 71908 CB/HCP4AL angular contact ball bearing will be used for the accelerated tests, which is a smaller version of the bearings typically used in machine tool spindles. A special-purpose fixture has been specifically designed and manufactured to host this bearing (Fig. 6.5). The fixture allows internal water cooling and the application of different lubrication types: dry, air/oil, grease and oil. The fixture also permits the installation of embedded temperature and vibration sensors.

A total of 6 bearings have been tested. For the proposed bearing, the calculation module estimated a nominal end-of-life of 7 h, while the modified end-of-life, applying the test conditions, is 15 h. The conditions used in the tests were 4 kN of static axial load and 6200 rpm of rotation speed.

Fig. 6.4 FALEX test bench available at IK4-TEKNIKER installations

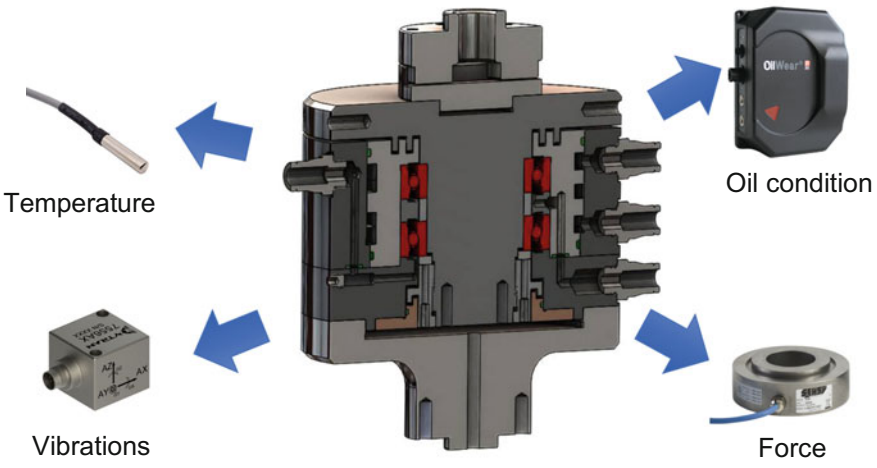

Fig. 6.5 Cross section of the design of the special fixture manufactured for the accelerated tests of the selected bearings (in red)

Table 6.1 Summary of the experimental tests (4 kN of static axial load and 6200 rpm of rotation speed)

#	Test stop time (h)	Failure	Comments
1	22	Greasing	–
2	34	Pitting	Regreasing after 20 h
3	20	–	Good condition
4	23	Greasing	–
5	18	Severe pitting	–
6	35	Micro-pitting	Regreasing every 5 h

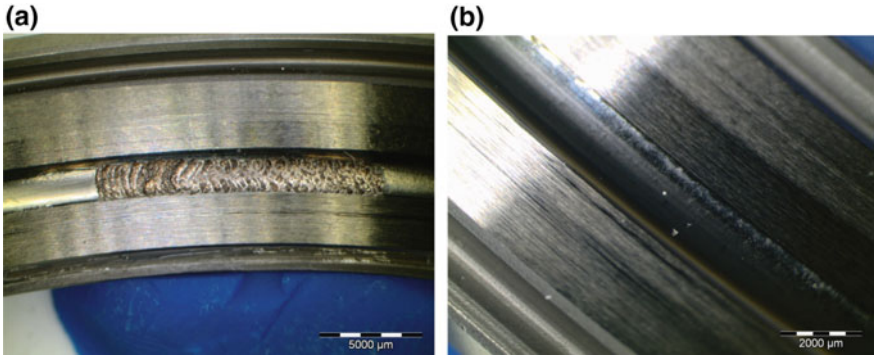

Fig. 6.6 Microscope images showing outer rings of the bearings: **a** #5 with severe pitting after 18 h; **b** #6 with micro-pitting after 35 h (with a regreasing every 5 h)

6.4.2 Results

Table 6.1 summarizes the results of the experimental tests. A big variance of end-of-life is observed, but always above the value determined by the calculation using the ISO 281 standard [9].

When analyzing the wear mechanism, lack of grease seemed to be the main problem, leading to pitting (Fig. 6.6) in the outer ring of the bearings. For these reasons, some of the tests were stopped after some time for a regreasing. By doing this, an extension of the end-of-life was observed.

6.4.3 Vibration Measurements

Figure 6.7 shows the evolution of the root mean square (RMS) in the whole studied frequency range (10–2000 kHz) of the vibration signal acquired during test #5. A sudden increase of vibration is observed at around 14 h, clear indicator that the bearing started to fail. The test continued until 18 h, showing a totally worn condition

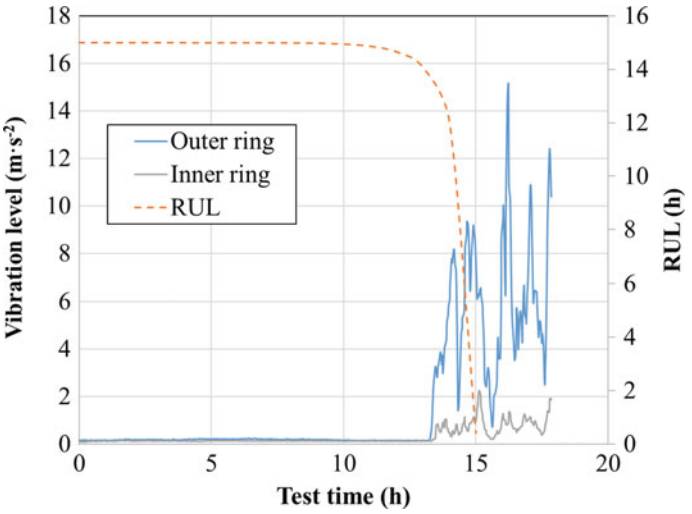

Fig. 6.7 RMS of the global vibration signal measured during test #5. Theoretical RUL evolution is plotted in dotted line

(Fig. 6.6a). The evolution of the theoretical remaining useful life (RUL) calculated for this bearing using the simulation module based on the ISO 281 standard is also presented.

The analysis of the frequency bands of interest for the selected bearing provides additional knowledge. An envelope analysis is applied in the frequency bands corresponding to the outer (1333 Hz) and inner rings (1560 Hz). Looking at the results obtained in test #5 again, bearing wear initiation can be detected where the vibration level at these bands increases (Fig. 6.8). In addition, it can be observed that higher vibration levels are measured in the frequency band corresponding to the outer ring, the one showing higher wear after visual inspection (Fig. 6.6).

6.5 Conclusions

A new approach for the study of bearing lifecycle performance is presented. The proposed approach is based on the well-known ISO 281 for end-of-life determination. The work is focused on bearings performance, but it can be easily extrapolated with other rolling-based elements like guideways and screw drives.

A specific tool has been developed that calculates the end-of-life of a specific bearing for a defined load cycle (forces and speeds in time). This tool allows bearing analysis through all its lifecycle. On the one hand, the module can be used in machinery design stage by providing an improved estimation of end-of-life by using load variation in time during the manufacturing cycle. This will allow a better selection

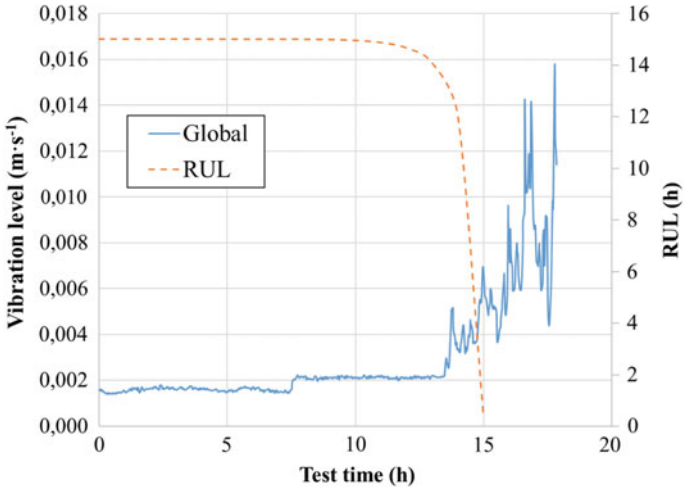

Fig. 6.8 Vibration level obtained applying envelope analysis to the frequency ranges corresponding to the outer and inner rings of the selected bearing (test #5). Theoretical RUL evolution is plotted in dotted line

of the critical components. On the other hand, the tool is prepared to be fed by real machine usage data (monitored). This way, remaining useful life of a component can be provided. In parallel, the usage of a condition monitoring system based on vibration measurement can be used to detect anomalous performance (out of the nominal behavior, like collisions).

Some preliminary validation tests have been done in a test bench available in IK4-TEKNIKER installations. The tests showed that the ISO standard underestimates the end-of-life of components. In addition, results provided by the vibration measurements showed the possibility to detect component failure in an early stage. This early detection will allow more efficient maintenance actions in industrial applications.

The proposed approach is aligned with some concepts aligned with current trends in ICT technologies: combination of different simulation models to improve estimations and integration of simulation models with monitored data to control system performance.

References

1. Sutar, M.D., Deshmukh, B.B.: Linear motion guideways—a recent technology for higher accuracy and precision motion of machine tool. Int. J. Innovations Eng. Technol. **3**(1) (2013)
2. Fleischer, J., Broos, A., Schopp, M., Wieser, J., Hennrich, H.: Lifecycle-oriented component selection for machine tools based on multibody simulation and component life prediction. CIRP J. Manuf. Sci. Technol. **1**(3) (2009)

3. Stribeck, R.: Kugellager fü r beliebige Belastungen. Zeitschrift des Vereines deutscher Ingenieure **45**(3), 73–9 (pt I) & **45**(4), 118–125 (pt II)
4. Goodman, J.: Roller and ball bearings. Proc. Inst. Civil Eng. **189**, 82–166 (1912)
5. Palmgren, A.: Ball and Roller Bearing Engineering, First edn., (trans.: Palmgren, G., Ruley, B). SKF Industries, Inc., Philadelphia, PA (1945)
6. Weibull, W.: A statistical theory of the strength of materials. In: Proceedings of the Royal Swedish Academy of Engineering Sciences, 45 pp., vol. 151, Stockholm, Sweden (1939)
7. Lundberg, G., Palmgren, A., Dynamic capacity of rolling bearings. In: Proceedings of the Royal Swedish Academy of Engineering Sciences, 50 pp., vol. 196, Stockholm, Sweden (1947)
8. Lundberg, G., Palmgren, A.: Dynamic capacity of roller bearings. In: Proceedings of the Royal Swedish Academy of Engineering Sciences, 32 pp., vol. 210, Stockholm, Sweden (1952)
9. ISO 281:2007: Rolling bearings—Dynamic load ratings and rating life
10. Halme, J., Andersson, P.: Rolling contact fatigue and wear fundamentals for rolling bearing diagnostics—state of the art. Proc. Inst. Mech. Eng. Part J: J. Eng. Tribol. **224**(4) (2010)
11. Cugnon, F., Berglind, L., Plakhotnik, D., Ozturk, E.: Advance modelling of machine tool machining process. In: ECCOMAS Conference 2017, Prague, 19–22 June 2017
12. Gugnon, F., Ghasempouri, M., Armendia, M.: Machine tools mechatronic analysis in the scope of Twin-Control project. In: NAFEMS World Congress 2017, Stockholm, 11–14 June 2017
13. Berglind, L., Plakhotnik, D., Ozturk, E.: Discrete cutting force model for 5-axis milling with arbitrary engagement and feed direction. Procedia CIRP **58**, 445–450 (2017)

Part III
Real Representation of the Machine Tool and Machining Processes

Chapter 7
Data Monitoring and Management for Machine Tools

Tobias Fuertjes, Christophe Mozzati, Flavien Peysson, Aitor Alzaga and Mikel Armendia

7.1 Introduction

Twin-Control concept combines the development of holistic simulation models with the knowledge of the performance of the real machines and processes. To deal with this second part, a data monitoring infrastructure must be implemented so that required information is acquired, managed and analyzed properly.

The approach used in Twin-Control consists in the installation of a local monitoring hardware that acquires internal variables of the machine, collects data of additional sensors and uploads all data to a cloud platform [1]. ARTIS Genior modular is used for the local monitoring, and PREDICT's KASEM® is used as cloud platform for data analysis. A fleet-level data analysis will be performed by integrating all the information coming from the different machines.

This chapter is structured as follows. After a brief introduction, an overview of the equipment to be monitored and integrated in Twin-Control is presented. The

T. Fuertjes (✉)
MARPOSS Monitoring Solutions GmbH, Egestorf, Germany
e-mail: tobias.fuertjes@mms.marposs.com

C. Mozzati · F. Peysson
PREDICT, Vandoeuvre-lès-Nancy, France
e-mail: christophe.mozzati@predict.fr

F. Peysson
e-mail: flavien.peysson@predict.fr

A. Alzaga · M. Armendia
IK4-Tekniker, C/Iñaki Goenaga, 5, 20600 Eiba, Gipuzkoa, Spain
e-mail: aitor.alzaga@tekniker.es

M. Armendia
e-mail: mikel.armendia@tekniker.es

M. Armendia et al. (eds.), *Twin-Control*,
https://doi.org/10.1007/978-3-030-02203-7_7

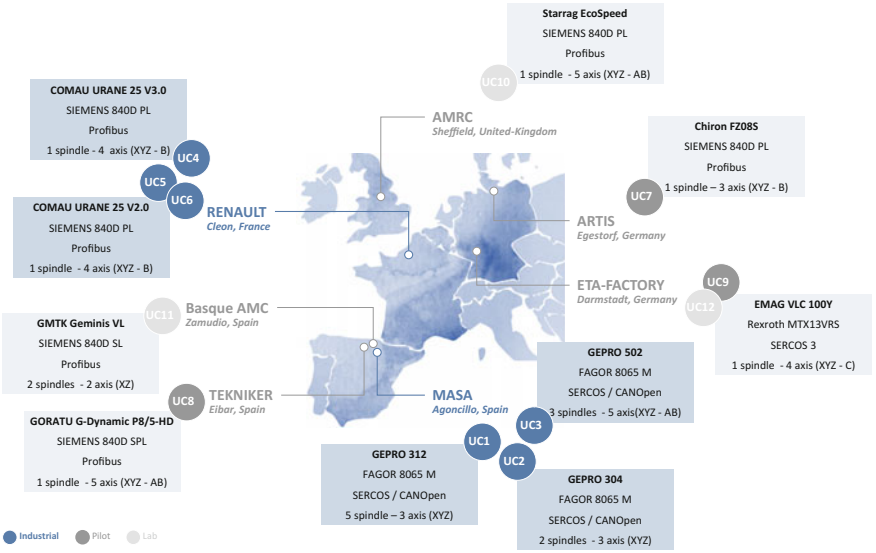

Fig. 7.1 Map of Twin-Control monitored and connected machine tools

third-section presents the different architectures proposed to cover all the use cases. Finally, the conclusions are presented.

7.2 Monitored Equipment

Figure 7.1 presents all the machine use cases monitored in Twin-Control project. As it can be observed, a total of 12 machine tools have been monitored. Each of the industrial validation scenarios includes three machines. For the aerospace validation scenario, located at MASA aerospace structural manufacturer installations (Agoncillo, Spain), three GEPRO machines were selected as use cases, named as Use cases 1–3. The machines present a similar architecture, but they differ in the number of axes and spindles. For the automotive validation scenario, located at RENAULT automotive component manufacturer (Cleon, France), three COMAU Urane machines were selected, named as Use cases 4–6.

Three more use cases have been monitored to test and validate Twin-Control developments during the project:

- Use case 7: CHIRON milling machine, located at ARTIS (Egestorf, Germany), to validate monitoring tools and test new features (NC Simulation).
- Use case 8: GORATU 5 axis milling machine, located at TEKNIKER (Eibar, Spain), to validate machine tool characterization procedure.

– Use case 9: EMAG machine, located at the ETA-FACTORY (Darmstadt, Germany), to test and validate energy efficiency models.

Finally, three additional machines, located at relevant research locations, have been taken to implement Twin-Control features and present them to the scientific and industrial community:

– Use case 10: Starrag EcoSpeed milling machine, located at the AMRC (Sheffield, UK), to disseminate process models and monitoring developments.
– Use case 11: GMTK vertical lathe, located at the recently opened Basque Advance Manufacturing Centre (Zamudio, Spain), to show Machine Tool characterization procedure, among other features.
– Use case 12: a second EMAG machine, located at the ETA-FACTORY (Darmstadt, Germany), to promote energy efficiency features.

The different use cases show a heterogeneous mixture of CNC models and communication-field buses, which represent the typical state for machine tool users. With this variety, it is difficult to determine a unique local monitoring architecture. In the next section, the different implemented architectures are detailed.

7.3 Implemented Monitoring Architecture

In each use case, monitoring hardware has been installed. Figure 7.2 presents a diagram showing the generic monitoring architecture used in Twin-Control project. However, depending on use case specifications and requirements, this generic architecture is adapted.

The modular configuration provided by ARTIS is perfectly suited to cover the heterogeneous applications. Figure 7.3 shows the integrated hardware in two of the industrial use cases.

ARTIS Genior modular (GEM) is the data acquisition module that can get real-time CNC/PLC data (around 100 Hz sampling, depending on the application). Also, an HMI visualization with any PC which is connected to the plant network is possible. For the real-time connection with the CNC, two different protocols are available. For the aerospace use cases, with FAGOR 8065 CNCs, an ARTIS FAGOR-CANopen protocol has been developed. This protocol allows a real-time monitoring of 32 bytes per sample. For the Twin-Control project, 28 bytes have been used to process data and 4 bytes have been reserved to identification and process information. To increase the number of possible real-time monitored signals, the CANopen sample rate was reduced to 4 ms. By combining two CANopen channels, real-time monitoring of 56 bytes (24 variables) with a sample rate of 8 ms is provided. For the machines located at the automotive validation scenario, mounting SIEMENS 840D CNC, PROFIBUS protocol is used to connect ARTIS GEM with machines PLC. This protocol enables system to exchange up to 16 CNC sensor signals in parallel. For some other use cases, as GORATU machine located at TEKNIKER, two of these devices are installed to increase the real-time monitoring variables up to 32.

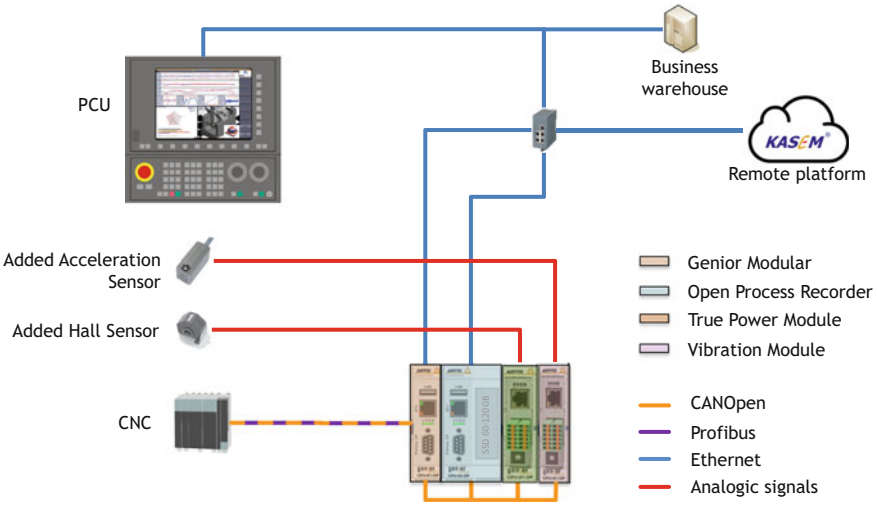

Fig. 7.2 Generic monitoring architecture applied in Twin-Control project

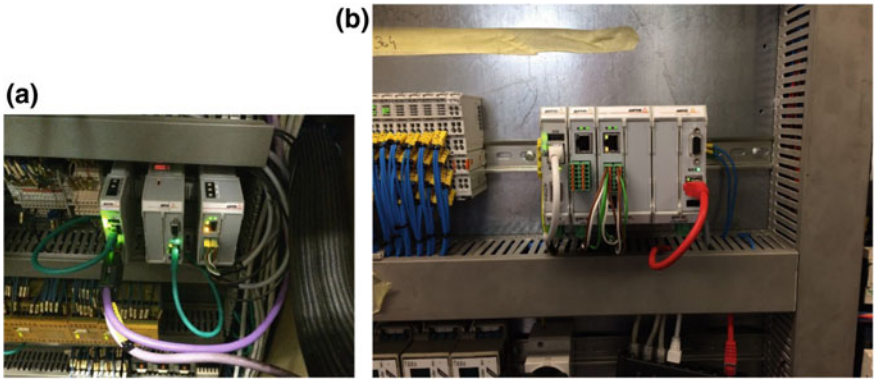

Fig. 7.3 Monitoring hardware installations in Twin-Control: **a** COMAU Urane machine from automotive validation scenario; **b** GEPRO 502 machine from aerospace validation scenario

Depending on the use case and its requirements, different variables have been configured to be monitored. Also, for each variable, it has been defined if real-time information is needed. As a sample, the real-time variables monitored in the two industrial validation scenarios are presented in Table 7.1.

Using the ARTIS GEM device, visualization of monitored data in machine tool HMI (Fig. 7.4) is possible for Windows XP-based controllers, using Ethernet connection and the GEM-Visu software.

ARTIS Online Process Recorder (OPR) is connected to the GEM for data storage purposes (240 GB capacity). It is also capable of monitoring non-real-time data using OPC, as a second data source. In addition, GEM and OPR could exchange real-

Table 7.1 Example of real-time (10 ms sampling) variables monitored in machines from aerospace and automotive validation scenarios

Aerospace validation scenario Gepro 502	Automotive validation scenario COMAU Urane
Target position X	Target position X
Target position Xb	Target position Y
Target position Y	Target position Z
Target position Z	Target position B
Target position A	Real position X
Target position B1	Real position Y
Real position X	Real position Z
Real position Xb	Real position B
Real position Y	Real power X
Real position Z	Real power Y
Real position A	Real power Z
Real position B1	Real power B
Real position B2	Spindle torque S
Real position B3	Torque X
Real power X	Velocity Y
Real power Y	Machine true power
Real power Z	ACC X
Real power A	
Real power B1	
Spindle torque S1	
Spindle torque S2	
Spindle torque S3	
Spindle speed S2	
Machine true power	

time information using CANopen, for example, in case of critical alarm information remotely detected inside the data management system (KASEM®).

ARTIS OPR shows a special feature in the EMAG machines located at the ETA-Factory (Darmstadt, Germany). Since the energy models are based on ON-OFF switching signals of the Bosch Rexroth control and the machine power aggregates, an OPC-UA interface has been developed. The energy efficiency models, developed in MATLAB/Simulink, are running at the OPR, and the signals are read from the control via OPC-UA. By using ARTIS GEM as additional software, it is also possible to monitor the energy model results in the GEM and visualize the results in the GEM-Visu (Fig. 7.5).

As an example, Table 7.2 presents the non-real-time variables monitored by the OPR devices installed in the industrial validation scenarios.

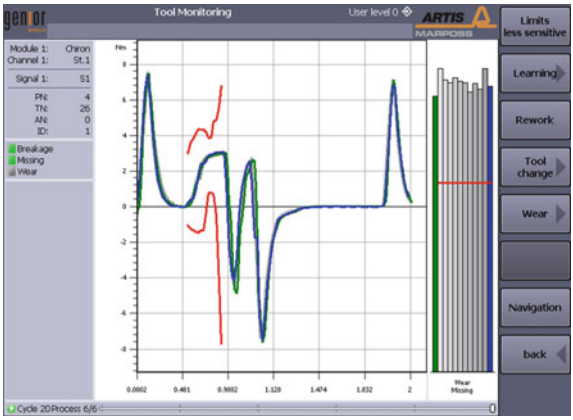

Fig. 7.4 GEM-Visu for visualization of monitored signals

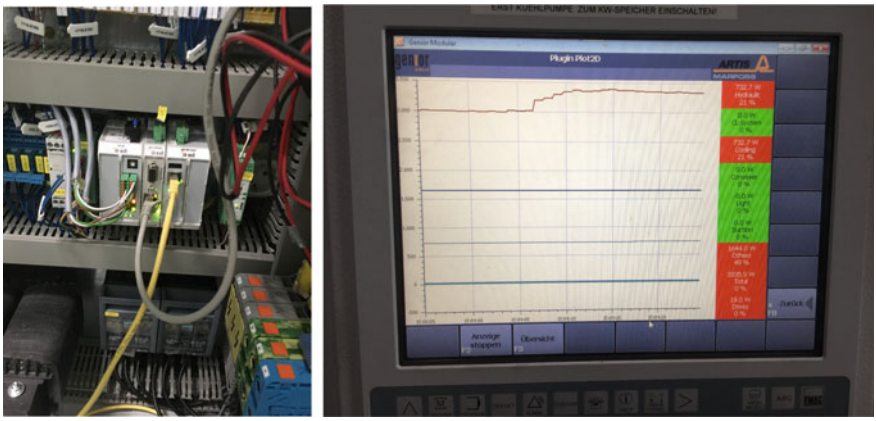

Fig. 7.5 Monitoring installation at the EMAG machine (ETA-Factory): hardware installation and screenshot of ARTIS HMI displaying energy consumption results

ARTIS True Power (TP) module sends power measurements from installed hall sensors to the GEM. CANopen protocol is used to make sure that the signals could be transferred under real-time conditions. The hall sensors are equipped directly at the main power supply of each machine (Fig. 7.6). Through the measuring of all three phases of the main power supply based on the TP module, it is possible to get the machine true power under real-time conditions.

ARTIS Vibration Measurement (VM) module has been also installed in different use cases. Processes accelerometer measurements real-time (internal sample rate of 25 kHz) and sends indicators (e.g. RMS) to GEM through CANopen protocol. For example, automotive use cases were provided with a vibration monitoring with sample frequencies of 25 kHz. To allow a vibration monitoring with sample rates

Table 7.2 Example of non-real-time (1 s sampling) variables monitored in machines from aerospace and automotive validation scenarios

Aerospace validation scenario Gepro 502	Automotive validation scenario COMAU Urane
Time	Time
Spindle speed S1	Process mode (G 00/G 01)
Spindle speed S2	Hydraulic system status
Spindle speed S3	High pressure cooling status
Hydraulic system status	Low pressure cooling status
Spindle temperature S1	Workpiece counter
Spindle temperature S2	FMD signals
Spindle temperature S3	Part info for RENAULT
Backlash X	RMS (15–1000 Hz)
Backlash X1	RMS (15–5000 Hz)
Backlash Y	RMS (5% around RPM tool 4)
Backlash Z	RMS (5% around RPM tool 12)
Backlash B1	RMS (5% around RPM tool 15)
Backlash B2	
Backlash B3	

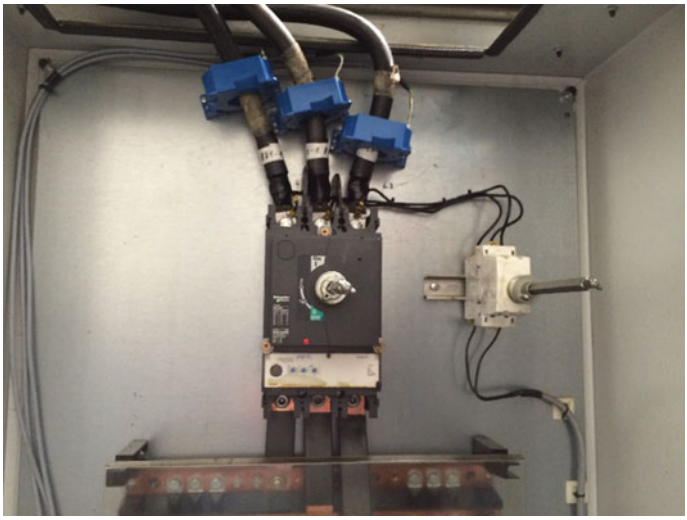

Fig. 7.6 Hall sensors installed in the main electrical input for energy monitoring purposes in GEPRO 502 machine from aerospace validation scenario

of 25 kHz, a new firmware for the VM module was developed and installed. This firmware stored the vibration data with a sample frequency of 25 kHz at the OPR. Inside the OPR, an automatic analyzing function was developed, which calculate the

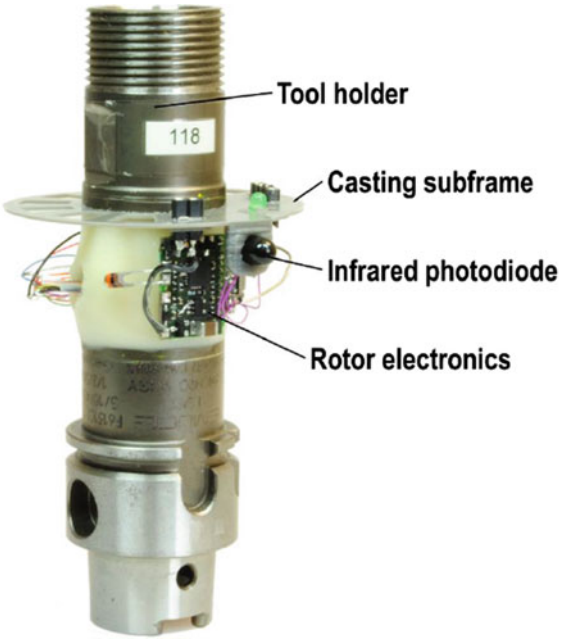

Fig. 7.7 ARTIS DDU-4 K-Wisy wireless force monitoring device from MARPOSS monitoring solutions

RMS values for five frequency bands and send the result continuously via GEM to the GEM module (Table 7.2).

ARTIS DDU-4K-Wisy (Fig. 7.7) is a new device from MARPOSS Monitoring Solutions that has been installed in the Starrag EcoSpeed machine, located at the AMRC (Sheffield, UK). It consists in a tool holder with embedded force and temperature measurement capabilities that is used for in-process force monitoring. The DDU 4K-Wisy is based on a HSK 32 tool holder which is equipped with eight strain gage rosettes each containing two mutually perpendicular grids. Via this measurement configuration four different measuring values are captured: torque, axial force and the axial tool holder deflection in two directions (perpendicular). To acquire temperature-compensated signals, each pair of strain gages is interconnected to four separate Wheatstone bridges. To log the generated data, a wireless transmission on the ISM radio band (around 2,4 GHz) is used along with a corresponding radio receiver which either can be connected to ARTIS monitoring devices via CAN bus or to a standard PC via USB.

7.4 Cloud Data Management

Fleet-wide proactive maintenance functionalities consist of the construction of model coupling data analytics and expert knowledge. Raw data and machine-level computed

information are therefore a major input of the cloud platform which is powered by PREDICT's KASEM® solution. The platform is accessible via the Internet and hosted on a secure server.

Data transfer from machine to the platform requires some flexibility to match with IT and production constraints. Indeed, in factories, machine tools are connected a production Ethernet which is used to exchange synchronization information between machines, gantry, robots and various management and control systems. Depending on the size and the age of the factory, networks can be close to saturation and a continuous transfer of high sampling rate data could impact the network availability and introduce losses of information packets. In addition, from cyber-security point of view, IT department is often reluctant to "connect" production network to the Internet because bad-intentioned people could get into the network and take control of equipment for instance.

In view of theses constraints, various data transfer architectures have been applied according to use cases. In case of laboratory and pilot machine tools, OPR has a direct connection to the cloud platform. For the industrial use cases, intermediate servers have been used, and these servers are connected to the production network and enable local data storage and edge computing. For the aerospace scenario, data from the OPR is automatically uploaded to the local KASEM® platform inside MASA facilities through MASA network; then this server, also connected to the Internet, manages the data transfer to the cloud as depicted in Fig. 7.8. In this case, local server also acted as a partition between machine network and Internet.

For the automotive scenario, IT constraints were more important, and to enable the data transfer a specific architecture has been developed in collaboration with the IT architects. This architecture is also based on a local platform hosted in a RENAULT data centre in the Renault Technocentre (Guyancourt, France) and connected to the production network as shown in Fig. 7.9. Server S1 hosts KASEM® solution, and knowledge base is hosted by server S2. Server S3 is a file storage server used for binary files. Finally, an intermediate Renault/Nissan system is used for secure transfers between the local and fleet platforms. In this case, architecture management—installation, configuration and update—can be made only from user connected to Renault network.

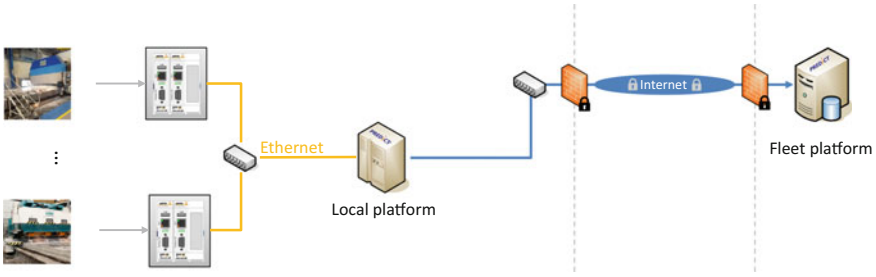

Fig. 7.8 Data exchange configuration for the aerospace validation use case

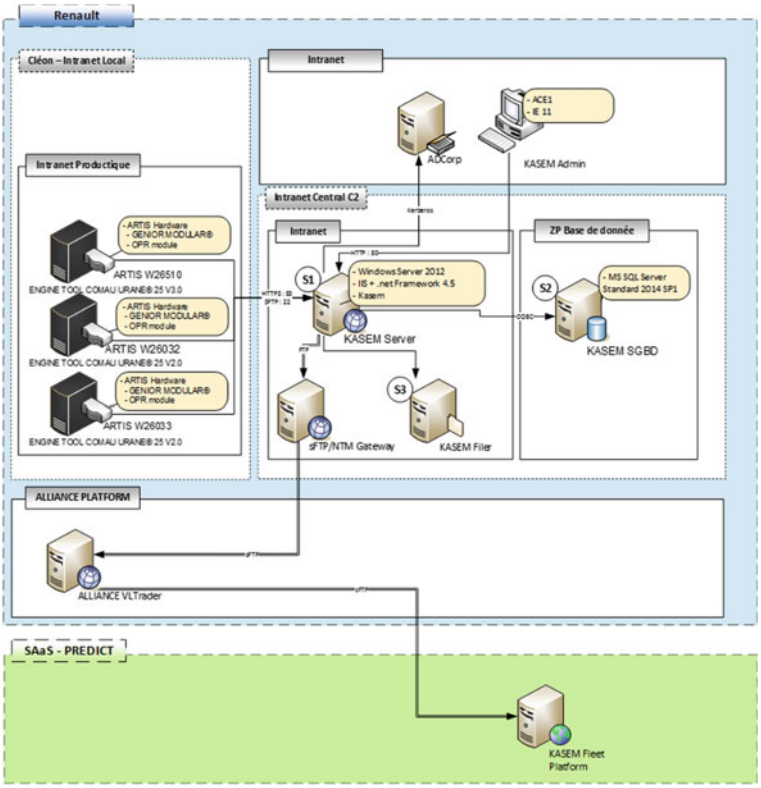

Fig. 7.9 Data exchange architecture for automotive use case

About every 10 min, each machine—OPR module—sends and receives real-time data from/to the local or fleet platform which represents around 5 MB transferred in batch mode. About every 60 min, each machine—OPR module—sends and receives non-real-time data from/to the local or fleet platform which represents around 6 MB in batch mode. The total amount of data stored per machine could be 600 GB per year. Inside KASEM® platform, there is a specific service able to index, read and archive binary with a life cycle management of acquisition channels. Regarding transfer protocols, WebDAV and FTP are the default options for upload stream. Once the Internet connection is set up and running, it is possible to download and see a report generated by KASEM® with the Genior modular HMI Plug-in.

Cloud platform is accessible at https://twincontrol.kasem.fr, with restricted access to authorized users. A screenshot of the home page of KASEM® platform is shown in Fig. 7.10. This interface provides the chance to visualize collected time series, computed information and stored reports, download data, and even advanced tasks like indicator generation via algorithm implementation.

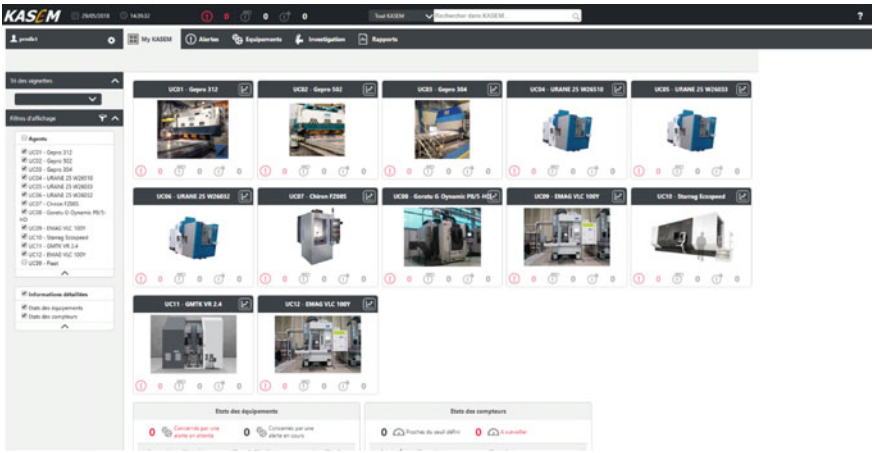

Fig. 7.10 Home page of KASEM server showing the connected use cases in the data management system

7.5 Conclusions

This chapter presents the monitoring infrastructure installed in a total of 12 machines used for implementation of Twin-Control at different levels: industrial evaluation, scientific validation and dissemination.

At local level, the monitoring architecture is based on a modular configuration. ARTIS devices are used and configured according to each use case specifications and requirements. The modular system can synchronously acquire internal variables from the CNC/PLC (real-time and non-real-time data), as well as signals from additional sensors like accelerometers, hall sensors and force transducers. This flexible approach provides the opportunity to include a wide range of equipment in the monitored fleet and is perfectly adapted to the usual configuration of end-users, with very different machines in their installations.

The data monitored at local level is uploaded from ARTIS OPR modules to a cloud platform. The PREDICT's KASEM® platform has been storing information from most of the use cases during almost two years in Twin-Control project. Hence, the proposed architecture has been validated and has provided an excellent source of real data used as a basis for the rest of developments of Twin-Control.

The capabilities of the installed infrastructure are not limited to data monitoring and storage. In following chapters, other capabilities like advance indicator calculation, fleet analytics and even the possibility to integrate model-based control actions in the machine will be covered.

Reference

1. Prado, A., Alzaga, A., Konde, E., Medina-Oliva, G., Monnin, M., Johansson, C.-A., Galar, D., Euhus, D., Burrows, M., Yurre, C.: Health and performances machine tool monitoring architecture. In: E-maintenance Conference, Luleå, Sweden, 17–8th June 2014

Chapter 8
Behaviours Indicators of Machine Tools

Flavien Peysson, David Leon, Quentin Lafuste, Mikel Armendia, Unai Mutilba, Enrique Guruceta and Gorka Kortaberria

8.1 Introduction

The behaviour of a machine tool is the set of actions and operations made by the machine sub-systems in conjunction with themselves and the machine environment. The expected behaviour can be defined as the capacity of a machine tool to achieve its objective: to produce parts with specified quality at high production rates [1].

These concepts can be monitored through sensor measurements. The characteristics of the sub-systems allow to interpret the expected behaviour from the machine. However, raw data are highly influenced by external and internal conditions. The behaviour of the sub-system can influence the one of another sub-system from the machine tool. By computing contextualized, and comparable over the time, indicators, from sensors measurement and machine operating conditions, it is possible to

F. Peysson (✉) · D. Leon · Q. Lafuste
PREDICT, Vandoeuvre-lès-Nancy, France
e-mail: flavien.peysson@predict.fr

D. Leon
e-mail: david.leon@predict.fr

Q. Lafuste
e-mail: quentin.lafuste@predict.fr

M. Armendia · U. Mutilba · E. Guruceta · G. Kortaberria
IK4-Tekniker, C/Iñaki Goenaga, 5, 20600 Eibar, Gipuzkoa, Spain
e-mail: mikel.armendia@tekniker.es

U. Mutilba
e-mail: unai.mutilba@tekniker.es

E. Guruceta
e-mail: enrique.guruceta@tekniker.es

G. Kortaberria
e-mail: gorka.kortaberria@tekniker.es

M. Armendia et al. (eds.), *Twin-Control*,
https://doi.org/10.1007/978-3-030-02203-7_8

monitor the machine behaviour and highlight its changes. The quality of the indicators and, consequently, of the monitoring requires a consistent acquisition that is representative of the system dynamics.

Behaviour indicators extraction of a machine tool can be done continuously by the exploitation of the workpiece program and existing machine sensors, or with specific characterization programs using existing sensors and/or additional sensors. Behaviour continuous monitoring using raw measurements is discussed in Sect. 8.2. The characterization tests of machine tools processed occasionally are discussed in Sect. 8.3. Finally, the conclusions are summarized in Sect. 8.4.

8.2 Extraction from Machining Raw Measurements

To continuously monitor the machine behaviour, it is possible to extract indicators from the raw existing sensors measurement during the machine workpiece production. Given the available collected data, it is possible to compute indicators representative of the machine and its sub-systems status. To give a sufficient representation of machine tool behaviour, it is recommended to have a minimal set of information that is synthesized in Table 8.1.

A machine is composed by a set of linear and rotating axes, at least one spindle and a set of auxiliary systems to ensure good machining conditions such as lubricant system, cooling system, air system, machining coolant system and hydraulic group. An overview of the machine behaviour is given by merging the results of its subsystems. Therefore, information about each of them is required. The axis behaviour indicators can be built based on real position, drive current and temperature. In some cases, such as vertical axis, it can be equipped with a compensation system. The axis balance pressure has then to be considered. Behaviour indicators for spindle can be based on speed, current and temperature. The auxiliary systems can be mainly

Table 8.1 Minimal raw measurement set for behaviour monitoring

System	Sensor	Operating condition
Workshop	Temperature	
Machine tool		Cycle tool change
Axis	Real position	
	Current	
	Temperature	
Spindle	Speed	Tool Number
	Current	
	Temperature	
Pumps/tanks	Pressure	

described by the actions of their pumps and tanks where output pressure analysis gives a good representation.

Indicators should be computed from specific operating conditions. The knowledge of workpiece cycle start/end, tool changes and tools in use are then highly recommended for a more accurate analysis. The knowledge of the machine tool environment conditions, such as the workshop inner temperature, is a plus, especially for temperature- and current-based indicators.

8.2.1 Indicator Extraction Process

When it is working, a machine tool and its sub-systems are solicited from various ways and with intensive efforts to produce a part. The solicitations depend on the different machine tool operating conditions. To observe machine behaviour, it is convenient to isolate and observe sensors measurements according to these conditions. The observation is available by extracting business indicators from isolated sensors measurement as depicted in Fig. 8.1.

Collected raw sensors data are, first, consolidated and made reliable, and then, the operating conditions of the machine tool are computed as explained in Sect. 8.1.1. Indicator extraction process from these conditions is detailed in Sect. 8.1.2.

8.2.2 Machine Operating Conditions

A machine tool operates in a workshop and aims at performing successive operations to a raw material to produce a finished workpiece. Each operation may involve the use of a specific tool and axis movements with optimized machining parameters, such as spindle speed or feed rate, for instance. The structuration of machine operating conditions is illustrated in Fig. 8.2, containing the following layers: production, cycle, step, tool change (TC) and move (M).

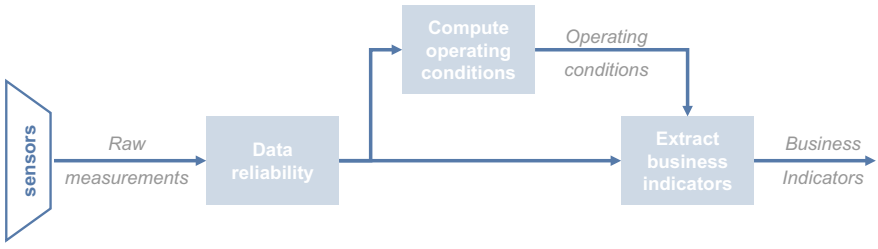

Fig. 8.1 From raw sensors' measurements to indicator extraction

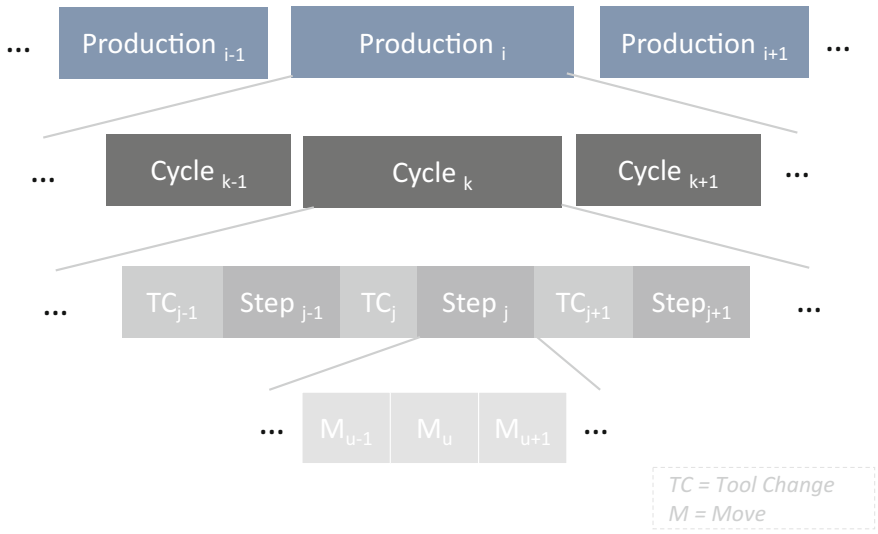

Fig. 8.2 Machine operating conditions

At the top level, the production phase characterizes uninterrupted sequences of machining cycles where the machine tool can produce from one to multiple workpieces of, possibly, different types. A machining cycle is the production of one workpiece. It is composed of successive steps, i.e. an operation such as drilling, boring, finishing with a specific tool and tool changes. For a specific workpiece type, the number of steps and the length of cycles remains constant if the program parameters remain unchanged. Within each step, several moves are performed, such as linear or circular motion, fast or slow, machining or not. Each move can be associated to a single G-Code line of the machining program. Such decomposition allows the observation of specific behaviour and to monitor weak signals. The example in Fig. 8.3 illustrates condition monitoring necessity. In this example, the spindle torque reproduces the effects of a tool change (in blue).

The different operating conditions can be collected directly from the machine numerical command. If it is not the case, they should be inferred from the raw sensors measurements such as axis positions. It is suitable to prioritize the first solution as it contains more reliable information describing the machine state. Algorithms based on raw sensors measurement depend on the relevance, the sampling rate and the synchronicity of the crossed data.

The machine tool efforts are different from one condition to another; to study the behaviour of the machine or a specific sub-system, it is recommended to observe sensor measurement independently from one condition to another. Moreover, the behaviour analysis is possible by extracting indicators from the dataset of sensors' measurements collected in each specific condition as explained in the next section.

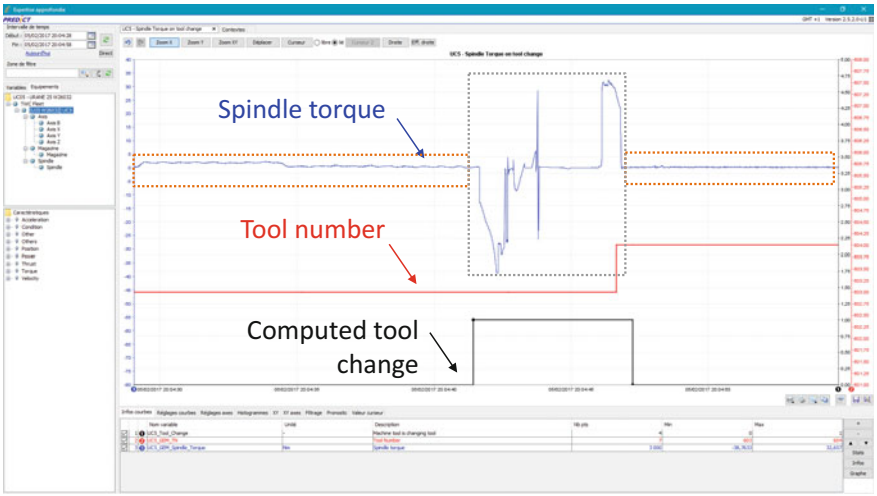

Fig. 8.3 Example of tool change detection for step decomposition

8.2.3 Indicator Processing

Rather than using the overall dataset to understand the behaviour, indicators based on descriptive statistics are computed to summarize the dataset. The indicators commonly used to describe a data collection distribution are (Fig. 8.4).

- The central tendency or centre of the distribution given by the mean and the median.
- The dispersion given by the percentiles, extreme values and standard deviation. A percentile is a value below which a given percentage of the data collection falls. The most frequently used percentiles are:
  - The median or 50th percentile.
  - The lower and upper box, respectively, the 25th and 75th percentile.
  - The lower and upper whisker, respectively, the 5th and 95th percentile.

8.2.4 Example of Indicators

In this section, two examples of indicator extraction are presented. The first one is focused on tool behaviour, based on spindle torque observed in a specific machining step. The second one aims at monitoring axis dynamic behaviour.

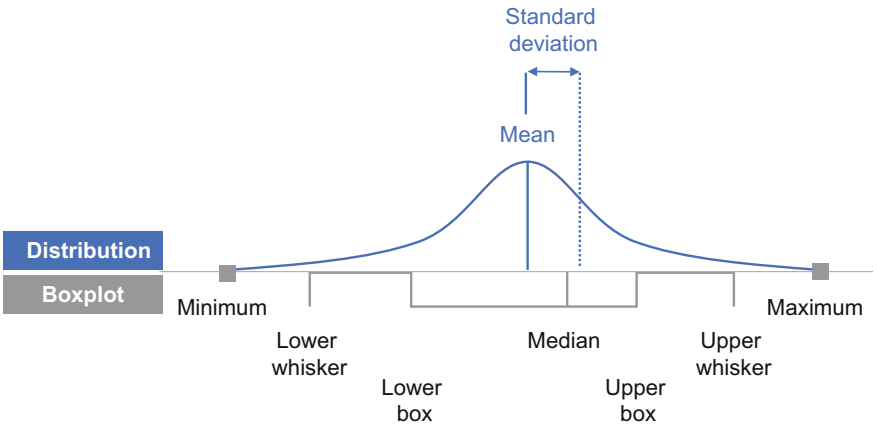

Fig. 8.4 Descriptive statistics: representation of distribution and box plot data

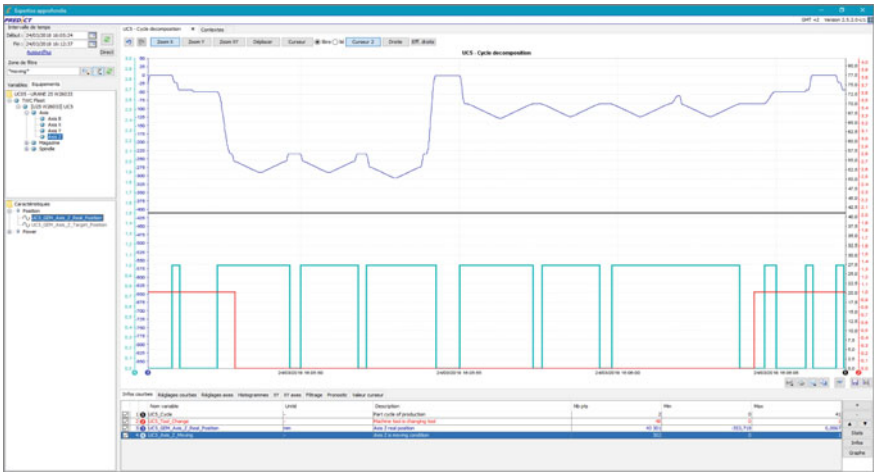

Fig. 8.5 Example of machining step decomposition. In blue, *Z*-axis position; in red, the tool changes; and in green, axis moving conditions

8.2.4.1 Spindle Torque When Machining at a Specific Step—Tool Behaviour

To observe a tool behaviour, one should focus on a specific step and extract indicators from spindle torque sensors when machining. A specific step is depicted in Fig. 8.5, where the red curves correspond to the tool change phases and the cyan curve shows phases where *Z*-axis is moving. The blue curve represents the *Z*-axis position.

As shown by the *Z*-axis position, this step consists of successive drilling operations. In Fig. 8.6, the spindle torque associated to this step is represented by the

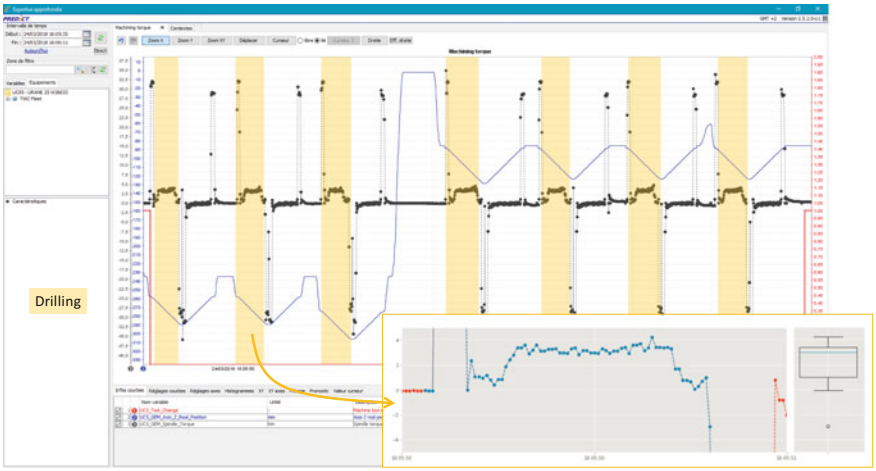

Fig. 8.6 Spindle torque behaviour in drilling operation: full drilling step (back) and zoom in spindle torque behaviour in a specific drill (front)

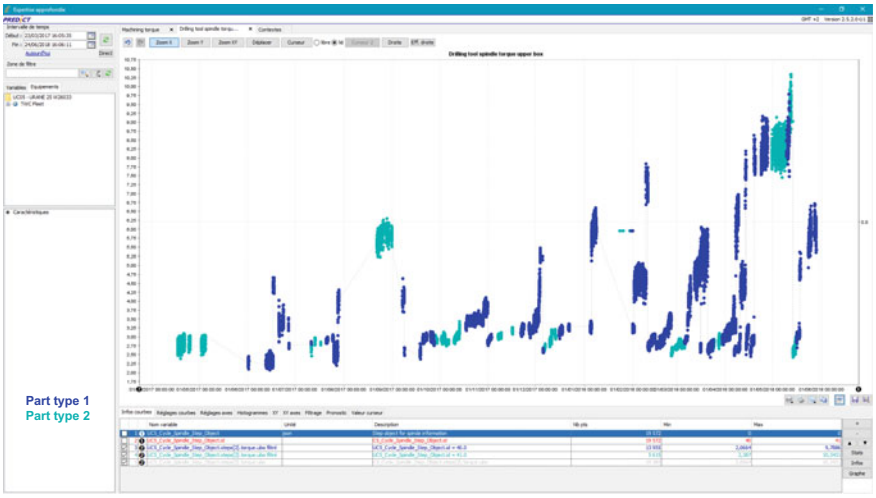

Fig. 8.7 Spindle torque drilling upper box indicator for a specific tool

black curve. To capture the tool usage behaviour within this step, the drilling operation should be analysed only when the tool is cutting the workpiece. These phases are marked by the yellow areas.

As shown in the detailed view of Fig. 8.7, the upper box data is a good representation of tool behaviour drilling. The evolution of this indicator with time is plotted in Fig. 8.7.

This example shows the evolution of tool behaviour, characterized by spindle torque upper box, for a machine programmed to produce two types of workpieces, part 1 and part 2. Each data on the graph represent the spindle torque upper box. Thanks to this indicator, it can be observed:

– Tool changes: ruptures are visible each time the tool is replaced.
– Tool wearing: for each new tool, the indicator's value is around 3 Nm and increases with use.

8.2.4.2 Axis Thrust When Axis Is Moving Linear—Axis Dynamic Behaviour

An axis linear move is composed of three phases: acceleration, linear displacement and deceleration. These steps are visible observing the axis position as illustrated in Fig. 8.8. The monitoring of axis thrust, illustrated by the black curve, during acceleration and deceleration phases gives an overview of the dynamic efforts required by an axis to move.

Hence, the following indicators may be extracted:

– Lower whisker characterizes *X*-axis thrust required to accelerate.
– Upper whisker characterizes *X*-axis thrust required to decelerate.
– Mean gives an indicator of axis balance.

In Fig. 8.9, the evolution of *X*-axis dynamic behaviour is represented, characterized by the mean thrust. A specific move for each processed part type has been defined. The exact same conditions could not be found between the two parts types'

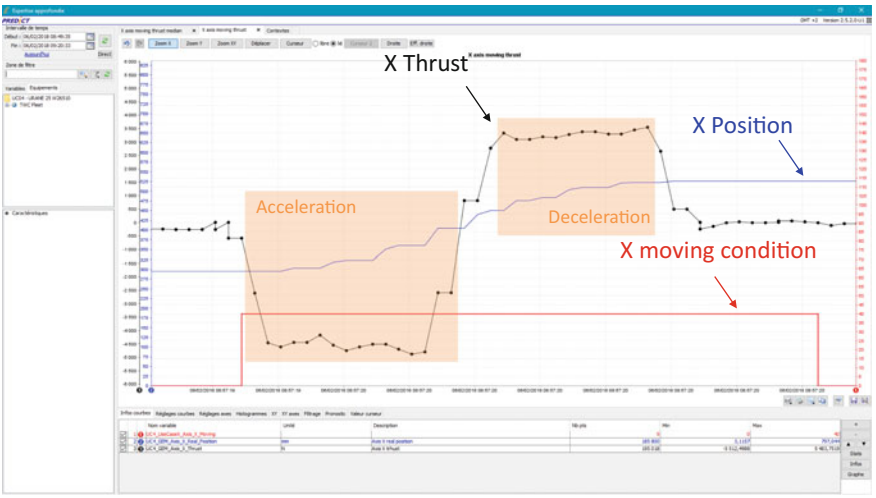

Fig. 8.8 *X*-axis moving thrust behaviour

Fig. 8.9 *X*-axis moving mean thrust

operations, leading to different values for the same indicator depending on the part being operated. For each move, the indicator analysis gives the same observation: with the use of the machine, *X*-axis thrust centre drifts until a certain point and then resets to the initial value. The breaking point is in fact due to a maintenance operation, leading to the conclusion that the value decrease was due to the axis degradation.

8.3 Machine Tool Characterization Tests

The analysis of indicators obtained from raw measurements during conventional machining operation is sometimes difficult, especially when trying to determine the condition of the machine tool. Perturbations, like the machining process itself, can hide the real performance of the machine tool. In addition, it is sometimes difficult to get repetitive movements from which comparable indicators can be obtained, especially in small batch sectors like aerospace.

In this line, a characterization procedure for machine tools has been defined, validated and implemented in Twin-Control project. The objective is to provide the opportunity to the end-user to perform a very simple and fast characterization of the machine tool, under controlled conditions. This way, a periodic checking is possible, leading to a better track of machine tool condition over time.

Next, the different proposed tests are presented.

8.3.1 Diagonal Positioning Error Measurement

The aim of this test is to determine the volumetric performance of a machine tool through a fast and reduced procedure. To achieve a volumetric performance indicator, diagonal positioning measurement is done in two diagonals of the machine tool. This way, it can be known if machine continues under specifications or not. The measuring procedure is based on an indirect method; it means that not just positioning error of each of the three linear axes is achieved, but perpendicular error between each pair of axes too.

This measuring procedure is suitable for three axes machine tools without moving table (bed type, column type, gantry type) or rotary axis. Moreover, the considered range is between 400 and 20,000 mm for the largest axis length of a machine tool.

As a reference, four measurements per year are suggested, one every three months. However, depending on the results of the volumetric performance indicator, architecture of the machine and workshop ambient conditions, the frequency of the tests could be varied and adapted on each case.

Diagonal positioning measurement in medium-large machine tools requires from an interferometry laser-based measuring system with the capacity to do the tracking of a mirror/retroreflector placed on the machine tool spindle. Either laser tracer or laser tracker measures the relative movement/displacement of a retroreflector from the initial point, based on their interferometry laser-based system. Both measuring devices can track a retroreflector placed on the machine tool´s spindle, allowing the measurement of machine tools movement in a fast and easy way, without special set-ups or fixing tools. This is the main advantage compared with common laser interferometry, which requires a tricky set-up process for this kind of measuring procedures where several axes of the machine tool are interpolated to create a special diagonal.

The measuring procedure is based in the ISO 230-6 [2] and consists of measuring two opposite diagonals carried out by the machine, such as B1-E1 and G1-D1 in Fig. 8.10. A diagonal positioning machine cycle needs to be programmed with stops at, at least, four equidistant points per metre. If the measuring range is short, the number of points should be higher. Indeed, not only the spatial position of the machine is measured, but also the distance between predefined (objective) points.

ETALON AG provides the most suitable software to manage this measure, Trackcheck [3]. If it is connected to the machine tool and measuring device, it automatically detects machine stops to perform a measurement. When the measurement has been successfully completed, the software calculates the mean bi-directional positional deviation which is graphically represented. A report summarizing the results is also provided.

This test provides a quick view of the geometric condition of the machine tool, but its aim is not to provide quantitative data. If the results show deviation with respect to reference values, a complete volumetric measurement should be performed to map the geometric errors of the machine tool and to be able to compensate them.

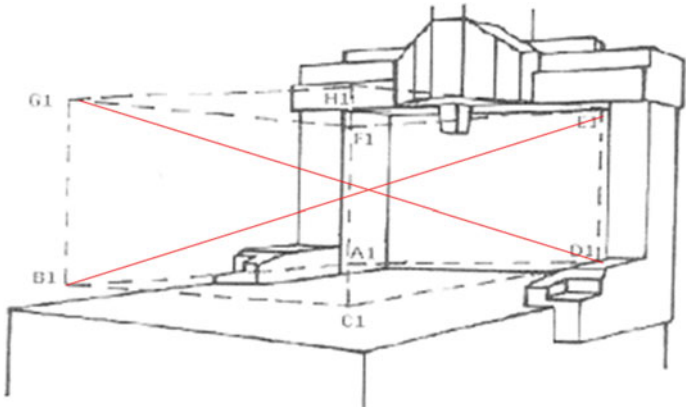

Fig. 8.10 Two opposite diagonal measurements [2]

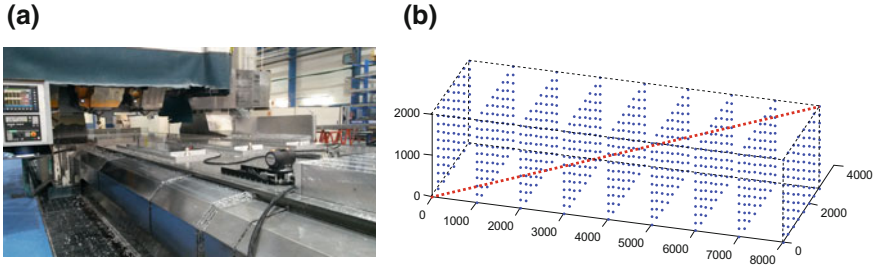

Fig. 8.11 Validation of diagonal error measurement test: **a** laser tracker installed in GEPRO 502 machine; **b** example showing the measurement points needed for the complete volumetric characterization (blue) and the diagonal measurement (red)

This procedure has been validated in different machines. Next, the results obtained in one of the use cases from the aerospace validation scenario, GEPRO 502 machine (Fig. 8.11a), are presented. As indicator, maximum value of the mean bi-directional positional deviation (xi) is obtained from the measured diagonal, according to [1], for each measured point. In all cases, results obtained in a complete volumetric error characterization, with a test time of around 10 h, are compared against an error measurement in a machine diagonal, with a duration of around 30 min (Fig. 8.11b).

Figure 8.12 shows the results obtained for the GEPRO 502 machine with the complete volumetric characterization and the diagonal measurement. A direct correlation between both measurements exists since the machine tool's maximum volumetric positioning error is between 250 and 300 μm for both cases. When validating diagonal measurement against the volumetric mapping of each machine, it can be concluded that positioning error correlates properly between results, but perpendicularity does not. It seems that the model that converts diagonals into positioning and perpendicularity errors does not fit to the model of the volumetric error modelling. Anyway, for

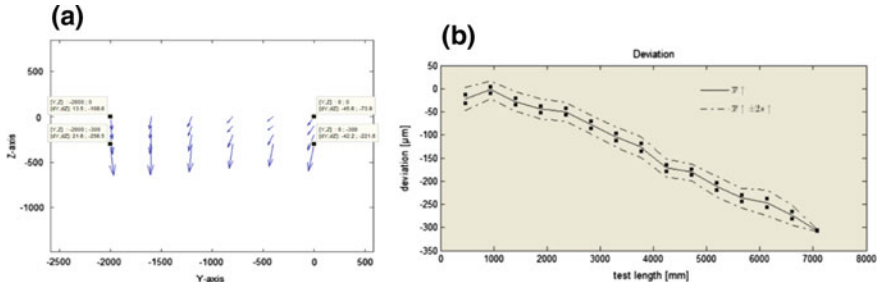

Fig. 8.12 Error measurements obtained in the GEPRO 502 machine: **a** complete volumetric characterization—*YZ*-plane; **b** space diagonal

a qualitative detection of machine geometric performance's deviation, the proposed test is valid.

8.3.2 Artefact Measurement Using Touch Probe

The main objective is to carry out a fast and reliable "health check" of the machine geometric performance, verifying whether the relative position/orientation between the machine tool coordinate system and the working volume is within the expected tolerances, using an artefact as a reference for the measurements.

The procedure consists of measuring the centre or position of several features (e.g. spheres) of an artefact located in the working volume with the touch probe and the corresponding software that allows doing the measurement. The proposed measuring process is automatic (using a CNC macro) and suitable to have the chance to export the results from the CNC.

A KONDIA MAXIM machine tool, located at IK4-TEKNIKER (Fig. 8.13a), has been used to validate this test. This machine has a moving table where the artefact is mounted and fixed during the measurements (Fig. 8.13b). In addition, the KONDIA machine provides the possibility to use a Renishaw touch probe with external software (Power Inspect) [4].

As cited above, a calibrated artefact located and fixed on the machine tool volume is measured to analyse the geometrical stability of the machine tool. The artefact is comprised of four spheres, and these geometries are measured each time to assess their position according to machine tool coordinate system and thermal environmental conditions. During the measurements, temperature is monitored to establish a relationship between the dimensional measurements and thermal ones.

For the validation, the measurements have been repeated over a certain period (24 h) to study the effect of thermal variations. After the tests, data are processed to correlate the geometrical instability with the thermal environmental condition variation. The result depicted in Fig. 8.14 shows the deviation of the position of the

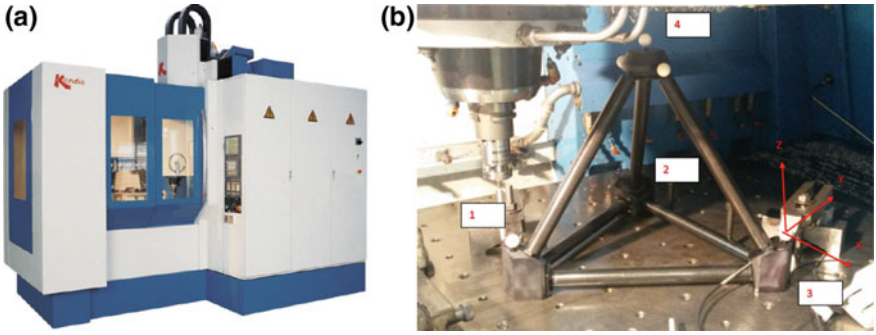

Fig. 8.13 **a** KONDIA MAXIM machine tool; **b** artefact mounted in the machine

four spheres of the artefact during part of the validation process. It can be observed that the positions of the sphere centres measured by the machine and the touch probe are not stable according to temperature variations. The measurements registered for 9 h clearly prove that the coordinate system of the machine tool and therefore its kinematics are not constant against thermal influences.

For an increase in T^a of approximately 5 °C (comparing to the starting state), the maximum drift of the machine is established in Z-direction (inverse to gravity direction) and is around 60 μm. Moreover, as all the centres present the same behaviour, a lack of stability of the artefact is discarded. The drift in X- and Y-directions is lower than in Z-direction for this kind of machine tool.

With these results, it can be concluded that the indicator, maximum deviation in X–Y–Z of any of the spheres for a certain temperature will be enough to determine the thermal stability of the machine. If the obtained indicator is above the determined threshold, to be characterized before, the machine will need to be examined in deep.

8.3.3 Dynamic Stiffness Measurement of Tool/Part

The objective of this test is to control the dynamics stiffness of the machine tool. A hammer test is proposed to evaluate the dynamic performance of the machine tool [5].

On the one hand, the force sensor at the hammer serves to provide a measurement of the amplitude and frequency content of the energy stimulus that is applied to a test object. On the other hand, accelerometers are used to measure the machine's structural response due to the hammer force. A single triaxial accelerometers located at the spindle will be used. A multichannel Fast Fourier Transform (FFT) analyser is needed to carry out the signal acquisition, sensor conditioning and FFT processing.

If possible, both excitation and measurement will be carried at the machine tool spindle. Different resonant frequencies must be identified and characterized with the following indicators: frequency, dynamic compliance, damping ratio and direction of excitation.

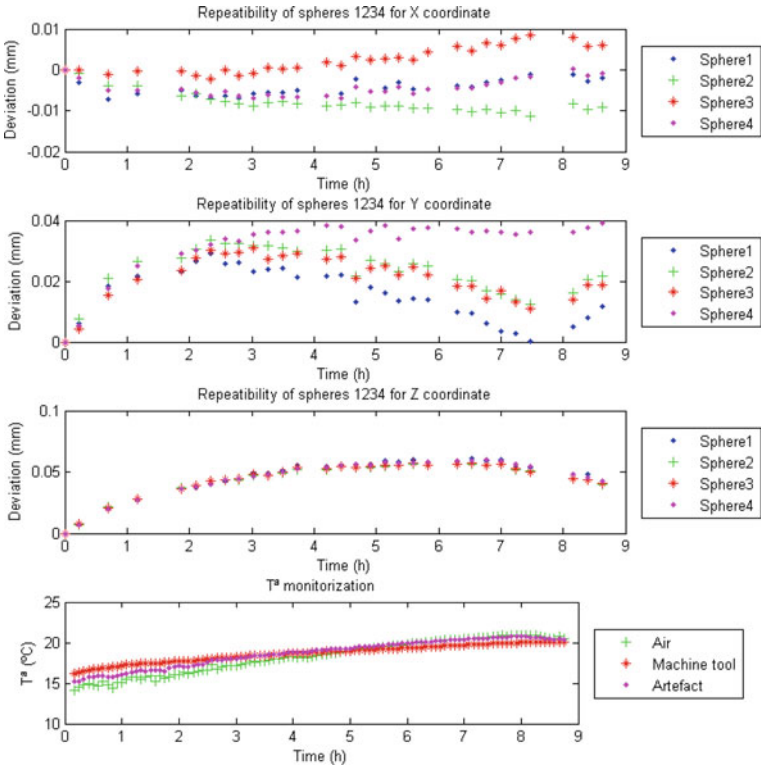

Fig. 8.14 Results of sphere positioning variation and temperature variation

A complete modal analysis has been carried out on the GORATU D-Dynamic machine located in IK4-TEKNIKER. Modal analysis consists of the experimental identification of vibration mode frequencies and the correspondent mode shapes. To do that, the machine is hit by a hammer and the vibrations are measured by accelerometers located in all the structure of the machine as depicted in Fig. 8.15.

Figure 8.16 presents the frequency response of the different points of the machine in *X*-direction when the disturbance, i.e. hammer force, is also done in *X*-direction. Two main resonance frequencies are identified, at 82 and 124 Hz. When using a single accelerometer at the tool tip, which is the aim of the proposed test, the frequencies will be accurately identified, since the obtained curve is part of the bunch of curves presented in the previous part. However, the measurement of a single point will not be enough to represent vibration mode shapes, but this is not the aim of the proposed periodic measurement.

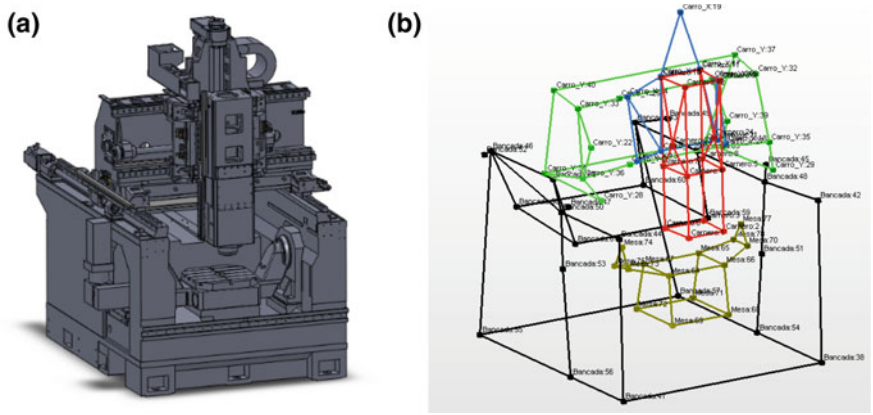

Fig. 8.15 Validation of dynamic stiffness characterization in the GORATU G-Dynamic: **a** diagram showing structural components; **b** points where accelerometers were located

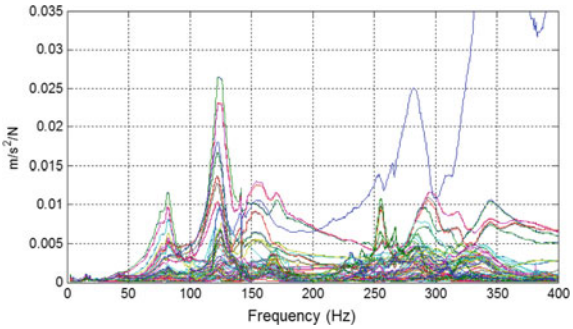

Fig. 8.16 Frequency response diagram showing vibrations of the different points of the GORATU machine in X-axis when excited in X-axis

8.3.4 Feed Drive and Spindle Auto-Characterization

In this case, a very fast characterization of the dynamic response of the feed drives and spindles of the machine tool is proposed. The idea is to execute very simple movements under controlled conditions while monitoring internal variables of the machine tool. The proposed sequence of movements is:

1. Back and forth displacement of each linear axis.
2. Circular interpolation of each pair of axes.
3. Spindle rotation at constant speed.

Each movement is a simplification of a more complicated test. For example, circular interpolation and the monitoring of internal position sensors is a simplification of the ball-bar test [6], which is commonly applied for machine tool geometric evaluation. Ball-bar test requires a specific hardware to track the position of the spindle

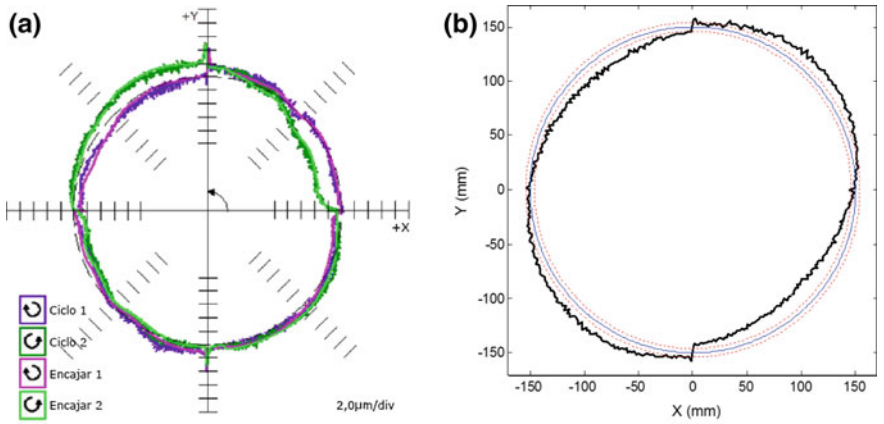

Fig. 8.17 Validation of the circular interpolation test from the feed drive auto-characterization procedure. Results obtained in a circular interpolation of the *X*- and *Y*-axes of the GORATU G-Dynamic machine: **a** results from the report available after the ball-bar test; **b** results obtained by using internal sensors for measurement

Table 8.2 Comparison of the indicators obtained in the circularity tests

	Ball-bar (µm)	CNC (linear scales) (µm)
Reversal peaks	2.5	2
Backlash	0.5	4
Circularity	8.3	10

during a circular interpolation. In Fig. 8.17, a report generated by a ball-bar device during a circular interpolation is compared with the results obtained in the same test by using linear scale position.

Table 8.2 summarizes the most important indicators obtained with both approaches to analyse circular interpolation performance. Although the simplified approach does not provide a quantitative estimation of the desired indicators, it provides an approximate idea and can be used for a qualitative analysis. The internal control variable measurement approach is not aimed to replace the ball-bar test to determine interpolation performance of the machine tool, but to provide the chance to quickly evaluate changes in the performance of a machine tool without installing the required hardware.

The complete sequence of movements is programmed in ISO code and is fed to the machine. By making use of monitoring capabilities implemented in Twin-Control project [7], data are continuously acquired during the test. The monitored data are uploaded to the fleet server, where it is processed to obtain relevant indicators like friction, backlash, inversion peaks and maximum power in feed drives, and power consumption in spindles. If an accelerometer is installed in the spindle, vibration analysis can be performed, providing relevant indicators to estimate its condition [8].

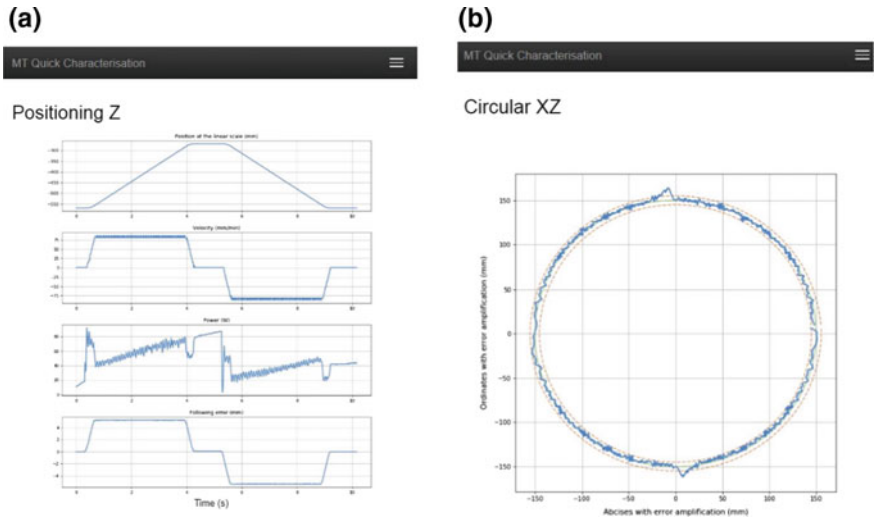

Fig. 8.18 Sample of the machine tool characterization test report generated on KASEM® after the auto-characterization: **a** linear translation of the *Z*-axis; **b** Circular interpolation of *X*- and *Z*-axes

The results of the tests are available in the cloud platform, KASEM®, just after tests execution. Indicators are managed together with the rest of indicators coming from the normal operating condition of the machine and, in case a deviation from nominal conditions of the machine tool is detected, a warning is generated. Apart from that, after each test execution a report is generated where the obtained indicators are summarized, and the user can analyse in detail the performance of each test as shown in Fig. 8.18.

The proposed test is totally automated and does not require special skills to machine tool operator nor special equipment. Test duration can vary depending on machine size, number of axis and dynamics, but it is always below 5 min.

Although the proposed procedure is not aimed for a quantitative characterization of the machine, it is very well suited for a qualitative analysis of machine tool condition. In addition, the short duration and its simplicity make it suitable for a periodic execution, leading to a better control of machine condition during its life cycle.

8.4 Conclusions

The behaviour of a machine tool is observable by computing contextualized information from sensors measurements. Two indicator extraction methodologies were described in this section. The first one exploits the in-production sensors' measurements to extract statistical features from specific machine operating conditions, and

the second one exploits the results of specific tests, called characterization tests, performed by the machine.

Both methodologies are based on known machine context exploitation. To have a full overview of the machining process and capacities, it is recommended to analyse indicators from both methodologies:

- The raw sensors' measurements indicator extraction offers high volume of data and is performed in parallel of the production. Nevertheless, the machine capabilities observed depends on the program performed such as indicators that illustrate only a part of the machine capabilities.
- The characterization test approach allows to observe the overall machine tool capacities as entire axis moves are performed under controlled conditions. Nevertheless, it requires to perform a specific program interrupting the production for about five minutes.

References

1. Tlusty, J.: Dynamics of high speed machining, ASME J. Eng. Industry **108**, 59–67
2. ISO 230-6.: Test code for machine tool—Part 6: setermination of positioning accuracy on body and face diagonals (Diagonal displacement tests) (2002)
3. http://www.etalon-ag.com/en/products/lasertracer/
4. http://www.hexagonmi.com/products/software/software-for-portable-measuring-arms/powerinspect
5. ISO 230-8.: Test code for machine tools—Part 8: Determination of vibration levels (2010)
6. Čep, R., Malotová, S., Kratochvíl, J., Stančeková, D., Czán, A., Jakab, T.: Diagnosis of machine tool with using Renishaw ball-bar system. MATEC Web Conf. **157**, 01006 (2018)
7. Armendia, M., Euhus, D., Peysson, F.: Twin-control: a new concept towards machine tool health management. In: 3rd European Conference of the Prognostics and Health Management Society. Bilbao, Spain, 5–8 July 2016
8. Olabarrieta, E., Konde, E., Guruceta, E., Armendia, M.: New approach for bearing life cycle control. In: 6th International Conference on Through-life Engineering Services, TESConf 2017, Bremen, Germany, 7–8 November 2017

Chapter 9
Non-intrusive Load Monitoring on Component Level of a Machine Tool Using a Kalman Filter-Based Disaggregation Approach

Johannes Sossenheimer, Thomas Weber, Dominik Flum, Niklas Panten, Eberhard Abele and Tobias Fuertjes

9.1 Introduction and Motivation

Today's society is increasingly concerned with ecological awareness in order to protect the environment. The political and social discussions focus on greenhouse gas emissions and rising global average temperatures. Furthermore, the total world consumption of primary energy is estimated to increase by 28% between 2015 and 2040 [1]. For that reason, the EU climate strategy aims to gradually reduce greenhouse gas emissions and increase the share of renewable energies, combined with improvements in energy efficiency [2].

As almost half of the global primary energy demand in 2017 will be caused by the industrial sector [3], there is considerable room for action to achieve the mentioned EU climate goals [2]. Progressive digitalization plays a major role here, as it offers the potential to make production processes more energy efficient. Furthermore, optimization approaches can be identified by transparent energy flows [4]. Within the

J. Sossenheimer (✉) · T. Weber · D. Flum · N. Panten · E. Abele
PTW TU, Darmstadt, Germany
e-mail: j.sossenheimer@ptw.tu-darmstadt.de

T. Weber
e-mail: t.weber@ptw.tu-darmstadt.de

D. Flum
e-mail: flum@ptw.tu-darmstadt.de

N. Panten
e-mail: panten@ptw.tu-darmstadt.de

E. Abele
e-mail: info@ptw.tu-darmstadt.de

T. Fuertjes
MARPOSS Monitoring Solutions GmbH, Egestorf, Germany
e-mail: tobias.fuertjes@mms.marposs.com

M. Armendia et al. (eds.), *Twin-Control*,
https://doi.org/10.1007/978-3-030-02203-7_9

Twin-Control project, which develops new concepts for simulating machine tools and the machining processes, the presented work was developed. These models, which are developed within this project, show both, the possibilities of making production processes more energy efficient and also take other life cycle characteristics such as the optimization of maintenance into account [5].

Measuring energy[1] values is an essential prerequisite for implementing energy efficiency measures through

- comparisons with other plants, departments, assembly lines, machines, components over time,
- defining adequate control measures to react early on to deviations/inefficiencies,
- setting and pursuing realistic targets and
- providing information on energy or power demands, costs, emissions and trends.

One way to obtain measured values is by applying temporary mobile measurements. Mobile measurements give an overview of the energetic status quo of a machine tool. Nevertheless, for comprehensive analyses of the machine's components, the use of stationary, permanent in-depth monitoring is better suited. In order to obtain performance data for the individual components, a distinction can be made between two methods:

(1) Hardware-based measurements (intrusive)
(2) Non-intrusive measurement techniques.

Hardware-based measurements of power and energy at component level require high investments in sensors and the associated devices. Non-intrusive measurement methods such as non-intrusive load monitoring (NILM) or non-intrusive appliance load monitoring (NIALM) [6] can be a cost-effective solution for obtaining detailed energy data using a power disaggregation. The NILM measurement method can detect individual devices within the performance data by analysing voltages and currents from a higher-level single point of measurement. Since the individual devices have different properties for steady-state and transition states in both reactive and active power, these so-called *energy signatures* can be used to assign the measured power to an individual component. At the point of common coupling (PCC), the loads of the devices are superimposed and then the individual curves are extracted from the aggregated data by pattern detection algorithms. In addition, control data of inferior components can be used to estimate the individual load using system identification approaches [7]. In this way, the Kalman filter-based disaggregation approach presented in this chapter allows a continuous energy monitoring at component level of machine tools with only one sensor needed at the machine tool's electric PCC.

[1] In this chapter, the electrical energy and electrical power are meant, when energy and power are mentioned.

9.2 Related Work

Several NILM solutions have already been developed in recent years within the residential sector [6, 8–11]. They are used to derive the energy demand of home applications such as refrigerators, lamps, vacuum cleaners, televisions and toasters. The energy data calculated by the NILM method may not be as accurate as the measured data, but it is sufficient in most cases for energy monitoring applications. For industrial applications, there are no comparable approaches of energy disaggregation and only few publications exist [7, 12–14]. Furthermore, in typical production environments, there are many sources of interference for NILM systems, such as basic electrical appliances and highly dynamic devices. One example is a speed-controlled motor with inverters, which may inhibit the deployment of disaggregation systems [12]. To minimize disturbances in industrial applications and to improve the accuracy of the algorithm, the machine states can be correlated to the aggregated power curves as proposed in [7, 13]. Since machine data acquisition (MDA) in modern production manufacturing facilities is already frequently used to calculate key performance indicators (KPIs) or to plan maintenance cycles, this strategy is particularly helpful. Thus, available industrial big data helps to provide better insight into the machine's energetic performance by applying power disaggregation algorithms.

9.3 Kalman Filter-Based Disaggregation Approach

The goal of the Kalman filter is to determine system states as accurately as possible, which can only be calculated and measured with an uncertainty. The Kalman filter works with a prediction step and a correction step. In the prediction step, the desired states of a system are calculated using a state-space model. In the meantime, the uncertainty of the result is calculated from the initial uncertainty (covariance) and an estimation error representing the inaccuracy of the calculation. In the correction step, the estimated value and the measured value are compared, while both contain an inaccuracy. The estimated value and the uncertainty can be set using R. E. Kalman's algorithm as shown in [15].

9.3.1 NILM Through Kalman Filter-Based Power Disaggregation

For the application of the Kalman filter to the energy disaggregation problem of a machine tool, the electrical power consumption of each auxiliary unit is defined as a condition to be determined. There is no state-space model with which the electrical power can be estimated. Furthermore, the individual states cannot be measured directly. Only the total power (P_{total}) consumed by the machine tool is measured by

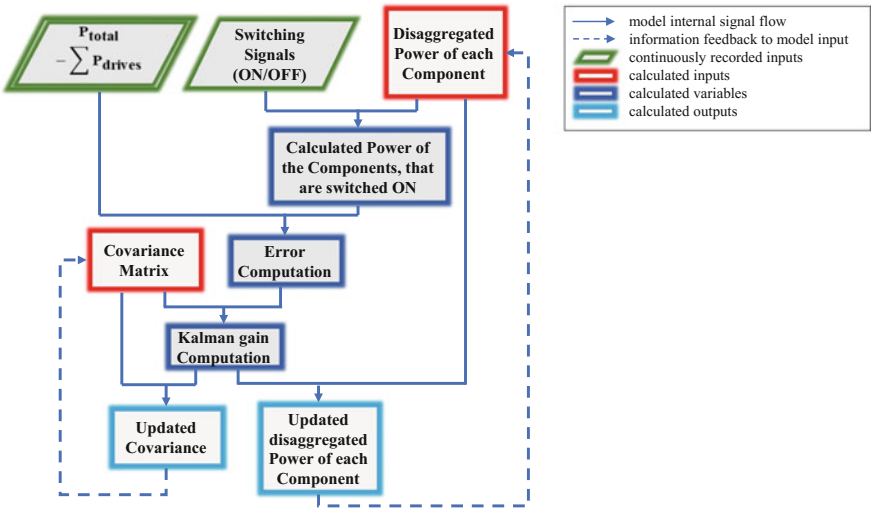

Fig. 9.1 Information flow chart of the applied Kalman filter

an external sensor. In addition, PLC data such as the power of each drive (P_{drive}) and the switching states (on/off) of the individual auxiliary units is used.

The states are updated according to the equations of R. E. Kalman via the so-called Kalman gain by comparing the sum of the power of all switched-on auxiliary units with the total power consumption subtracted by the accumulated power of the drives. The updated states are now used as the basis for a new comparison with the total output of the auxiliary units. Following this procedure, the states are updated successively. An overview of the Kalman filter-based power disaggregation approach is schematically displayed in Fig. 9.1.

9.3.2 Differentiation of Dynamic and Constant Electrical Power Consumers

There are two different consumption patterns for the auxiliary units. On the one hand, there are systems, which are also referred to constant consumers, and on the other hand, there are dynamic consumers. Constant consumers have a uniform performance plateau, which can be determined relatively accurately with the presented approach. In contrast, the power consumption of dynamic consumers, like speed-controlled motors, fluctuates even without a change of state. Other than consumers with constant power consumption, dynamic consumers are assumed to have an uncertainty within the measurements, whereby the inaccuracy (covariance) of the respective state is maintained. For constant loads, the uncertainty of the static loads converges towards zero as time progresses. This means that the performance allocated to the system is

increasingly less affected by fluctuations in the measured total power, while dynamic loads continue to allow performance adjustments.

9.3.3 Extension of the Kalman Filter Using Peak Shaving and Damping Factors

The algorithm for this application case has been extended to counteract undesirable developments. To improve the convergence for constant loads during the teach-in process, a damping factor and a peak shaving factor were introduced.

A single damping factor has been assigned to all auxiliary units with constant consumption behaviour, which artificially reduces the uncertainty of the respective states. Negative consumption, i.e. the generation of energy, is excluded in the model due to the unlikely occurrence. On this account, the Kalman gain must not lead to a negative state. By implementing a nonnegative condition in the filter, the resulting deviation of measured total power and the sum of the switched-on aggregates is distributed to other aggregates. In the case that the approximate power consumption of the auxiliary units or their dynamics is known, this information can be taken into account.

The peak load factor was introduced to neglect peak loads that occur when the ancillary units are started up from the disaggregated power. For this purpose, the initial condition is held for a few seconds after the component has been switched on, before the actual teach-in process begins. Otherwise, the load peak would falsify the teach-in process. Errors in the teach-in phase due to peak loads can thereby be avoided. Apart from the distinction between dynamic and statistical loads, and if available the average consumption of the components, no further user input is required for the presented approach.

9.4 Implementation and Validation of the Presented NILM Approach

The online monitoring is implemented by integrating the disaggregation algorithm into an existing process and tool monitoring system called Genior Modular of MARPOSS Monitoring Solutions GmbH. This monitoring system can be supplemented with additional sensors by adding additional transmitters. In this case, a transmitter for measuring the total power consumption of the machine is connected to the Genior Modular via CANopen communication. The integration of embedded software, like in this case the disaggregation algorithm, is realised by an additional OPR device of MARPOSS Monitoring Solutions GmbH. Because an existing data acquisition and analysis architecture can be used, the effort for the user and costs are reduced. In this

way, the Kalman filter-based disaggregation approach can be simply retrofitted on existing machine tools.

An exemplary application on the EMAG VLC100Y CNC turning machine is presented in this chapter. This machine is located in the model factory for energy efficiency (ETA-Factory) on the campus of the Technische Universität Darmstadt in Germany. The turning machine is controlled by a programmable logic control (PLC) from Bosch Rexroth, which records the required switching states of the units and the power consumption of the drive units via OPC-UA communication. The modelled power consumption can be visualized locally on a HMI or transferred to a higher-level platform. In addition to power consumption modelling at the component level, an analysis of the available data is also included.

The turning machine contains the following auxiliary units:

- hydraulic pump
- chip conveyor
- cooling lubricant pump
- suction
- electric control cabinet
- combined other consumers.

The hydraulic pump, the suction and the electric control cabinet are classified as a constant consumer, while the cooling lubricant pump is a dynamic consumer. Both consumer types are constantly switched on during machining. The chip conveyor is a constant consumer which is switched on or off sequentially during the manufacturing process. All other dynamic and constant auxiliary units of the machine tool are summarized under combined other consumers. These combined other consumers are attributed with higher measurement uncertainties than normal consumers. In addition, the measurement uncertainty is increased or, respectively, decreased with each switch-on or switch-off process in order to absorb the load peak that occurs.

For the validation of the presented non-intrusive load monitoring approach with a Kalman filter-based disaggregation, a temporary mobile measurement was conducted. The results of the disaggregation are compared to measured mean power signals of the listed auxiliary units in Fig. 9.2. The corresponding evaluation results are discussed in the following sections and are shown in Table 9.1. Besides the measured mean power consumption, the mean disaggregated power consumption, the corresponding root mean square deviation as well as the relative error are listed for all auxiliary units. The root mean square deviation and the relative error are calculated according to Eqs. (9.1) and (9.2), respectively. The relative error is the quotient of root mean square deviation and the measured power at switched-on component state.

$$\text{root mean square error} = \sqrt{\frac{\sum_{i=1}^{N} \left(P_{\text{measured}\,i} - P_{\text{disaggregated}\,i}\right)^2}{N}} \tag{9.1}$$

$$\text{relative error} = \frac{\text{root mean square error}}{P_{\text{measured (when switched on)}}} \tag{9.2}$$

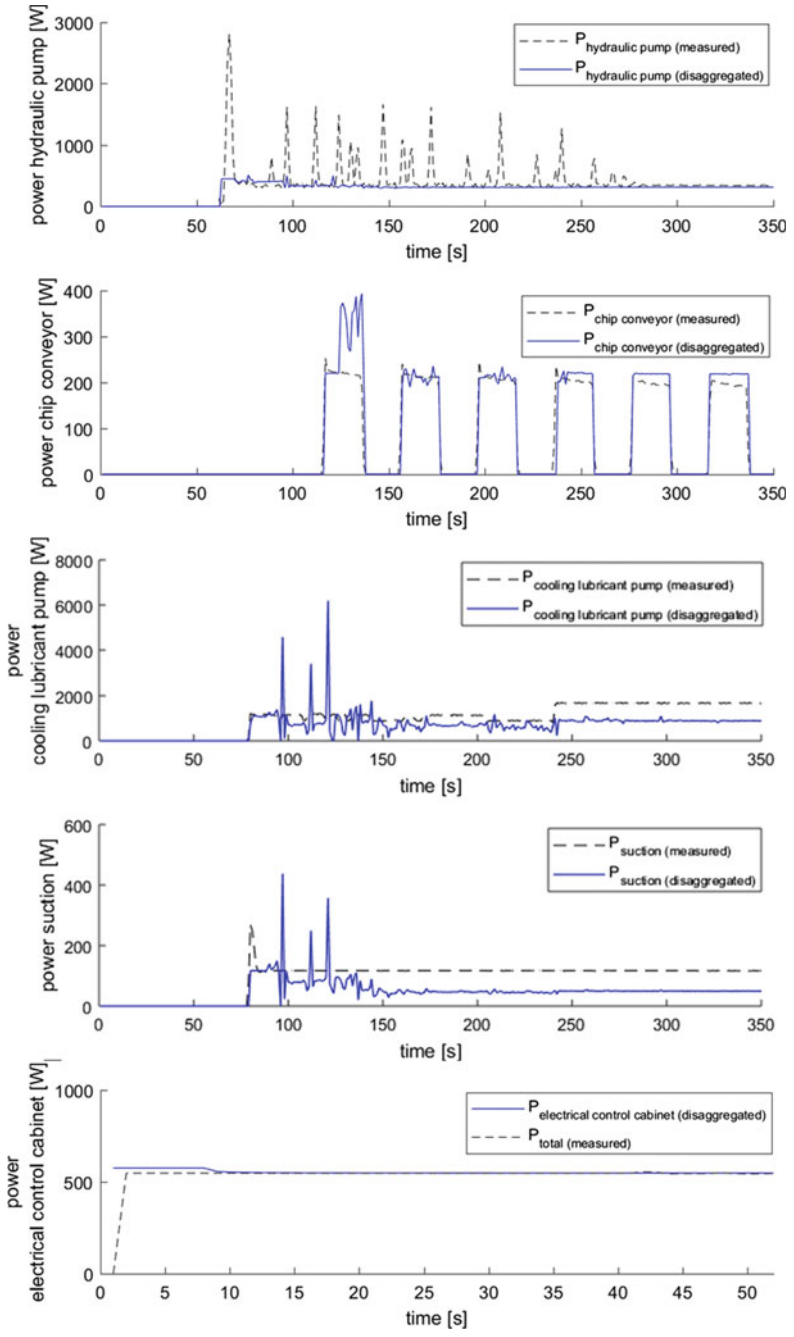

Fig. 9.2 Comparison of disaggregated and measured power for the auxiliary units with the corresponding switching states

Table 9.1 Evaluation results of the Kalman filter-based disaggregation approach on the EMAG VLC100Y turning machine

Auxiliary unit of the machine tool	Consumer type	Mean measured power consumption[a] [W]	Mean disaggregated power consumption[a] [W]	Root mean square deviation [W]	Relative error [%]
Hydraulic pump	Constant	448.5	328.29	114.2	25.5
Cooling lubricant pump	Dynamic	1288.0	847.7	439.4	34.1
Chip conveyor	Constant	201.0	229.47	12.1	6.0
Suction	Constant	535.3	551.8	49.8	42.2
Electrical control cabinet	Constant	546.3	551.8	16.9	3.1
Combined other consumers	Dynamic	Not measureable	1368.1	–	–

[a]The mean includes only power signals at switched-on component state

Since the hydraulic control of the turning machine is an accumulator charging control, the measuring signal (first diagram in Fig. 9.2) has large peak loads that can be attributed to the reloading of the hydraulic accumulator. Since the hydraulic unit is defined as a constant load, these load peaks are not transmitted to the disaggregated signal. Even when defining the hydraulic pump as a dynamic consumer, these sudden peaks cannot be assigned to a single component without additional information about the hydraulic recharging process. Instead, these load peaks are now distributed among the dynamic consumers, but the major part of the peak is attributed to the combined other consumers due to its higher measurement inaccuracy. In order to integrate the hydraulic load peaks into the disaggregated power, an additional model input signal would be necessary which describes the state of the hydraulic accumulator charging process. These inaccuracies explain the high relative error, but when neglecting the load peaks in the measured signal, the base load of the hydraulic pump was met very well with the disaggregation.

The example of the chip conveyor clearly shows how the sensitivity of the algorithm decreases over the time in which the component is switched on (second diagram in Fig. 9.2). While the disaggregation is initially falsified by other disturbances during the first switch-on process, the required power of the chip conveyor is better met during the subsequent switching processes and is ultimately properly trained. The teach-in phase can be better used with sequentially switched consumers, since the individual switching processes are each accompanied by the interference of varying intensity, which is why the actual power requirement is met more accurately.

The measurement data of the cooling lubricant pump (third diagram in Fig. 9.2) shows an example of a component that requires several energy levels within one manufacturing cycle. This is because the cooling lubricant is fed through nozzles of different sizes, depending on the tool used and the current machining process. In this case, a higher power level is reached after about 240 s. From this time on, the cooling lubricant is sprayed in large quantities and at high pressure to rinse away chips from the workpiece during the milling process. Different power levels could be differentiated by taking into account the nozzles switching signals. In this case, the classification of the cooling lubricant pump as a constant consumer would be recommended.

The disaggregated power curve of the suction (fourth diagram in Fig. 9.2) shows how the load peak factor prevents a falsified training due to the initial load peak, which is almost twice as high as the later power consumption. Nevertheless, the further disaggregated power curve is subject to strong fluctuations, and the trained-in disaggregated power is far too low, which primarily results from the load peaks of the hydraulic accumulator charging circuit. For this reason, the disaggregated power consumption of the suction has a high relative error.

The constant energy requirement of the electrical control cabinet can only be trained at the beginning of the measurement. Here, the machine is in an energy-reduced standby mode, which is why all auxiliary units are switched off and only the control cabinet is supplied with power. After about 55 s, the machine is switched to the machining mode and the auxiliary units are turned on successively. At this point in time, the algorithm has already trained the power of the electrical control cabinet due to the damping factor. The disaggregated power and the measured power correlate well (fifth diagram in Fig. 9.2), which is also visible in the low relative error of the component.

In general, the accuracy of disaggregation increases if the individual components are switched on one after the other and have enough time for the teach-in process. However, this is not always possible due to the technical restrictions and the request for short cycle times. The delay of the switching processes of the auxiliary units during the examined turning process is shown in Fig. 9.3. To obtain more precise results, the individual components could be switched on and off one after the other, starting from the standby state of the machine, in which they are initially all switched off. As this is rarely possible in industrial environments and because the goal was to find an automated procedure, which does not require a manual teach-in process, this method has been dispensed within this series of tests.

9.5 Conclusion and Outlook

The presented cost-effective disaggregation approach to monitor the energy consumption at component level is possible through the use of a Kalman filter with the information of the component's switching states and the overall power consumption. The approach was tested on a laboratory machine tool and validated with a

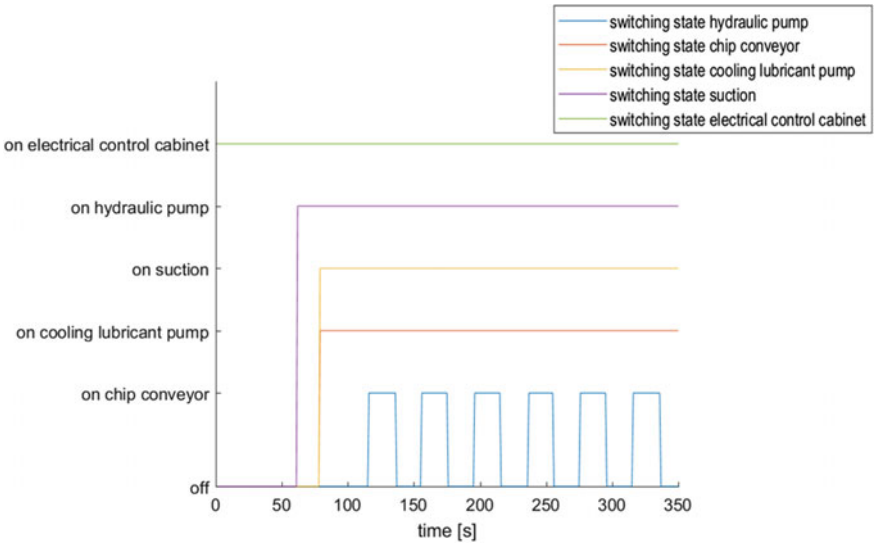

Fig. 9.3 Illustration of the switching states of the auxiliary units over one production cycle

temporal measurement of the component's power consumption. Based on the evaluation results, the limitations of the concept are shown. For example, load peaks, which often arise in hydraulic accumulator charging circuits due to recharging of the accumulator, need further input signals related to the hydraulic recharging process in order to obtain more precise disaggregation results. The distribution of these load peaks to other components can distort the disaggregation results. The advantages of the disaggregation of cyclical loads are discussed, as well as the relevance of the switching state correlation of the individual auxiliary units.

Even if an exact power disaggregation of industrial components is difficult, the presented approach offers a cost-effective and simple possibility to estimate the energy demand on component level. Further investigations are necessary to decrease the influence of the limitations in order to increase the accuracy of the power disaggregation.

References

1. U.S. Energy Information Administration: International Energy Outlook 2017. Available online at https://www.eia.gov/outlooks/ieo/pdf/0484(2017).pdf (2017). Checked on 11/28/2017
2. European Commission: Climate Strategies & Targets. Available online at https://ec.europa.eu/clima/policies/strategies_en (2017). Updated on 11/27/2017, checked on 11/28/2017
3. Exxon Mobil Corporation: 2017 Outlook for Energy: A View to 2040. Irving, Texas. Available online at http://cdn.exxonmobil.com/~/media/global/files/outlook-for-energy/2017/2017-outlook-for-energy.pdf (2016). Checked on 11/28/2017

4. Posselt, G.: Towards Energy Transparent Factories, 1st edn. (2016) (Sustainable Production, Life Cycle Engineering and Management). Available online at http://dx.doi.org/10.1007/978-3-319-20869-5
5. Armendia, M.: Twincontrol. A New Concept for Machine Tool and Machining Process Performance Simulation. Available online at http://twincontrol.eu/wp-content/uploads/sites/11/2016/05/twincontrol-flyer.pdf (2016). Checked on 11/28/2017
6. Hart, G.W.: Nonintrusive appliance load monitoring. Proc. IEEE **80**(12), 1870–1891 (1992). https://doi.org/10.1109/5.192069
7. Panten, N., et al.: A power disaggregation approach for fine-grained machine energy monitoring by system identification. Procedia CIRP **48**, 325–330 (2016). https://doi.org/10.1016/j.procir.2016.03.025
8. Froehlich, J., et al.: Disaggregated End-Use Energy Sensing for the Smart Grid. IEEE Pervasive Comput. **10**(1), 28–39 (2011)
9. Iyer, S.R., et al.: Energy disaggregation analysis of a supermarket chain using a facility-model. Energy Build. **97**, 65–76 (2015). https://doi.org/10.1016/j.enbuild.2015.03.053
10. Sankara, A.: Energy Disaggregation in NIALM Using Hidden Markov Models. Missouri University of Science and Technology, Rolla, Missouri (2015)
11. Zoha, A., et al.: Non-intrusive load monitoring approaches for disaggregated energy sensing. A survey. Sensors (Basel, Switzerland) **12**(12), 16838–16866. https://doi.org/10.3390/s121216838 (2012)
12. Trung, K.N., et al.: An innovative non-intrusive load monitoring system for commercial and industrial application. In: Xuan-Tu, T. (Hg.) International Conference on Advanced Technologies for Communications (ATC), pp. 10–12, Hanoi, Vietnam, pp 23–27 (2012)
13. Gebbe, C., et al.: Estimating machine power consumptions through aggregated measurements and machine data acquisition. AMM **655**, 61–66 (2014). https://doi.org/10.4028/www.scientific.net/AMM.655.61
14. Wichakool, W., et al.: Smart metering of variable power loads. IEEE Transac. Smart Grid **6**, 189–198 (2015)
15. Marchthaler, R., Dingler, S.: Kalman-Filter. Available online at, Einführung in die Zustandsschätzung und ihre Anwendung für eingebettete Systeme (2017). https://doi.org/10.1007/978-3-658-16728-8

Chapter 10
Utilizing PLC Data for Workpiece Flaw Detection in Machine Tools

Johannes Sossenheimer, Christoph J. H. Bauerdick, Mark Helfert, Lars Petruschke and Eberhard Abele

10.1 Introduction

Digitization is rapidly changing our entire economy and our society. The number of connected devices, like IT infrastructural connected objects, sensors and programmable logic controllers (PLCs) [1], is currently increasing rapidly [2]. Thus, until 2020 the number of devices connected to the Internet is expected to rise to eight billion [3]. This applies not only to the areas of household, traffic and mobility, infrastructure and buildings, but also to the industry. Data is currently considered the most valuable resource [4] and is even called "gold of the future" [5].

Larger industrial companies have recognized the value of their own production data and are using different analytic methods to improve the production process. Despite this, small- and medium-sized enterprises still have great difficulties in collecting and utilizing production data.

Internal machine data such as PLC and bus data can be used not only for process control, as is usually the case, but also for condition and quality monitoring, as well as energy efficiency [1]. In addition, data analysis can prevent high economic losses due

J. Sossenheimer (✉) · C. J. H. Bauerdick · M. Helfert · L. Petruschke · E. Abele
PTW TU, Darmstadt, Germany
e-mail: j.sossenheimer@ptw.tu-darmstadt.de

C. J. H. Bauerdick
e-mail: bauerdick@ptw.tu-darmstadt.de

M. Helfert
e-mail: helfert@ptw.tu-darmstadt.de

L. Petruschke
e-mail: petruschke@ptw.tu-darmstadt.de

E. Abele
e-mail: info@ptw.tu-darmstadt.de

M. Armendia et al. (eds.), *Twin-Control*,
https://doi.org/10.1007/978-3-030-02203-7_10

to late detection of workpiece flaws. A diagnosis of insufficient workpiece quality on a machine tool can be categorized into the following five groups [6]:

- Observations by the user of the machine,
- Diagnosis by measuring and testing equipment,
- Diagnosis by testing workpieces,
- Diagnosis by additional sensors,
- Model based or signal analytical diagnosis.

Conventional quality control systems can only be applied to randomly chosen samples and are cost-intensive and error-prone. As a consequence, monitoring systems are more and more automated. For these monitoring systems, only the diagnosis with additional sensors as well as model based or signal analytical diagnosis is utilizable [6]. These types of diagnosis allow an early detection of workpiece flaws as well as an identification of their causes [7]. As scrap is reduced, the safety, reliability and profitability of products are improved as well [8].

As described in [9], monitoring systems are divided into direct and indirect measuring systems, depending on whether the parameters to be monitored are observed directly (e.g. cutting force in machine tools) or indirectly via correlated data. For example, measurements of the spindle's power consumption can be correlated to the cutting forces [9–11]. Because the environmental influences and the usage of cooling lubricant impedes direct measurements in machine tools, indirect monitoring systems are usually used. As the costs for additional sensors have to be minimized [12], this article focuses on signal analysis diagnostics using machine internal sensors, such as those which are used within the drives.

Furthermore, there are some model-based prediction methods for surface roughness in machining processes [13, 14], but there are no known methods for identifying typical workpiece flaws from pre-processing like moulding or forging. Typical flaws of these pre-processes are listed in [15, 16]. Based on previous work, which showed that workpiece flaws can be detected through drive-based PLC data [1], this chapter outlines an automated method for monitoring workpiece quality using machine drive-based signals in machine tools. Because the analysed signals are sensitive to tool wear, this aspect is examined in the second part of this chapter.

10.2 Automated Quality Monitoring Using Drive-Based Data

In order to show the automated workpiece flaw detection method, a test series, which is subdivided into preliminary and main tests, is examined in this chapter. The preliminary tests investigate the face turning of a solid cylinder for various cutting parameters and are used to develop a statistical concept for automated flaw diagnosis. Within the main tests, the developed concept is applied to a real production process, in which different machining steps of a control disc for a hydraulic pump, which is manufactured at the ETA Factory, a model factory for energy and resource

Table 10.1 Relevant processing steps with the appendant machining parameters of the main tests

Processing step	Cutting velocity v_c	Cutting depth a_p	Feed rate f
	[m/min]	[mm]	[mm/rev]
Exterior scrubbing	180	2.0	0.3
Face scrubbing	180	2.0	0.3
Exterior finishing	300	0.2	0.25
Face finishing	300	0.2	0.25

efficient production at the Technische Universität Darmstadt, is analysed. The solid cylinder is made of 42CrMoS4 and the forged brute of the control disc of 8CrMo16.

Workpiece flaws like for example blow holes, shrink holes and incorrectly placed boreholes are simulated in the tests by boreholes of different sizes. The machine tool on which the tests are undertaken is a vertical turning machine of type EMAG VLC100Y with a Bosch Rexroth PLC of the type Motion Transfer Extreme (MTX). Table 10.1 shows the relevant processing steps and parameters of the control disc manufacturing process which is examined in the main tests.

10.2.1 Information Flow and Evaluation Process

To control the movements of the axis, the actual values of the machine drives are constantly measured at the frequency inverter and transmitted to the PLC via the fast automation bus Sercos. The signal flow and the evaluation workflow are shown in Fig. 10.1.

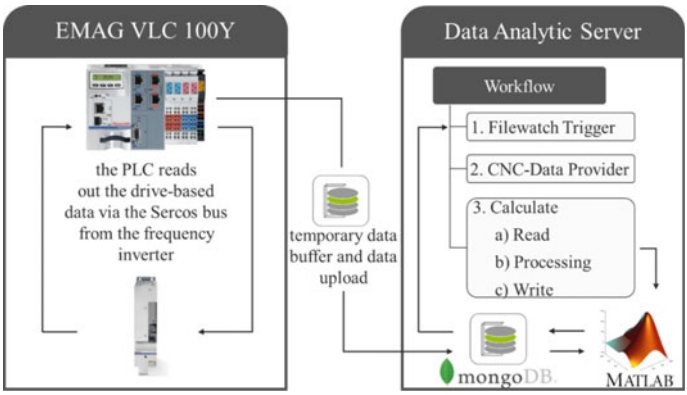

Fig. 10.1 Signal flow and the evaluation workflow

The drive-based signals are read out at a sampling rate of 2 ms with a software called MTX efficiency workbench (EWB). This data is buffered until the end of the measurement. In parallel, the Data Analytic Server (DAS, formerly Generic Data Server), a workflow-based software framework by Bosch Rexroth introduced in [1], detects the end of the recording with a filewatch trigger and executes a workflow consisting of the CNC-DataProvider and a computational activity. The CNC-DataProvider imports the buffered EWB data into the database used by the DAS called MongoDB. In the next step, the calculate activity evaluates this data using a precompiled MATLAB DLL which contains the necessary MATLAB functions for workpiece flaw diagnosis and writes the diagnostic results back into the MongoDB. This workflow-based evaluation method enables fully automated workpiece flaw analysis in parallel to the production.

10.2.2 Sensitivity Analysis and Signal Processing Steps

A sensitivity analysis was carried out to select appropriate drive-based signals for evaluation. Available signals include the current values of position, speed, power, force and momentum of each axis. In addition to the actual position of the spindle, which is needed to locate the flaw on the workpiece, the following five signals form a feature vector that represents the input for the analysis:

- The current position value of the x-axis
- The current position value of the y-axis
- The current position value of the z-axis
- The current spindle power value
- The process force of the x-axis, which is the only feed axis during the tests.

While the current position of the axis is measured directly at the engine encoder and the process force is derived from a model, the actual power of the axis is calculated by measuring the DC link voltage and current at the frequency inverter [17]. As a result, it was found that the interference caused by the flaw can be detected in a better way in the five signals by analysing the difference between the averaged last three signals and the currently measured signal. This formula is represented in Eq. 10.1, where i is the number of the currently measured signal. The resulting calculated signal calc.signal oscillates about zero and is not affected by the scale of the signal's trend.

$$\text{calc.signal}_i = \frac{\sum_{j=1}^{3} \text{signal}_{i-j}}{3} - \text{signal}_i \tag{10.1}$$

The peaks of the signals caused by the flaws can be easily detected in the calculated signal, as depicted in Fig. 10.2. The calculated signal for the five analysed characteristics is plotted over the radius of the workpiece for the facing process of the full cylinder, whose bores have a diameter of 2.0, 1.5 and 1.0 mm, respectively,

at a distance of 9, 18 and 27 mm to the workpiece centre. Three empirically chosen tolerance bands, which are divided into multiple sections, mark a certain standard deviation to the mean value of the currently measured signal. The advantage of dividing the tolerance bands into equidistant sections is the ability to detect small flaws even if the noise's amplitude varies over the workpiece radius.

10.2.3 Workpiece Flaw Detection

A diagnosis of workpiece flaws includes an identification of the flaw, a localization on the workpiece and a quantification of the flaw.

Possible workpiece flaws are detected if the calculated signal exceeds the narrowest tolerance bands. With the corresponding actual position information of the feed and spindle axis, the potential workpiece flaws are localized in the next step. In order to quantify the potential workpiece flaw, a new parameter called intensity of diagnosis IoD was introduced. The IoD indicates the accuracy of the flaw diagnosis and the distribution of the IoD over the workpiece's surface can give more detailed insight into the flaw's size. According to Eq. (10.2), the IoD is the quotient of the number of features F that simultaneously manifest a trespass of the smallest tolerance band and the total number of features F_{tot} multiplied by the quotient of the number of the largest tolerance band T of all features that was trespassed and the total number of tolerance bands T_{tot} times one hundred. If the workpiece shows frequent and locally concentrated of measurements with a high IoD,

$$\text{IoD} = \frac{F}{F_{\text{tot}}} * \frac{T}{T_{\text{tot}}} * 100 \tag{10.2}$$

After the evaluation of the drive-based data, the results of the workpiece flaw analysis, their position and quantification are combined and transferred onto a virtual image of the workpiece, which is displayed in Fig. 10.3. If a potential flaw is identified, because its corresponding data points trespass one of the tolerance bands, the information of its location and its intensity of the diagnosis is mapped on the virtual workpiece image. Areas on the workpiece that show both a locally concentrated high frequency of flaw identifications and an IoD above 75% are thus caused by strong variations between the currently measured and previously measured signals, which clearly indicates a potential workpiece flaw. Areas on the workpiece surface with IoDs below 20% can be correlated to noise in the signal. High IoDs on the outer boards of the workpiece are due to deviations from a perfectly circular workpiece rotation, which is explained in greater detail in the following paragraphs. The virtual image is later transmitted to the machine operator and supports the quality control and source inspection process. As shown in a close-up view of the repartition of the IoD on the virtual image of the workpiece in Fig. 10.4, it is even possible to derive the diameter of the boreholes.

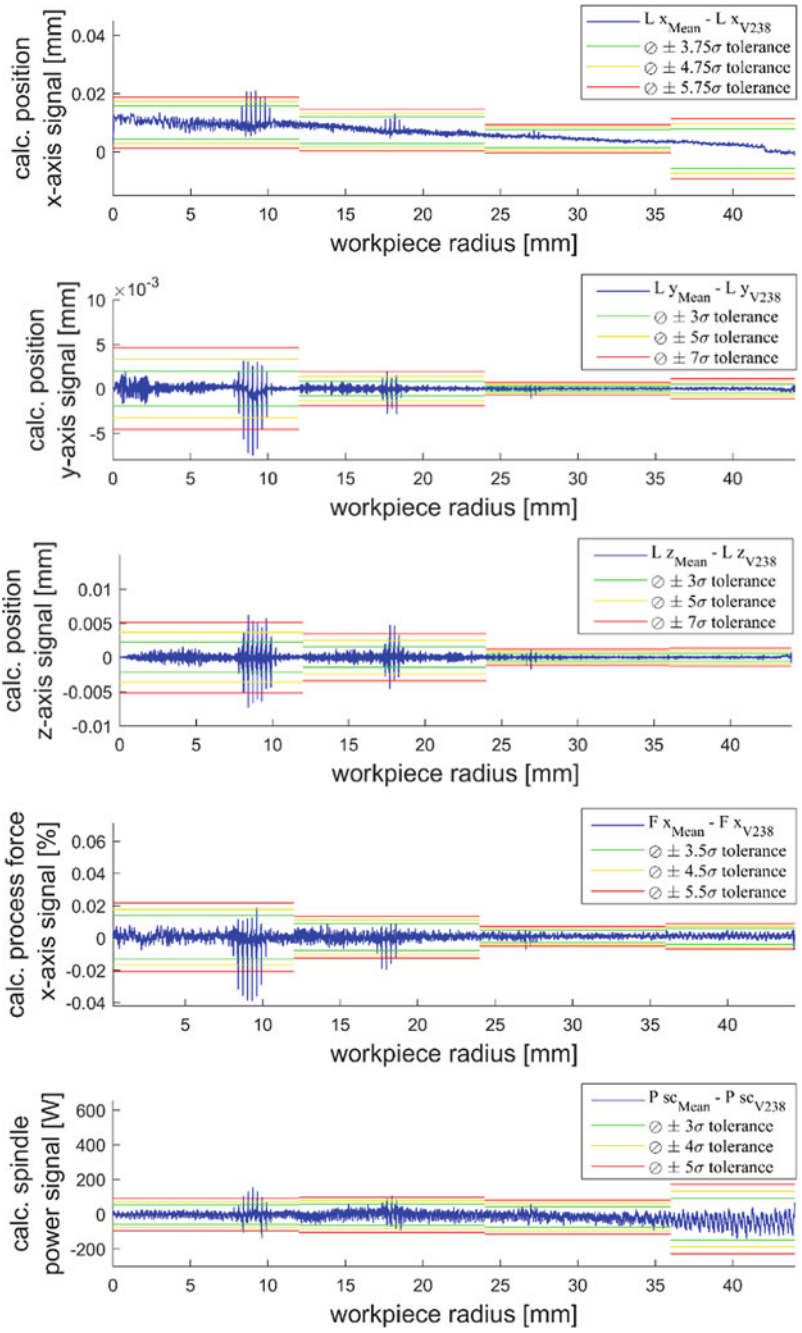

Fig. 10.2 Graph of the difference between the averaged last three signals and the currently measured signal of a full cylinder with three bores for the face turning process (in blue) over the workpiece radius. Additionally, tolerance bands in green, yellow and red which are divided into four sections surround the calculated signal

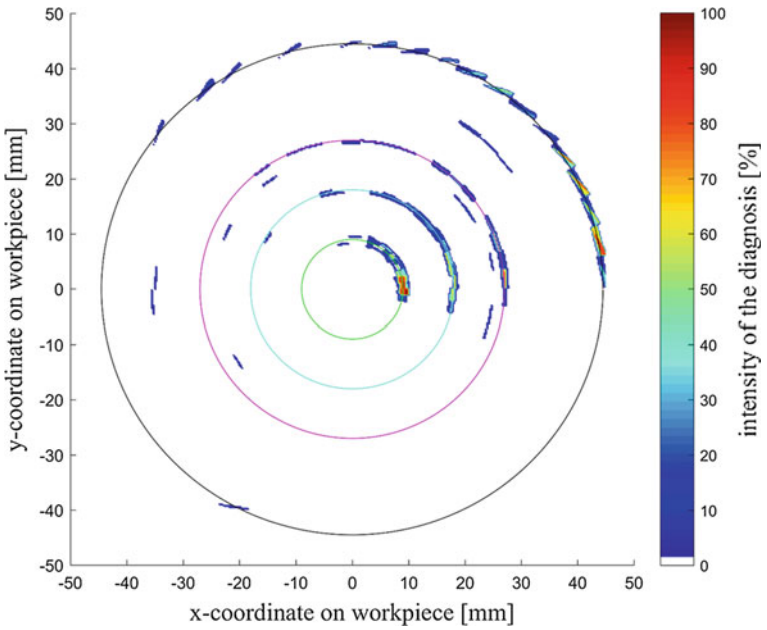

Fig. 10.3 Repartition of the intensity of the diagnosis *IoD* over the virtual image of the full cylinder end side, which is bordered by the blue line, during the face turning process. The green, magenta and cyan line mark the radial position of the three boreholes on the full cylinder

10.2.4 Evaluation and Limits of the Presented Concept

A diagnosis is considered to be accurate if the displayed intensities of the diagnosis at the corresponding locations of the virtual workpiece image match well with the size and position of the actual borehole. As explained in this section, the choice of the analysed process steps impacts whether the diagnosis delivers accurate results or not. A high-precision diagnosis was achieved both for the examined face turning process of the full cylinder and for the face scrubbing of the forged unmachined part of the control disc. The analysis of the face finishing process and the exterior scrubbing of the unmachined part resulted in an inaccurate diagnosis.

These differences in the accuracy of the diagnosis for the different process steps result from the great influence of the relation between the selected cutting parameters and the accuracy of the diagnosis. The diagnosis becomes less accurate at high cutting speeds and feed rates because less data is recorded over the workpiece surface. In addition, the quality of the diagnosis deteriorates at cutting depth of less than 1 mm because the plastic deformation of previous cutting steps reduces the effective size of boreholes.

The face scrubbing of the unmachined workpiece is characterized by moderate cutting speeds and feed rates with simultaneously high cutting depths. Therefore, the

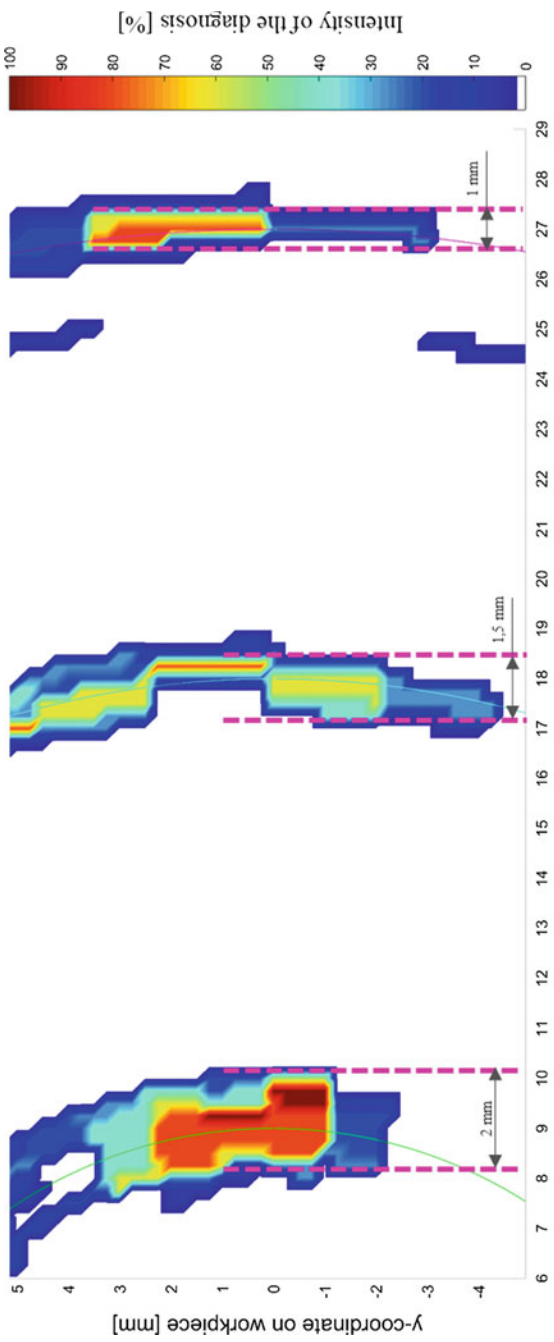

Fig. 10.4 Close-up view of the intensity of the diagnosis *IoD* on the virtual image of the workpiece, where the diameter of the boreholes is indicated by magenta-coloured dotted lines

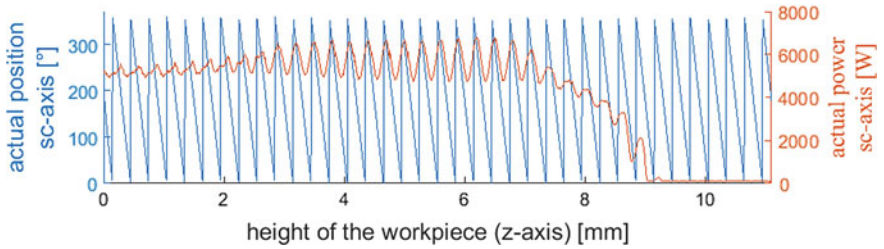

Fig. 10.5 Ratio between the actual spindle position in degree and the actual spindle power (sc-axis) over the height of the distance covered by the exterior scrubbing process

accuracy of the diagnosis proved to be better than with the finishing steps, which use high cutting speeds, low feed rates and very small cutting depths.

Flaws on the side surface of the unmachined part were not detected during the exterior scrubbing, because the flaw's influence on the signal is negligible compared to that of the initially not perfectly round rotating unmachined part. At each revolution of the workpiece, the signals of the five features show large oscillations due to the fact that the flaw, which is located at a covered distance of 7.7 mm form the exterior scrubbing process, cannot be identified. This is seen in Fig. 10.5, which shows the relation between the actual position and the power of the spindle. The flaw could have been detected in the second turning step if the exterior scrubbing process of the unmachined part was divided into two steps each with half of the current cutting depth.

Although the tool wear influence is reduced by focusing on the calculated signals based on the average of the last three cutting processes, noise from progressive tool wear is added to the signal. The noise increases the standard deviation of the signal and thus the size of the tolerance bands. This makes it more difficult to detect flaws in the workpiece.

10.3 Influence of Tool Wear on Machine Drive-Based Signals

In order to investigate the influence of the process parameters on the tool wear and to better understand the resulting surface roughness, further experimental series were executed. A face turning process is, therefore, conducted multiple times with different combinations of cutting parameters and analysed for their influence on tool wear, surface roughness and specific energy consumption. The investigated cylinder consists of 42CrMoS4 and GARANT CNMG120408-SG HB7035 inserts are used with a PCLNR 2525 M12 AFR231 tool holder. In these experiments, the already mentioned EMAG VLC100Y machine tool is used, and the surface roughness is measured after each test run with a mobile MarSurf Perthometer M2 measuring device. The process

parameters are selected with regard to the face scrubbing process of the hydraulic control disc in order to examine ten different cutting parameter combinations. Based on the basic process parameters listed in Table 10.1, one parameter is modified within a certain range, and the other two parameters are maintained constant (Table 10.2). Considering the differences between the material of the cylinder and the hydraulic control disc, a cutting depth (a_p) of 1.5 mm is used as basis.

As also [18, 19] describe, the main influence on tool wear results from an increasing cutting speed. An increase of the feed rate leads to an increase of the surface roughness but has no essential impact on the tool wear, which corresponds with the results of [18, 20]. By increasing the cutting depth neither the surface roughness nor the tool wear is affected significantly, as is also the case with [18, 21]. In accordance with [21, 22] an increase in each of the analysed cutting parameters leads to a reduction in specific energy consumption by increasing the material removal rate.

Furthermore, the impact of tool wear on the power consumption of the spindle is compared for two different combinations of cutting parameters. For this purpose, the cutting parameter combination A with a cutting speed of 180 m/min, a cutting depth of 1.5 mm and a feed rate of 0.3 mm/rev plus the cutting parameter combination B with a cutting speed of 220 m/min, a cutting depth of 1.5 mm and a feed rate of 0.3 mm/rev are chosen. For cutting parameter combination A, representative data rows of the face turning process after a different number of cuts of an insert are shown in Fig. 10.6. It is observable that the spindle power increases with increasing material removal due to tool wear.

In Fig. 10.6, the corresponding spindle power consumption for cutting parameter combination B is displayed. It is obvious that the power consumption varies between the first and 56th cut. Also, this cut represents the last cut for the tool before the test is completed. The latter is associated with a clearly higher power consumption, and the pattern shows irregularities which do not occur with an unworn cutting edge. Figure 10.6 also indicates that the processes with the cutting parameter combination B are shorter because of the higher cutting speed, but also have a higher power consumption because of the higher required spindle speed.

Besides the signals analysed in Sect. 2.2, the power consumption of the axis drives was evaluated for tool wear analysis. It is visible that a change is detected in the power consumption of the x-axis, y-axis and z-axis with increasing tool wear. The corresponding power consumption of the drives of these axes is shown in Fig. 10.7 for cutting parameter combination B. A significant deviation can be determined for

Table 10.2 Range of cutting velocity, cutting depth and feed rate

Cutting velocity v_c	Cutting depth a_p	Feed rate f
[m/min]	[mm]	[mm/rev]
160	0.5	0.15
180	1.0	0.2
200	1.5	0.25
220	2.0	0.3

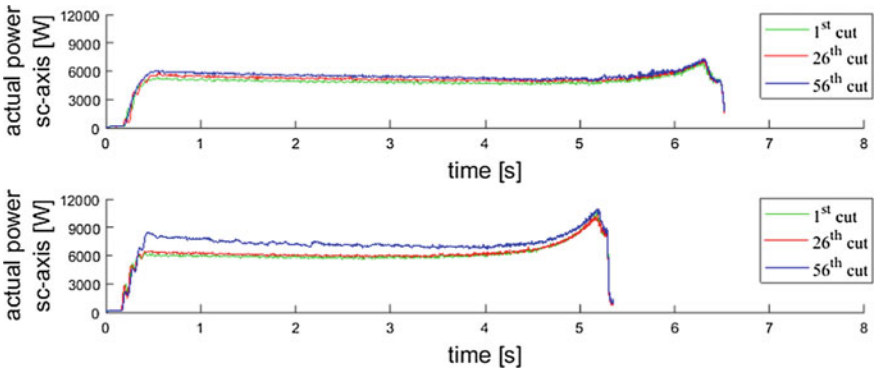

Fig. 10.6 Actual spindle power (sc-axis) with cutting parameter combination A (upper figure) and B (lower figure) according to different numbers of cuts

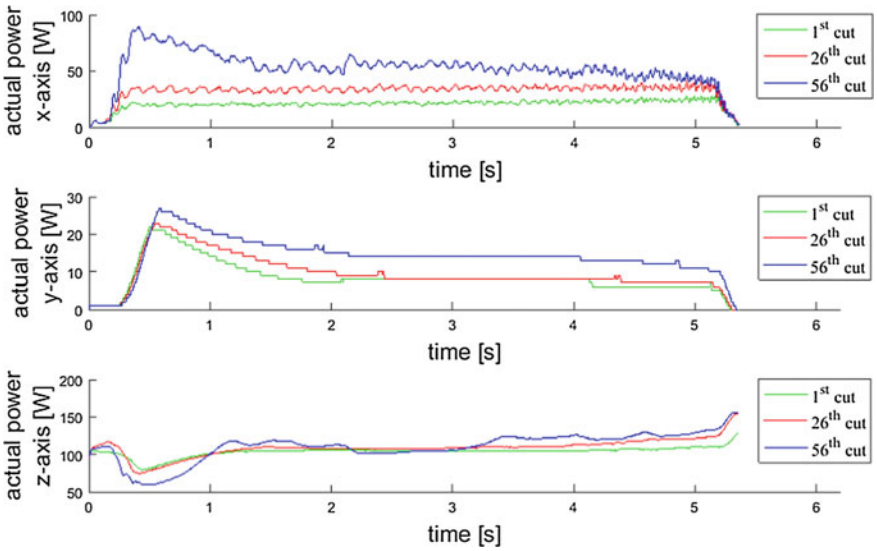

Fig. 10.7 Actual power of *x*-axis, *y*-axis and *z*-axis with cutting parameter combination B according to different numbers of cuts

the last cut of the *x*-axis. The curve shows both deviating and a higher level of the characteristic curves with a peak at the beginning of the process. Additionally, the power consumption curve of the *y*-axis changes with increasing tool wear. There is a shift to the right and when the tool wear is higher, the curve is at a higher level of power consumption. In contrast, the *z*-axis does not have higher power consumption, but in that case higher fluctuations in power consumption occur with increasing tool wear.

The data is collected in one measurement and is available both for improving the flaw detection algorithm by automatically adjusting the barriers as tool wear and with it signal noise increases, and for automatic and proactive identification of worn inserts.

10.4 Conclusions

This paper presents an automated approach to component failure diagnosis. For this, drive-based data are measured at high frequency and evaluated after completion of the recording. Workpiece flaws, like shrink holes, which are represented by boreholes of different diameters, can, therefore, be reliably detected, located and quantified. Following diagnosis, quality assurance is supported by purposefully prepared data as the display of a virtual image of the workpiece with the intensity of the diagnosis plotted at the corresponding position. In addition, investigations of cutting parameter combinations have shown that the cutting speed has a significant impact on tool wear. The increasing tool wear is clearly identifiable in the power consumption of the axis drives and the main spindle power. This information is useful for both, automated proactive tool replacement and improved flaw detection. The limitations of the concept, like the influence of process parameters and tool wear have been pointed out and offer starting points for future research.

Acknowledgements This chapter is based on the publication at Procedia CIRP (Volume 72, 2018, Pages 357–362) of the work "An automated procedure for workpiece quality monitoring based on machine drive-based signals in machine tools" presented by Christoph J. H. Bauerdick, Mark Helfert, Lars Petruschke, Johannes Sossenheimer and Eberhard Abele at the 51st CIRP Conference on Manufacturing Systems (https://www.sciencedirect.com/science/article/pii/S2212827118304165).

References

1. Bauerdick, C.J., Helfert, M., Menz, B., Abele, E.: A common software framework for energy data based monitoring and controlling for machine power peak reduction and workpiece quality improvements. Procedia CIRP **61**, 359–364 (2017)
2. Bundesministerium für Wirtschaft und Energie: Digitale Strategie 2025. http://www.de.digital/ (2016). Accessed 15 Dec 2017
3. Postscapes and Harbor Research: What Exactly is the Internet of Things? https://www.postscapes.com/what-exactly-is-the-internet-of-things-infographic/ (2014). Accessed 15 Dec 2017
4. The Economist: The World's Most Valuable Resource is No Longer Oil, but Data. The Data Economy Demands a New Approach to Antitrust Rules. Regulating the Internet Giants. https://www.economist.com/news/leaders/21721656-data-economy-demands-new-approach-antitrust-rules-worlds-most-valuable-resource (2017). Accessed 15 December 2017
5. Lohsse, S., Schulze, R., Staudenmayer, D.: Trading Data in the Digital Economy Legal Concepts and Tools. Nomos/Hart (2017)

6. Walther, M., Verl, A.: Antriebsnahe Maschinendiagnose. Zuverlässigkeit und Diagnose in der Produktion, Fortschritt-Berichte VDI, Düsseldorf (2007)
7. Tönshoff, H.K., Wulfsberg, J.P., Kals, H., König, W., van Luttervelt, C.A.: Developments and trends in monitoring and control of machining processes. CIRP Ann. **37**(2), 611–622 (1988)
8. Grosch, J.: Schadenskunde im Maschinenbau. Charakteristische Schadensursachen – Analyse und Aussagen von Schadensfällen. Kontakt & Studium 308. expert, Renningen (2014)
9. Wang, L. (ed.): Condition monitoring and control for intelligent manufacturing. Springer series in advanced manufacturing. Springer, London (2006)
10. Tlusty, J., Andrews, G.C.: A critical review of sensors for unmanned machining. CIRP Ann. **32**(2), 563–572 (1983)
11. Gontarz, A.M., Hampl, D., Weiss, L., Wegener, K.: Resource consumption monitoring in manufacturing environments. Procedia CIRP **26**, 264–269 (2015)
12. Weck, M., Plapper, V., Groth, A.: Sensorlose Maschinenzustandsüberwachung. VDI-Z integrierte Produktion, vol. 142 (2000)
13. Asiltürk, İ., Çunkaş, M.: Modeling and pre-diction of surface roughness in turning operations using artificial neural network and multiple regression method. Expert Syst. Appl. **38**(5), 5826–5832 (2011)
14. Kant, G., Sangwan, K.S.: Predictive modelling for energy consumption in machining using artificial neural network. Procedia CIRP **37**, 205–210 (2015)
15. Rossmann, A.: Probleme der Maschinenelemente erkennen, verhüten und lösen. Typische verfahrensspezifische Fehler, Probleme, Mechanismen 3. Turbo Consult, Karlsfeld (2012)
16. McEvily, A. J.: Metal Failures. Mechanisms, Analysis, Prevention (2002)
17. Bosch Rexroth, A.G.: Rexroth IndraDrive, Drive Controllers MPx-02; MPx-03; MPx-04. Parameter Description, Lohr a. Main (2006)
18. Rajemi, M.F., Mativenga, P.T., Aramcharoen, A.: Sustainable machining. Selection of optimum turning conditions based on minimum energy considerations. J. Clean. Prod. **18**(10–11), 1059–1065 (2010)
19. Camposeco-Negrete, C.: Optimization of cutting parameters for minimizing energy consumption in turning of AISI 6061 T6 using Taguchi methodology and ANOVA. J. Clean. Prod. **53**, 195–203 (2013)
20. Guo, Y., Loenders, J., Duflou, J., Lauwers, B.: Optimization of energy consumption and surface quality in finish turning. Procedia CIRP **1**, 512–517 (2012)
21. Helu, M., Behmann, B., Meier, H., Dornfeld, D., Lanza, G., Schulze, V.: Impact of green machining strategies on achieved surface quality. CIRP Ann. **61**(1), 55–58 (2012)
22. Mativenga, P.T., Rajemi, M.F.: Calculation of optimum cutting parameters based on minimum energy footprint. CIRP Ann. **60**(1), 149–152 (2011)

Part IV
Integration of the Twin Concept

Chapter 11
Simulation of Machining Operations Based on the VMT Concept

Frédéric Cugnon and Jean-Pierre Delsemme

11.1 Introduction

The simulation of machining operations in close interaction with the machine tool dynamic behaviour requires two main modelling components. First, to accurately simulate the dynamics of modern high-speed machine tools, a mechanical model that represents the flexibility of all components and their interactions is needed [1]. To create this mechatronic model of a machine tool (virtual machine tool), 3D MBS and FEA methods are used for mechanical aspects and 1D modelling for the CNC. As described in Chap. 2, an integrated methodology is proposed for the mechanical aspects, and it combines MBS capabilities in a nonlinear FEA [2] solver called SAMCEF Mecano [3]. It enables accurate modelling of the machine by considering FEA models of the components connected by a set of flexible kinematical joints. Additional models are implemented to deal with drive-trains and motors dynamics. Furthermore, an integrated cutting force model is used to capture force interactions between the tool and the workpiece to fully capture the dynamic behaviour of the machine tool. Within the scope of the Twin-Control project, the VMT concept was used to model two machines, a high-speed four-axes box-in-box machine from Comau and a large three-spindle five-axes machine from Gepro. The two models are shown in Fig. 11.1.

Furthermore, an integrated cutting force model is used to capture force interactions between the tool and the workpiece to fully capture the dynamic behaviour of the machine tool during the machining operations. This chapter deals with the integration of this cutting force model with the developed VMT module.

F. Cugnon (✉) · J.-P. Delsemme
Samtech S.a., a Siemens Company, Liège, Belgium
e-mail: frederic.cugnon@siemens.com

J.-P. Delsemme
e-mail: jean-pierre.delsemme@siemens.com

M. Armendia et al. (eds.), *Twin-Control*,
https://doi.org/10.1007/978-3-030-02203-7_11

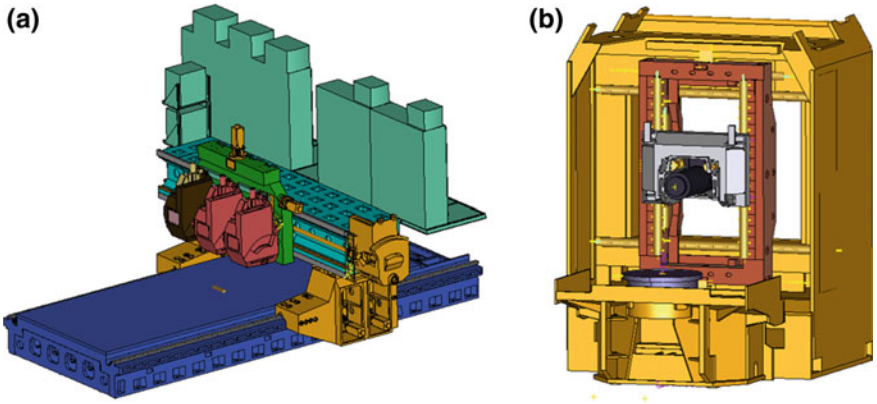

Fig. 11.1 Virtual machine tool models developed in Twin-Control project: **a** Gepro 502 machine; **b** Comau Urane 25V3 machine

11.2 Machining Module

The considered cutting simulation approach is compatible with the virtual machining paradigm. Derivation of the forces acting on the cutting edges of the milling tool is a two-step procedure. First, the geometric and volumetric properties of the removed material are computed. Second, process dependent heuristic is applied on the tool move spatial data to compute cutting force components. The process for obtaining cutting forces is illustrated in Fig. 11.2. This method is widely described in Chap. 3 of the book. This section focusses only on its integration in the Mecano software.

The cutting force module [4], originally developed in MATLAB, is converted to a single DLL to be called in the SAMCEF simulation. An overview of the cutting force module structure is shown in Fig. 11.3. The cutting force module is composed of three primary sections (labelled a–c in Fig. 11.3) which execute the key functions of the cutting force model. These sections are combined into a single module, and the different sections are only called as necessary using the desired RunFlag input value. The first step of the cutting force module, Fig. 11.3a, generates the discretized tool mesh based on the tool dimensions and mesh resolution data. The constant edge

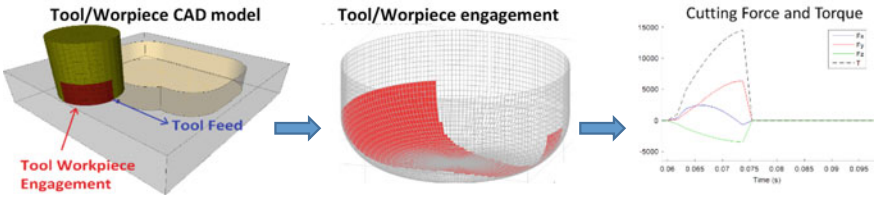

Fig. 11.2 Cutting force estimation approach

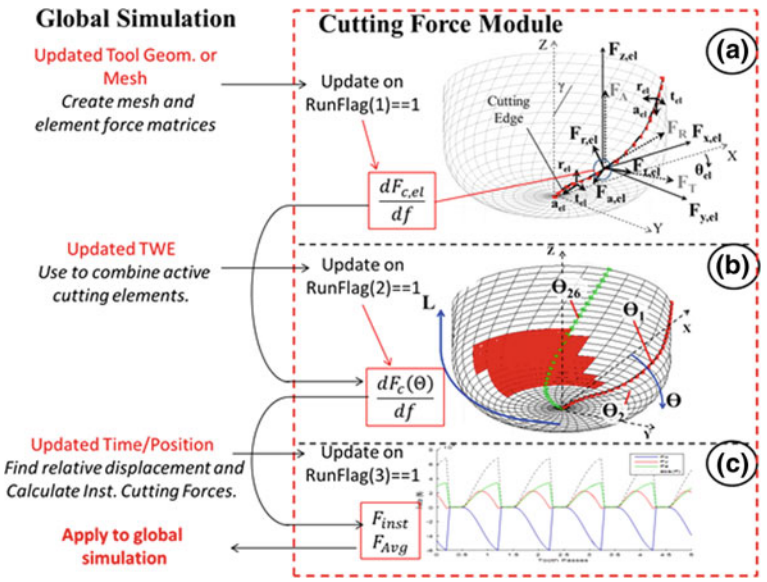

Fig. 11.3 General set-up of the cutting force module

effect vectors, $F_{e,XYZ,el}$, the cutting force matrices, $Q_{c,XYZ,el}$, are also generated in this first step. This first step is only called once at the beginning of the simulation and at each tool change. The second step, Fig. 11.3b, updates the TWE tool mesh and determines average cutting forces based on the nominal feed direction and feed per tooth. The second step of the module is called when the TWE obtained from the ModuleWorks module is updated. The third step, Fig. 11.3c, determines the instantaneous, angle-dependent cutting force based on the tool rotational speed and the current simulation time. Step three is called during for each SAMCEF iteration to access required instantaneous forces.

11.3 Coupling Architecture

The mechanical model of the machine tool is coupled with three additional simulation modules (Fig. 11.4). For the CNC modelling, a MATLAB Simulink model that is converted to C-code is used and included in a dynamic library thanks to MATLAB Coder capabilities. As the cutting force module is also based on MATLAB programming, the same approach of creating a dynamic library from C-code generated by MATLAB Coder is selected. The simulation C++ program for tool-workpiece engagement (TWE) computation is also converted to a dynamic library that can be called from C-code functions.

In SAMCEF Mecano, two specific elements have been developed to manage these dynamics libraries. The first one, called DIGI element, allows coupling the mechanical model to any Simulink model and, in particular, control systems. The implemented staggered method is a fixed time step sampling, where both codes will exchange data (positions, forces …). Both codes manage their own time step and can compute several instants between two sampling times without updating exchanged data. This weak coupling is usually stable thanks to the small sampling times imposed by the control loops, which imposes passing times to the Mecano solver.

A strong coupling between the mechatronic model of the machine tool and the machining simulation tool is implemented. Practically, a specific cutting force element, called TOOL element, has been developed. It considers the dynamics of the tooltip combined with the tool-workpiece engagement (TWE) determined from ModuleWorks toolpath generation and simulation libraries. The resulting relative motion of the tool with respect to the workpiece (TP) is used as input to generate cutting forces (CF). These are applied on the machine model at the spindle tip and generate some excitation to the model. To fulfil equilibrium at each step of the time integration process a Newton–Raphson iterative scheme is used, where cutting forces are updated, and the associated iteration matrix is generated at each iteration. As explained in Sect. 2.1 of this book, the computation of cutting forces is done in a single module that can be called in three different ways. Before starting the time integration (or when the tool is replaced/changed for the considered spindle), the module is initialized. Once the process starts, the TWE is computed for each current individual cut, and the machining module is updated. Finally, the module is called every time that force evaluation is required. Cut definition is obtained from the tool

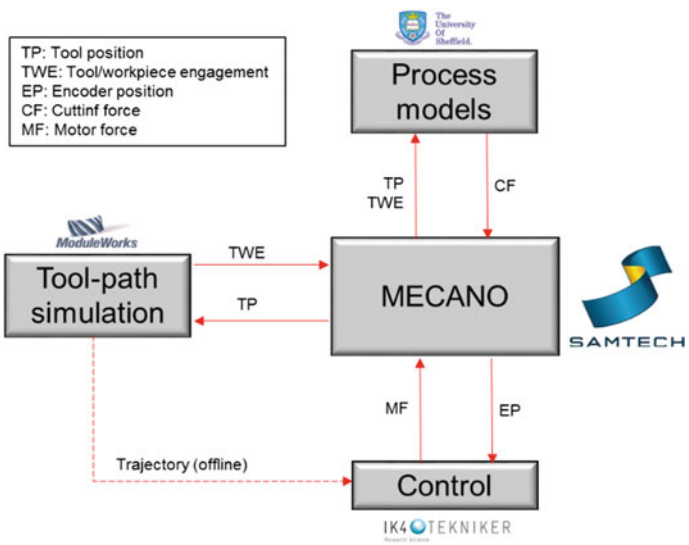

Fig. 11.4 Coupling scheme for the integrated simulation model

computed kinematics projected in the workpiece reference frame. According to a user-defined cut length, TWE is updated as soon as (Tc time) the tool as moved of this characteristic length since previous update. For accurate TWE computation, the cut length should be chosen significantly bigger than the spatial discretization used in ModuleWorks software. As TWE computation changes the workpiece geometry when a cut is performed, the corresponding DLL can only be called once during the considered cut. The flow chart of Fig. 11.5 has been implemented to combine this constraint with the need of having a strong coupling between the machine model and the cutting forces.

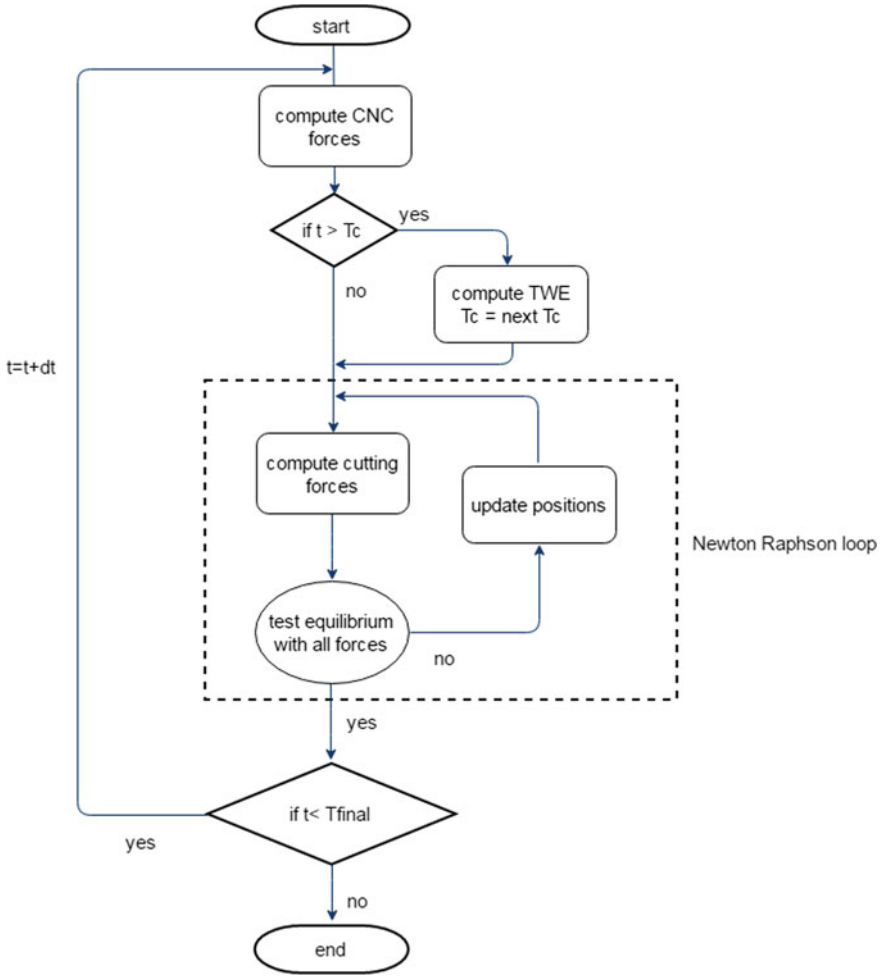

Fig. 11.5 Computational flow chart of the integrated simulation model

11.4 Simulation of Machining Sequences

11.4.1 Simple Machining Process with the High-Speed Box-in-Box Machine

The model of an Urane 25V3 machine from Comau is used to demonstrate that the VMT concept allows simulating a machining process, considering the virtual machine tool in its real conditions, accounting for all interactions between mechanical, control and machining [5, 6]. Thanks to the dedicated TOOL element, the interaction between the tool and the workpiece (rigidly attached to the machine plate—see Fig. 11.6) is defined.

The simulated machining process is the following:

- Move z-axis forward to have a cutting depth of 4 mm.
- Move y-axis up to simulate one cutting pass (milling with an end-milling cutter) as shown in the zoom of Fig. 11.6. The nominal tool y-velocity is 1.9 m/min.
- Tool spinning velocity is 12,250 rpm.
- Technological parameters correspond to two cutters end-milling tool that machines an aluminium holed workpiece.

Some simulation results are shown below. Figure 11.7 shows forces generated by the linear motors to realize the manufacturing process. It can be noticed that these forces are mainly caused by both machining and inertia forces. Figure 11.8 shows the position of the tooltip along the three-axes of the machine with three different scales corresponding to the min-max range of each measure, the magnitude of X-axis vibration is no more than a few microns, while Y-axis magnitude is 110 mm.

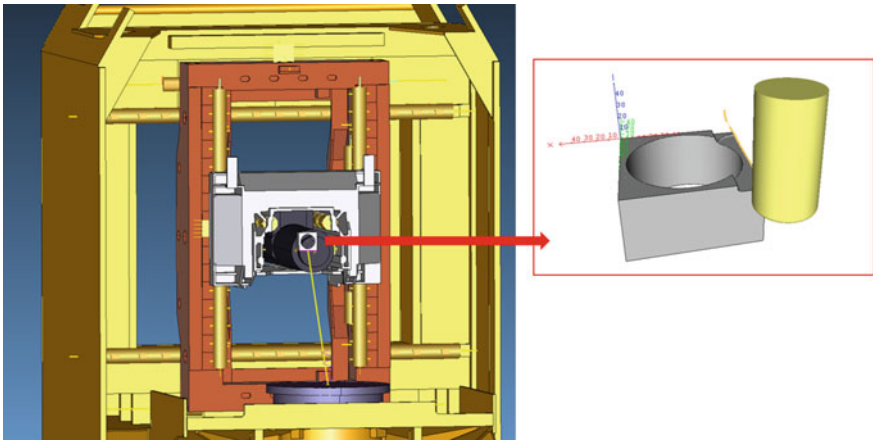

Fig. 11.6 Simple machining process application: sample workpiece on Comau Urane machine

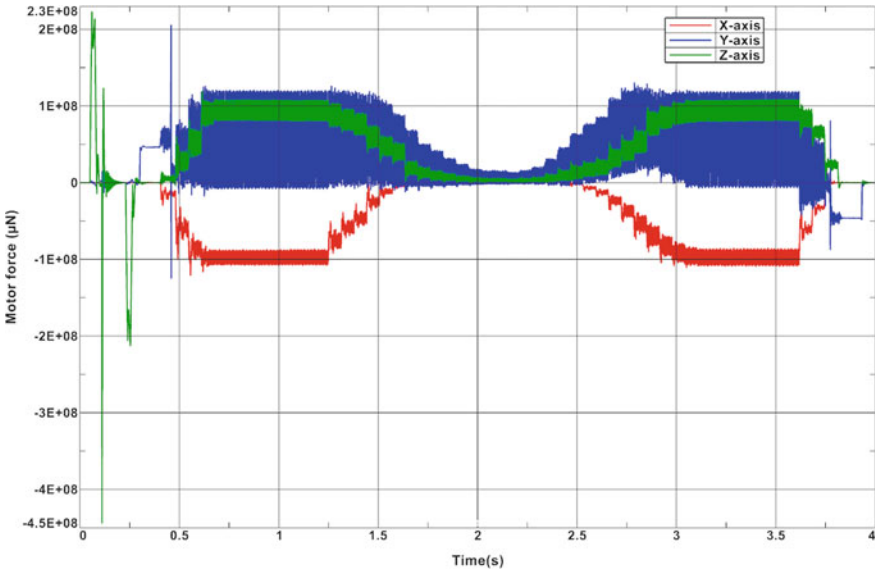

Fig. 11.7 Forces in linear motors calculated in the simulations done in the high-speed box-in-box machine

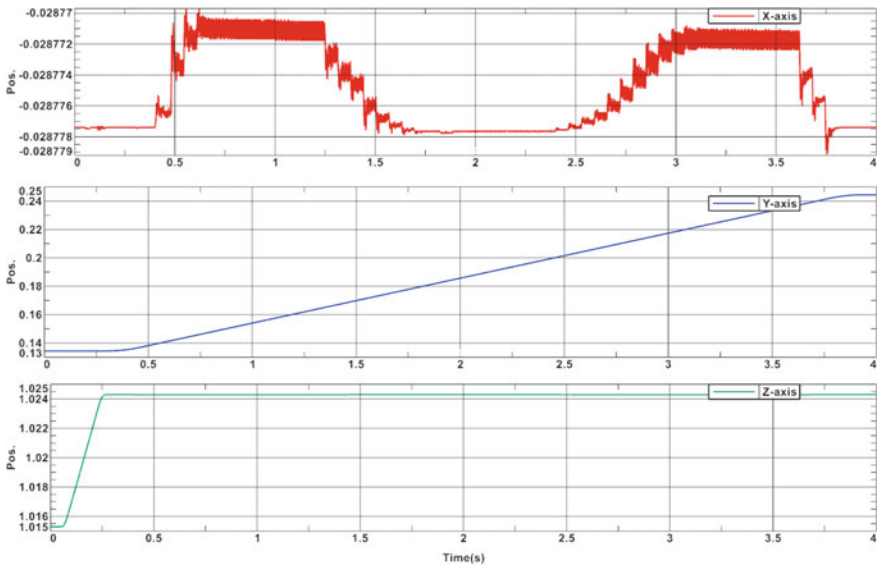

Fig. 11.8 Tool positions calculated in the simulations done in the high-speed box-in-box machine

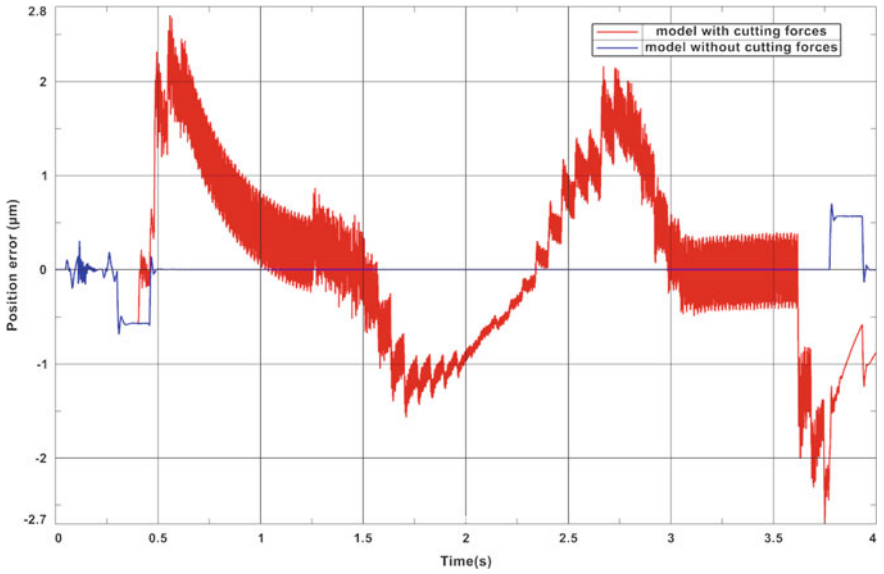

Fig. 11.9 Influence of cutting forces on positioning error in the simulations done in the high-speed box-in-box machine

To highlight the influence of the cutting forces on the machine dynamics, Fig. 11.9 shows the positioning error along the moving axis, if they are considered (red curve) or not (blue curve) in the model. Figure 11.10 shows the same kind of comparison for the tool velocity along Y-axis, vibrations induced by the machining forces are observed.

Finally, some sensitivity analyses highlighted the influence of the manufacturing conditions on the cutting forces. Figure 11.11 compares the cutting force along the move direction in 3 different cases: nominal (red), faster move ($v = 3.8\ \text{m min}^{-1}$—blue) and deeper cut (7 mm—green). Shown results are average force computed as post-processing results from the TOOL element.

11.4.2 Machining Process with Tool Change on a Multi-spindle Machine

The Gepro 502 machine, another use case of Twin-Control project, is now considered to present another simple machining process. It also considers all interactions between mechanical, control and machining models. Thanks to the dedicated TOOL element, the interaction between the tool and the workpiece (attached to the table—see Fig. 11.12) is defined. In this simulation, tool changes and multiple spindles are considered. The simulated machining process is the following:

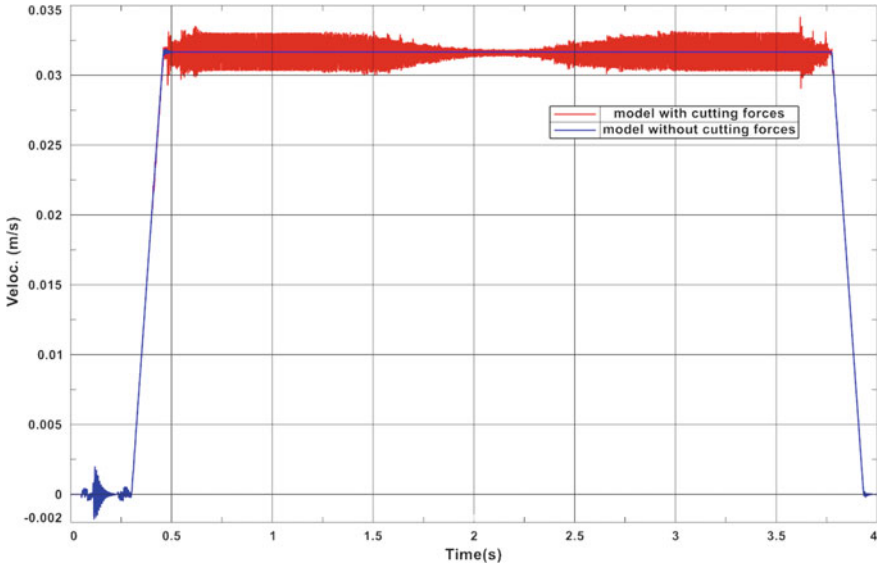

Fig. 11.10 Influence of cutting forces on tool velocity in the simulations done in the high-speed box-in-box machine

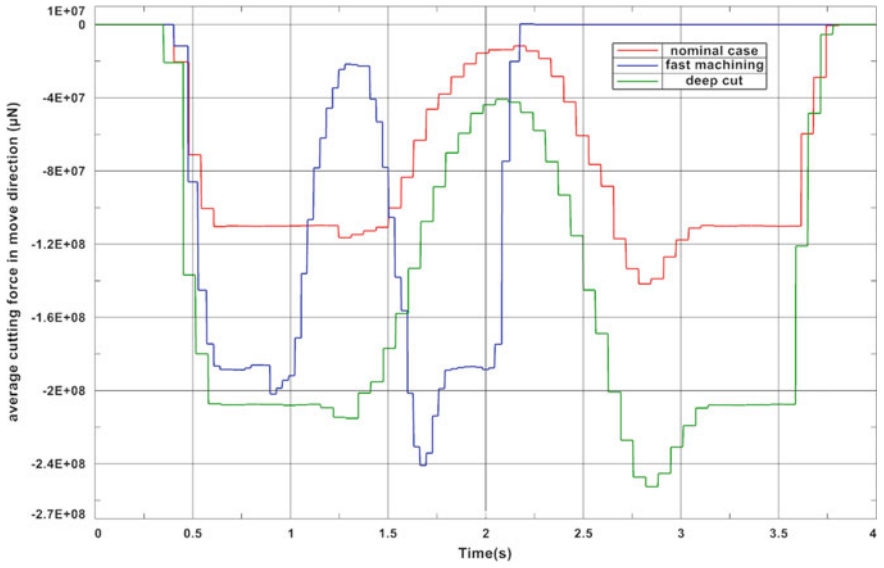

Fig. 11.11 Influence of machining conditions on cutting forces

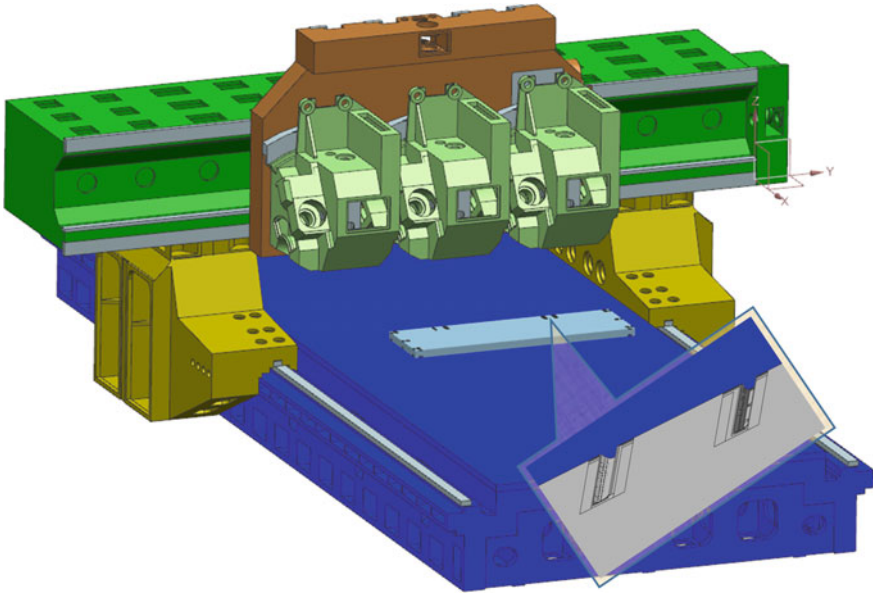

Fig. 11.12 Machining with tool change (Gepro 502 machine)

- Spindle 1 (right) is equipped by an end-milling tool (Diameter 10 mm–three cutters–corner radius 2 mm).
- Spindle 2 (centre) is equipped by an end-milling tool (Diameter 12 mm–two cutters–corner radius 6 mm).
- Z-axis is moved down to have a 4 mm cutting depth.
- X-axis is moved forward to simulate a first cutting pass. The nominal tool x-velocity is 3 m min^{-1}.
- Set spindle speed to 12,250 rpm.
- Once first pass is done, tools get out of the workpiece, and the machine gets back to its initial configuration. Tools are exchanged between both spindles, machine is shifted in the Y-direction and the operation is repeated.

During the simulation, the CAD representation of the workpiece is updated at each evaluation of the TWE. At the end of the simulation, this STL file is made available to the user for evaluation of the final workpiece geometry, including the effects of errors in the tool motion. The final workpiece configuration is shown on the machine CAD model, the effect of the tool change (zoomed area) is clearly observed.

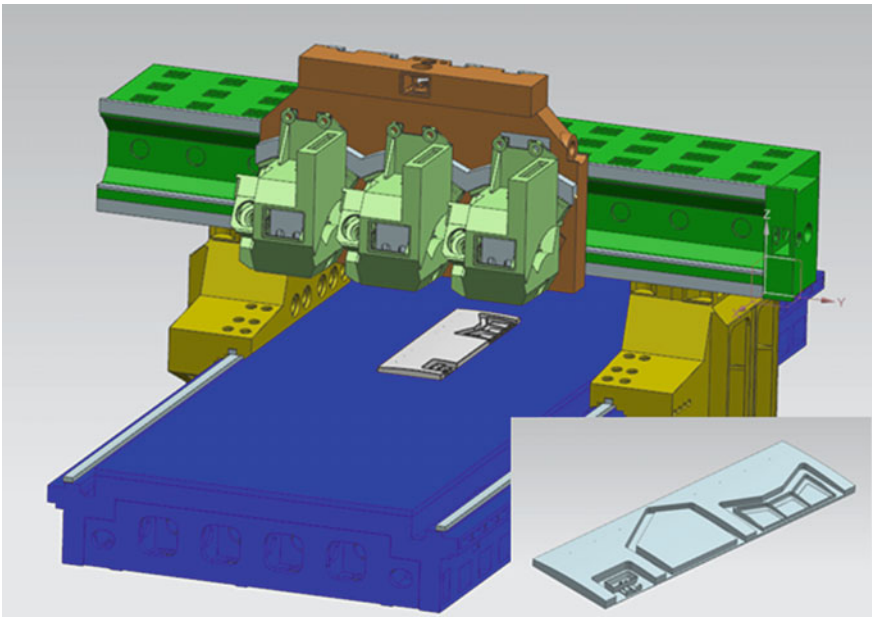

Fig. 11.13 Machining a complex piece with a five-axes machine (GEPRO 502)

11.4.3 Industrial Machining Process

In this chapter, the Gepro's five-axes machine is considered. It is used to manufacture an aluminium workpiece defined as Twin-Control target project application, which includes all type of machining operations done with this machine [7, 8].

Figure 11.13 shows how the workpiece is positioned on the machine to realize the central machining operation. The final geometry is shown in the bottom left of figure. This three-axes machining operation is realized by the central spindle of the machine, using a 3 cutters end-milling tool rotating at 15,000 rpm. Figure 11.14 shows the machined workpiece. This CAD representation (STL format) is an output of the simulation. It is made available to the user for evaluation of the final workpiece geometry, including the effects of errors in the tool motion. On the zoomed area, one can clearly see the footprint of the tool, and the upper left part of the figure shows the executed tool trajectory.

Figure 11.15 shows the evolution of the cutting forces at the tool level (upper graph) during the machining process, and the associated spindle torque (lower graph). Figure 11.16 shows tooltip position, where successive zooms highlight mechanical vibration at both structural natural frequencies of the structure and cutting frequency.

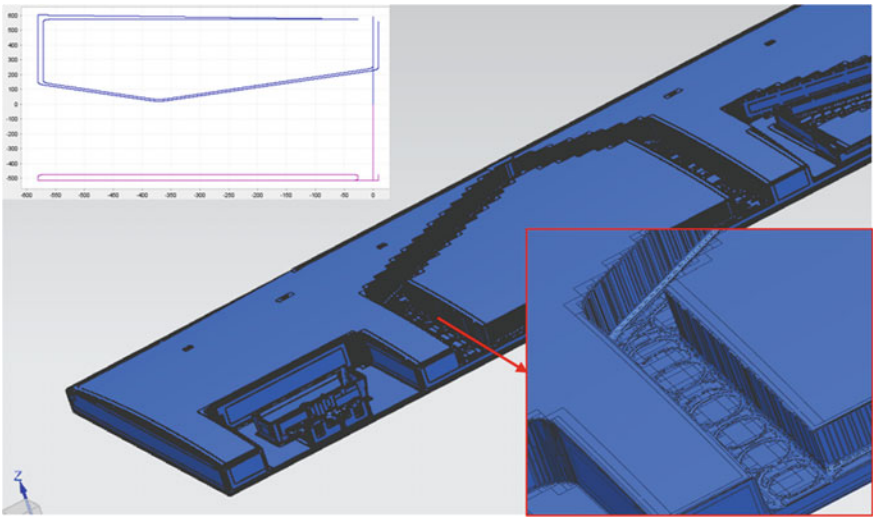

Fig. 11.14 STL CAD representation of the machined piece

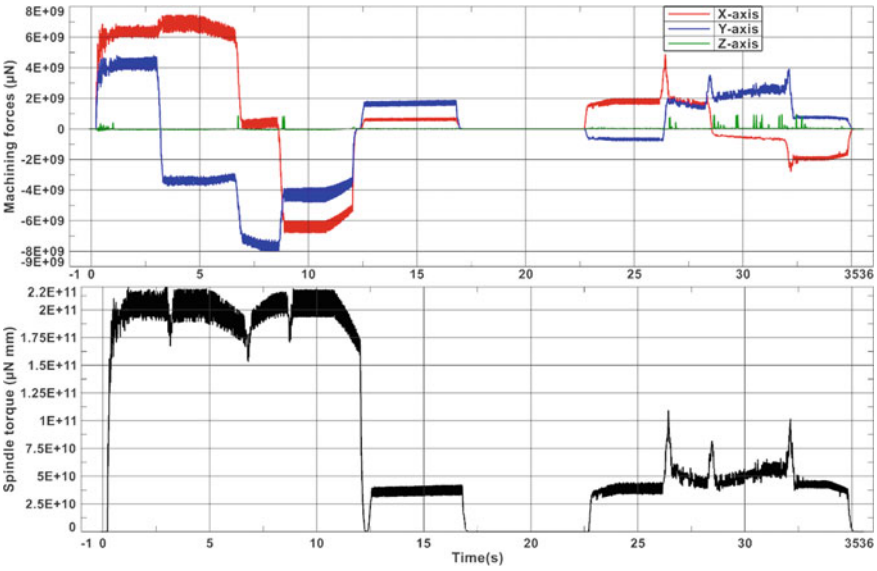

Fig. 11.15 *X*, *Y* and *Z* cutting forces—Spindle torque

This machining sequence of about 1 min is simulated in about 2 h on a normal laptop. Even if far away from real time, this is acceptable for this kind of accurate model (142,000 time—steps–4176 degree of freedom) used for designing new machine or preparing machining sequence, but not for on-line monitoring.

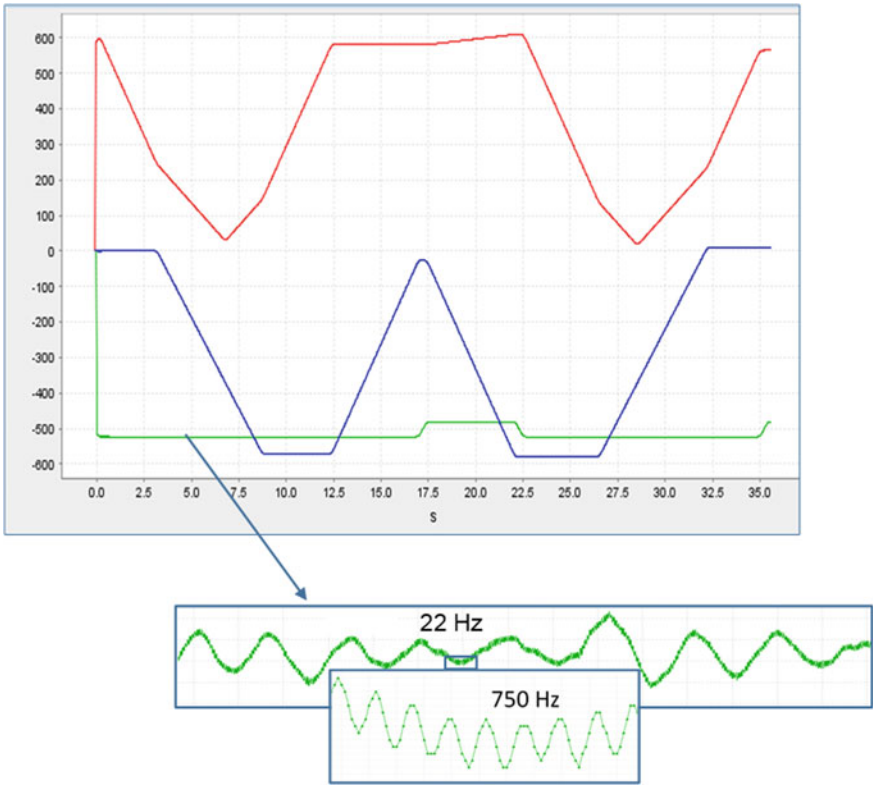

Fig. 11.16 Tooltip position (X, Y and Z)

11.5 Conclusions

The VMT concept is used for virtual prototyping of machine tools in working conditions. The proposed technology has been applied to build mechatronic flexible multibody models of several machines. This virtual machine tool is fully coupled to a cutting force module. This approach provides comprehensive simulations capabilities for virtual machine tool prototyping in machining conditions. The resulting Twin-Control simulation package is intended for both machine tool builders for design activities and machine tool users to improve their processes. In both cases, this virtual model can be used to avoid performing many costly physical tests.

References

1. Morelle, P., Granville, D., Goffart, M.: SAMCEF for Machine Tools resulting from the EU MECOMAT project, NAFEMS Seminar–Mechatronics in Structural Analysis, May 2004, Wiesbaden, Germany (2004)
2. Géradin, M., Cardona, A.: Flexible multi-body dynamics: a finite element approach, John Willey& Sons (2001)
3. Samtech (2017). SAMCEF V18.1 User manual
4. Berglind, L., Plakhotnik, D., Ozturk, E.: (2017). Discrete Cutting Force Model for 5-Axis Milling with Arbitrary Engagement and Feed Direction. In 16th CIRP Conference on Modelling of Machining Operations, June 2017, Cluny, France
5. Cugnon, F., Ghassempouri, M., Armendia, M.: Machine tools mechatronic analysis in the scope of EU Twin-Control project", Nafems world conference, June 2017. Stockholm, Sweden (2017)
6. Cugnon, F., Berglind, L., Plakhotnik, D., Ozturk, E.: Advance modeling of machine tool machining process. Eccomas Thematic conference on Multibody Dynamics, June 2017, Prague, Czech Republic (2017)
7. Cugnon, F., Berglind, L., Plakhotnik, D., Armendia, M.: Simulation of machining operations using the virtual machine tool concept. ASME 14th International Conference on Multibody Systems, Nonlinear Dynamics, and Control, August 2018, Quebec City, Canada (2018)
8. Cugnon, F., Berglind, L., Plakhotnik, D., Armendia, M.: Modeling of machining operations based on the virtual machine tool concept. 5th Joint International Conference on Multibody System Dynamics, June 2018, Lisbon, Portugal (2018)

Chapter 12
Cyber-Physical System to Improve Machining Process Performance

Mikel Armendia, Tobias Fuertjes, Denys Plakhotnik, Johaness Sossenheimer and Dominik Flum

12.1 Introduction

There are several tools to optimize machining processes in the design stage [1–3]. After the correct set-up of the designed process, it is run in the machine tool by an operator in production conditions.

Under ideal conditions, the operator should only run the process every time a new part is clamped in the fixture. However, different events can take the process from these ideal conditions: Tool wear or breakage, machine tool condition variation, excess/absence of material in raw surfaces, variation of workpiece material, variation in cooling conditions, etc.

In addition, there is always some margin to improve the performance of a designed process once it is in production, for example, feed rate increase to increase productivity or feed rate reduction when process does not go as expected (e.g. chatter occurs)

M. Armendia (✉)
IK4-Tekniker, C/Iñaki Goenaga, 5, 20600 Eibar, Gipuzkoa, Spain
e-mail: mikel.armendia@tekniker.es

T. Fuertjes
MARPOSS Monitoring Solutions GmbH, Egestorf, Germany
e-mail: tobias.fuertjes@mms.marposs.com

D. Plakhotnik
ModuleWorks GmbH, Aachen, Germany
e-mail: denys@moduleworks.com

J. Sossenheimer · D. Flum
PTW TU, Darmstadt, Germany
e-mail: j.sossenheimer@PTW.TU-Darmstadt.de

D. Flum
e-mail: D.Flum@PTW.TU-Darmstadt.de

M. Armendia et al. (eds.), *Twin-Control*,
https://doi.org/10.1007/978-3-030-02203-7_12

Twin-Control aims to overcome these effects by the application of CPSs based on model-based control techniques. CPSs are defined as smart devices that interact with the machine (through sensors and actuators) to increase its performance [4]. In this case, different developments of Twin-Control project in modelling are embedded in the monitoring hardware or the control of the machines to affect its performance.

After this introduction, Chaps. 2–7 present the different CPS-based control strategies in Twin-Control. Finally, the conclusions are presented.

12.2 Process Monitoring

Process monitoring using ARTIS hardware can be split into two different applications. First, process monitoring by learning. Second, process monitoring by simulation.

Learning-based process monitoring is a key feature of ARTIS process monitoring systems. The process monitoring is based on process signals of the machine control. Furthermore, the process monitoring could be based on additional sensor signals (e.g. vibration and force). Genior Modular is the main module of ARTIS hardware. In this module, the interface to the machine control as well as the HMI is provided. The process monitoring algorithm and the determination of the limits and parameters are calculated on the Genior Modular device, as well. For the user, the QNX-based Genior Modular provides an intuitive HMI to configurate the process monitoring task. The system determines all limits and parameters automatically. Additional input keys provide the possibility of making certain adjustments. In detail view display mode, these input keys are immediately visible. In multi-view display mode, it is necessary to first select one of the windows in order to make the keys visible. The user has the possibility to manually adjust the limit, being less or more sensitive to process changes.

For the learning process, some reference processes must be executed in advance. The system calculates automatically how many learn steps must be performed. Apart from that, a manual adjustment of the learning process repetitions is possible.

Once the learning is complete, the process monitoring can be started. Figure 12.1 shows a visualization software GEM-Visu. Next, the most important indicators of this visualization are listed.

- Line graphics:
  - Green curve: learned signal curve
  - Grey curve: signal curves of the last 10 processes are displayed
  - Blue curve: current signal curve
  - Red curve (1): lower breakage limit
  - Red curve (2): upper breakage limit
- Bar graphics:
  - Red line (3): missing limit (indicates that a tool is not installed)

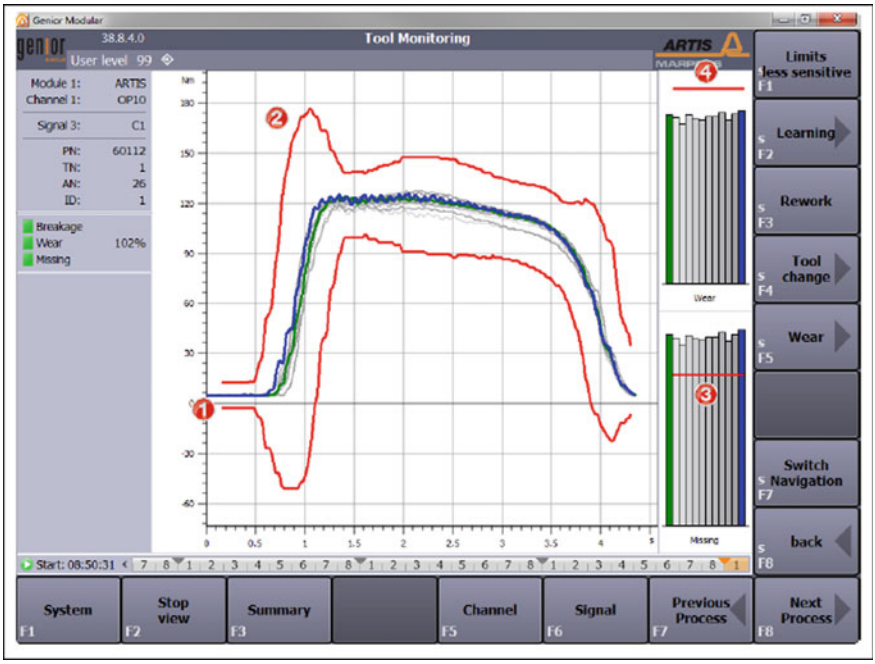

Fig. 12.1 Genior modular visualization for process monitoring

– Red line (4): wear limit
– Green bar: area value of the learned process
– Grey bar: area value of the previous ten processes
– Blue bar: area value of the current process.

The alarm reaction could be configured by the user. So, the system could send just a warning or fully stop the machine.

Process monitoring by learning is suitable for large batch manufacturing, where stable conditions are present for the learning stage and the process monitoring strategy can be applied for a long time. However, for small to medium batch size sectors, like aerospace, this approach is not useful.

For this case, Twin-Control proposes a simulation-based process monitoring. As a first step, process models are run in a PC which is connected, via CAP-Logger, to the control of the Starrag EcoSpeed located in the AMRC installations. The CAP-Logger is a small client program that connects to the GEM-CNC server via TCP and stores the requested data in CSV format. The GEM-CNC server is a service running on Siemens Solution Line HMIs. It forwards the TCP requests to the Siemens CAP-API, and it sends the response back to the CAP-Logger via TCP.

Measured axis positions and spindle speed are used as input of the models which provide spindle torque estimations. These estimations can be compared to spindle torque measurements that are also done by the ARTIS equipment (Fig. 12.2).

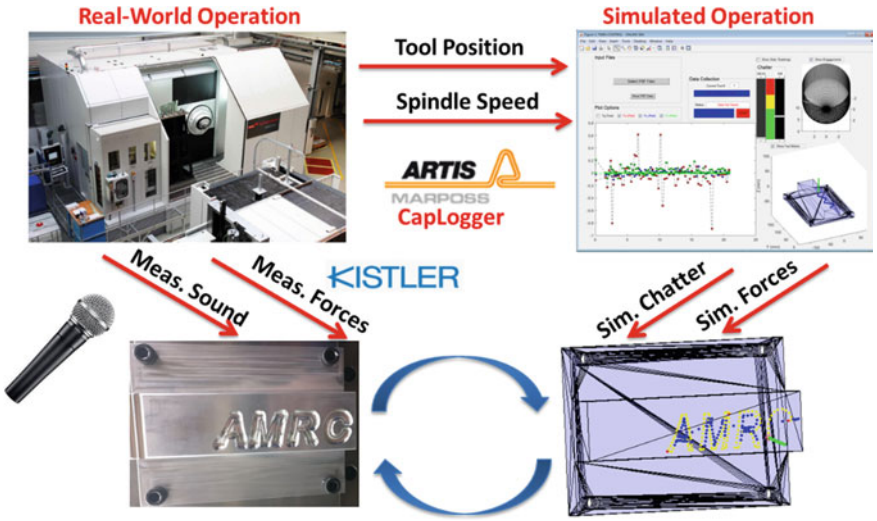

Fig. 12.2 System architecture of the pilot line set-up at the AMRC, showing the flow of data between the real and simulated operations

This strategy could be used to implement a simulation-based process monitoring. For that, process models need to be integrated into the ARTIS hardware and run in parallel to the real process (Fig. 12.3). Simulation results will provide the nominal conditions instantaneously, equivalent to the learned reference values used in the learning-based process monitoring, and could be used to fix the thresholds for a simulation-based process monitoring approach.

12.3 MT Operating Condition Adaptation for Life Increase

The knowledge of machine tool condition is very useful for maintenance activity planning. Early detection of (possible) problems in the machine tool allows more efficient maintenance actions, maximizing machine uptime.

Early detection of future anomalous situations with the machine tool avoids undesirable machine tool breakage, and consequent unforeseen production stops.

Two approaches, both based on feedback generated by models implemented by TEKNIKER in KASEM, are defined towards this end. Both models, although using different approaches, can identify or estimate that the machine tool is going to have a problem. Thanks to this feedback, ARTIS hardware can adapt, normally smooth, working conditions of the machine tool to extend machine tool life and wait for the next planned maintenance action.

The first approach is the integration of end-of-life models developed in Twin-Control project in the monitoring architecture. This feature provides the chance to

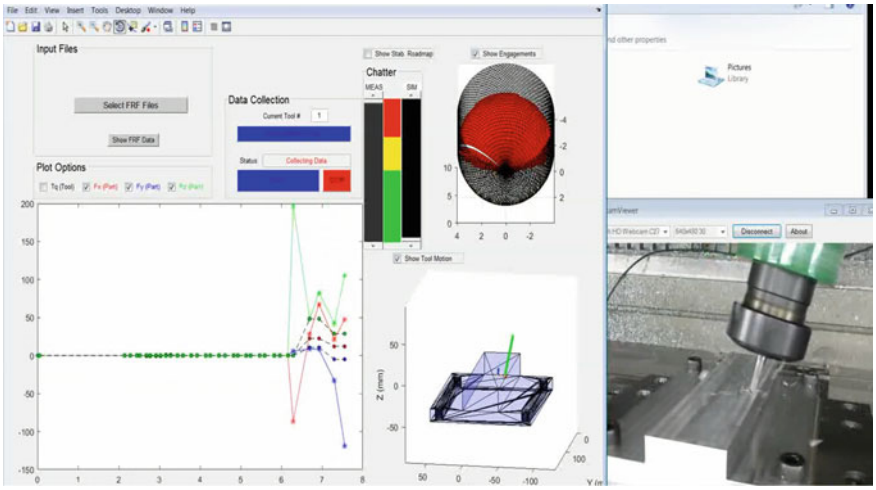

Fig. 12.3 Screenshot showing the Twin-Control process models GUI, fed with real input data coming from the machine. The estimations are directly compared with measurements of the real process, presented in lower right corner

estimate the remaining useful life (RUL) of the critical components of a machine tool by accounting for the real usage (monitored) conditions. The end-of-life models could be integrated at local or fleet level. For Twin-Control, KASEM has been the choice for this implementation. When the RUL estimated by the end-of-life model falls below a predefined limit, KASEM generates a warning towards the planning of a maintenance action (change of bearing or spindle).

A second approach is based on the results coming from the machine tool characterization tests that consist in a series of quick tests that allow a good characterization of machine tool condition. The indicators calculated from these tests are compared to the ones obtained in nominal conditions and, in case deviations occur, anomalous condition of the machine is determined. Again, even if this procedure can be implemented at local or cloud level, KASEM has been chosen as platform in Twin-Control project.

As in the case of a problematic RUL value, when any indicator of the MT characterization test gets over the defined threshold, KASEM generates a warning towards the planning of a maintenance action.

Apart from this warning at maintenance management level, Twin-Control can automatically adapt machine tool performance to its condition. According to the next planned maintenance stop and the RUL value, ARTIS Genior device system can smoothen machining conditions (reduce feed rate and/or spindle speed) to avoid component breakage. The ARTIS GEM-CNC server, installed in the machine control, receives the commands from the ARTIS GEM-OA (Genior Modular with Open Architecture) to change the current value of R-parameters that define cutting conditions (feed rate and/or spindle speed).

As an alternative to the automatic modification of machining conditions, since manufacturers do not want to decrease productivity automatically, a warning showed by the ARTIS HMI or the ARTIS telegram remote control will suggest the operator with some new cutting conditions.

12.4 Energy Monitoring System on Component Level

A cost-effective approach to monitor the energy consumption at component level has been developed by using a Kalman filter and the information of the component's switching states, which has been explained in greater detail in Sect. 3.3.

The ARTIS OPR device records the required switching states of the different components (via OPC UA) and the power consumption of the drive (via internal signal monitoring). Additionally, the total power consumption of the machine is acquired by an ARTIS true power module. The energy disaggregation algorithm, which is based on the Kalman filter, is embedded in the ARTIS OPR.

An EMAG VLC100Y turning machine, located at the ETA Research Factory of the Technische Universität Darmstadt, has been used to implement and validate this development. The disaggregated power consumption at component level can be visualized locally on the HMI of the machine using ARTIS GEM-Visu (Fig. 12.4) or transferred to a higher-level platform, like SCADA or MES. This ensures immediate feedback on energy demand.

Even if an exact power disaggregation of industrial components is difficult, the algorithm offers a cost-effective and simple possibility to estimate the energy demand on component level. Since existing data acquisition and analysis architecture was

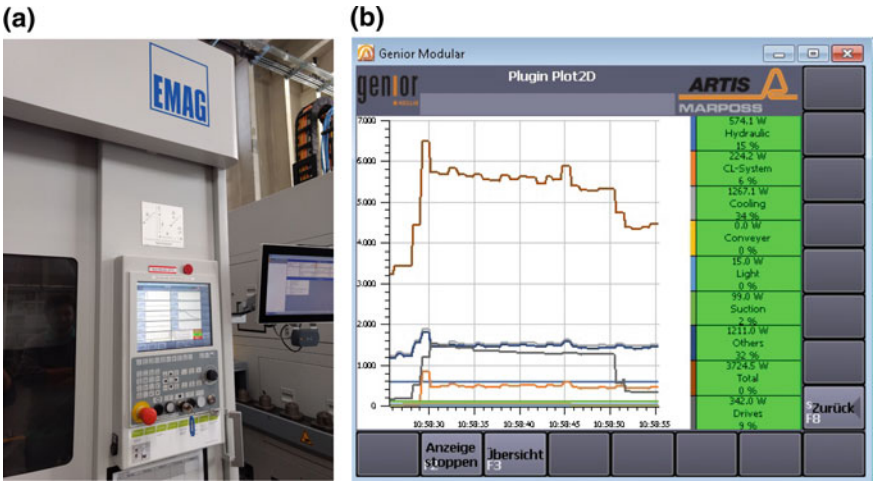

Fig. 12.4 Visualization of the component energy monitoring: **a** machine HMI; **b** ARTIS GEM-Visu

used, the implementation effort and costs could be reduced, compared to hardware-based energy monitoring on component level. The presented approach can thus be used for cost-effective energy monitoring.

12.5 Telegram Remote Control

Currently, there is no possibility to interact with the monitoring hardware from outside, so that a physical connection to the machine is needed. By using an open-source chat software for the GEM devices, a PC or a smart device could be connected to these devices from everywhere in the world.

With this approach, it is possible to get information about the status of each connected device (e.g. serial number, number of alerts, IP address) without a physical connection to it. Furthermore, it is also possible to interact with the GEM device (Fig. 12.5). Based on the configuration of the telegram adapter, monitoring configurations could be adapted via smart devices or PCs.

The telegram adapter could be installed in the GEM device or the OPR. Also, it is possible to install the telegram adapter at a plant server or PC, which has a network connection to the monitoring hardware. For connecting the monitoring hardware with a chat group, in the telegram adapter, just the IP address of the target GEM device must be configured.

For Twin-Control, a chat group was implemented, in which the GEM devices of the ARTIS, MASA and TEKNIKER use cases are involved.

12.6 Adaptive Feed Rate Control

In complex machining processes, chip flow varies according to the deep of cut, tool geometry and the programmed spindle speed. To guarantee maximum productivity, it is interesting to keep continuous chip flow control. To do that, feed rate must be adapted according to monitored spindle consumption to achieve desired variables.

Adaptive control (AC) is an option for ARTIS Genior Modular systems. This option controls the programmed feed rate of a cutting cycle to maintain a constant load on the tool during the entire cutting cycle (Fig. 12.6). This way, feed rate will be increased when the cutting power, e.g. spindle acceleration, is low (good tool condition and less chip removal). The software algorithms automatically slow down feed force if tool condition (wear) or material quality (e.g. texture, hardness) changes. This function is active during the process monitoring. To provide this feature, ARTIS Genior Modular uses the real-time connection to the machine control. By overwriting, e.g. R-parameters in the machine control, the feed rate of a cutting cycle is optimized.

Adaptive feed rate control has been implemented in the GEPRO 502 machine of MASA. This way, when the spindle is underworking, the feed rate is increased; when the spindle is overworking, the feed rate is reduced. The objective is to maximize

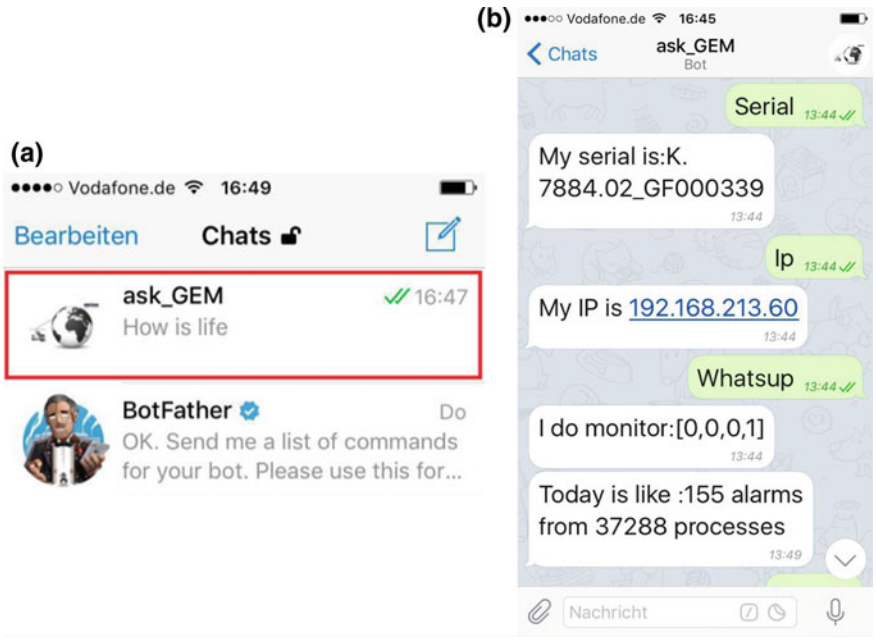

Fig. 12.5 Screenshots of the telegram adapter feature: **a** ask_gem chat within telegram app; **b** example of the contents of the chat

productivity by keeping the material removal rate high during all the process. To test this, a scalloped sample part has been used.

12.7 CNC Simulation and Collision Avoidance System (CAS)

During real machining operations, process visibility is often limited due to small safety windows or high coolant flow. Apart from that, due to undefined position of additional equipment (fixture, toolholder, workpiece, etc.) in the machine tool working volume, collisions are common. Both issues are very critical from the operator's point of view. To overcome these problems, the availability of a virtual representation of the machine tool, replicating the movements that the real machine is executing, can be very useful.

Material removal simulation is performed within ModuleWorks libraries, for which the proper simulation environment must be established first. The simulation models require the following parameters: the initial geometry of the stock material, geometric definition of the cutting tools, machine tool kinematics and a sequence of the commanded machine axis moves. Once the virtual machining set-up being initial-

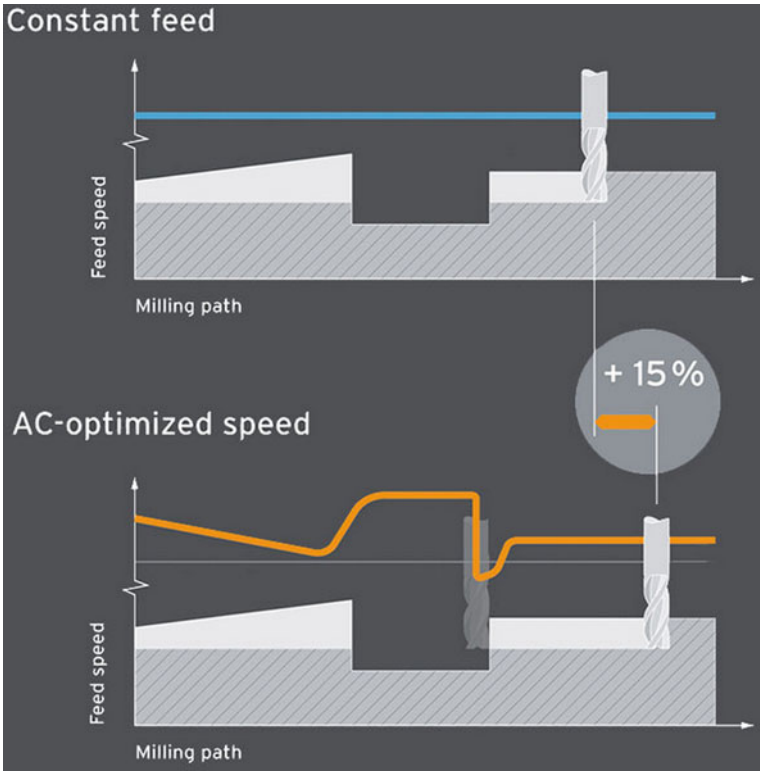

Fig. 12.6 Diagram presenting ARTIS adaptive control optimized feed rate strategy

ized, ModuleWorks simulation can retrieve input signals to change and add cutting tools, execute new cutting tool moves. During the simulation steps, the internal data structure representing the shape of in-process stock material has been continuously updating to reflect the changes made by cutting tools. For each simulated move, the output is a set of results showing the status of the tool–workpiece interaction during the move (whether material has been cut, a collision between machine tool element or cutting tool and stock material has been detected, etc.) Optionally, a tessellated (triangulated) 3D surface of the simulated workpiece can be computed for further visualization and analysis. The analysis is supported due to applying of different colorization options (coloured by tool indices, feed or another measured data). The simulation libraries are designed to be integrated on the level of the HMI or CNC unit (as shown in Fig. 12.7) to retrieve actual positions of the machine tool axes for exact computation of the relative positions of the tools and workpiece in the simulation environment. Such an approach reduces integration efforts to visualize the results and provides both verification and clash detection during different processes maintain time responsiveness.

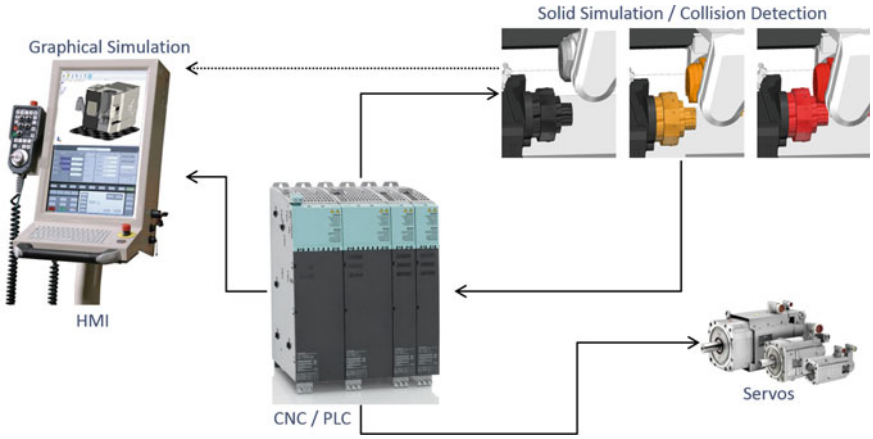

Fig. 12.7 Integration of ModuleWorks simulation

Since ModuleWorks libraries use the tri-dexel model for material shape representation, that is capable of staying memory and time consistent over machining time, this approach leads to efficient computation with a low response time that satisfies real-time conditions for machining applications.

ModuleWorks CAS takes the real axis positions, machine geometries and workpiece position and uses the same motion data as the real servos to provide a fully integrated and visually realistic simulation of the machine kinematics, tools, jaws, clamps and fixtures as well as the material removal process. The real-time collision avoidance is based on the look-ahead functionality provided by CNCs. The look-ahead is a method for trajectory planning, for which a CNC precomputes several future moves. If ModuleWorks simulation runs on the "future" moves, a message of a reported collision may be passed to the machine control before the actual collision occurs. The communication can basically be maintained through a variety of standard APIs and protocols (Focas, EtherCAT, Profinet, etc.). Collision detection and avoidance are available in both auto and jog modes using this look-ahead motion data. CAS implementation is based on the access to OPC/UA interface of the machine tool to retrieve different data via the interface along with internal processing of the geometries of the in-process stock and set-up components, as shown in Fig. 12.8.

The new functionality foresees collisions that may happen in the future. In addition to in-time simulation, simultaneous computation threads consider machine tool positions at some time upfront. The predicted position is examined towards potential collisions and may signal to halt the machine, and colliding machine tool elements are highlighted in red in Fig. 12.9.

CAS integration has been proved to be an efficient solution to withstand collision risk with different operational modes in machining critical components. Huron, a leading French manufacturer of very high-performance 5-axis machining centres for continuous machining of complex parts, has integrated CAS into Huron's

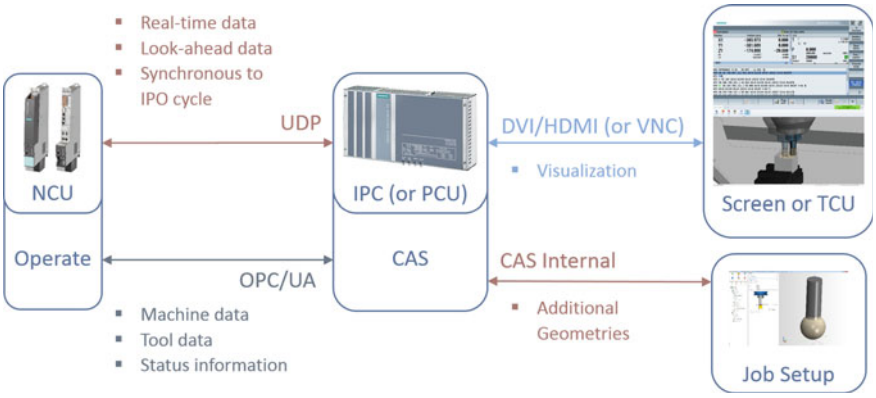

Fig. 12.8 Design of the collision avoidance system for Siemens 840D CNC

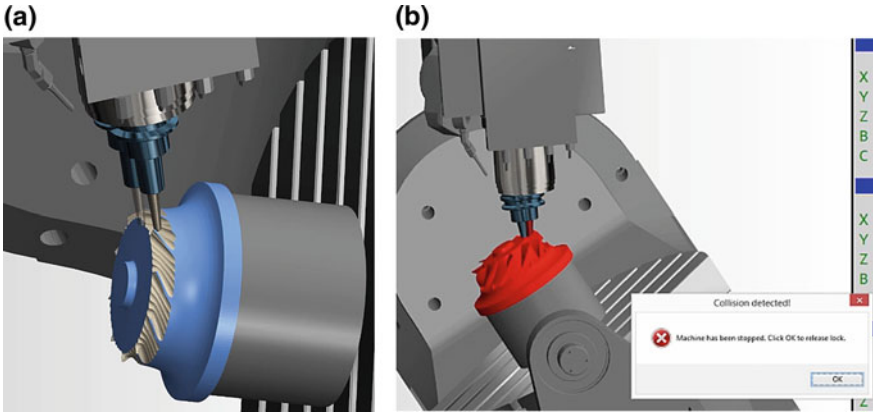

Fig. 12.9 ModuleWorks CAS in action: **a** look-ahead position (transparent); **b** CAS alarm on HMI to stop the machine

high-performance product lines, including KX 50 L, a high-performance double column machining centre, and K3X 8 FIVE, a machine from the range of very high-performance 5-axis bridge-type machining centres.

12.8 Conclusions

This document presents an overview of the model-based control strategies developed in Twin-Control project and applied using the CPS approach. Part of the modelling activities carried out in Twin-Control project has been implemented at workshop level. This way, virtual representation of the machine is linked to the real

representation and can modify its performance to improve productivity (adaptive control), increase machine uptime (collision avoidance system), optimize tool life (process monitoring), improve maintenance actions (automatic machining condition smoothening) and even to improve the communication with operators (telegram adapter). Most of the applications are based on a standard monitoring equipment, like ARTIS devices used in Twin-Control project, and hence, high costs are avoided. The different features have been validated at both laboratory and industrial level.

References

1. Berglind, L., Plakhotnik, D., Ozturk, E.: Discrete cutting force model for 5-axis milling with arbitrary engagement and feed direction. Procedia CIRP **58**, 445–450 (2017)
2. https://www.malinc.com/products/machpro/
3. https://www.cgtech.com/products/about-vericut/optipath/
4. Berger, C., Nägele, J., Drescher, B., Reinhart, G.: Application of CPS in machine tools. In: Jeschke, S., Brecher, C., Song, H., Rawat, D. (eds.) Industrial Internet of Things. Springer Series in Wireless Technology. Springer, Cham (2017)

Chapter 13
Fleet-Wide Proactive Maintenance of Machine Tools

Flavien Peysson, Christophe Mozzati, David Leon, Quentin Lafuste and Jean-Baptiste Leger

13.1 Introduction

From the capacity of production depending on machine tool availability, it becomes a day-to-day concern for maintenance operator and production manager. Each stop in production constitutes a loss of earning that should be anticipated to allow an efficient planning of maintenance operation and to avoid unscheduled production downtime. Condition-based maintenance solutions at a machine level provide the operator with tools that support monitoring of the machine's behaviour and highlight behaviour changes. However, machine tools as large engineering systems have multiple subsystems and equipment of different natures (electrical, mechanical, hydraulics, electronics, etc.) following different fault rates and modes in which behaviour may differ from specific phases of their life cycle due to events and maintenance history. Supporting proactive maintenance at a fleet level provides summarized information and means of comparison and investigation for decision-making.

F. Peysson (✉) · C. Mozzati · D. Leon · Q. Lafuste · J.-B. Leger
PREDICT, Vandoeuvre-lès-Nancy, France
e-mail: flavien.peysson@predict.fr

C. Mozzati
e-mail: christophe.mozzati@predict.fr

D. Leon
e-mail: david.leon@predict.fr

Q. Lafuste
e-mail: quentin.lafuste@predict.fr

J.-B. Leger
e-mail: jean-basptiste.leger@predict.fr

M. Armendia et al. (eds.), *Twin-Control*,
https://doi.org/10.1007/978-3-030-02203-7_13

13.1.1 Fleet-Wide Approach and Industrial Challenges

Originally referred to a group of ships or aircrafts [1], the term fleet is used in the industrial domain to refer to a set of machines, generally the whole of an owner's system. Technically, the fleet is considered as set of entities composed of similar sub-systems which behaviours are comparable [2]. From the capacity to process a workpiece being the objective of a machine tool, the objective of a fleet of machine tools is considered as its capacity to process a batch of workpieces. Fleet-wide approach of objectives is then twofold: to provide augmented and synthetized information at a fleet level and to provide higher diagnostics and prognostics capacities.

The condition-based monitoring allows to monitor the global behaviour of the fleet, i.e. its capacity to achieve its objectives, by providing indications of the health state of each sub-system. Monitoring the behaviour at a fleet level aims at informing maintenance operators and managers about the health and availability of each machine, as well as the global fleet by merging and extracting information from indicators.

In addition to the benefits for maintenance management, the fleet-wide approach provides tools to improve and capitalize failure analysis and investigation. Indeed, it allows machine behaviours' comparison and experience feedback sharing at a fleet level allowing better fault detection and isolation. Both objectives require a well formalized and structured knowledge.

13.1.2 Building the Fleet-Wide Approach

At the bottom of the fleet, the sub-systems attached to a machine tool such as axis, spindle and auxiliary systems such as hydraulic group, coolant, system, cooling system, could be monitored independently from each other. Using condition-based monitoring, it is possible to build behaviour indicators not biased by the characteristics of other sub-systems, thus being able to respond in real time considering the state of each sub-system. Despite being a powerful tool for maintenance operator to ensure a correct and quick diagnosis, the combinatory explosion caused by each indicator with its own dynamic could lead to a deteriorated legibility. The number of alarms and information on the fleet-wide level would exceed human abilities. It is then recommended to build bottom-up fleet-wide approach [3] by monitoring the machine's sub-system health, to provide information to monitor the machine's health and, then, the fleet's health.

The fleet-wide approach allows maintenance operators and management to get a general view of the state of the fleet and support the decision-making to ensure the fleet mission. This approach also allows to compare sub-systems at different levels and uses the results of maintenance and events history to be reused for upcoming events. The challenge of fleet-wide approach is to build tools that support monitoring health states for each level: fleet, machine and sub-systems, and allow the compar-

isons while not being invasive for users. A knowledge base uniting semantic and systemic approach of the fleet must be considered.

13.2 Fleet-Wide Knowledge Base Architecture

Health assessment provides relevant information highlighting abnormal health in the monitored component, sub-system or system, but it does not provide the necessary information to identify the root causes to fix the degradation process. For this purpose, a global modelling of the fleet is required at different levels to formalize both the maintenance knowledge and the processes, mainly monitoring, diagnostic and prognostics, to achieve proactive fleet management.

Knowledge modelling rely, first, on the machinery domain-specific concepts formalization, leading to machine tool fleet detailed description and second, to the structuration of the different concepts by the description of both vertical, i.e. between level, and horizontal, i.e. in a specific level, interactions.

13.2.1 Machine Tool and Related Concepts Definition

In the process of modelling the fleet level using a semantic approach, each level is defined in a vertical approach while clearing the concepts that allow health status definitions and horizontal comparison of the different levels of the fleet. First, different levels are identified, from each a set of definitions and concepts arises, as depicted in Fig. 13.1.

Focussing first on the machine tools level, its definition is given by "a machine driven by power that cuts, shapes or finishes metals or other materials" [4]. As a large number of machines and concepts could be included in this definition, this work is focused on the general concepts emerging from modern machines tools powered with electrical power and composed of at least one electro-spindle and at least three axes. At this level, the availability of the machine will be consolidated with information concerning the health status of the sub-systems to describe the general status of the machine [5].

The sub-system level describes the functions of the machine tools that are necessary to manufacture the workpiece. This example focusses on the axis unit sub-system that represents the moving parts of the machine necessary for the positioning of the spindle or the workpiece. The axis unit, depending on machine design, can be composed of at least three linear axis and rotational axes. The technologies and features used for conception can be different depending on the designer choice. Considering the diversity of possibility for the components of this sub-system, it is necessary to define a set of rules based on ontology that eases the horizontal level comparison and expertise sharing between equivalent sub-system of other machine tools and their

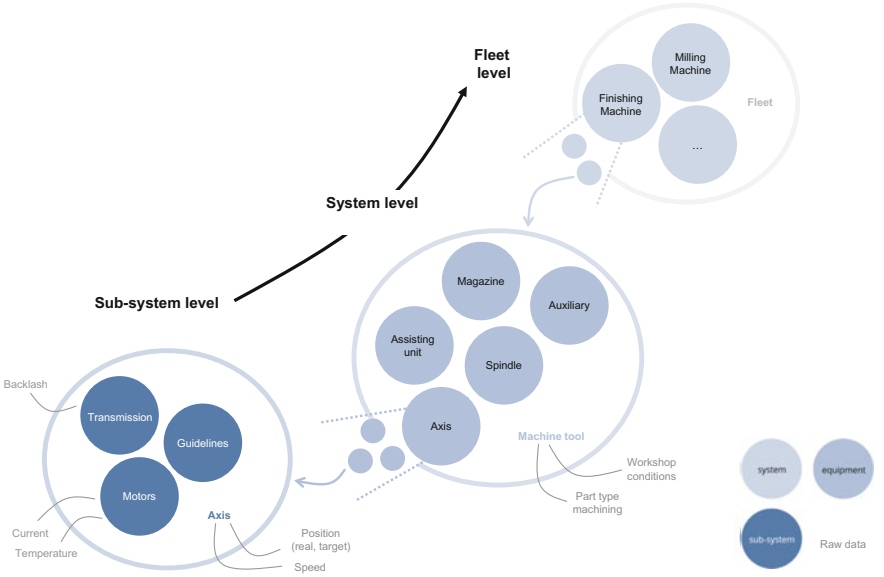

Fig. 13.1 Machine tool fleet representation of the semantic modelling

equipment (axis in this example). Four levels to classify the contextual information are discussed in [6] to provide comparison facilities:

- Technical context is the description of a system in terms of technical features. For instance, the three linear axes are composed of linear motor, sliding system, guideline, cooling system associated, etc. Even if the design and dimensions of the component are different, this description allows comparisons of the features of the linear axis to be considered.
- The service context and operational context are complementary to the technical context.
  - The service context aims at describing the solicitations that the system endures. For example, considering the axes of the same machine, the three linear axes are designed for different purpose. As a common nomenclature, the Z axis is parallel to the spindle, while the X and Y axes form the plane perpendicular to the spindle direction; X being defined as the longest of X and Y. The solicitation will be different depending on machining executed along Z axis (e.g. drilling) or executed along X and Y axes (e.g. boring).
  - The operational context defines the operating condition of a system. Using knowledge and information related to the operational context helps to go through the interactions of the systems and build the approach that isolates the equipment characteristics. The operational context could be used to isolate a comparable behaviour of the axes and overlook the interactions between, for example, one axis moving while the other are maintaining their position.

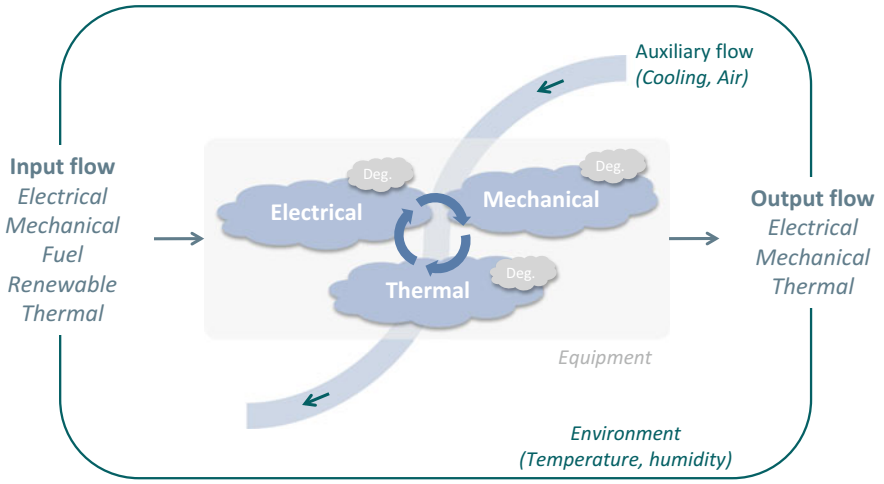

Fig. 13.2 Functions of a sub-system and interactions with its environment

- The performance context is the description of the ability of the system or equipment to accomplish its mission. Mainly depending of the expected performances of the machine itself, the performances of a sub-system are to be used as complementary information to model the knowledge.

At the equipment level, a general approach knowledge modelling and behaviour indicator can be defined using the descriptions associated with the sub-system and the equipment itself given by the semantic study. However, the information about each equipment is visible only through data, making the data acquisition the key for the study of the equipment. The semantic approach aims here at defining the inputs to build the algorithms that compute the indicators combining both sensor measurements, such as current, temperature and the internal control variables such as spindle machining, not machining, targeted position, targeted speed. It is recommended to anticipate the monitoring plan of the behaviour before defining data collection plan.

The semantic definition, while being indispensable to the fleet description, is not sufficient by itself to describe properly the interactions occurring between the sub-systems at different levels, especially for diagnostic purpose. The representation on Fig. 13.2 summarizes the interactions of an equipment with its environment. The input flow coming from other sub-systems can influence the functions associated with the equipment as the output flows depending of the function influence the functions depending on them. A systemic approach describing for each machine, depending on its conception, the functioning and malfunctioning as well as the interactions between the flows is presented below.

13.2.2 Functional and Dysfunctional Analysis

Once the knowledge of machine tool domain is defined, these concepts are then integrated and structured in a knowledge base to describe each level of the fleet. A systemic approach [7] is being considered to build a description of the machine and its components by its functions (what the components are supposed to do), their consumed or produced flows (how the components interoperate) and anticipate how they could malfunction. Although the malfunction modelling tends to be sufficient to help the process of decision-making, the functional modelling is the start point to structure the root cause analysis.

The functional modelling describes the interoperability of the components and provides tools to identify the probable root causes of the events. Figure 13.3 shows a simplified example of the functional modelling of the three-dimensional axis unit using KASEM® knowledge modelling tool. The whole view shows how the function "to move the spindle along the *X*, *Y* and *Z* axes". Hence, the function of the axis unit is operated. This function is refined in three sub-functions representing the three-axis sub-systems as shown by the green arrows. Each of them could then be refined in sub-levels describing the components of the axis such as linear motor, cooling system, guiding system, etc. The arrows represent the flows consumed and produced by the function. In this example, the main purpose of each axis is to produce a mechanical movement, while consuming electrical energy provided by the plant. Each flow here is defined by characteristics, shown with the colour code. The yellow and black arrows represent electrical energy and the red arrows mechanical energy.

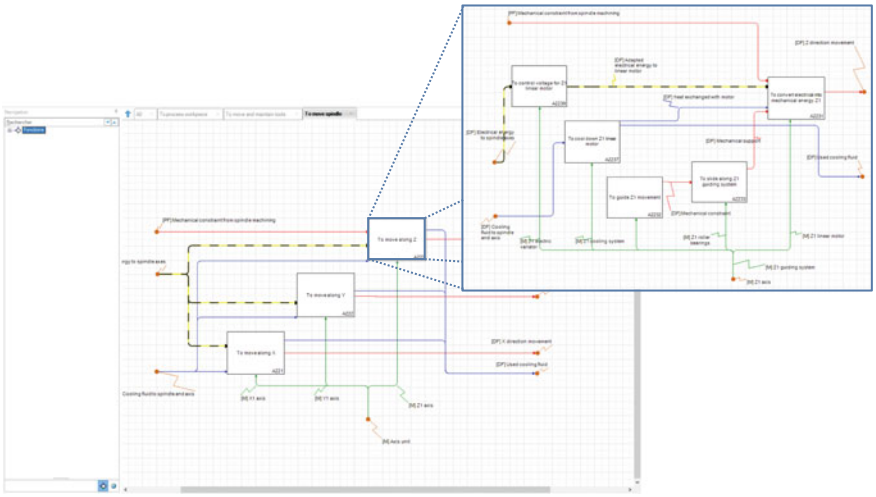

Fig. 13.3 KASEM® knowledge modelling tool—functional analysis of the three-dimensional axis unit

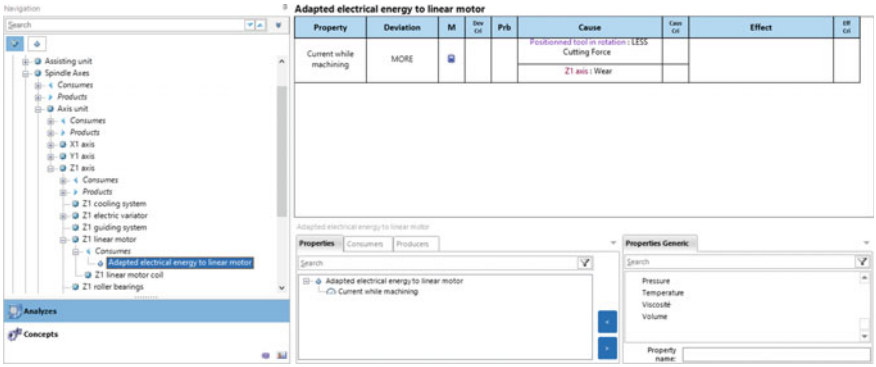

Fig. 13.4 KASEM® knowledge modelling tool—HazOp view of the axis current while machining flow

The malfunction of the system is studied using the HazOp—Hazard and Operability—analysis that identifies the possible deviations of the flows in combination with the study of the possible degradations and criticality of the functions provided by FMECA—Failure Modes, Effects and Criticality Analysis. Each flow deviation and function degradation can be associated with a probable cause and/or effect. The causes can be external, such as human intervention, plant conditions degradation, or internal. Using the same logic, the internal causes could be from another flow deviation or function degradation from another sub-system of the same machine. Following this principle, the interoperability between the sub-systems leads to build a root cause analysis of potential malfunctions. For instance, Fig. 13.4 shows the HazOp of the possible deviations of the flow: "adapted electrical energy entering the motor of the *Z* axis" of the machine tool. Two possible causes were identified here for the deviation "more current while machining". None of these causes could be identified as root cause in case of a deviation of the flow. Using the causal chain as depicted in Fig. 13.5, some root causes appear at level 2. Using associated monitoring of the possible root causes and manual procedures, the operator then determines the real cause of the detected flow deviation.

The functioning and malfunctioning of modelling is implemented in the knowledge base of the platform to structure its inference engine. Each event can lead to supply a common feedback of the fleet that helps diagnostic and decision-making by providing the most common cause and root cause for each event type encountered.

13.2.3 Combination of the General Concepts and Analysis to Build Fleet-Wide Architecture

The systemic approach is combined with a semantic approach, both providing tools that help the fleet management purpose [3]. The semantic approach aims at defining the general concepts related to each level of the fleet. The ontology-based definitions

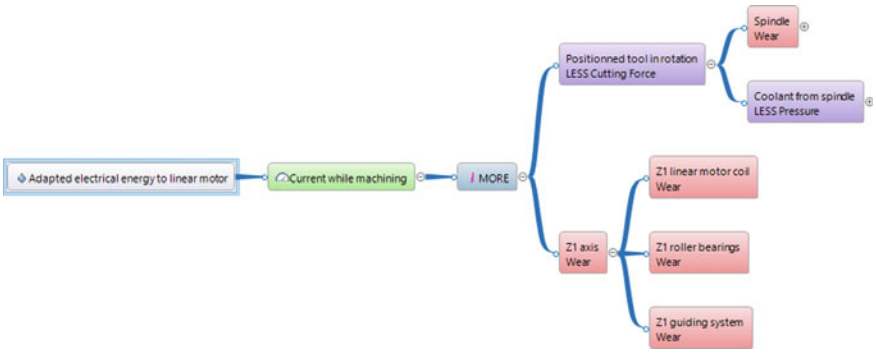

Fig. 13.5 KASEM® knowledge modelling tool—root cause analysis view of current while machining deviation

support the characterization of intrinsic rules for a generic monitoring of machines different regarding the design and the components. It also defines the concepts that are necessary to build the root cause analysis that profits from the feedback provided by the fleet-wide management. The systemic modelling is built using definitions from the semantic modelling. The functional analysis is designed for any specific machine design, using only generic functions and flows to represent its equipment and their interactions. The dysfunctional modelling then profits from the generic deviations and degradations commonly associated with the flows and function. Finally, the root cause diagrams can be automatically generated using the information provided by the systemic modelling and profits from the feedback on functions and equipment regarding their definitions.

13.3 Maintenance Platform Services

To offer support to maintenance personnel, a set of maintenance-related services must be integrated into a dedicated maintenance platform. KASEM®—Knowledge and Advanced Services for E-maintenance—which is developed, maintained and improved by PREDICT, is a platform that offers such services and is dedicated to proactive and predictive maintenance to help operators and experts to take the right decision at the right time. The efficiency, flexibility and operability of the platform are mainly based on its service-oriented architecture, as depicted in Fig. 13.6.

KASEM® platform integrates mandatory services such as data storage, as well as administration services that regroup all aspects relative to user management (profile definition, user authentication, user rights). In addition, the platform integrates the following services:

- *Data Visualization* gathers all the tools and ways to communicate a clear and efficient information to the users (statistical graphics, plots, information graphics,

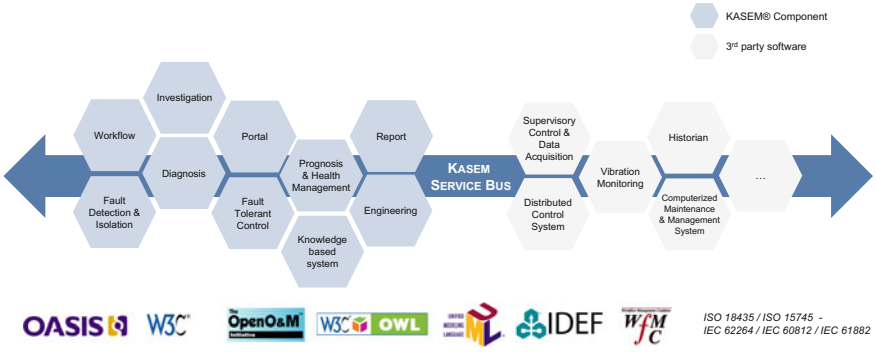

Fig. 13.6 KASEM®, service-oriented architecture (SOA) platform

tables, and charts) and to help users to analyse data by providing tools adapted to the type of information to be investigated. It aims at making complex information more accessible, understandable and usable.

- *Event management* gathers all the tools and ways to generate events relative to systems' status (fault detection, prognostics, health) and to manage these events (validation, cancellation).
- *Analysis and Investigation* gathers all the tools and ways to analyse and understand events and to take the right decision. It regroups all the possible actions that help to identify the causes of an event.
- *Knowledge sharing* gathers all the ways to create and consult system's documentation and information.

In the following, these four main services are discussed.

13.3.1 Data Visualization Services

To visualize its data, an end-user has three kinds of tools according to the type of information to be checked, the level of details needed or the profile of the user and its expectations:

- Dynamic time series for the visualization of historical raw and computed data set as well as real-time information.
- Custom reports that show specific view of the data set on a specific period.
- Dashboard that shows specific dynamic views based on real-time data information.

Dynamic time series visualization is available into the KASEM® platform thanks to its integrated E-Visualization tool, which user interface is represented in Fig. 13.7. This tool aims at performing a detailed expertise on systems by analysing systems' data. It offers from simplest to more advanced capabilities such as:

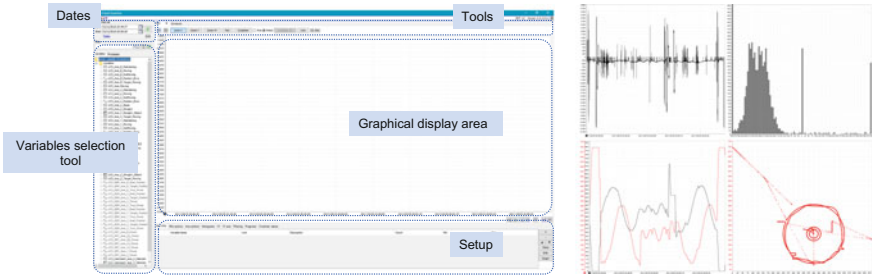

Fig. 13.7 KASEM® data visualization: (left) e-visualization tool, (right) built-in charts

- Collected data visualization as time series. Variable curves can be loaded into a graphical display area. Multiple variables can be loaded into a same view, they can be easily scaled (manual configuration of axis, attached to another variable axis) and manipulated (colour, stroke and point types, display type).
- Reusable contexts creation. Indeed, the tool allows to save all the loaded variables of a graphical display area and their custom setup into a context that is reuseable. By this way, it is possible to load a memorized context into different periods to compare situations.
- Built-in tools to analyse situations such zooming, filtering or comparing variables. Moreover, user can perform histograms and *XY* graphs.

Hence, KASEM® e-Visualization offers to a user the capacity to easily manipulate and analyse systems' historical or real-time data set. It fits well for performing expert analysis on a system but has limited capacity of synthesization.

To this purpose, report or dashboard definition is required. Reports and dashboards allow to visualize information in an organized way and to perform further analysis or point out advanced information built from raw variables. They both aim at having a focus on specific aspects of a dataset, yet they differ from several aspects.

A report is defined as a document that contains information organized in a narrative, graphic or tabular form and aims at being communicated or presented in oral or written form. On the other hand, a dashboard characterizes "a visual display of the most important information needed to achieve one or more objectives". Table 13.1 summarizes the main differences.

Examples of specific views that can be extracted from knowledge base data are presented in Fig. 13.8. On the left, a radar chart that is sent each week to specific user is shown. This chart displays an overview of the amount of data collected from its machine tool's fleet. On the right, an example of dashboard displaying machine tool system usage data.

Data visualization service is one the most important features for Operation and Maintenance, allowing to create specific static or highly dynamic views per user core business and user level of knowledge about the system. Today, in addition to be user-adaptive, this service must also be device-adaptive to fit all displaying technologies: desktop, laptop, tablet, smartphone and smart watches.

Table 13.1 Report and dashboard differentiation

Report	Dashboard
Static: historical information defined by date ranges	**Dynamic**: automatically updated real-time information
To be shared: structured information for the audience	**Specific to user**: for the user of a system and system management purpose
Singular: any modification to it will be seen by each person of the audience	**Exclusive**: modification on a user's dashboard does not affect any other dashboard
Generated as a file: more often PDF files	**Interactive Web pages**: based on technologies such as D3.js (JavaScript library for manipulation documents based on heterogeneous data)

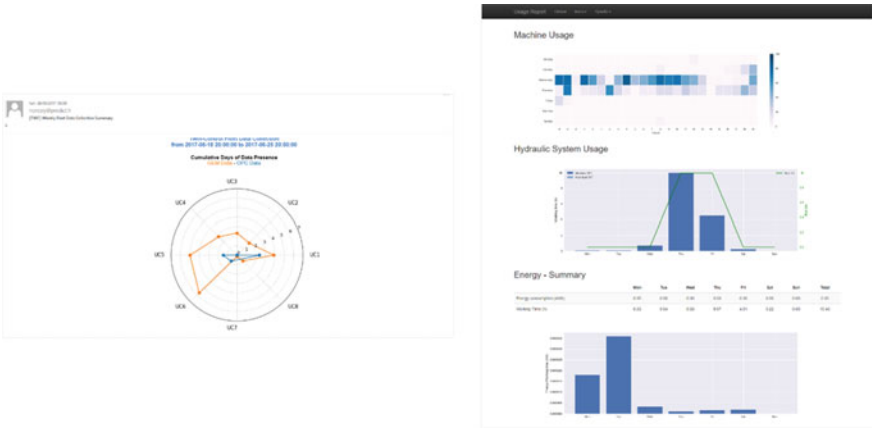

Fig. 13.8 Examples of advanced data visualizations: collected data report sent periodically by e-mail (left), system usage Web dashboard (right)

13.3.2 Event Management Services

An event is a message indicating that something has happened on the monitored system. From Prognostics and Health Management (PHM) point of view, an event can, for example, symbolize that the system behaviour has changed or that there is a high risk of faults [8]. Event management service has, thus, several roles: to generate events and notify users that event occurs, as well as to provide tool to follow event life cycle.

Event generation is the part of the service in charge of running data analysis algorithms on new collected data from monitored systems. Elementary services of data manipulation are orchestrated to build up the platform knowledge and to generate alert as illustrated in Fig. 13.9. In this figure, algorithms are depicted in grey, collected

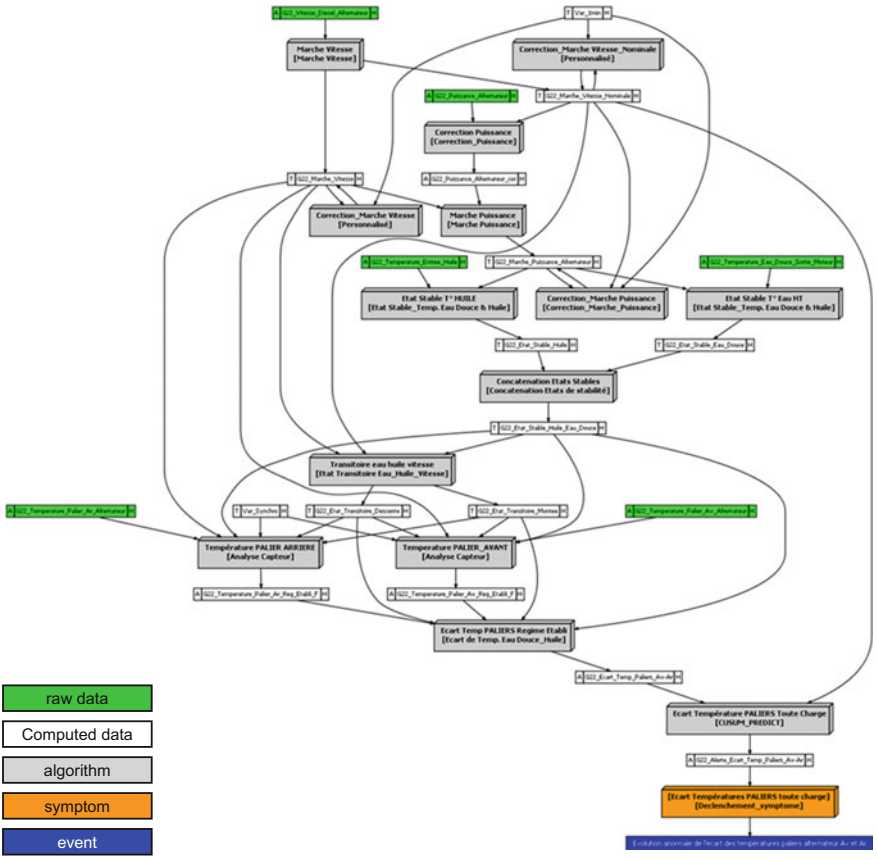

Fig. 13.9 An example of an algorithm chain for event generation, from raw data to proactive event

data in green, and white elements represent part of the computed knowledge. The event, illustrated in blue, is generated at the end of the algorithmic chain.

For a given event, once the sequence is computed and if the event is active, it is necessary to prevent the right users. According to the application, these users can be defined within event level and location. User is alerted that a new event has occurred by e-mail, SMS or thanks to notifications that can be pushed up on a smart mobile device. Then, the users need to have tools to follow-up all events which they are responsible of.

PHM events are mainly linked to degradation anticipation and degradation detection. Events represent state changes in the spatial discretization of the faults metrics. They can, hence, evolve when metrics increase and decrease, but also disappear. Generally, for a given event, its level is represented by an integer number between 1 and 10 (the highest the level is, the closer of the degradation it is). To follow the status

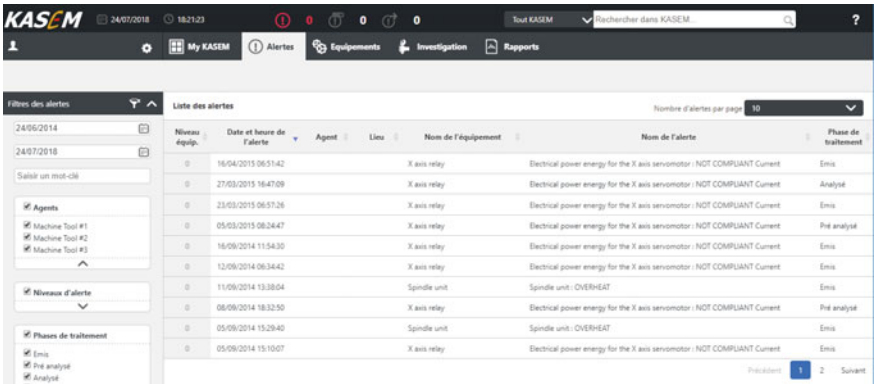

Fig. 13.10 KASEM® event console

of active events, the KASEM® events console, reproduced in Fig. 13.10, summarizes all details about the last evolution of each active events:

- Event occurrence and last state dates;
- Location of the equipment (component, sub-system or fleet) attached to the event;
- Description and type of the event;
- Level of the event;
- Additional buttons to visualize event data.

13.3.3 Analysis and Investigation Service

An event occurs when an abnormal behaviour has been detected. Analysis and investigation service is then necessary to explain what the causes are—diagnostic—and the consequences—prognostic—of this event. This analysis and investigation process is organized in a workflow and results in event analysis and capitalization that improves event feedback.

The KASEM® workflow process is schematized in Fig. 13.11. It consists in a sequence of interactions and actions between the platform, the system and operators. The different steps are:

- *Preliminary analysis*: In this step, the event veracity is checked by a user. If a true event has occurred, a diagnostic can be performed for this event. In other cases, the event is rejected.
- *Diagnostic*: In the field of investigation, this step aims at identifying the potential causes of the event and it can potentially result in consequences identification. This step can be completed by performing analysis to refine the diagnostics. When the diagnostics are accepted, i.e. when the causes have been identified, the event analysis can be finalized.

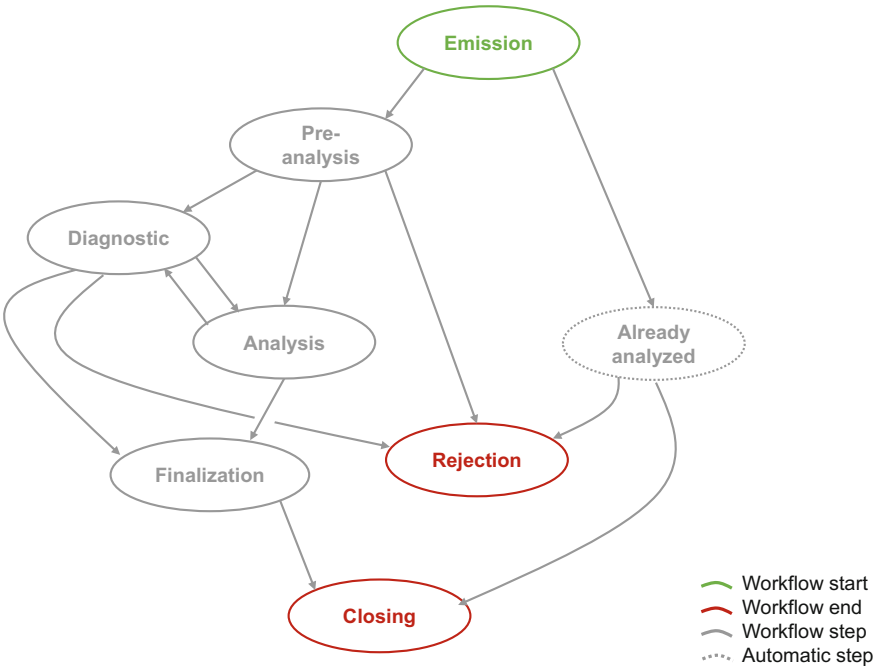

Fig. 13.11 KASEM® event analysis and investigation workflow

- *Analysis*: This phase aims at refining the potential causes by querying complementary analysis. After an analysis, further diagnostic may be performed if needed or the event may be finalized or rejected.
- *Finalization*: In this step, the most probable cause is selected, event is closed, and the overall analysis is stored into the knowledge base to expand available experience feedback.

The experience feedback is all the accumulated information about causes and consequences that have been held on the different events of a system. It aims, on the one hand, at optimizing the decision-making process when an event appears; and on the other hand, at pointing out recurrent problems towards the objective of continuous improvement of the system.

Experience feedback is improved with fleet dimension as it is shared by all its individuals. Hence, the bigger is the fleet, the greater is the feedback. Nevertheless, to cope with individuals' heterogeneity a knowledge model based on ontology should be used for better reuse of data, like maintenance history, reliability analysis, failure analysis, data analysis at fleet level to provide knowledge from similar but non-identical systems [6].

13.3.4 Knowledge and Information Sharing Service

From a system context, the knowledge defines all the documentation, analysis, schemes and any element that make a system more comprehensive. Through KASEM®, the knowledge storage as well as the knowledge creation is made available. Indeed, it is possible to add documentation relative to a system, a sub-system or a component. Moreover, it is possible to perform and store advanced system analysis like functional and dysfunctional analysis.

Sharing service includes ways to exchange information from the platform. KASEM® Representational State Transfer—REST—API enables automatic exchange of information with other platforms or tools. The API provides a secure and accredited access to the business-oriented Web services. Information can thus be read or written by executing a simple HTTP request. This offers a high level of interoperability with all conventional languages such as .Net, Java and Python.

Hence, the platform enables to:

- centralize and provide easy-to-access documentation and information for all the users;
- share up-to-date information to all the users by providing direct access to newly created information.

13.4 Conclusion

This chapter presents advanced services that are required for a fleet-wide proactive maintenance platform to provide the right information at the right time to the right person and to assist this person in decision-making. For this purpose, advanced operation and maintenance services like data visualization service, event management service, analyse and investigation service and knowledge sharing service must be provided. Within Twin-Control project, the platform KASEM®, developed by PREDICT, has been deployed to centralize data and knowledge on twelve machine tools and several generic algorithms have been developed to evaluate machine health and generate early detection events to anticipate machine failure.

Flexibility is a key point in the SOA platform for operation and maintenance services [9], and there are two levels of flexibility. Service-oriented architecture is the first level with the possibility to only use needed services and thus only pay for the used services. The second level of flexibility corresponds to service itself that must fit with the application constraints.

References

1. Medina-Oliva, G., Voisin, A., Monnin, M., Peysson, F., Leger J-B.: Prognostics assessment using fleet-wide ontology In: Proceedings of Annual Conference of the Prognostics and Health Management Society, Montreal, Minneapolis, MN (2012)
2. Medina-Oliva G., Peysson F., Voisin A., Monnin M., Leger, J-B.: Ships and marine diesel engines fleet wide predictive diagnostic based on ontology, improvement feedback loop and continuous analytics In: Proceedings of 25th International Congress on Condition Monitoring and Diagnostics Engineering Management, pp. 11–13Helsinki, Finland (2013)
3. Monnin, M., Leger, J.-B., Morel, D.: Proactive facility fleet/plant monitoring and management. In: Proceedings of 24th International Congress on Condition Monitoring and Diagnostics Engineering Management, Stavanger, Norway, (2011)
4. https://www.collinsdictionary.com/dictionary/english/machine-tool
5. Abichou B., Voisin A., Iung B.: Bottum-up Capacities Inference for Health Indicator Fusion with Multi-Level Industrial Systems, Proceedings of 2012 IEEE Conference on Prognostics and Health Management, Denver, CO, pp 1–7 (2012)
6. Medina-Oliva, G., Voisin, A., Monnin, M., Leger, J.-B.: Predictive diagnosis based on a fleet-wide ontology approach. Journal of Knowledge-Based Systems **68**(1), 40–57 (2014)
7. Monnin M., Voisin A., Leger J-B., Iung B.: Fleet-wide health management architecture, Proceedings of Annual Conference of the Prognostics and Health Management Society, Montreal, Quebec, Canada (2011)
8. Peysson, F., Ouladsine, M., Outbib, R., Leger, J.-B., Myx, O., Allemand, C.: A generic prognostic methodology using damage trajectory models. IEEE Trans. Reliab. **58**(2), 277–285 (2009)
9. Fernandez, S., Mozzati, C., Arnaz, A.: A Methodology for Fast Deployment of Condition Monitoring and Generic Services Platform Technological Design, Proceedings of Annual European Conference of the Prognostics and Health Management Society, Bilbao, Spain

Chapter 14
Visualization of Simulated and Measured Process Data

Denys Plakhotnik, Luke Berglind, Marc Stautner, Dirk Euhus, Erdem Ozturk, Tobias Fuertjes and Yavuz Murtezaoglu

14.1 Introduction

Over the last century, companies and research institutions have put significant efforts into improving the performance of machining operations. The progress was achieved in improving tool life through optimization of cutting tool geometry, cutting material, coolants, and coatings. Nowadays, these advances can be considered traditional and, to a large extent, this area seems to be over-researched, resulting in marginal output from research. In order to push back the frontiers of industrial practice, more sophisticated tools and approaches must be used to address process monitoring and controlling the conditions of the machine and tool [1].

D. Plakhotnik (✉) · M. Stautner · Y. Murtezaoglu
ModuleWorks GmbH, Aachen, Germany
e-mail: denys@moduleworks.com

M. Stautner
e-mail: marc@moduleworks.com

Y. Murtezaoglu
e-mail: yavuz@moduleworks.com

L. Berglind · E. Ozturk
The Advanced Manufacturing Research Centre (AMRC), Boeing, University of Sheffield, Sheffield, UK
e-mail: l.berglind@amrc.co.uk

E. Ozturk
e-mail: e.ozturk@amrc.co.uk

D. Euhus · T. Fuertjes
MARPOSS Monitoring Solutions GmbH, Egestorf, Germany
e-mail: dirk.euhus@artis.marposs.com

T. Fuertjes
e-mail: tobias.fuertjes@mms.marposs.com

M. Armendia et al. (eds.), *Twin-Control*,
https://doi.org/10.1007/978-3-030-02203-7_14

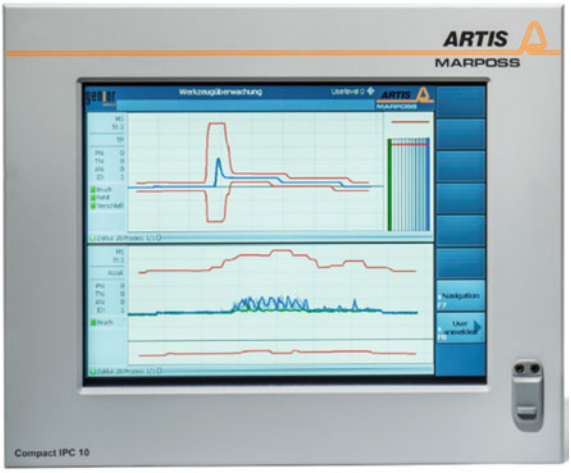

Fig. 14.1 Visualization of the process parameters is plotted as a set of charts

Since computer numerical controls (CNCs) are used in almost all kinds of production processes, there is a way to improve CNCs such that the entire production chain may benefit from such an improvement. Because CNCs depend on the production cycles of the hardware to which they are connected, CNC implementations need to assure a certain level of interoperability. The technological standards of current CNC user interfaces do not provide the rich user experience expected of today's HMIs. In addition, not all available information is connected and provided to the user. Information such as the current axis values and machining program are displayed as text, and only experienced users are able to use the information directly. When new data is introduced into these systems, either by exchanging the CNC, by adding hardware to the system or by adding simulation software, it is difficult to connect this new data to the information currently in the system.

Although many researchers and commercial entities are involved into the development of software and hardware solutions for process monitoring, one of the most comprehensive studies in the field [2] reveals marginal exposure of the development in the area of visualization of the process monitoring. In general, the review papers in monitoring of machining operations [2, 3] do not emphasize the importance of visualization. Measurements from additional hardware can be displayed as plots, as shown in Fig. 14.1, but it is difficult to correlate a position on the plot with the programmed toolpath and the machine values at that instance in time.

Moreover, it seems that most of the publications target visualization of simulation results only. Apparently, computing of cutting forces and other process parameters can become an important issue for the industry, because it may facilitate reduction in ramp-up time and associated costs for batch production. Process monitoring data are often used to tune process parameters for batch production. Several parts are machined before the batch production in order to define the specification of a stable process. In contrast, a fully fledged virtual machining environment will result in

reliable prediction of cutting conditions without performing real trials. It is likely that postprocessing and analysis of the data acquired after actual machining will become nearly obsolete after virtual manufacturing paradigm becomes an industry standard. Simulation approaches will avoid performing expensive trials. Creating a strategy that combines measurement and simulation data sources has a high potential.

Based on the preliminary studies, several gaps between process monitoring and visualization have been identified. The following list highlights approaches that may bring benefits in the manned analysis of the process monitoring data:

- Geometric simulation/verification based on the measured machine axis positions;
- Colorization of the simulated workpiece geometry based on the simulated/measured process parameters (spindle torque, cutting forces, etc.);
- Comparison of the simulated and measured process parameters.

On the software side, the aim is to replace the standard data display methods (tables, graphs, etc.) with a graphical interface that shows the current shape of the workpiece and the machine to enable users to immediately see what is currently happening. This directly connects the real world of the process, the machine, and the workpiece with the data at a certain instant in time. This allows users to directly find correlations and problems and apply the needed modifications to the process.

This chapter presents visualization functionalities provided by ModuleWorks to Twin-Control. This includes explanation of the principles of the underlying 3D simulation methods along with the description of the developed visualization features providing advanced visualization of measured and simulated cutting force values that are mapped on the predicted shape of the workpiece.

14.2 3D Volumetric Simulation

There exist several techniques which have been developed to model virtual workpieces and removing any material that interferes with the geometry of a tool moved along a path (solid modeling [4, 5], Z-map [6], and Dexel approach [7]). In this paper, a discrete modeling method based on tri-Dexel volume representation [8] is used, which is an improved version of the Dexel model. The tri-Dexel model represents a volume as a manifold of evenly distributed linear segments, or Dexels, in three orthogonal directions, as depicted in Fig. 14.2a. In the current paper, geometric software which applies the tri-Dexel model is used because tri-Dexel model has proved to be an efficient data structure with reliable performance and precision, which is very important for a computation routine running in an iterative loop. The material removal has been simulated using ModuleWorks engine that calculates discrete intervals intersecting with the swept volume of a moving tool. The start and end points of all subtracted intervals indicate the boundary of the removed volume and hold information about their spatial position and inverted normal vectors of the tool sweep envelop. Dexel spatial positions, surface normal vectors, and signatures of the intersecting tools are sufficient to reconstruct the part surface, as shown in Fig. 14.2b.

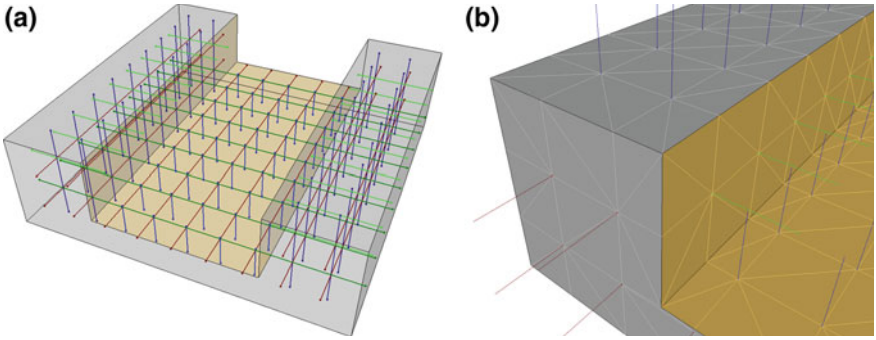

Fig. 14.2 Use of the tri-Dexel model: **a** tri-Dexel model (red, green, and blue segments are the Dexels in X, Y, and Z directions); **b** triangulation and triangle coloring derived from the Dexel points and normal vectors

14.3 3D Simulation and Interfaces Combined

To connect the real-world shapes, a virtual representation of the machine and the current shape of the workpiece need to be maintained throughout the entire process. ModuleWorks uses its industry-proven MachSim (the machine and its kinematic) and CutSim (actual shape of the workpiece during the manufacturing process) software to create the 3D representation of the workpiece geometry and machine that can then be integrated into the CNC user interface.

For the Twin-Control project, this methodology has been extended and optimized. It has developed an interface to exchange internal simulation data for processing analytic modules that allow the prediction of process behavior such as stability and cutting forces. To display this information to the user at the machine, a second interface connects this data with the workpiece shape that was calculated in parallel. The other interfaces take real-world measurement data and integrate it into the same representation of the workpiece shape. The virtual system is completed by a system that delivers warnings to users and delivers additional security to the machine. Users can directly correlate data with the current shape of the workpiece. On the machine, this system can stop the process to avoid crashes and other unwanted process errors.

As shown in Fig. 14.3, the process monitoring data are split into spatial data related to the cutter position and a process parameter, which will be visualized. The measured machine axis positions are used to re-simulate material removal in CAM software. The workpiece simulation holds only geometry data describing the material left after the simulation. Finally, the workpiece geometry is enriched with the measurement values. In this particular case, the Genior Modular system provides spindle torque.

To demonstrate developed software features, a simple pocketing operation (four-pocket milling) is used (as shown in Fig. 14.4). In order to improve usability and ergonomics of visual inspection, colorization of milling tool, toolpath, and machined surface has been implemented. However, visualization is only one aspect of part

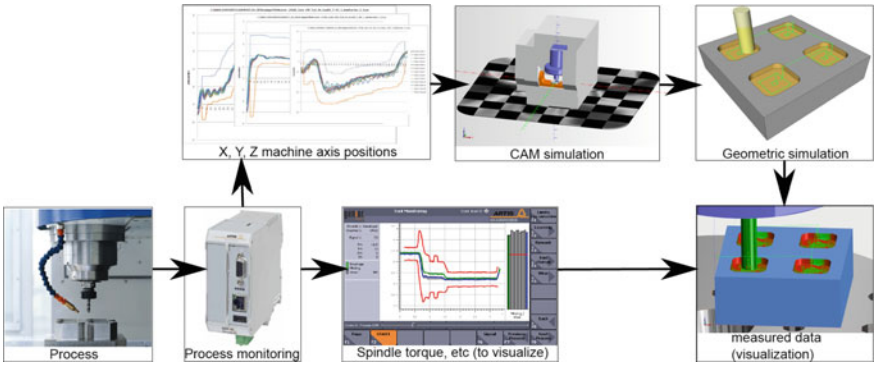

Fig. 14.3 Workflow to combine simulation of measured machine movements and process data

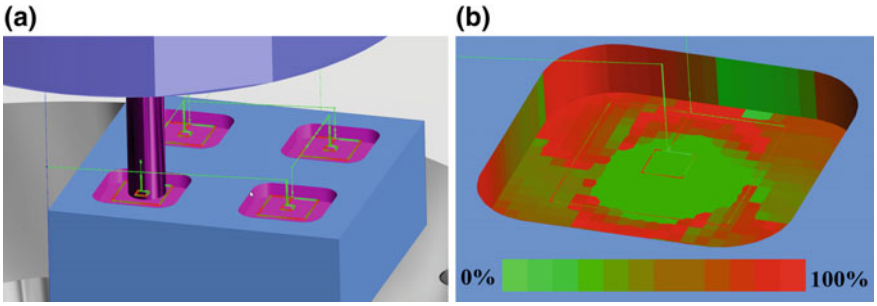

Fig. 14.4 Visualization of pocket milling machine: **a** colorization of cutting/rapid moves; **b** colorization of spindle torques

quality inspection. Figure 14.5 depicts a Chiron milling machine equipped with the developed software–hardware functionality. The simulation screen shows the actual status of the workpiece shape, in which material removal simulation is performed considering measured axes positions. Online inspection of the process is always available regardless of the workpiece visibility (for instance, due to coolant mist). Closer look on a single pocket is shown in Fig. 14.4b. The spindle torque (%) was measured every 0.06 mm for constant feed. The length of a pocket toolpath is about 73 mm.

Another visualization feature, which may not be extremely useful in the industrial settings, is mapping of the difference between measured and expected/simulated data. As an example, researchers or scientists are allowed to depict the relative error of their force models and the measurements of the actual machining. Figure 14.6 shows how two sets of data can be represented on a 3D surface of the simulated part. This approach should ease finding typical machining case scenarios (corner machining, pocket machining, etc.) at which simulation models fail more often by highlighting them.

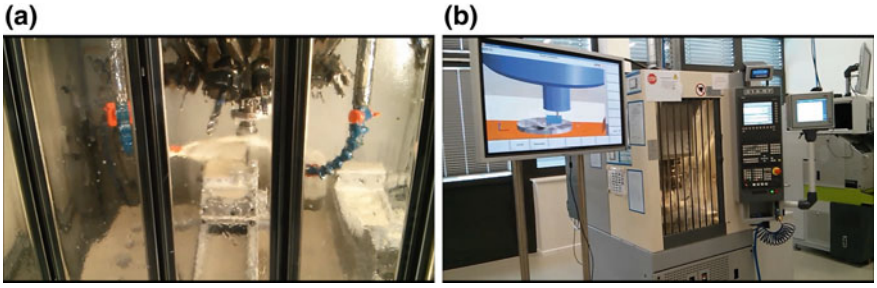

Fig. 14.5 Observation of the milling process on a Chiron machine: **a** through the machine housing; **b** on the simulation screen

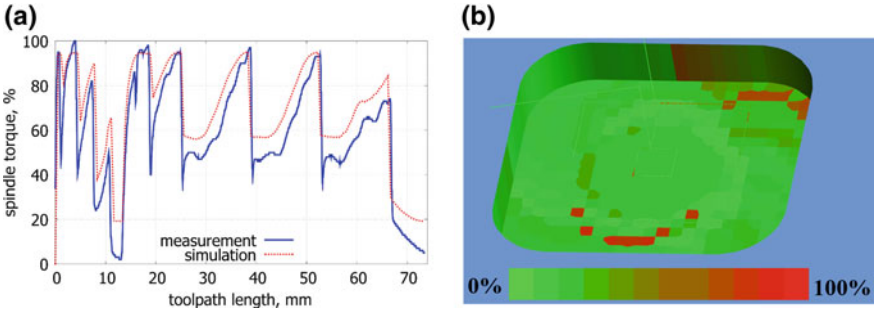

Fig. 14.6 Visualization of the difference between measured and simulated data: **a** input data; **b** mapping of the difference on the 3D surface

Additionally, one experimental visualization feature for advanced simulation has been developed. In generic simulation, all cut points are painted with one uniform color. However, some tool properties, like tool deflection, wear, depend on the point on the tool that removes material. Applying the simulation data along with the feature yields a surface depicting proper input values for the parts of the cutting tool that are in contact in machining time, as shown in Fig. 14.7. Calculation of the contact points considers five-axis motions via quaternion interpolation.

14.4 Additional Visualization Features

Besides, there have been developed another several visualization methods that can facilitate to optimize machining operations:

- Visualization of the tool–workpiece engagement. Figure 14.8 shows the contact area between a tool and the workpiece. This functionality is useful to analyze how cutting forces change along a part program.

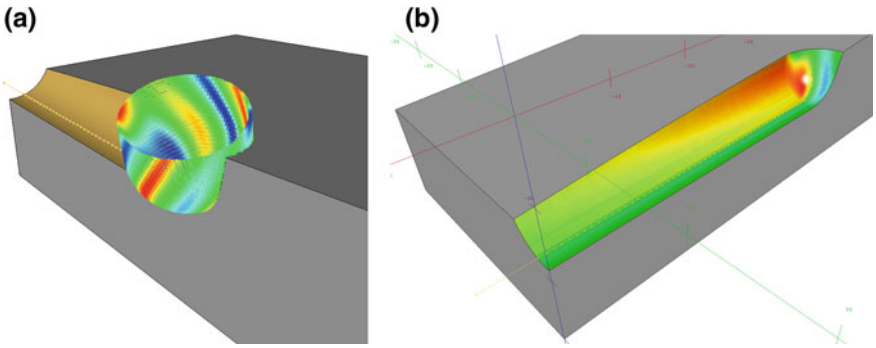

Fig. 14.7 Non-uniform colorization: **a** tool data set at one tool position; **b** mapping of all tool data sets onto the machined surface

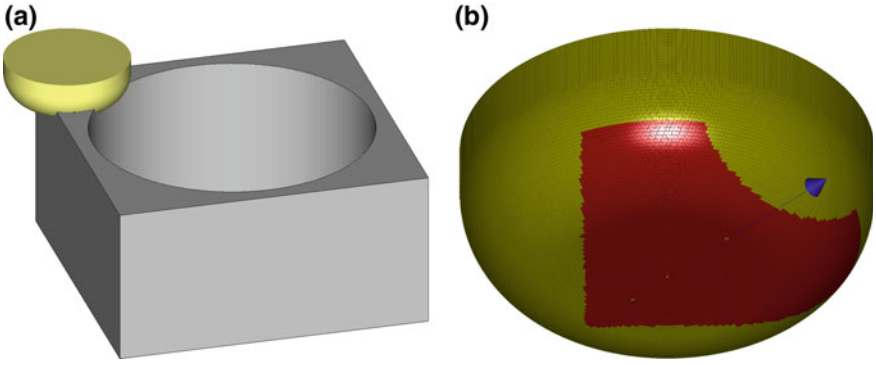

Fig. 14.8 Visualization of the tool-workpiece engagement: **a** tool-workpiece setup; **b** engagement area

- Visualization of the cutting marks on the machined surface. Figure 14.9a shows which surface outlook can be expected after grinding. This feature is expected to be necessary for aesthetic applications.
- Visualization of future shape and position of machine components. Figure 14.9b shows two tools and spindles. The transparent ones are attributed to the future positions acquired from the CNC as the output of the look-ahead functionality. The real axis positions, machine geometries, and workpiece position are taken into account. The predicted position is examined toward potential collisions and may signal to halt the machine before the actual collision occurs.

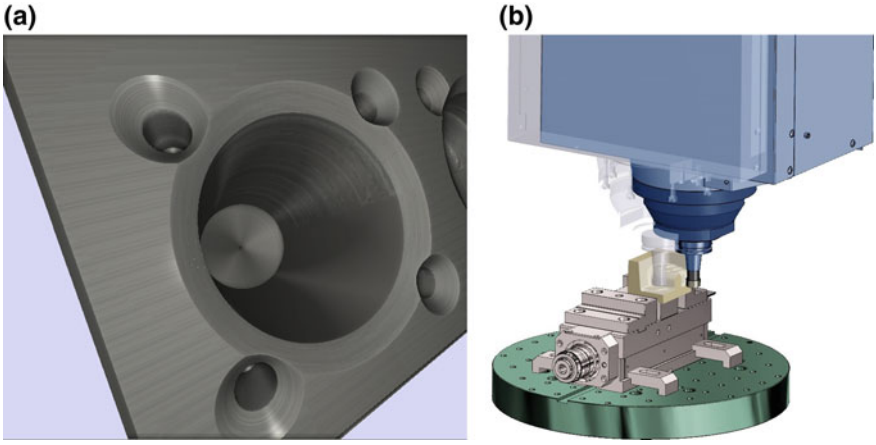

Fig. 14.9 Additional visualization features: **a** grinding textures using the shader technology; **b** visualization of the future machine position (transparent)

14.5 Conclusions

Integration of the process monitoring data into CAM simulation is a tangible progress in the evolution of the CAx chain. Previously, the analysis of the cutting process measurements could not be performed in the CAM environment. In an extended CAM, immediate access to stored process parameters allows more robust verification and modification of NC programs. Three-dimensional machined surface colored according to the measurement can be analyzed more intuitively than graph plots. Also, it can be detected whether the extreme or unfavorable cutting conditions do really affect the machined surface. In a case of an actual or foreseeable failure, results of cutting force simulation can be exploited for operation re-planning to avoid tool and workpiece damage.

References

1. Ulsoy, A.G., Koren, Y.: Control of machining processes. J. Dyn. Syst. Meas. Control **115**(2B), 301–308 (1993)
2. Teti, R., Jemielniak, K., ODonnell, G., Dornfeld, D.: Advanced monitoring of machining operations. CIRP Ann. Manuf. Technol. **59**(2), 717–739 (2010)
3. Stavropoulos, P., Chantzis, D., Doukas, C., Papacharalampopoulos, A., Chryssolouris, G.: Monitoring and control of manufacturing processes: a review. In: 14th CIRP Conference on Modeling of Machining Operations (CIRP CMMO), vol. 8, pp. 421–425 (2013)
4. Lazoglu, I., Boz, Y., Erdim, H.: Five-axis milling mechanics for complex free from machining. CIRP Ann. Manuf. Technol. **60**, 117–120 (2011)
5. Boz, Y., Erdim, H., Lazoglu, I.: Modeling cutting forces for 5-axis machining of sculptured surfaces. In: 2nd International Conference, Process Machine Interactions (2010)

6. Kim, G., Cho, P., Chu, C.: Cutting force prediction of sculptured surface ball-end milling using Z-map. Int. J. Mach. Tools Manuf **40**, 277–291 (2000)
7. Boess, V., Ammermann, C., Niederwestberg, D., Denkena, B.: Contact zone analysis based on multidexel workpiece model and detailed tool geometry representation. In: 3rd CIRP Conference on Process Machine Interactions (2012)
8. Benouamer, M.O., Michelucci, D.: Bridging the gap between csg and brep via a triple ray representation. In: Proceedings of the Fourth ACM Symposium on Solid Modeling and Applications, SMA '97, ACM, pp. 68–79, New York, NY, USA (1997)

Part V
From Theory to Practice

Chapter 15
Twin-Control Evaluation in Industrial Environment: Aerospace Use Case

Mikel Armendia, Mani Ghassempouri, Guillermo Gil, Carlos Mozas, Jose A. Sanchez, Frédéric Cugnon, Luke Berglind, Flavien Peysson and Tobias Fuertjes

15.1 Introduction

Within Twin-Control project several features have been developed and validated at research level, showing promising results, as presented in the previous chapters of the book. However, since its gestation, Twin-Control project has aimed to provide

M. Armendia (✉)
IK4-Tekniker, C/Iñaki Goenaga, 5, 20600 Eibar, Gipuzkoa, Spain
e-mail: mikel.armendia@tekniker.es

M. Ghassempouri
COMAU France, Castres, France
e-mail: mani.ghassempouri@comau.com

G. Gil · C. Mozas
Mecanizaciones Aeronáuticas S. A. (MASA), Agoncillo, Spain
e-mail: ggil@masa.aero

C. Mozas
e-mail: cmozas@masa.aero

J. A. Sanchez
GEPRO Systems, Durango, Spain
e-mail: jasanchez@geprosystems.com

F. Cugnon
Samtech S.a., a Siemens Company, Liège, Belgium
e-mail: frederic.cugnon@siemens.com

L. Berglind
The Advanced Manufacturing Research Centre (AMRC) with Boeing, University of Sheffield, Sheffield, UK
e-mail: l.berglind@amrc.co.uk

F. Peysson
PREDICT, Vandoeuvre-lès-Nancy, France
e-mail: flavien.peysson@predict.fr

T. Fuertjes
MARPOSS Monitoring Solutions GmbH, Egestorf, Germany
e-mail: tobias.fuertjes@mms.marposs.com

M. Armendia et al. (eds.), *Twin-Control*,
https://doi.org/10.1007/978-3-030-02203-7_15

the required industrial validation. In this line, two validation use cases are presented in the project, from two of the more demanding sectors in European industry and with very different requirements: aerospace and automotive. This chapter presents the results obtained in the application of Twin-Control in the aerospace use case.

Section 15.2 of this chapter provides a summary of the validation use case. In Sect. 15.3, the applied industrial evaluation approach is presented. Section 15.4 deals with the implementation activities and the obtained results, including the impact caused by these features in the end-users. Finally, the last section covers the conclusions.

15.2 Use Case Description

The aerospace validation scenario is located at Mecanizaciones Aeronáuticas S.A. (MASA) plant in Agoncillo, near Logroño in Spain. For the evaluation, GEPRO 502, 512 and 304 machine tools are used. The architecture of the three machines is similar, but they differ in the number of axes, dynamic capabilities, spindle type, etc. Even of the three machines have been monitored, the GEPRO 502, depicted in Fig. 15.1, has been used as the main reference to implement Twin-Control features.

For the aerospace use case, a new machining process, illustrated in Fig. 15.2, has been used. This process has been defined for the project and combines features of different test pieces usually applied by MASA for internal validations. The part is a

Fig. 15.1 General view of the GEPRO 502 machine, available in MASA installations, used in the aerospace validation scenario

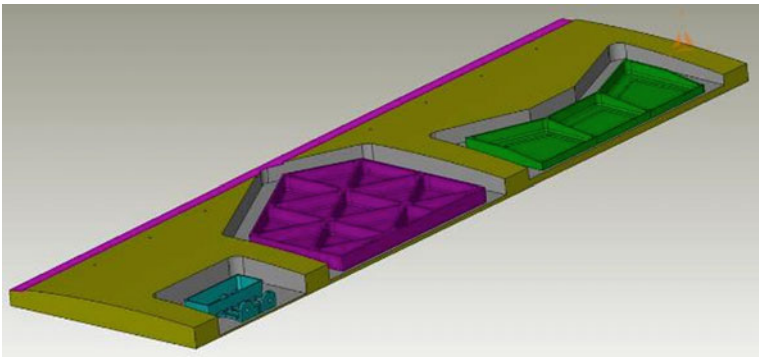

Fig. 15.2 Part used in the aerospace validation use case

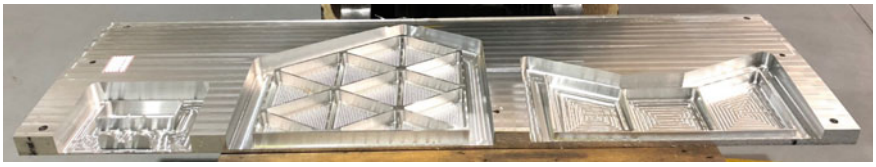

Fig. 15.3 Validation part machined at MASA

large plate of aluminium that is manufactured using 3- and 5-axis milling, as well as drilling operations. Its dimensions are $2000 \times 600 \times 65$ mm.

The evaluation is mainly focused in the triangular pocket region in the middle, represented by purple region in Fig. 15.2. This geometry requires movements aligned in the X- and Y-axes, as well as interpolated movements of these two axes. Through this test the machine tool precision in the linear axis, X and Y, can be evaluated, both when they work individually and interpolated. During the corner machining of the triangular pockets, the machine performs feed rate, acceleration, cutting direction and chip thickness that allow evaluating the dynamic performance of the machine (speed, acceleration and jerk) and the quality of this type of operation.

The validation part has been machined several times (Fig. 15.3) to acquire data through the monitoring system and use it for the validation of the different Twin-Control features. The machined validation part is shown in Fig. 15.3.

15.3 Evaluation Strategy

The evaluation strategy will be linked to the different scenarios of use (SOU) defined by the aerospace end-users at the beginning of the project:

– Scenario of Use 1: Machine tool design
– Scenario of Use 2: Process design
– Scenario of Use 3: In-line operation
– Scenario of Use 4: Maintenance

For each scenario of use, results obtained with Twin-Control are presented, and the impact on end-users is evaluated.

15.4 Scenario of Use 1: Machine Tool Design

The tools and capabilities developed in Twin-Control create a new design environment for machine tool builders which allow to optimize the machine design through simulations. Since in aerospace, process performance overcomes energy efficiency in importance, and the work has been focused in the first feature.

15.4.1 Virtual Machine Tool with Integrated Process Models

15.4.1.1 Implementation and Results

A FEM-based kinematic and dynamic model of the GEPRO 502 machine has been done using SAMCEF Mecano software. The model, represented in Fig. 15.4, covers machine structure, feed drives and integrates control. Specific validation of this simulation model was performed by using hammer tests and positioning movements. The results are presented in Sect. 2.1 of this book.

The machining module has been configured for the three machines of the aerospace use case. For that, characteristics of the cutting tools applied in the validation use case have been collected and stored in a table shape database, reproduced in Table 15. 1, to be used by the simulation tool.

The integrated simulation tool developed in the Twin-Control project is validated by comparing simulated data with data measured during the real process shown in Fig. 15.3.

Once the CAD model of the validation workpiece, shown in Fig. 15.2, is positioned properly on the CAD model of the machine, it is translated to STL format in order to be used in the VMT model depicted in Fig. 15.5.

Validation consists of simulating four machining sequences as shown in Fig. 15.6: a roughing operation of the external groove (blue path), a roughing operation of one triangular pocket (red path), a finishing operation of the vertex of the pocket (black path) and finishing operation of the walls of the pocket (green path). Position target functions replicated from the ISO code executed in the machine are used to feed the Virtual Machine Tool model.

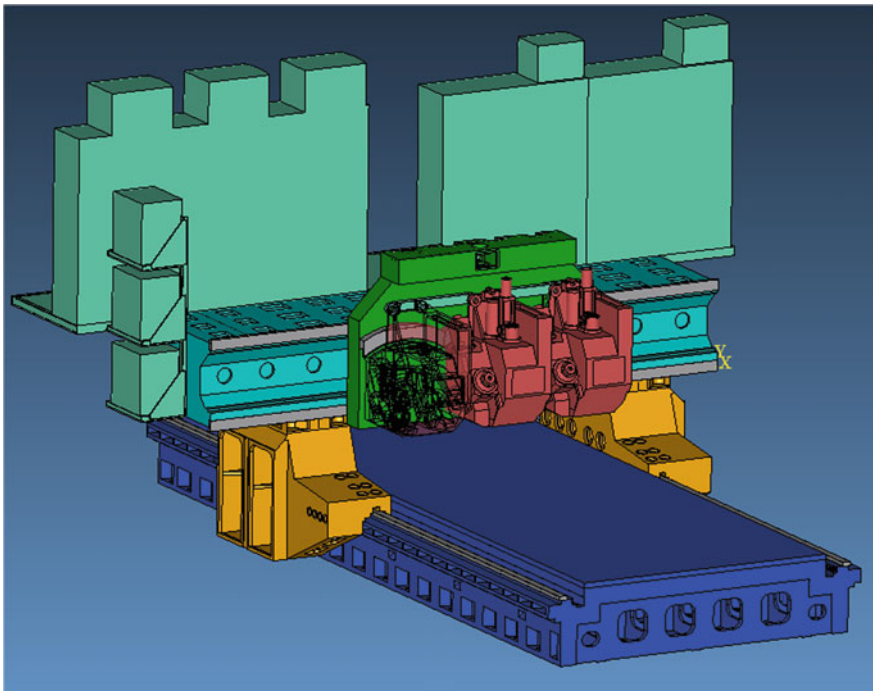

Fig. 15.4 CAD model of the GEPRO 502 machine used for the its Virtual Machine Tool model

The blue machining sequence in Fig. 15.6a, defined as external groove, can be decomposed in 9 equivalent trajectories at different heights defined by the axial depth

Table 15.1 Characteristics of the tools needed in aerospace use case

Tool #	D	Rc	Beta	Lam	Nflut	ToolDir	Zmax
1	50	4	0	0.610865	3	0	15
2	25	4	0	0.610865	3	0	30
3	5	–	0	0.610865	2	0	20
4	40	4	0	0.610865	3	0	15
5	25	5	0	0.610865	3	0	30
6	20	5	0	0.610865	3	0	20
7	20	0	0	0.610865	3	0	20
8	20	4	0	0.610865	3	0	20
9	16	4	0	0.610865	3	0	20
10	30	15	0	0.5236	2	0	10

D Tool Diameter [mm]; *Rc* nose radius of tool [mm]; *Beta* taper angle of tool [rad]; *Lam* Helix angle [rad]; *Nflut* Number of flutes [−]; *ToolDir* cut rotation direction [−]; *Zmax* max Z value for virtual tool [mm])

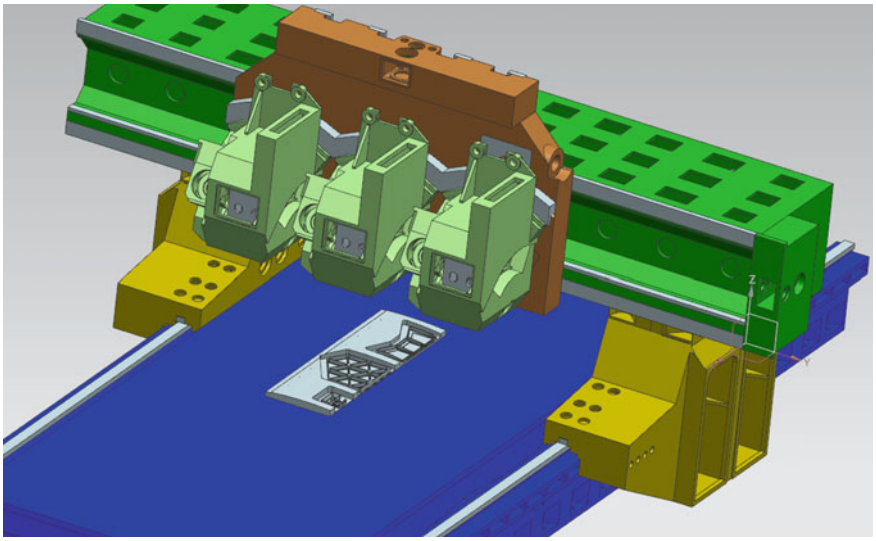

Fig. 15.5 CAD model of the workpiece positioned on the machine model

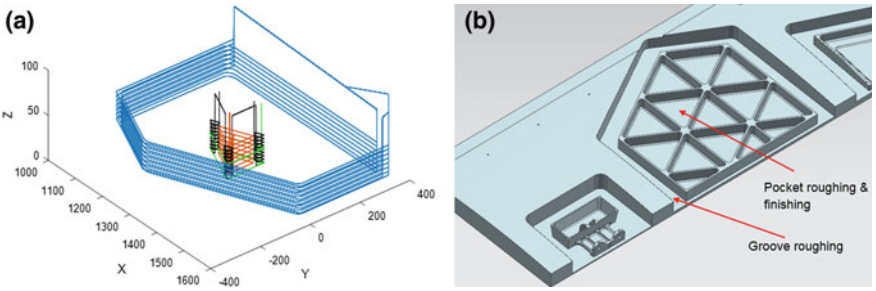

Fig. 15.6 Machining sequences for the validation of machining performance in the aerospace validation scenario

of cut of 5 mm. For each pass, the workpiece STL file generated from the previous one is used, replicating the real machining procedure. In Fig. 15.7, the evolution of the groove machining using the simulation tool is presented graphically.

After the external groove, the triangular pocket roughing is simulated, corresponding to the red machining sequence of Fig. 15.6a. Again, the roughing process is separated in different phases which are simulated taking into account the workpiece geometry of the previous pass. After the roughing operation, triangular pockets are finished by applying two steps. The first one consists in the corner finishing and corresponds to the black machining sequence of Fig. 15.6a. Each vertex is machined by performing three passes at different heights. The second finishing step consists in the wall finishing of the triangle pockets and corresponds to the green machining

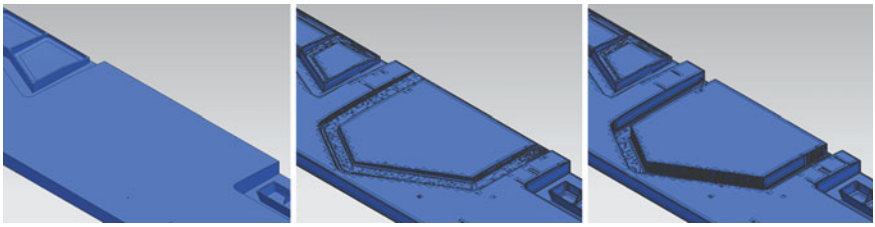

Fig. 15.7 CAD (STL) evolution during the simulation of the external groove machining in the aerospace use case

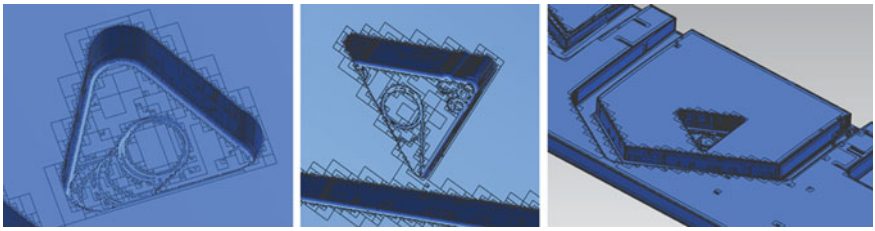

Fig. 15.8 Triangular pocket machining simulation sequence (from left to right): roughing, corner finishing and wall finishing

sequence of Fig. 15.6a. In this case, two passes at different heights are performed. Figure 15.8 presents the complete sequence to machine the triangular pockets.

Figures 15.9 and 15.10 show the simulation results for the pocket roughing and wall finishing operations, respectively, comparing them to the monitored data during real machining at MASA. Although some errors can be observed for some steps of the process, surely due to tool-workpiece engagement estimation inaccuracy, the obtained results match quite well, specially, for roughing operations where higher forces are present.

15.4.1.2 Impact

GEPRO is not a general-purpose machine tool manufacturer. Each GEPRO machine is developed to machine a specific part or part family, always from aerospace sector. In some cases, due to the big size of the machines and the high costs, GEPRO works in the retrofitting of older machines to use the big structural components.

Due to small size of the company and the presented features, GEPRO does not fabricate prototypes for the new machine tool models. Indeed, as each machine is taken as a new development, all GEPRO machines can be taken as prototypes, but they must be completely functional in production.

The current product development stages reproduced in the top of Fig. 15.11, and the correspondent average duration, for GEPRO are:

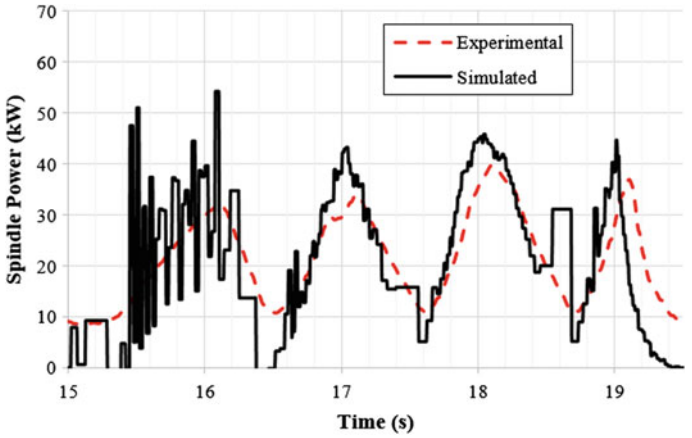

Fig. 15.9 Comparison of the simulation results obtained with the integrated simulation tool and real monitored data for the triangular pocket roughing operation

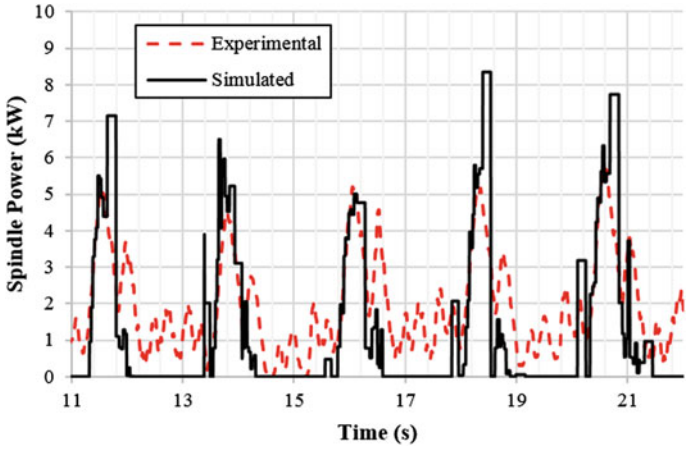

Fig. 15.10 Comparison of the simulation results obtained with the integrated simulation tool and real monitored data for the triangular corner finishing operation

– Conceptual design of the new machine (0.5 months)
– Detailed design (3–4 months)
– Design review and modifications (0.5 months)
– Component fabrication and purchasing (3.5 months)
– Assembly (2–3 months)
– Commissioning (2–3 months)
– Validation and optimization tests (0.5 months).

The application of Twin-Control in the product development of a company like GEPRO will have a direct effect in the commissioning stage, as shown in the bottom

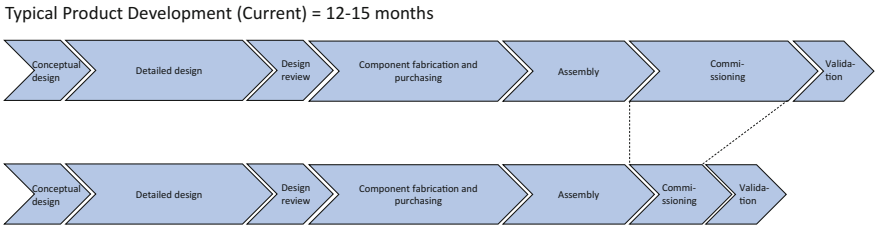

Fig. 15.11 Comparison of the current product development process for GEPRO and the proposed one with the application of Twin-Control

of Fig. 15.11. Indeed, if Twin-Control models are used in the design stage, the developed machine design will be optimized against the required manufacturing process. A reduction of a 10% in the total development time is expected. Contrary to COMAU case, this reduction affects all the machines manufactured.

15.5 Scenario of Use 2: Process Design

For this scenario of use, the integrated simulation tool and the process models developed in the project are of special interest. The possibility to simulate in advance the manufacturing processes provides a great chance to reduce design time and to define optimized processes, leading to a minimization of the set-up time and a better performance of the process.

15.5.1 Virtual Machine Tool with Integrated Process Models

15.5.1.1 Implementation and Results

The same implementation presented in scenario of use 1, machine tool design, is applied in this scenario. Apart from that, for the simulations carried out with the GUI containing the process models, additional hammer tests have been performed at the GEPRO machine to get the FRF of the tooltip with all the used tools Fig. 15.12 shows an example of FRF.

The collected machine data is applied directly in the process model's GUI, so that the simulated tool path follows the measured tool path. The resulting simulated spindle power is then compared with the measured spindle power. The simulated and measured spindle power data is shown for the external grooving, blue machining sequence in Fig. 15.6a with a previous facing operation, in Fig. 15.13.

A closer look at the external grooving operation shows that the measured data follows the same path as the measured data and that the results closely agree, especially

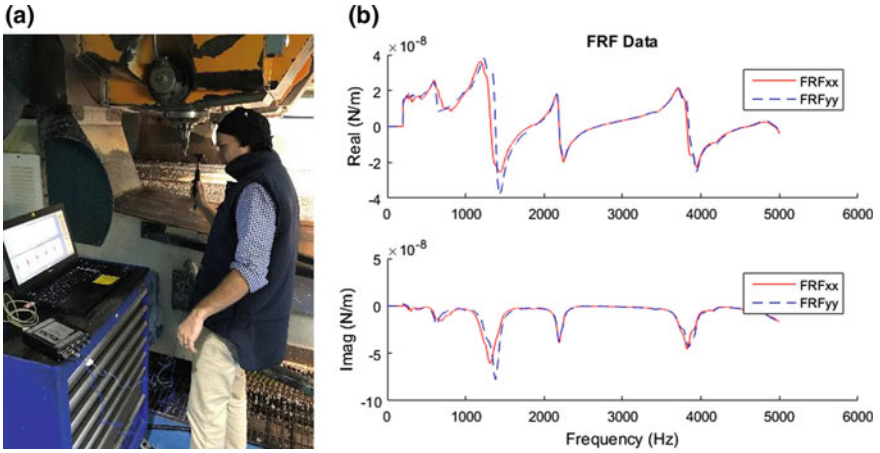

Fig. 15.12 Tool FRFs in the GEPRO 502: **a** Hammer tests. **b** Example of FRF for the tool #1 (from Table 15.1)

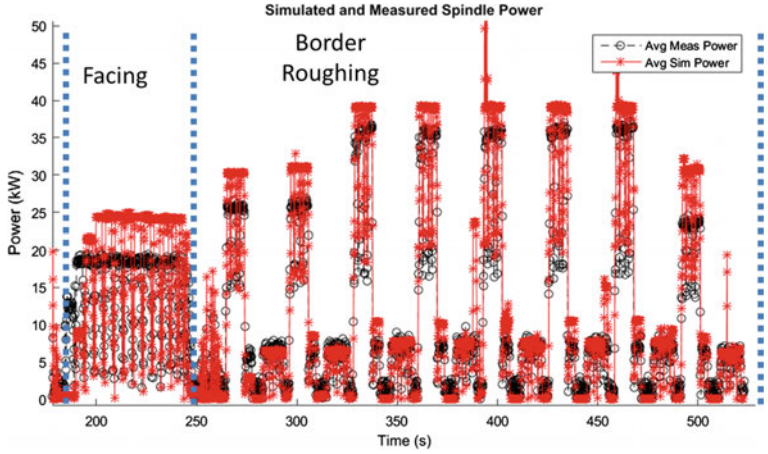

Fig. 15.13 External grooving operation of MASA process: simulated and measured spindle power

at the lower power levels. In Fig. 15.14, the different regions of the operation are identified, showing the amount of power required for each feature of the geometry.

The simulated and measured power results for the triangle pocketing are shown in Fig. 15.15. This operation is composed of a triangular roughing pass, a corner roughing pass and a finishing pass, and required two separate tools in the simulation. The results for the triangle feature also show close agreement between the simulated and measured power values, even at low power rates for the corner roughing and finishing passes.

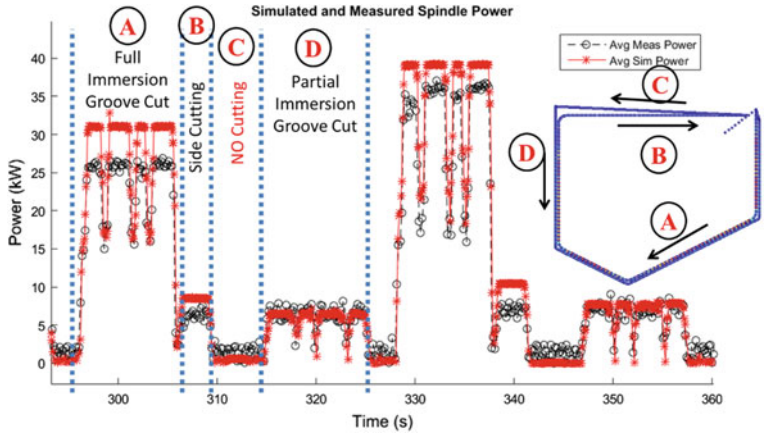

Fig. 15.14 External grooving operation of MASA process: detailed view of the simulated and measured spindle power for a single pass

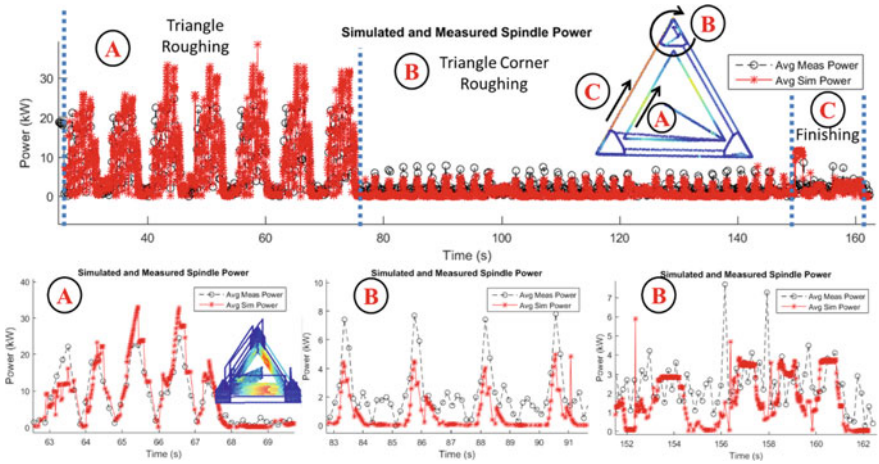

Fig. 15.15 Triangular pocket milling at MASA use case: simulated and measured spindle power

It can be concluded that the application including process models is a very useful tool for machine tool designers. Of course, it does not provide such a complete range of results as the integrated simulation model based on machine tool FEM, but simulations are faster to configure and run. Figure 15.16 shows a comparison of the results obtained for the triangular pocket roughing using the integrated simulation tool, the process model's GUI and the monitored data during real machining. It can be observed that both models' results are very similar and are close to experimental data.

A key aim of the Twin-Control concept is to improve process efficiency through integration of simulation and measurement. As a demonstration, the process simula-

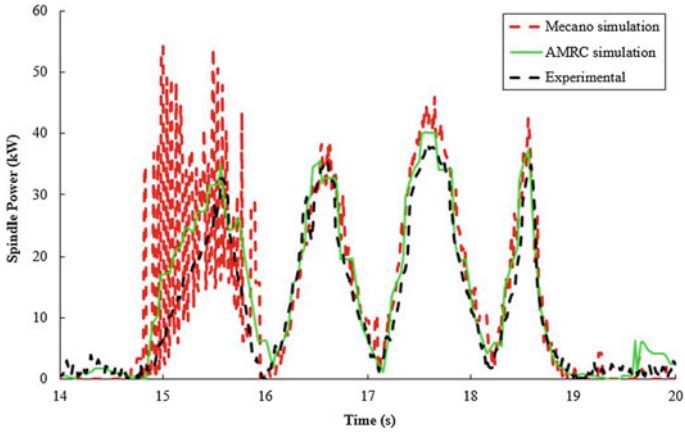

Fig. 15.16 Comparison of the results obtained with the integrated simulation tool (Mecano), process models (AMRC) and monitored values for

tion and measurements results from Fig. 15.15 have been applied to identify process improvements. Different strategies are tested on three triangular pockets, where each pocket is broken down into three operations (roughing, vertex finishing and wall finishing), and each operation is broken down, again, in three steps where machining conditions vary. A summary of the process parameters is provided in Table 15.2. For the pocket roughing operation (steps 5001–5003), the axial step is varied between 5 and 7 mm, so the number of roughing passes can be reduced. For the corner roughing operation (steps 5004–5006), the feed rate is varied between 6750 and 8100 mm/min, and for the wall finishing operation (steps 5007–5009), the feed rate is varied between 6750 and 8100 mm/min.

Three new triangular pockets have been machined at MASA using the process parameters from Table 15.2 and test if the new parameters produce an acceptable part. During machining, measurements of the machine axes and spindle torque are again collected through the installed monitoring system. This data provides an opportunity to verify if the simulations results can capture subtle changes in the process. Figure 15.17 shows the simulated and measured spindle power results for the three triangle roughing operations. At this scale, the simulation results closely follow the measured power results as the depth of cut is increased from 5 to 7 mm.

The results from Fig. 15.18 show the simulated and measured spindle torque for the vertex finishing operation, using three machining conditions. In this case, again, the simulation can predict small changes in power as the feed rate is increased, although the changes are smaller in this case.

The results from Fig. 15.19, that presents the comparison for the wall finishing operation, indicate that the measurement and simulation results track less accurately when the power or torque magnitudes are small.

The results from this second phase of trials at MASA have shown that the simulations are able to be used to improve new and existing processes. The ability to

Table 15.2 New parameters tested for aerospace pocketing operation (tool numbers are referred to the ones in Table 15.1)

Process steps	Description	RPM	Tool number	Axial depth (mm)	Feed rate (mm/min)	Feed per tooth (mm)
5000	Roughing milling of all the part and the exterior groove until $Z = 48$ mm	15,000	1	5	10,000	0.22
5001	Roughing milling of pocket 1 (3 mm to finish the wall)	15000	1	5	10,000	0.22
5002	Roughing milling of pocket 2 (3 mm to finish the wall)	15,000	1	6	10,000	0.22
5003	Roughing milling of pocket 3 (3 mm to finish the wall)	15,000	1	7	10,000	0.22
5004	Corner finishing pocket 1	15,000	8	11	6750	0.15
5005	Corner finishing pocket 2	15,000	8	11	7425	0.165
5006	Corner finishing pocket 3	15,000	8	11	8100	0.18
5007	Finishing of the pocket walls 1	15,000	9	16	6000	0.133
5008	Finishing of the pocket walls 2	15,000	9	16	6600	0.147
5009	Finishing of the pocket walls 3	15,000	9	16	7200	0.160

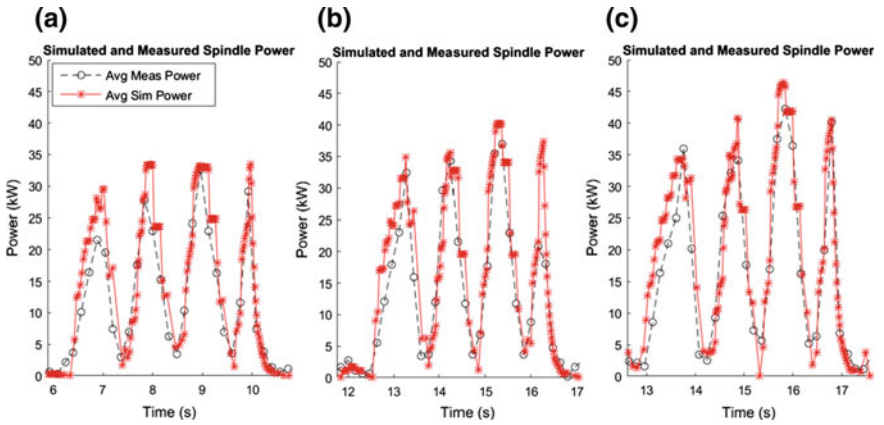

Fig. 15.17 Triangle roughing operation of **a** pocket 1 (operation 5001), **b** pocket 2 (operation 5002) and **c** pocket 3 (operation 5003)

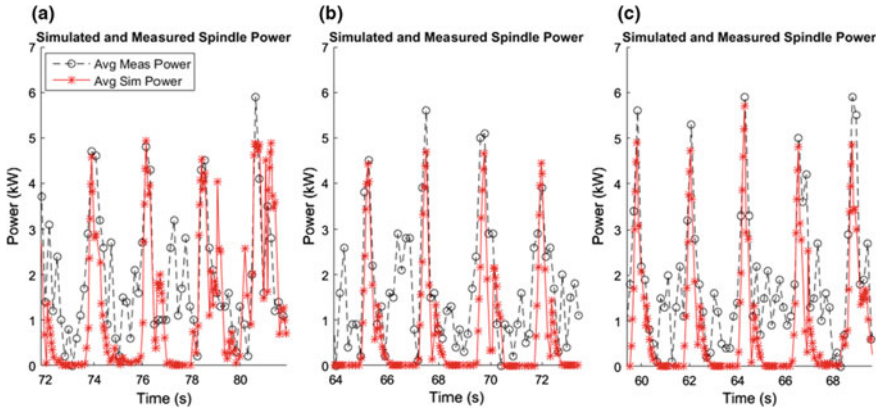

Fig. 15.18 Triangle vertex finishing operation of **a** pocket 1 (operation 5004), **b** pocket 2 (operation 5005) and **c** pocket 3 (operation 5006)

accurately simulate subtle changes to the process allows process planners to first identify potential areas of improvement and then be able to explore the effect each parameter will have on the process outcome. Ultimately, this process can be used to fully test new processes off machine and increase confidence in a process before the first part is produced.

15.5.1.2 Impact

Table 15.3 shows the phases to implement a new manufacturing process in MASA, from aerospace sector, including an estimation of the duration of each phase. Since

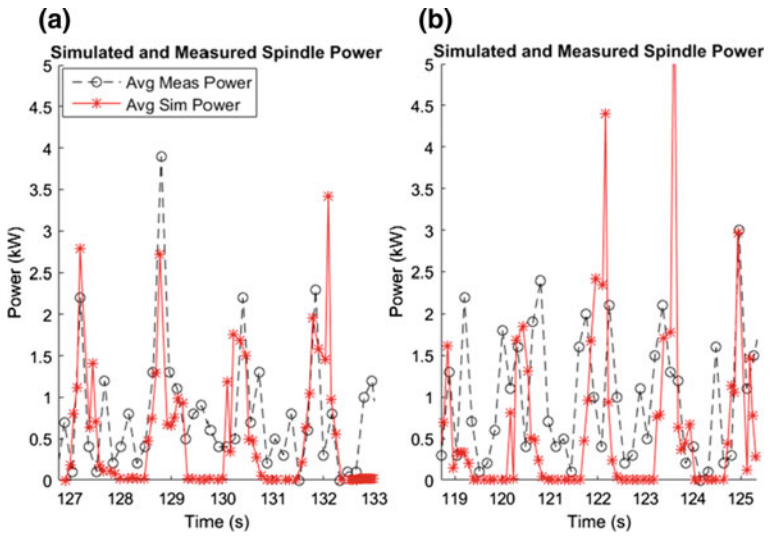

Fig. 15.19 Triangle wall finishing operation of **a** pocket 2 (operation 5008) and **b** pocket 3 (operation 5009)

Table 15.3 Average duration of the different stages of the new process design and set-up procedure for MASA (aerospace validation scenario) and the impact expected with the application of Twin-Control features

Activities		Duration (days)	Expected duration with Twin-Control (days)
1	Study of the geometry	5	5
2	Process definition	3	3
3	MT and tool choice	2	1
4	CNC programming and tooling design	21	21
5	Vericut simulation	3	5
6	1st part machining	1	
7	Inspection	2	
8	Final modification in process	6	
	Total average duration	45	35

small batches are usually required from customers, and hence, this implementation is performed with a high frequency.

In the third column, the impact expected by the application of Twin-Control process simulation capabilities is included. The biggest impact is expected in two stages:

– Machine Tool selection: MASA has several machines at its workshop, with very different configurations and characteristics. One of the most important steps for a successful process implementation is the selection of the best machine tool for

the specific process. With the implementation of Twin-Control simulations, the evaluation of the optimal site from MASA's machine tool park will be possible. Different simulations will provide the results (function transfers, vibrations …) and information to select the best machine tool configuration. With this, the machine tool selection stage will be reduced by a 25%.
– Process simulation and set-up: With the implementation of Twin-Control simulations, a comparison between a huge range of different tools and machining conditions can be done, allowing an optimization. In addition, MASA will be able to know before the machining in which operations the chattering risk exists, allowing the modification of machining conditions and the selection of the best alternative option. A reduction of process design and set-up time of around 60% is expected.

The average process implementation takes currently 43 days. With Twin-Control, it is expected to be reduced to 35 days. This is a reduction of the 20% in the development of the final process for get a serial production for a part.

15.6 Scenario of Use 3: Process Control

The machining process that is designed end set-up to obtain an optimized performance, as presented in scenario of use 2, is then run in the machine tool by an operator in production conditions.

Under ideal conditions, the operator should only run the process every time a new part is clamped in the fixture. However, different events can take the process from these ideal conditions such as tool wear or breakage, machine tool condition variation and excess/absence of material in raw surfaces.

Apart from this, the operator can usually modify process performance, for example, by modifying the feed rate when process does not go as expected (e.g. chatter occurs).

The application of Twin-Control in this scenario of use leads to a minimization of the impact of the undesirable events during production.

15.6.1 Local Machine Tool and Process Monitoring and Control Device

15.6.1.1 Implementation and Results

The monitoring equipment based on the ARTIS Genior Modular and updated in Twin-Control will be able to improve process control and facilitate operator's activities. Three new features developed in the project are of special relevance in this scenario.

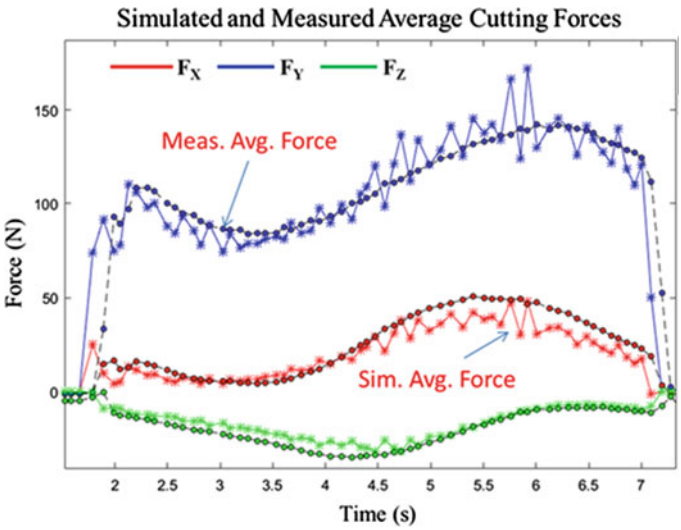

Fig. 15.20 Comparison of simulated and monitored results for the validation operation of the stability roadmap feature of Sect. 2.2 of the book

15.6.1.1.1 Process Monitoring

The well-known learning-based process monitoring feature from ARTIS Genior Modular is available at the aerospace use case but does not suit the short to medium batch size faced by MASA.

In this case, the state-of-the-art simulation-based process monitoring approach introduced in Chap. 12 of this book is of special interest. Preliminary results obtained in a Starrag EcoSpeed machine, located at the AMRC (Sheffield, UK), present the possibility to improve process control by embedding process models inside the monitoring hardware, as illustrated in Fig. 15.20.

The estimations done by the process models using real inputs from the machine can be used to determine the ideal conditions and fix thresholds that define anomalous performance of the process.

15.6.1.1.2 NC Simulation

The CNC simulation capabilities of ModuleWorks have been integrated in the ARTIS GEM-Visu HMI during Twin-Control project as depicted in Fig. 15.21. An implementation of the aerospace use case has been done by developing a simplified design of the GEPRO 502 machine. The virtual model has been created starting from STL files provided by GEPRO. By using current axis position data recorded by the OPR of the GEPRO 502 machine, the virtual representation of the machine replicates the movements done by the real machine.

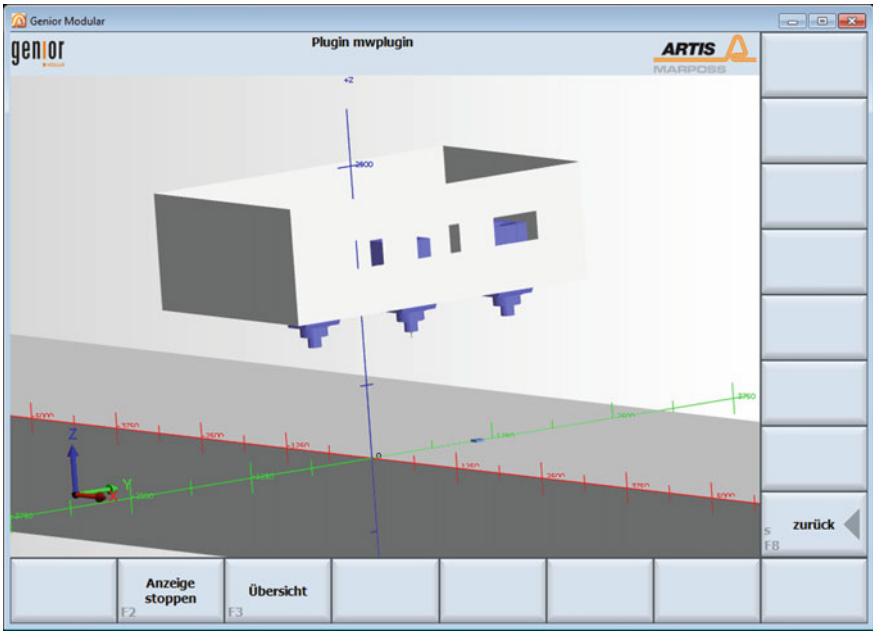

Fig. 15.21 Screenshot of ARTIS HMI showing CNC Simulation feature applied in a simplified GEPRO 502 machine

In machines where the process is not visible for operators, like the GEPRO 502 machine where an opaque curtain blocks the access to the machining region, this feature provides the chance to the operator to control the process.

15.6.1.1.3 Adaptive Control

Adaptive feed rate control has been implemented in the GEPRO 502 machine of MASA. This feature consists in the adaptation of feed rate according to spindle consumption and is performed by the ARTIS Genior modular installed in the machine. By applying this feature, when the spindle is under-working, the feed rate is increased; and, when the spindle is overworking, the feed rate is reduced. The objective is to increase productivity by keeping the maximum material removal rate during all the process. To test this, a scalloped sample part, represented in Fig. 15.22, has been used.

First, a learning stage was performed by machining the workpiece longitudinally at a constant feed rate, in this case 4000 mm/min, depicted in Fig. 15.23. This way, the target spindle consumption value is defined. This value of the spindle consumption will serve as a pattern when the adaptive control is activated.

After that, the adaptive control is activated, and a series of longitudinal machining operations are performed. This time, feed rate is automatically increased in the

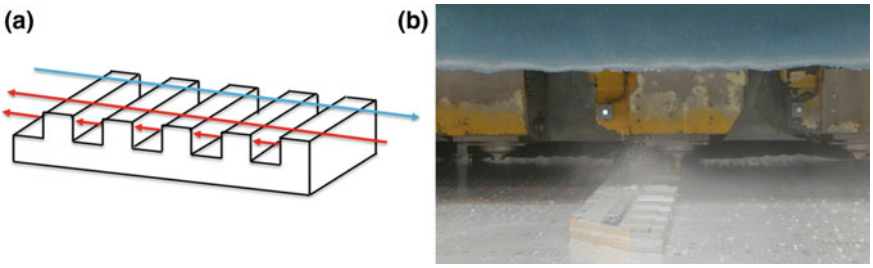

Fig. 15.22 Implementation of adaptive feed rate control in MASA use case: **a** diagram showing the adaptive control strategy on scalloped part: blue line shows the learning stage; red line shows the adapted stage. **b** Picture showing the real workpiece being machine in MASA case

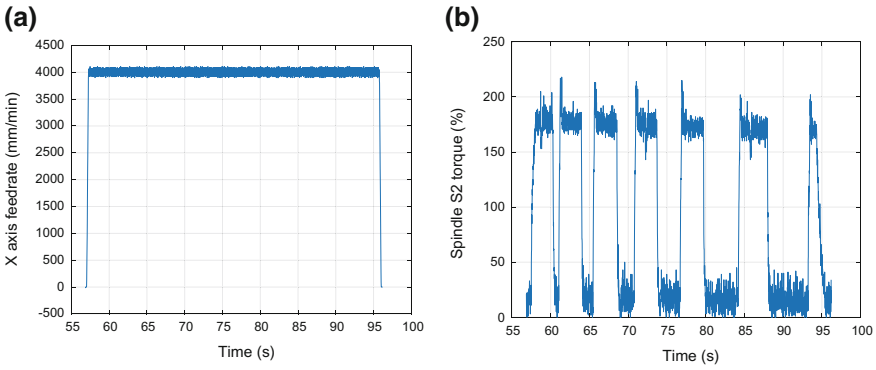

Fig. 15.23 Signals monitored during the learning stage of the adaptive control implementation in MASA use case: **a** constant feed rate. **b** Intermittent torque due to scalloped workpiece

regions with no material (Fig. 15.24), trying to reach the learned spindle torque (Fig. 15.23). In these regions, feed rate increases up to 5200 mm/min, which is the 130% of the programmed feed rate. This increase (130%) is a maximum limit fixed for safety reasons. Thereby, shorter machining times were achieved than without the adaptive control.

The differences between the learning stage and the adaptive control stage can be clearly observed in Figs. 15.23a and 15.24a. In the first case, the feed rate reaches values around 4000 mm/min and, in the second case, with the adaptive control active, the feed rate reaches values around 5200 mm/min.

15.6.1.2 Impact

The cycle time of the validation part selected for Twin-Control is approximately 24 h. The application of adaptive feed rate control will provide a reduction of a 10% in the total cycle time. The long travelling distances, the limitations in cutting conditions

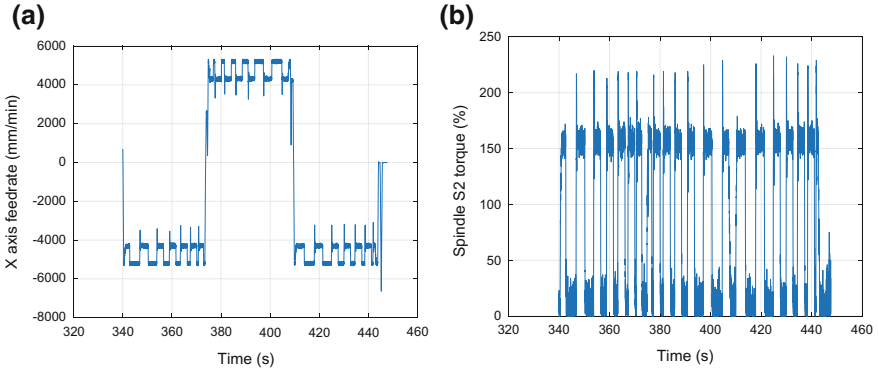

Fig. 15.24 Signals monitored during the adaptive machining in MASA use case: **a** constant feed rate. **b** Intermittent torque due to scalloped workpiece

caused by difficult-to-cut materials (e.g. titanium), and the intermittent cutting of typical pocket-type workpieces makes aerospace sector very prone to benefit from adaptive feed rate control.

MASA produces a total of 6000 parts per month, with approximately 1.20% of scrap parts. This fact, together with the high cost of the scrap parts (average of 600 and 2400 € for aluminium and titanium parts, respectively), makes any possibility to increase process reliability very interesting.

Nowadays, the scrap parts due to tool breakage are totally controlled for aluminium machining and no scrap parts are produced by this problem. In case of titanium machining, tool breakage is a problem and a cause of scrap part production. The application of Twin-Control simulation-based process monitoring will allow to predict tool breakage in advance and replace the tool in an early stage.

The average tooling cost for MASA is 6 and 30€ per machining hour for aluminium and titanium, respectively. By the application of Twin-Control simulation-based process monitoring, a reduction of the tooling cost of around 5–10% is expected in titanium machining. In the aluminium machining, it won't have a remarkable effect.

Collisions are quite common in the machines of the aerospace validation scenario, with an average of 20 collisions per year, since an opaque safety curtain is normally blocking the visualization of the machining area and the manufacturing of short batches that require manual set-up operations. The application of CNC simulation capabilities will allow the reduction of collisions in the machines, leading to a reduction of scrap parts and maintenance costs.

15.7 Scenario of Use 4: Maintenance

Preventive maintenance is the most common practice to guarantee machine tools performance in current industrial end-users. Preventive maintenance consists, most of the times, in scheduled actions according to machine usage time. Although this approach reduces machine failures, all the problems cannot be avoided. The proper analysis of the monitored data can help to anticipate to failures.

15.7.1 Fleet Management System

The cloud-based fleet-wide platform developed in Twin-Control project capitalizes all the information on all connected machines to support trend analysis of indicators, which is the first step towards predictive maintenance policy. Sections 3.2 and 4.3 of the Twin-Control book provide more insights into the fleet-wide platform developed in Twin-Control project.

15.7.1.1 Implementation and Results

Data from three machines located at MASA is uploaded to the cloud platform for machine tools hosted on a dedicated server (https://twincontrol.kasem.fr/). As machine operating data is one main input of the platform, reliability of machine tool connection is important. Every night, for 1 year and a half, behaviours indicators are extracted from raw data, operating and characterization test reports are generated.

MASA production cycle time is long, and parts are not produced in series. It means that to have comparable indicators between parts specific moves should be identified or requested, as done in the characterization tests. Additionally, laws between move indicator and for instance move length and distance can be characterized.

15.7.1.1.1 Y-Axis Power Consumption Drift

Analysis of power consumption of each Y-axis linear move according to speed and length shows a gap in the indicators from the 2017/06/22 when data transfer between machine and fleet platform is restored after few days, as depicted in Fig. 15.25. A maintenance activity report from MASA shows that during the week of the 2017/06/30 a problem with a chip accumulation in the Y-axis occurred, causing several components damage and replacement as shown in Fig. 15.26.

In this scenario, data transfer has been lost just before the drift of power. It can be assumed that the drift will be detected more than 3 days before.

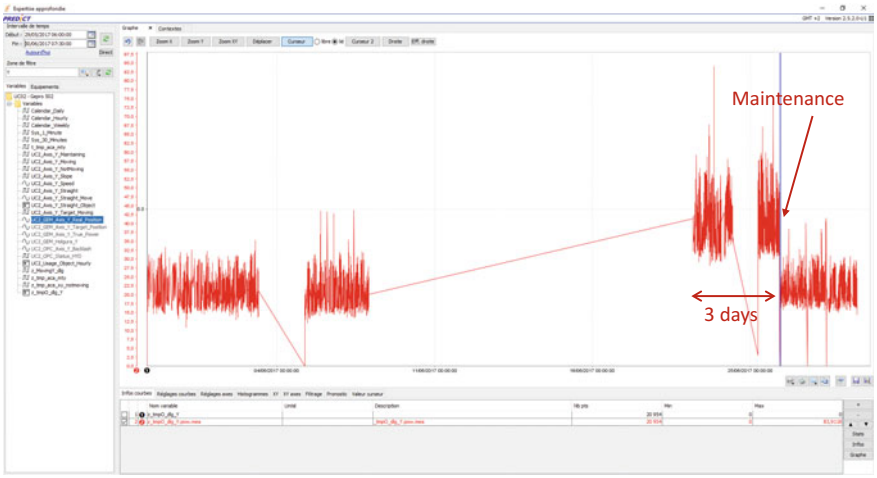

Fig. 15.25 Identification of anomalous performance of the *Y*-axis of GEPRO 502 machine using power-based indicators

MASA	**PARTE DE TRABAJO** **Mantenimiento Correctivo**	*7.535* Nº AVISO : 7.535
EDIFICIO : NAVE DE FABRICACION	**SISTEMA :** 502	**INSTALACIÓN :** EJE Y
COMUNICADO POR : GALILEA	**TELÉFONO :** 1500	**OPERARIO :** FELIX MARIN OCHOA
MÁQUINA : EJE Y	**NUMERO DE SERIE:** GENERICO 502	**FECHA :** 30/06/2017 **HORA :** 13:18
SITUACIÓN		
ANOMALÍAS DETECTADAS ROTO EJE Y TAPA BANDEJA B2. DENTRO DE CABEZAL LLENO DE VIRUTA PRENSADA **REPARACIÓN EFECTUADA** MODIFICAR AGUJEROS SOPORTE EJE NUEVO. SOLDAR SOLAPAS BANDEJA Y CAMBIADO BARREDOR MONTAR TAPA BANDEJA B2 CABEZAL LIMPIAR TODO EL CABESZAL POR DENTRO (TODO BIEN SOPLADO Y LUEGO CON ASPIRADOR)		

Fig. 15.26 Extract of MASA maintenance report from 2017/06 (in Spanish), indicating a maintenance action due to chip accumulation in *Y*-axis

15.7.1.1.2 Characterization Tests

Around 30 characterization tests have been made and analysed during the project. Due to its importance for MASA, this analysis is focused in the backlash indicator

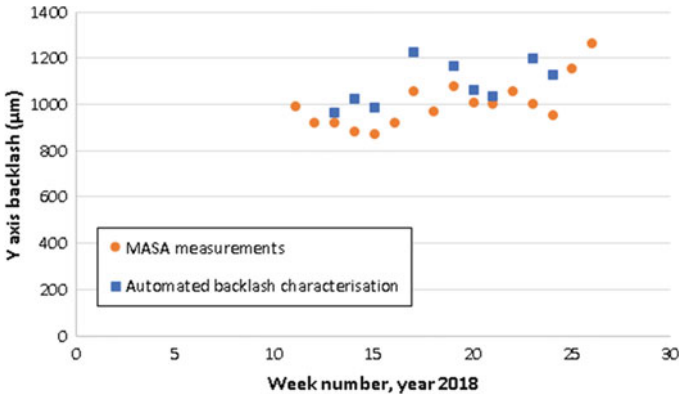

Fig. 15.27 Comparison of the Y-axis backlash obtained from circularity tests and through direct measurement

for the Y-axis, which is computed from the circularity tests. The trend of the Y-axis backlash calculated thanks to the characterization test is presented in Fig. 15.27, where the experimental measurements done by MASA are also plotted. It can be observed that the automated test is able to detect the same trend and provide good quantitative estimation of the backlash.

15.7.1.2 Impact

As mentioned before, MASA maintenance activities are based on preventive strategy. Periodic check of the most critical systems (axes backlash, hydraulic system and electrical components…) is performed by maintenance experts. This check supposes machine downtime and does not avoid machine failure.

With the application of a predictive maintenance strategy, MASA will be able to minimize the possibilities to suffer the failure. Thank to early detection of a drift in the machine behaviour, maintenance actions can be optimized, minimizing machine downtime. In addition, part of preventive actions could be eliminated, reducing overall maintenance costs and machine downtime.

Backlash of feed drives is one of the most critical aspects to get scrap parts in MASA. Currently, MASA checks the backlash manually, which is time-consuming. The implementation of MT characterization tests, where backlash is automatically determined makes easier the control of this parameter and minimizes the risk of getting a scrap part due to axis backlash. It is expected a reduction of the 10% in scrap parts due to this implementation.

Proactive events also contribute to the reduction of energy consumption of the machine because in most cases abnormal behaviours an equipment will increase its consumption with factors up to 3 as observed in MASA cases.

15.8 Conclusions

This chapter presents the implementation and obtained results of the technical developments done in Twin-Control project in the proposed aerospace industrial validation scenario. A specific approach for Twin-Control evaluation is defined, based on different scenarios of use defined in the project. The results and the impact of Twin-Control features are structured according to these scenarios of use.

Twin-Control shows a set of features that can help aerospace machine tool builders and users to improve their processes. A summary of the impact caused by the application of Twin-Control is listed next:

- A reduction of a 10% in the total development time of a new customized machine tool.
- A reduction of the 20% in the design and set-up of a new process.
- A reduction of 10% in cycle time.
- A reduction of tooling cost of 5–10%, depending on the workpiece.
- Reduction of machine downtime and maintenance costs thanks to predictive maintenance approach.
- A reduction of scrap parts of the 10%.

Chapter 16
Twin-Control Evaluation in Industrial Environment: Automotive Case

Mikel Armendia, Mani Ghassempouri, Jaouher Selmi, Luke Berglind, Johannes Sossenheimer, Dominik Flum, Flavien Peysson, Tobias Fuertjes and Denys Plakhotnik

16.1 Introduction

The previous chapters of this book have presented the different features developed in Twin-Control project, including results obtained in research environment. However,

M. Armendia (✉)
IK4-Tekniker, C/ Iñaki Goenaga 5, 20600 Eibar, Gipuzkoa, Spain
e-mail: mikel.armendia@tekniker.es

M. Ghassempouri
COMAU France, Castres, France
e-mail: mani.ghassempouri@COMAU.com

J. Selmi
RENAULT SAS, Powertrain Production Engineering Division (DIPM), Guyancourt, France
e-mail: jaouher.selmi@RENAULT.com

L. Berglind
The Advanced Manufacturing Research Centre (AMRC) with Boeing, University of Sheffield, Sheffield, UK
e-mail: l.berglind@amrc.co.uk

J. Sossenheimer · D. Flum
PTW TU, Darmstadt, Germany
e-mail: j.sossenheimer@PTW.TU-Darmstadt.de

D. Flum
e-mail: D.Flum@PTW.TU-Darmstadt.de

F. Peysson
PREDICT, Vandoeuvre-lès-Nancy, France
e-mail: flavien.peysson@predict.fr

T. Fuertjes
MARPOSS Monitoring Solutions GmbH, Egestorf, Germany
e-mail: tobias.fuertjes@mms.marposs.com

D. Plakhotnik
ModuleWorks GmbH, Aachen, Germany
e-mail: denys@moduleworks.com

M. Armendia et al. (eds.), *Twin-Control*,
https://doi.org/10.1007/978-3-030-02203-7_16

as this project has aimed to provide insights of industrial applicability and positive impact on end-users, a special effort has been done in the industrial evaluation.

Automotive sector is well-known for its large batch sizes and tight margin costs. Manufacturing processes are optimized at high level, and features like energy efficiency and maintenance are very relevant due to the correspondent cost reduction. In this line, the application of Twin-Control features is, thus, of special interests for this sector.

The chapter is structured as follows. After this introduction, an overview of the automotive validation scenario is provided in Sect. 16.2. In Sect. 16.3, the industrial evaluation approach applied in Twin-Control is presented. Section 16.4 presents the implementation and results obtained with Twin-Control features, with a special attention to the impact caused by these features in the end-users. Finally, the last chapter covers the conclusions.

Section 16.2 of this chapter provides an overview of the automotive validation scenario. In Sect. 16.3, the industrial evaluation approach is presented. Section 16.4 presents the implementation and results obtained with a special attention to the impact caused by these features in the end-users. Finally, the last section covers the conclusions.

16.2 Use Case Description

The automotive validation scenario is located at Cléon plant of RENAULT, in France. This plant produces gearboxes and engines for the RENAULT–Nissan Alliance car assembly plants all over the world. For the validation, three machine tools of the production line "Module 6", dedicated to the machining of the stator housing of RENAULT electric motor, were used.

This validation set of machines is composed by two COMAU Urane 25 V2.0 and one COMAU Urane 25 V3.0 machine centres. The three machines have the same basic characteristics; only versions of scales, tool magazine and control human machine vary. These machines, illustrated in Fig. 16.1, are composed of one spindle, four axes (X, Y, Z and B) and a palletizer with two clamping systems. They are controlled by a SIEMENS Sinumerik 840D CNC.

The process implemented in the presented line consisted in the machining of an aluminium housing, called CMOT part (Fig. 16.2), used in RENAULT's electric motors. Two machining steps are performed: OP110 and OP120. Face milling, drilling, tapping and boring are the most important machining processes. A complete description of the machining process was provided by RENAULT to the technical partners of Twin-Control.

By the end of the project, a new process was being set up for the selected manufacturing line. In this case, the machining of an aluminium carter illustrated in Fig. 16.3 is called POC part. Twin-Control simulation capabilities have been used to provide a feedback in the machining process design stage.

Fig. 16.1 COMAU Urane 25

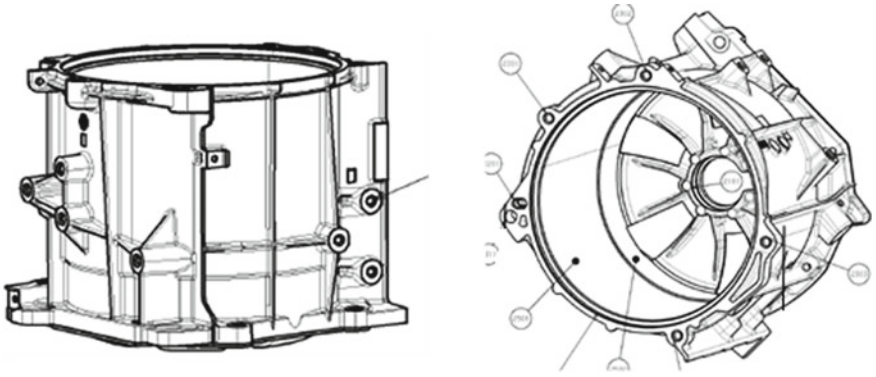

Fig. 16.2 General view of the CMOT part, used to validate most of Twin-Control features in the automotive validation scenario

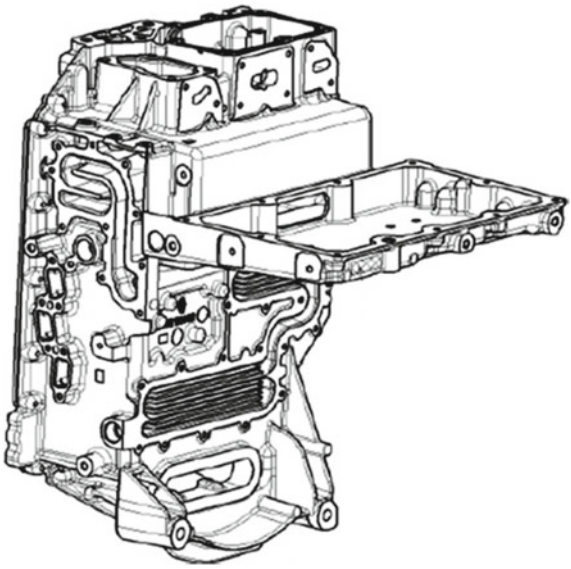

Fig. 16.3 General view of the POC part, implemented in the validation scenario at the end of the project

16.3 Evaluation Strategy

The evaluation approach defined in Twin-Control project is linked with the different scenarios of use (SoU) defined by the end-users at the beginning of the project:

- Scenario of Use 1: Machine Tool Design
- Scenario of Use 2: Process Design
- Scenario of Use 3: In-line Operation
- Scenario of Use 4: Maintenance
- Scenario of Use 5: Quality Control.

For each scenario of use, results obtained with Twin-Control are presented and the impact on end-users is evaluated.

16.4 Scenario of Use 1: Machine Tool Design

The tools and capabilities developed in Twin-Control create a new design environment for machine tool builders which allow to optimize the machine design through simulations. Since automotive energy efficiency is very relevant, the application of the developed energy simulation models is presented, together to the results obtained with the Virtual Machine Tool.

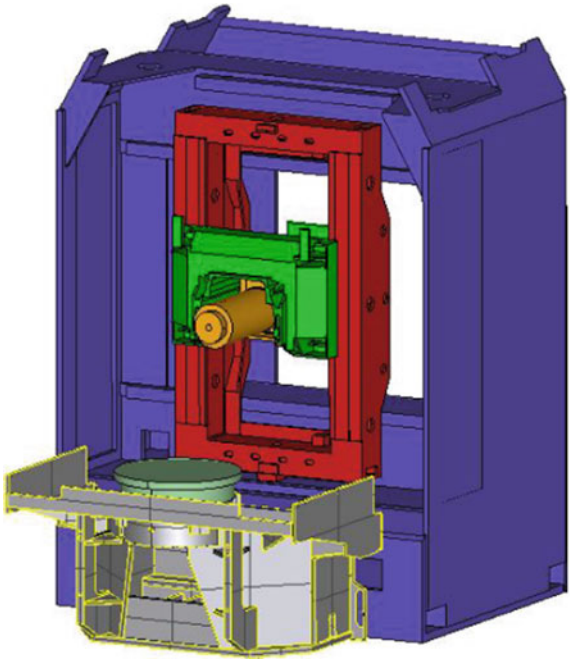

Fig. 16.4 CAD model of the COMAU Urane 25 V3.0 used for the its Virtual Machine Tool model

16.4.1 Virtual Machine Tool with Integrated Process Models

16.4.1.1 Implementation and Results

A Finite Element (FE)-based kinematic and dynamic model of the Urane 25 V3.0 machine has been done using SAMCEF Mecano software (Fig. 16.4). The model covers machine structure, feed drives and motion control loops. Specific validation of this simulation model was performed by using hammer tests and positioning movements. The results are presented in Sect. 2.1 of this book.

The virtual machining module has been configured for the automotive validation scenario. For that, characteristics of the cutting tools applied in the validation use case have been collected and stored in a table-shape database (Table 16.1) to be used by the simulation tool.

Results applying a sample part to the integrated simulation tool that combines machine tool dynamics and machining process are presented in Sect. 4.1 of this book. The integrated simulation tool has not been used for the validation part. Instead, within Scenario of Use 2, the process models have been directly applied.

Table 16.1 Characteristics of the tools needed in automotive use case

Tool #	D	Rc	Beta	Lam	Nflut	ToolDir	Zmax
1	8.5	0	0	0	2	0	205
2	8	0	0	0	2	0	182
3	M10	0	0	0		0	215
4	30	0	0	0	6	0	170
5	40	0	0	0	4	0	197
6	249	0	0	0	2	0	150
7	14	0	0	0	4	0	242
8	12	0	0	0	2	0	188
9	30	0	0	0	6	0	235
10	8	0	0	0	2	0	182
11	259	0	0	0	2	0	139
12	62	0	0	0	1	0	159
13	58	0	0	0	5	0	159
14	5	0	0	0	2	0	205
15	M6	0	0	0		0	215
16	10	0	0	0	2	0	160
17	5	0	0	0	2	0	205

D = Tool Diameter (mm); R_c = nose radius of tool (mm); Beta = taper angle of tool (rad); Lam = Helix angle (rad); Nflut = Number of flutes (−); ToolDir = cut rotation direction (−); Zmax = max Z value for virtual tool (mm)
Rc, Beta and Lam values for these tools are null since they have straight and plane cutting face

16.4.1.2 Impact

COMAU manufactures a standard family of machine tools for automotive industry. Each model of COMAU machine tools is manufactured and sold for more than several thousand units. So, it is necessary that each new machine be validated, tested and industrialized before being launched on the market and mass production. The current product development process of COMAU is illustrated in Fig. 16.5, and it takes an average of three years.

The first step in current product development process is to define, study and validate the concept of the new product. The second step is to study and manufacture a first prototype which will be used for internal validation tests. The third step is to study and manufacture a second "debugged" prototype which includes all improvements and/or modifications detected with the first prototype. The second prototype is tested in a real industrial condition (e.g. a customer product line). The last and fourth step is the product industrialization and adaptation for the serial and mass production. Usually, the first industrial project made by the new machine will be used for the industrial validation tests.

The application of Twin-Control in the product development process will have a direct impact on the prototyping stage, i.e. second and third steps, of the current

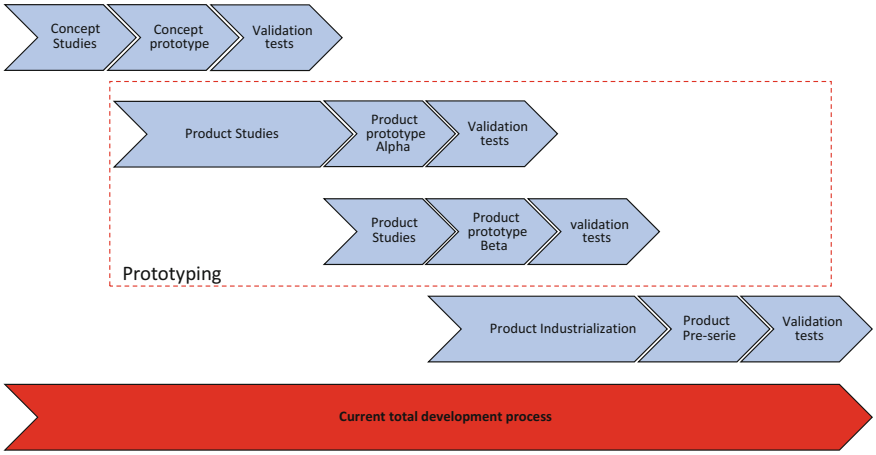

Fig. 16.5 Current product development process for COMAU

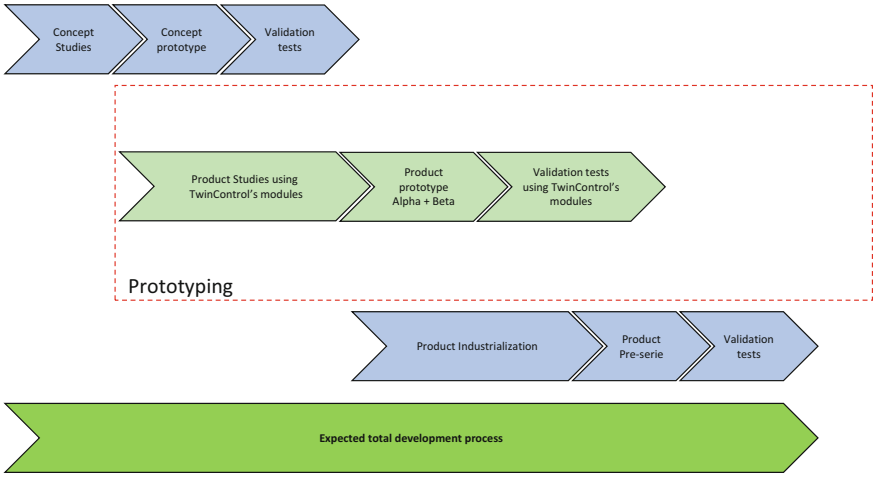

Fig. 16.6 Proposed product development process for COMAU with the application of Twin-Control

process. By using the virtual modules and tools developed by Twin-Control project, it could be possible to identify the main problems virtually and to solve and debug them during the study phases; it means that the major part of the product validation and tests could be done virtually, and the final validation could be done by the first prototype, as shown in Fig. 16.6. After internal tests and light modification, this first prototype could be shipped to a customer plant for industrial validation tests. It is expected a reduction of 10% in time and costs in the product development process with the application of Twin-Control.

Table 16.2 Overview of the current power consumption of the COMAU Urane 25 V3.0 during production and idle time

Component	Idle time mode		Production mode		Ratio between idle and production mode (%)
	Power consumption (W)	Ratio related to main connection (%)	Power consumption (W)	Ratio related to main connection (%)	
Main connection	9417.1	100	14262.4	100.0	66.0
Drives	27.4	0.3	2502.9	17.5	1.1
Cooling fluid pump	4338.3	46.1	4315.1	30.3	100.5
Hydraulic system pump	863.3	9.2	952.0	6.7	90.7
HP-coolant pump	661.3	7.0	2377.7	16.7	27.8
Cooling module	1808.2	19.2	1606.3	11.3	112.6
Other consumers	1718.6	18.2	2508.5	17.6	68.5

16.4.2 Energy Efficiency Models

16.4.2.1 Implementation and Results

The offline energy efficiency models, which are described in Sect. 2.3 of the book, have been applied in the automotive validation scenario. With the help of the developed library, COMAU Urane 25 V3.0 machine has been mapped. Manufacturer's information such as fluid or electrical plans has been used for this purpose. The parameterization of the component models is carried out via data sheets, which allow a simple adaptability to different applications.

To analyse the energy optimization potentials, all energy-relevant aggregates were measured. Table 16.2 shows the measurement results of the machine's current energy consumption. As described in this chapter, all three machine-related approaches to increase the energy efficiency (see Fig. 2.2 in Sect. 2.3) are applied to the Urane 25 V3.0 machine tool.

As the Urane 25 V3.0 machines were designed and manufactured about 15 years ago (2003), the components used at these machines (motors, pump, chiller, etc.) are less energy efficient compared to the components which are available on the market in 2018. By applying the offline energy simulation models, which are described in Sect. 2.3, the following measures and design modifications are proposed:

Table 16.3 Aggregated savings potential of COMAU Urane 25 V3.0 machine applying efficient components and design principles

Component	Current scenario	Scenario with energy-efficient components	
	Power consumption (W)	Optimized power consumption (W)	Reduction (%)
Main connection	**14262.4**	**9309.3**	**34.7**
Drives	2502.9	2439.6	2.5
Cooling fluid pump	4315.1	1227	71.6
Hydraulic system pump	952.0	289.1	69.6
HP-coolant pump	2377.7	2124.8	10.6
Cooling module	1606.3	720.3	55.2
Other consumers	2508.5	2508.5	0.0

- replacing the current electric drives with more efficient IE4 motors
- implementing a switch-off mode for the hydraulic system pump
- replacing the cooling fluid pump with a better-suited pump
- replacing the current chiller with a more energy-efficient chiller.

16.4.2.2 Impact

The overall energy savings potential of the COMAU Urane 25 V3.0 machine analysed in the automotive validation scenario by applying energy-efficient design principles and by using energy-efficient components is summarized in Table 16.3. A total energy reduction of the 34.7% can be achieved in the COMAU Urane 25 V2 and V3.0 machine. These components (or similar alternatives) are used in the last generation of the Urane 25 V8 machines.

16.5 Scenario of Use 2: Process Design

The process models developed in the project provide the possibility to simulate in advance the manufacturing processes analysing the effect of different process parameters. This way, end-users have a great chance to reduce design time and to define optimized processes, leading to a minimization of the set-up time and a better performance of the process.

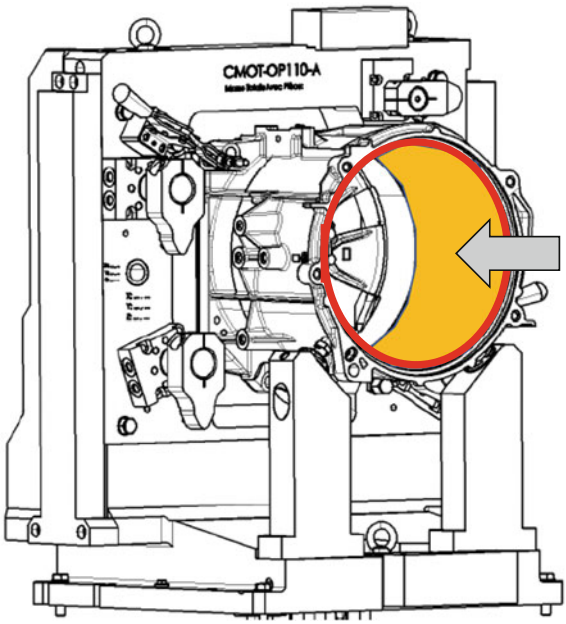

Fig. 16.7 Boring part operation in the automotive validation process

16.5.1 Machining Process Models

16.5.1.1 Implementation and Results

The Twin-Control process models have been applied to the boring operation of RENAULT's motor case of the automotive validation scenario, illustrated in Fig. 16.7. This operation is the most critical in the validation part.

A depiction of the simulation is shown in Fig. 16.8a, where the two-sided boring tool is modelled as a large-diameter drilling tool with two flutes.

One challenge for this simulation is that the original stock geometry is not known with certainty, where the stock ID from the forge set at 253 ± 1 mm is provided. Furthermore, the large size of the tool relative to the part geometry created issues for determining tool workpiece engagement with precision. To account for these issues, the part STL geometry is created with a tapered inner surface, which starts with an ID of 254 mm at the start of the cut, and 242 mm at the end of the cut. Additionally, the tool mesh and the engagement precision are set very fine to capture changes to the TWE due to small changes in the part ID.

The results of the simulation are shown in Fig. 16.8b, where the simulated torque is compared with the on-machine torque measurements. Both sets of torque data increase throughout the cut due to higher chip load as the stock ID decreases. The simulated data shows several locations where the torque drops to zero. These drops are due to errors in the TWE calculation, which are complicated here due to the large size of the tool relative to the part geometry. Ignoring these errors, the path of the

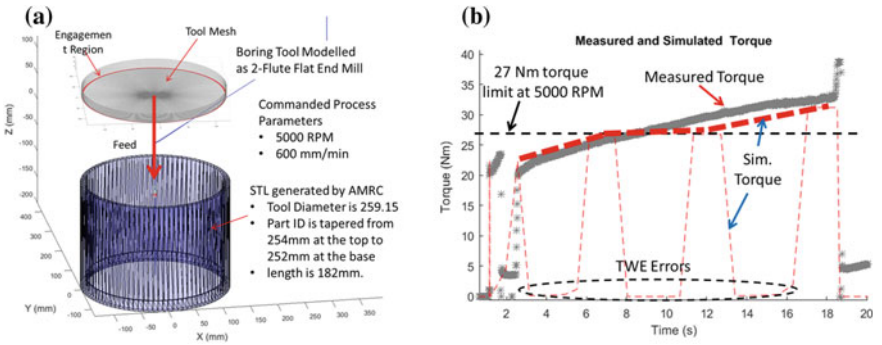

Fig. 16.8 Simulation of the big boring of the CMOT part: **a** description of the simulation; **b** obtained results

simulated torque indicated by the thick dashed line in Fig. 16.8b closely follows the measured torque profile throughout the cut.

Accurate torque predictions from the updated process model give process planners the opportunity to look for issues with a machining operation before a part is produced. Figure 16.8b shows an example of how this can be used to prevent torque overload. The spindle used here has a torque limit of 27 Nm at 5000 RPM. It can be seen from these results that the torque limit is surpassed close to the beginning of the cut. It is known from the machine measurement that the tool feed slows during the operation, and it is also possible the torque overload caused a decrease in the spindle RPM as well. The overall result is an operation which takes longer to complete than planned and which pushes the spindle to its performance limits.

A second implementation of the process models developed in Twin-Control is presented next. RENAULT needs to define the machining process to manufacture a new aluminium automotive part, and the process models are used as support tool. The part under consideration, which is shown in Fig. 16.3, has a large cantilever plate section which must be machined. Because of the large overhang, vibration issues are expected to be the greatest risk at this region. Two machining strategies will be simulated for this section which will result in different loads on the part, and the process with the lowest risk of chatter will be recommended. For the current simulations, the tool is modelled as a 32-mm-diameter, 5-fluted, zero-helix flat-end mill; the material is modelled as the same aluminium alloy as used in the previous example, the tool feed rate is fixed to 0.1 mm/tooth, and 2 mm of material is removed from the face of the part (Fig. 16.9).

Before the Twin-Control simulations are run, FEA analysis is used to predict the dynamic response of the part geometry when mounted to the machine. As the part is assumed to be flexible in this case, simulated part FRFs are used during dynamic analysis, and the tool is assumed to be rigid relative to the part. Considering the FEA model of Fig. 16.10, FRFs are computed performing harmonic responses on the desired frequency range with unitary loads on a set of selected nodes, while measuring the resulting accelerations (magnitude and phase) at the same nodes.

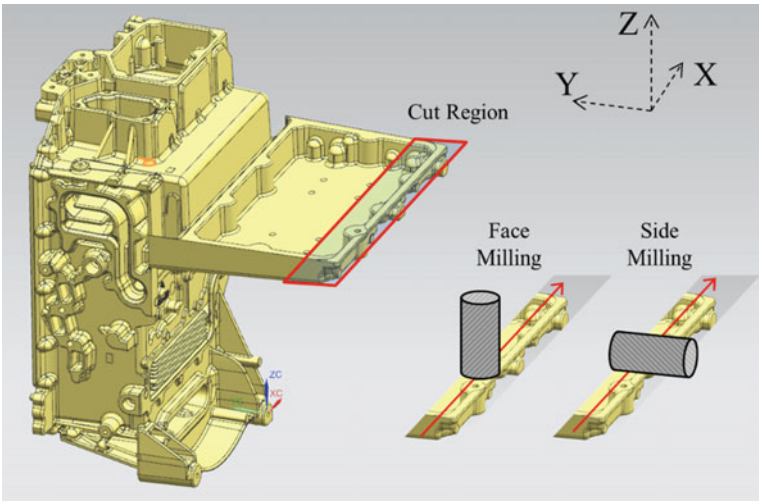

Fig. 16.9 New automotive part with large overhang region which will be simulated for both face and side milling

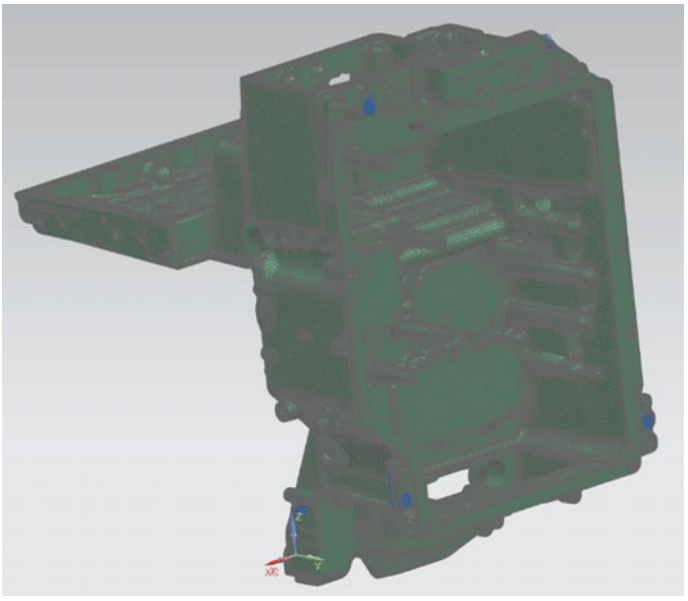

Fig. 16.10 FEA set-up to obtain part dynamic response of the POC part to be manufactured by RENAULT

The FEA simulations provided FRF data at multiple locations along the cut regions. To simplify the simulation process, only FRFs at the most flexible region of the cut are considered. Further, only FRFs in the most critical direction are con-

sidered for each process. In the current model, only radial cutting forces influence chatter for a flat-end mill, so the critical FRFs for the facing operation are FRF_{XX} and FRF_{YY}, and the critical FRF in the side milling operation is FRF_{ZZ}, as shown in Fig. 16.11a.

The resulting stability roadmaps for each simulation are shown in Fig. 16.11b. It is clear from the stability roadmap results that the two operations, while removing the same amount of material, differ greatly in terms of chatter risk. From the FRF data, the part is significantly more flexible in the Z-directions, and this flexibility increases likelihood of chatter for side milling, where radial forces act primarily in

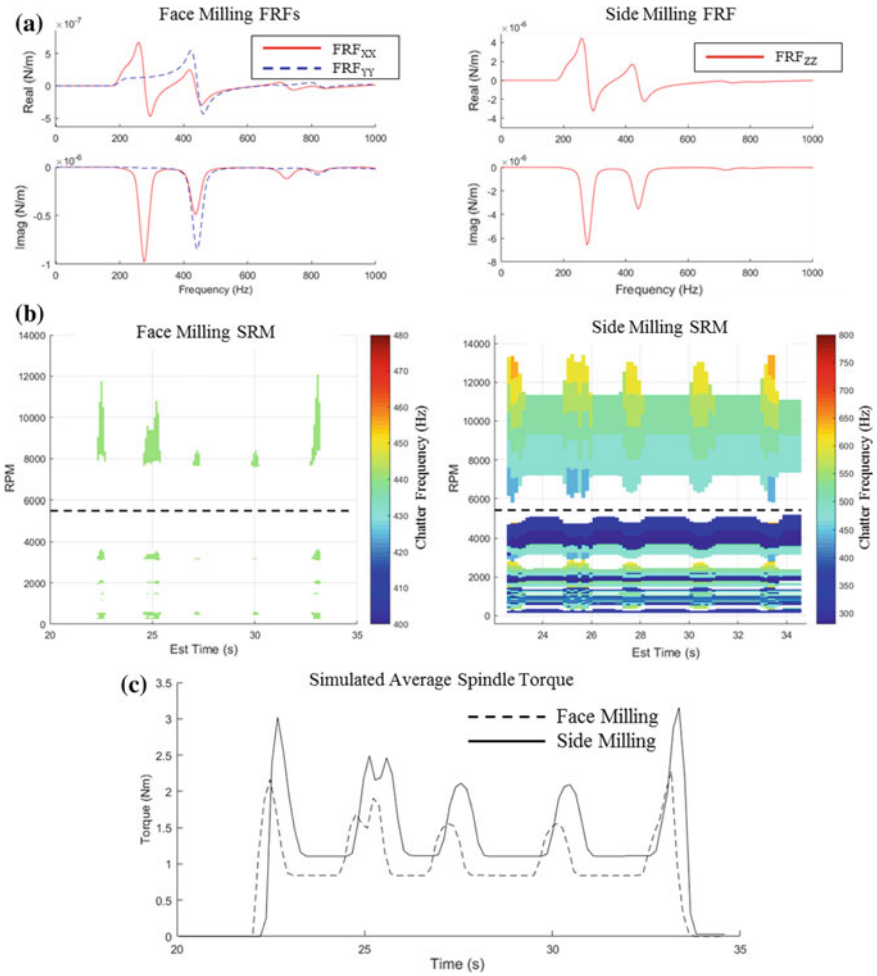

Fig. 16.11 **a** FRF data used for the facing and side milling simulations, **b** the resulting stability roadmaps from both simulations and **c** the resulting average simulated torque for both simulations

the *Z*-direction. The stability roadmap results for the face milling operation show a significant reduction in the chatter risk. This is due primarily to higher part stiffness in the *X* and *Y* directions.

To provide additional means of comparing the two operations, torque loads are also simulated to determine if there is a significant difference in process loads between the two strategies. The results from Fig. 16.11c show that the resulting process loads are similar in both strategies, with an approximate 20% difference between the two strategies throughout the operation. This result indicates the process should be decided based on the chatter simulations, where the results differ greatly between the two operations.

From the simulation results in Fig. 16.11, the facing operation is better suited to this application. While it is predicted that no chatter will occur at 5500 RPM for the side milling case, the conditions are close to the stability boundaries, and there is still a potential of chatter. The facing operation shows a larger separation between the stability boundaries, especially at 5500 RPM. Furthermore, the predicted spindle torque load is approximately 20% lower throughout the facing operation. As a result, face milling at 5500 RPM is recommended for this application with the current tool and part material. Note that these results and recommendations serve as a starting point for the process design based on the available information. At a later stage in development, the simulations should be updated with new data, such as actual part FRF measurements, to further improve the process design.

16.5.1.2 Impact

Table 16.4 presents the average duration of the different stages of the new process design and set-up procedure for RENAULT. The large batches required for their processes make this procedure very time-consuming since it requires the preparation of specific material for the process (fixture, tooling and even the machine).

In the third column, the impact expected by the application of Twin-Control features is included, which is mainly linked to the reduction of the process design stage, the reduction in time to select the best machine tool for the process, and a minimization of trials for process set-up. A reduction of the 11% of the total design time is expected.

16.6 Scenario of Use 3: Process Control

In Scenario of Use 2, features to optimize the design and reduce the set-up of machining process are presented. Under ideal conditions, the operator should only run the designed process each time a new part is required. However, real industrial conditions are far from being controlled and unexpected events can occur: tool breakage, collisions, variation of material and dimensions of raw parts, etc.

Table 16.4 Average duration of the different stages of the new process design and set-up procedure for RENAULT and the impact expected with the application of Twin-Control features

Indicative process steps and durations			
Activities		Duration (week(s))	Expected duration with Twin-Control (week(s))
1	Study of the part geometry	1	1
2	Process design proposal	6	4.8
3	Risk analysis	2	2
4	Trials and simulation for risk avoidance	12	9.6
5	Discussion and iteration with study department	8	8
6	Validation of the acceptable tolerances	2	2
7	Process drawing generation and machining tolerances définition	4	4
8	MT and tool supplier RFQ and purchase order	12	12
9	Tooling and machine purchase order	32	28.8
10	CNC program generation	2	2
11	Quality capabilities by the supplier	8	8
12	Shipment (machine, tooling, raw parts …)	2	2
13	Quality capabilities at the plant	4	4
14	Process certification	1	1
15	Manufacturing agreement	1	1
	Total average duration	**63**	**56.2**

The application of Twin-Control at machine operator level leads to a minimization of the impact of the undesirable events during production and to optimize productivity.

16.6.1 Local Machine Tool and Process Monitoring and Control Device

16.6.1.1 Implementation and Results

The monitoring equipment based on the ARTIS Genior modular and updated in Twin-Control will be able to improve process control and facilitate operator's activities. Three new features developed in the project, apart from the process monitoring available in ARTIS, have been implemented in this industrial scenario.

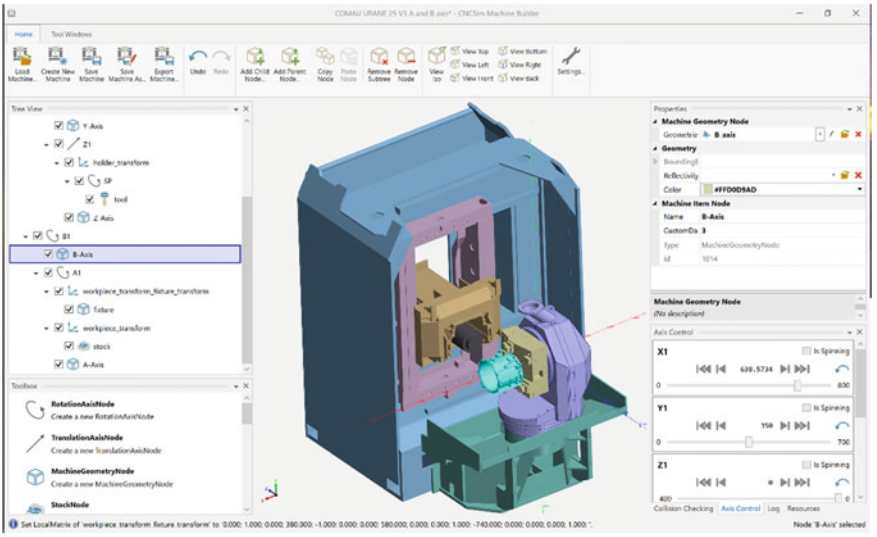

Fig. 16.12 Screenshot of the MachineBuilder application showing COMAU Urane 25 model

Collision Avoidance System (CAS)

The newly developed collision avoidance system (CAS), from ModuleWorks, provides real-time verification and clash detection during the milling process through CNC controllers. CAS has been implemented in the automotive validation scenario.

Implementation of CAS system is based on geometric computation of spatial positions of bodies that are involved in the machining process. As a mandatory prerequisite, a machine tool model must be provided to the CAS kernel. Such models must include not only the geometric descriptions of the machine tool components, but also kinematic dependencies and proper coordinate transformations of all machine elements to be considered.

To simplify the preparation of the machine tool data, MachineBuilder application has been developed, as shown in Fig. 16.12. MachineBuilder application has a dedicated graphic user interface allowing a CNC developer seamless integration of the existing CAD data of the machine tool into CAS system. The machine model includes machine elements along with fixture and stock geometry. The kinematic tree can be created within the application as well.

In addition to kinematics and geometry of the machine model, different collision-checking options may be applied. This way, the machine model elements to be considered for potential collisions are defined. For instance, a collision check between machine tool elements or between cutting tools and machine elements can be done, as shown in Fig. 16.13. It is also possible to specify any custom rules for machine elements defined in the kinematic tree.

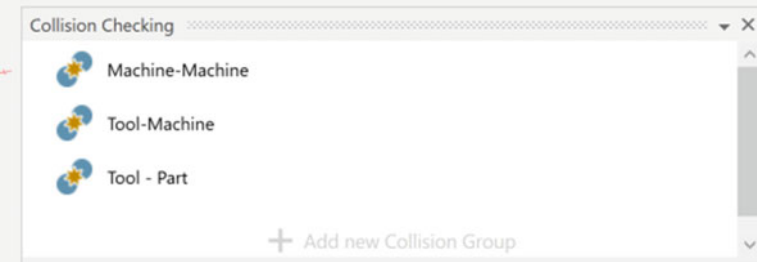

Fig. 16.13 Collision-checking options for CAS

Fig. 16.14 CAS integration of COMAU Urane machine in SIEMENS 840D control

Figure 16.14 shows the integration of the CAS model of the COMAU Urane machine tool in a SIEMENS 840D controller, the same used in the machines located at the validation scenario.

Collisions on the machines tools are usually result in expensive and lengthy repair and maintenance procedures. The risk of collisions becomes much higher if a new

operation is set up or changes in fixtures/tooling applied. Often such seemingly small changes are overlooked and executed on a machine without proper verification. CAS system can serve as the last guard to protect the equipment. If a collision is detected, the machining process is stopped before an actual collision occurs to prevent expensive machine damage and downtime. The end-users may assure that the human-factor or inefficient verification software will cause production losses.

Energy-Based Condition Monitoring

In the following paragraphs, the results obtained through the application of the Kalman-Filter-based disaggregation algorithm in the frame of the automotive use case of the Twin-Control project are described. The aim is to determine the energy requirements of the machine tool at component level.

Since the gearbox production has a central coolant treatment system, only the machine's auxiliary units are examined. The electric power consumption of the components was measured during a temporary measurement over several production cycles. The cooling module could only be measured as one unit, but for the disaggregation it is subdivided into its components, which are a cooling compressor and a fan. The collective consumer called "other consumers" includes all electrical auxiliary units of the machine, which are not listed above. As can be seen in Fig. 16.15 most

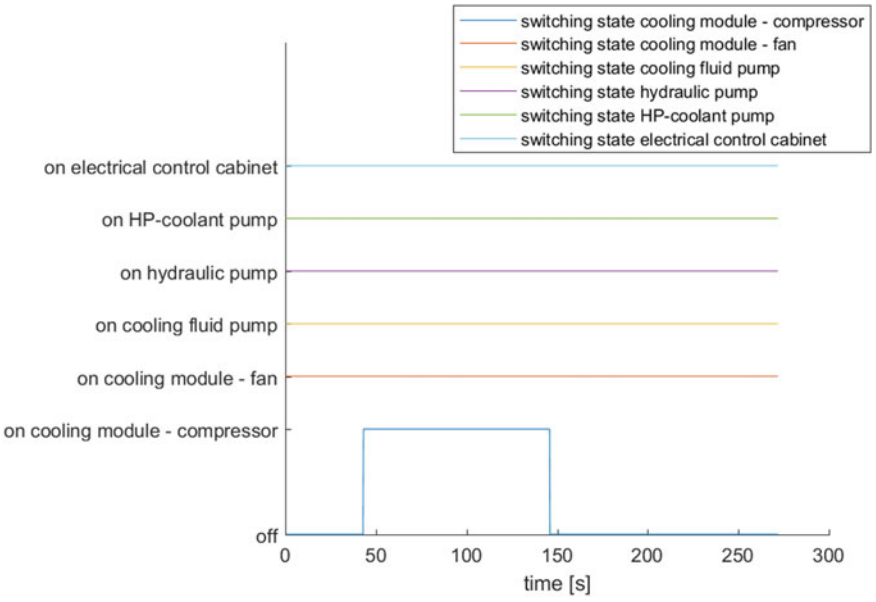

Fig. 16.15 Overview of the switching states of the auxiliary units of the COMAU Urane 25 V3.0 machine

Table 16.5 Evaluation results of the Kalman-filter-based disaggregation approach on the COMAU Urane 25 V3.0 machine tool

Auxiliary unit of the machine tool	Consumer type	Mean measured power consumption (W)	Mean disaggregated power consumption (W)	Root mean square deviation (W)	Relative error (%)
Cooling fluid pump	Constant	4314.9	4200.2	153.5	3.5
Hydraulic system pump	Constant	2273.9	577.9	363.9	16.0
HP-coolant pump	Constant	2273.9	1512.2	844.3	37.1
Cooling module fan	Constant	438.03	238.15	147.3	55.1
Cooling module compressor	Constant	4148.7	3941.3	1469.6	35.4
Electric control cabinet	Constant	–	183.1	–	–
Other consumers	Dynamic	–	4428.7	–	–

auxiliary units are constantly switched on during the production mode. Only the compressor of the cooling module is a cyclic consumer, while the fan of the cooling module is constantly switched on. Therefore, except for the collective component "other consumers", all components are regarded as constant consumers.

Figure 16.16 compares the measured and disaggregated power for the production mode. Table 16.5 compares the average measured values and the average disaggregated power values with the errors, which calculated according to Eqs. 1 and 2 in Sect. 3.4 of this book.

The accuracy of disaggregation increases if the individual components are switched on one after the other and have enough time for the teach-in process. However, this is not always possible due to the technical restrictions and the request for short cycle times. Since most components of the COMAU Urane 25 V3.0 machine tool are permanently switched on, the influence of the initial conditions is dominant. Therefore, a good training process, which requires either stepwise switched components or multiple successive switching operations of the same component, is not possible in this case. The presented disaggregation approach is much better suited, and will give better approximations of the consumed power, for machines that have such a training phase.

Since the power consumption of the fan of the cooling module could not be measured separately, the measured power was determined from the power of the entire module when the compressor is switched off. According to the electrical circuit dia-

gram, the nominal power of the fan is 620 kW, which confirms the approximation of the fan's actual power consumption. Decisive information to map the load peaks of the hydraulic pump (second diagram in Fig. 16.16) or the HP-coolant pump (third diagram in Fig. 16.16) of the COMAU machine is missing. Significantly, more precise results could be achieved if the corresponding signals were integrated into the disaggregation model. Furthermore, the consequently falsified disaggregation, which is distributed to all other components, would be lower. Therefore, the accuracy of the disaggregation of the other components could also be increased. The disaggregation results of the cooling fluid pump (first diagram in Fig. 16.16), the cooling module's fan and the cooling module's compressor approximate the measured power consumption relatively well.

The presented approach can be used for cost-effective energy monitoring. Even if an exact power disaggregation of industrial components is difficult, the presented approach offers a cost-effective and simple possibility to estimate the energy demand on component level.

Implementation of a Demand-Oriented Control

Currently, the Urane 25 V3.0 machine installed at RENAULT is used with two operating modes, a production mode and an idle mode. The power consumption of the two operating modes is shown in Table 16.2. The axes are not moved in idle mode, and therefore have only low power consumption, but no automated switch-off has been realized. During idle mode, the power consumption of the other auxiliary units deviates only slightly from the power consumption in production mode. The cooling module compressor is switched on and off in a timed manner, which is why the power consumption is also independent of the operating mode. The HP-coolant pump and the hydraulic pump have reduced power consumption because the requirements for these components are reduced in idle mode, but there is no automatic switch-off.

After consultation with COMAU and based on the results provided by the disaggregation approach and the offline measurements, the following operating modes for the Urane machine tool are proposed. The operating modes are already available on the Urane 25 V3.0, but currently they are not used by RENAULT.

- Production mode
- Operational mode
- Stand-by mode
- Switched-off mode.

When implementing a demand-oriented control of the auxiliary units, the technical restrictions and start-up times must be respected. The proposed operation modes consider the existent restrictions and switch off the modules only when it is safe for the components and the machine. In production mode, after 1 min of inactivity, the drives, the hydraulic system pump and the HP-coolant pump are switched off to operational mode. The breaks of the drives are of course activated during this time. After 10 min of inactivity, the machine is switched to stand-by mode, which means

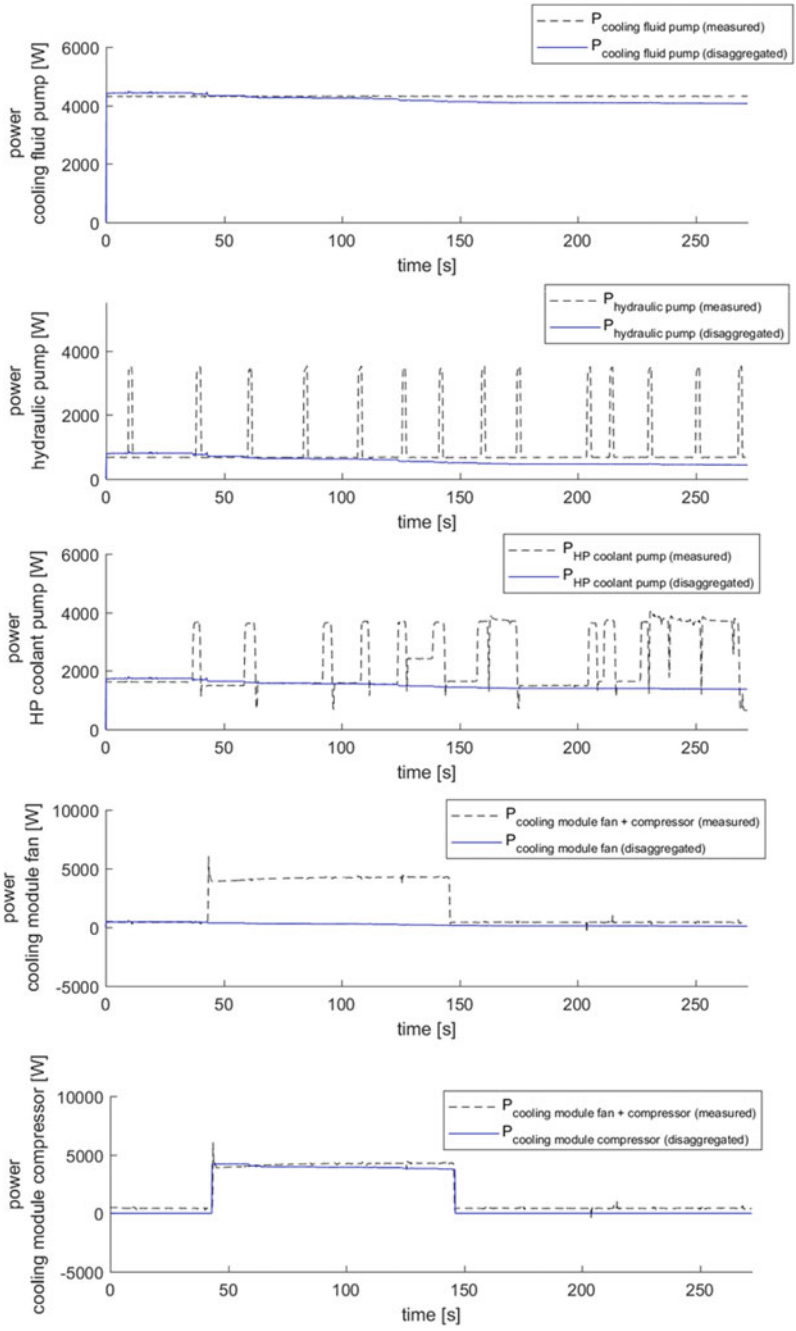

Fig. 16.16 Comparison of disaggregated and measured power for the auxiliary units of the COMAU Urane machine

Table 16.6 Implementation of a demand-oriented control for the COMAU Urane 25 V3.0 machine

Component	Power consumption (W)			
	Production mode	Operational mode (after 1 min)	Stand-by mode (after 10 min)	Switched-off mode (after 1 h)
Main connection	14262.4	7639.9	1718.6	0.0
Drives	2502.9	0.0	0.0	0.0
Cooling fluid pump	4315.1	4315.1	0.0	0.0
Hydraulic system pump	952.0	0.0	0.0	0.0
HP-coolant pump	2377.7	0.0	0.0	0.0
Cooling module	1606.3	1606.3	0.0	0.0
Other consumers	2508.5	1718.6	1718.6	0.0

that the cooling fluid pump and the cooling module are additionally switched off. In the last step, the machine is automatically switched off after 1 h. Table 16.6 gives an overview of the energy consumption in the energy-optimized scenario.

Figure 16.17 shows the power consumption of the drives and other consumers of the COMAU Urane 25 V3.0 machine and the correspondent machine state (1 for producing and 0 for idle time) for a certain period of measurement. Based on these machine states, the downtime frequency and the duration were calculated, as shown in Fig. 16.18. Even if most of the idle times have short duration, there are several events showing long idle times. The reduction of energy consumption during this stop periods will lead to great reduction in the total energy consumption for each machine.

To prevent downtime due to waiting periods during the start-up phase of the machine, the Urane should be automatically started, after longer switched-off periods, 15 min before the first production order is scheduled in the production planning system.

16.6.1.2 Impact

The cycle time of the validation part selected for Twin-Control is 7.4 min and represents the typical process carried out by RENAULT. Due to the high level of optimization at process design stage due to its impact in the large batch, there is no big expectation from the application of adaptive feed rate control and its impact in the cycle time.

RENAULT can produce up to 7000 parts per month at Cleon plant, with a very small rate of scrap part production (average of 25 scraps per month). This fact, together with the limited cost of each scrap part (for the validation part it is around

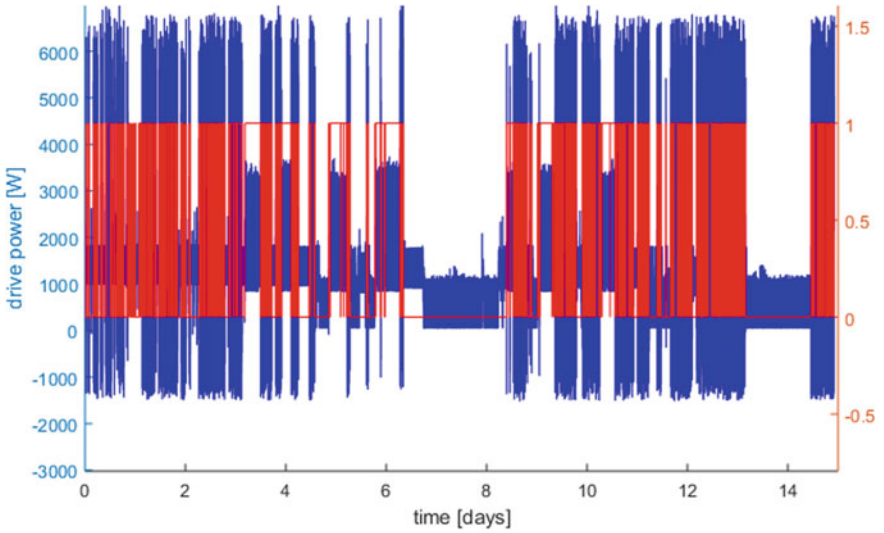

Fig. 16.17 Power consumption of Urane's drives and other consumers (in blue) with the machine state (1 = producing 0 = idle time) for the period of 1 to 15 of April 2018

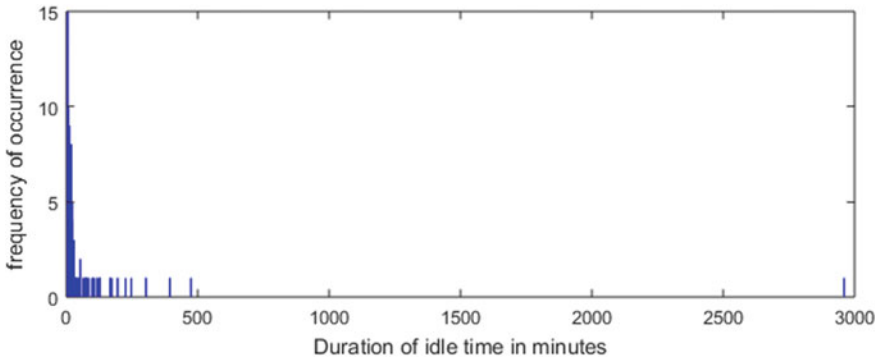

Fig. 16.18 Frequency of machine idle time for the period from 1 to 15 of April 2018

119 €), highlights the great automatization and process control of RENAULT and the limited impact of Twin-Control feature application.

A very small percentage of the total part cost is assigned to tooling. This is mostly caused by small tool wear in aluminium machining. The tool life is expected to increase from 5 to 10% with the application of Twin-Control process monitoring. However, the impact to the overall process is very limited.

For collisions, once the process is set up, machines work in automatic mode and performing the same process. Hence, no collisions occur in this use case.

Regarding the non-intrusive energy monitoring, the choice of the switching signals has a high impact on the accuracy of the disaggregation. Table 16.5 compares the

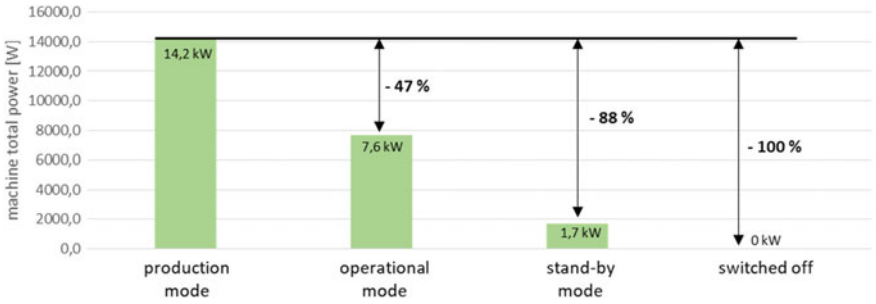

Fig. 16.19 Energy savings potential of demand-oriented control of the COMAU Urane 25 V3.0 machine tool

average measured values and the average disaggregated power values with the errors. By applying this approach with additional switching information, good estimations of the energy consumption on component level will be possible. A survey among different measuring equipment manufacturers showed that the costs for sensors, data evaluation modules, their implementation and maintenance for a hardware-based measurement set-up are between 8.000 and 18.000 €, while the costs for a non-intrusive measurement are approximately below 3.500 €. At this point, it must be emphasized that these are common market prices and not the prices of individual manufacturers. The actual cost savings depend on the number of auxiliary units, the implemented sensors and power analyser modules, as well as the workload during commissioning. Therefore, considerable cost savings can be realized on each machine by implementing a non-intrusive energy monitoring algorithm.

Due to the implementation of a demand-oriented control, the energy consumption of the Urane 25 V3.0 machine tool can be reduced during idle time, as presented in Fig. 16.19. Compared to the production mode, the power consumption of the machine can be reduced by 47% in the operational mode, by 88% in the stand-by mode and by 100% when it is switched off. When considering the actual production scenario of the machine, which is shown in Fig. 16.17 for the period 1–15 April 2018, a total energy saving of 35% can be realized through the implementation of a demand-oriented control.

16.7 Scenario of Use 4: Maintenance

Main activity to ensure good performances of machine tools consists in preventive maintenance intervention. Most of the time these interventions are scheduled according to machine operating hours or number of produced parts.

Although that systematic preventive maintenance reduces, the number of unexpected failures not all is avoided. On the remaining failures, a small percentage is not predictable, but most of them can be anticipated by analysing behaviour drifts of the machine tools.

16.7.1 Fleet Management System

The cloud-based fleet-wide platform for machine tool developed in Twin-Control project runs performance and health index algorithms on a huge number of machine tools that automatically upload collected data on the fleet server.

Algorithms are based on a multi-criteria analysis framework. They are parametrizable to fit with machine's specific characteristics and usage. Also, they are robust to consider real working conditions of machine tools.

The cloud-based fleet-wide platform capitalizes all the information on all connected machines to support trend analysis of indicators, which is the first step towards predictive maintenance policy.

16.7.1.1 Implementation and Results

Within the project, the cloud platform for machine tools is hosted on a dedicated server and available at https://twincontrol.kasem.fr/. RENAULT machine's fleet, used for the evaluation of the automotive use case, is composed of three machines. For this industrial use case, fleet-wide platform receives and analyses data in batch flow.

RENAULT produces small parts in series with a short cycle time. It means that, for each part behaviours, indicators are computed and, then, a trend analysis is performed for each indicator. Next, some examples of the results obtained in the fleet-wide platform are presented. These results present the detection and correlation of different events, which will serve as reference for predictive maintenance actions in the future.

16.7.1.2 Spindle Over-Speed Fault

According to machine program phases, i.e. for a couple tool and operation, several indicators have been defined mainly based on the spindle torque evolution. One of them is based on the saturation length during machining. Figure 16.20 compares the torque raw signal, while machining with tool 5504 in two different dates. Graphs show that at the end of cutting the torque reaches the maximum level. These observations are linked to the simulation results obtained applying the process models, as depicted in Fig. 16.8, where it was estimated a required torque for the boring operation that was very close to the spindle limits. Either tool wear or excessive raw material can lead to the spindle overload.

By following the trend of the saturation length per cycle, over-speed fault of the spindle is anticipated as depicted in Fig. 16.21. In the presented case, anticipation time is around 15 h. Fault is confirmed by RENAULT computer maintenance management system (CMMS), where a replacement of the tool is indicated at the fault time, as shown in Fig. 16.22.

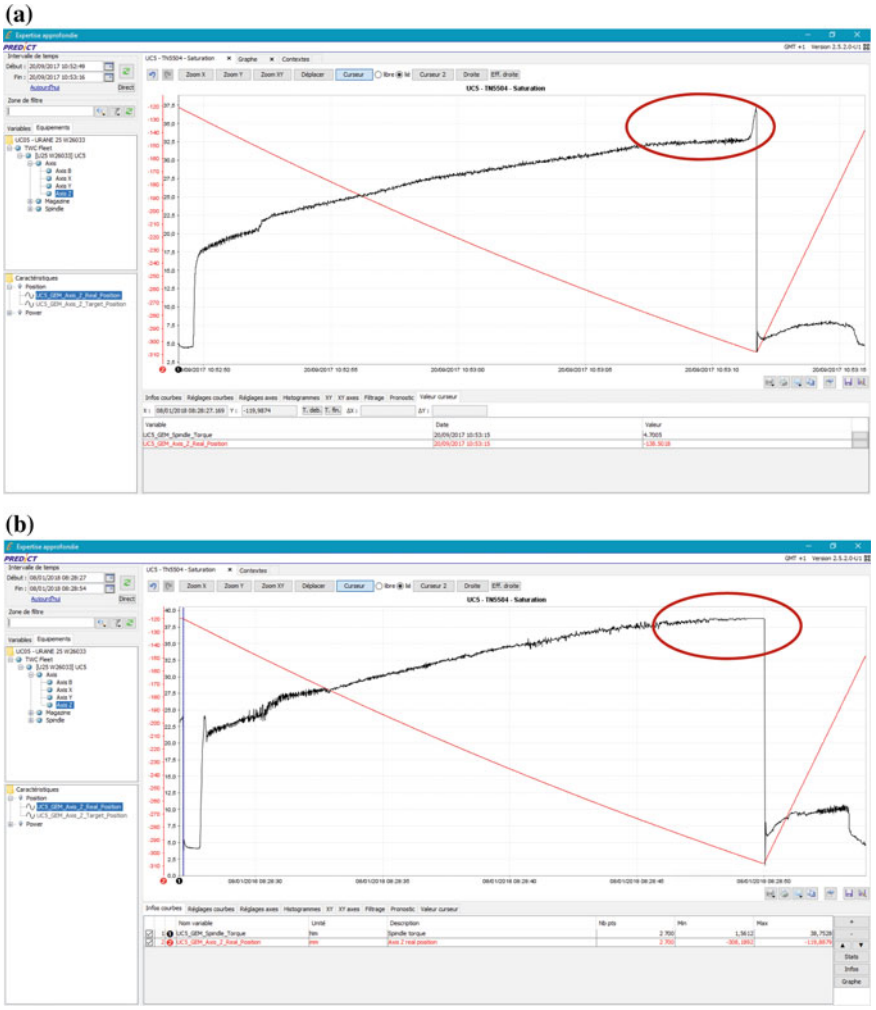

Fig. 16.20 Torque raw signal while machining with tool 5504: **a** September 2017; **b** January 2018

Tool Wear

Spindle torque-based indicators can be used to follow the tool wear curves. Several experimental studies show that the tool wear is given by a characteristic law depicted in Fig. 16.23. Three zones are considered: the adaptation zone (1), the linear wear zone (2) and the accelerated wear zone (3). Systematic tool change is based on a theoretical evaluation of the end on linear wear zone.

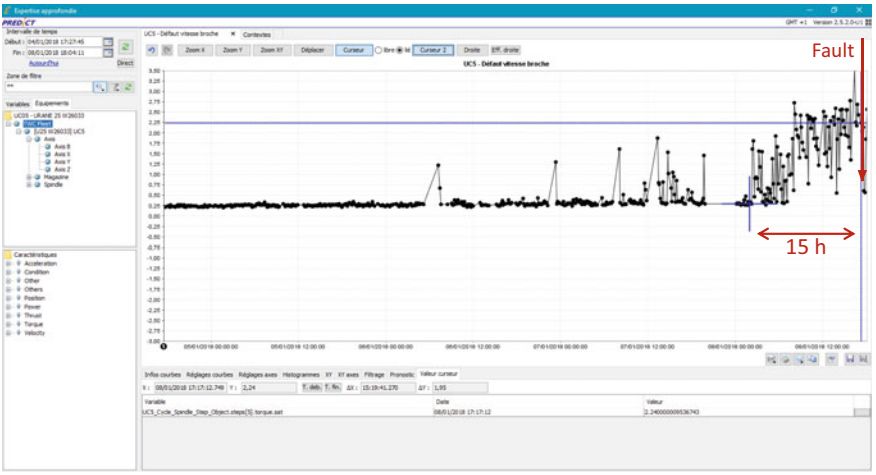

Fig. 16.21 Spindle over speed fault anticipation

S02	21177607	01	:
B2B	1	03	1151969 / 22009927
10/01/18	3		
	CEL	AB04556	vitesse broche

s: Défaut vitesse broche
c:
r:
v:

Le 10/01/2018 soir:
Le défaut se produit toujours avec le même outil, le T5504.
Vu avec le CDL pour changer l'outil dans un premier temps. A surveiller.

Fig. 16.22 Extract from RENAULT CMMS, Spindle speed fault on 2018/01/10 (in French)

Figure 16.24 shows an example of the tool wear estimation for tool 5208 based on spindle torque measurement. The accelerated tool wear zone can be clearly identified in both operations made with this tool for each workpiece. Accelerated wear zone is detected around 130 parts before is changed. As shown in Fig. 16.25, tool is replaced by RENAULT based on "frequency", i.e. maximum parts produced counter is reached, and not for accelerated wear. Machining with tools in the accelerated wear zone increases risks of both tool breakage and quality problems on the workpiece.

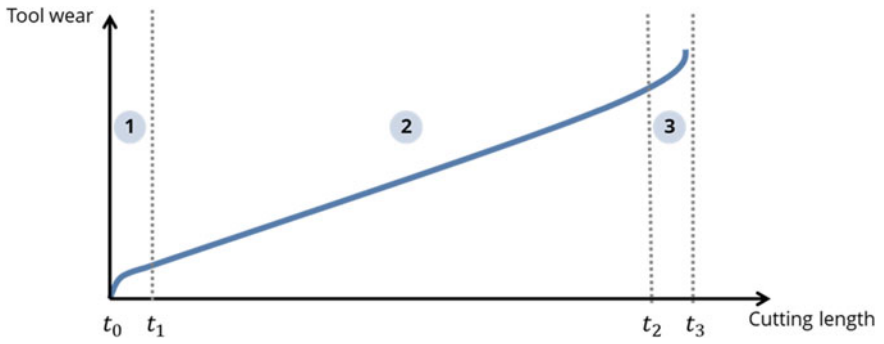

Fig. 16.23 Characteristic law of tool wear

Fig. 16.24 Accelerated tool wear zone detection

BILAN SUIVI CHANGEMENT D'OUTILS ANNÉE 2017

ATELIER Carter Flex 4556

A : DESROCHES				B : ANNE / VILLEDIEU				C : RENAU		
N°outil	Fréquence en minutes	Nbres de minutes	Mois	Date	Semaine	Cause	Commentaire	CU	Module	Equipe
T 5206	600 Mn	300	DÉCEMBRE	18/12/2017	51	autre	3d nc	52	6	b
T 5206	600 Mn	10	DÉCEMBRE	18/12/2017	51	autre	axe c	52	6	b
T 5206	600 Mn	600	DÉCEMBRE	05/12/2017	49	frequence		51	6	b

Fig. 16.25 Extract from RENAULT Tool replaces tracking system (in French)

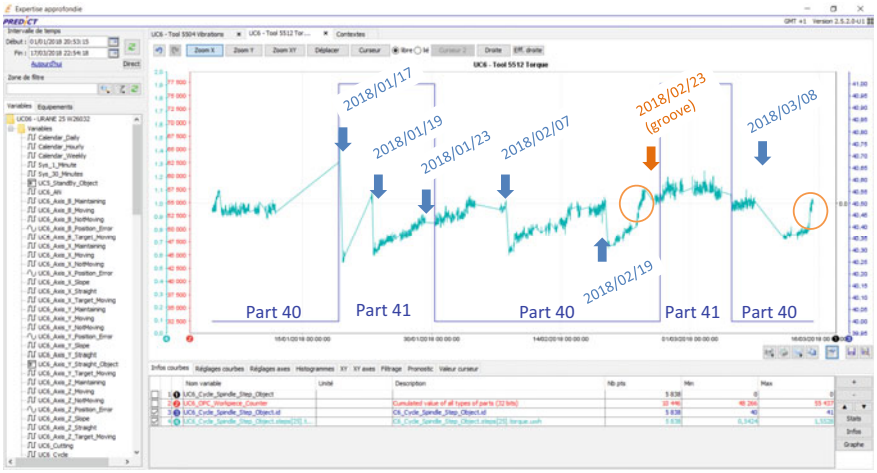

Fig. 16.26 Comparison of torque-based indicator and tool replace dates (Tool 5512)

Another example of tool wear is reproduced in Fig. 16.26 and shows the mapping of the indicator and the tool tracking system according to the two kinds of workpiece. The comparison highlights the correlation between rupture in torque-based indicators and replaces dates and shows two accelerated wear events (circled). Indeed, the first zone caused some grooves on the workpiece.

Workpiece Streaks

Trend analysis of torque-based indicators when not cutting, i.e. when tool comes out the workpiece, has been correlated to streak failure detection in the machined part. In this case, the considered behaviour is not an accelerated increase, but an abnormal decrease as depicted in Fig. 16.27.

Streaks were detected on one workpiece during quality control and caused by a problem on a valve in antivibration system as shown the extract of the CMMS in Fig. 16.28.

16.7.1.3 Impact

Main benefit proactive events are that machine tool users do not suffer the failure. They have time before the drift become a failure to take decision. Indeed, the knowledge of the drift allows to investigate and to identify the root causes in advance and according to the dynamic of the drift:

1. Wait for the next planned machine stop without stopping production by keeping drift under control using compensative maintenance actions. For instance, in case

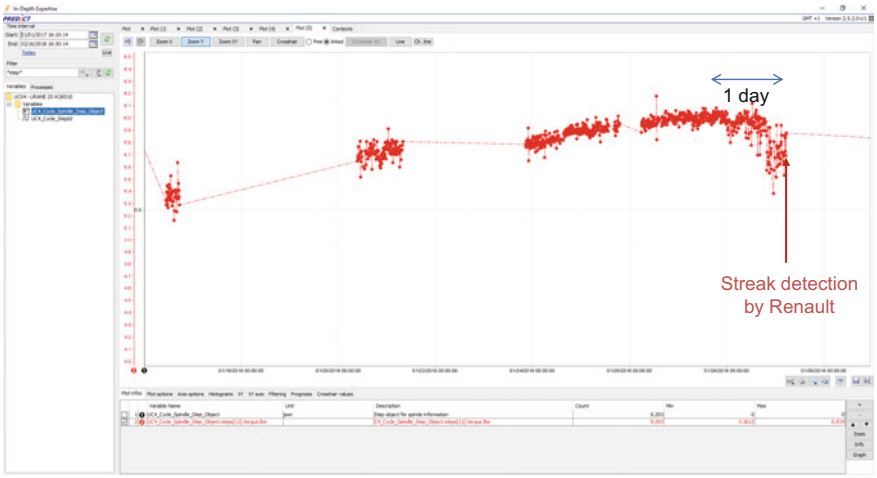

Fig. 16.27 Indicator behaviour before streak detection

S05	21324200	01	:
B2B	3	02	1075377 / 22011448 :
30/01/18	1		
	NDC	AB04556	Présence de stries dans le fut

s: Présence de stries dans le fut
c: valve de séquence de l'anti-vibration HS
r: fait changement de la valve et de l'accu
v: non

Fig. 16.28 Extract from RENAULT CMMS, streak detection on 2018/01/30 (in French)

of chip accumulation in one axis motor, a solution could be to clean the affected area periodically.

2. Find the right time to make the intervention. By instance, in case of shift-operating workshop use time between shift change having everything prepared before.

In case of linear motor failure, used in COMAU machines, the replace of the motor takes around 20 h for two experimented maintenance technicians. It means that, in case of motor failure, it is necessary to call off-duty people which adds extra costs to the intervention and increases machine downtime. In this scenario, the knowledge of the risk of failure several days in advance will avoid, at least, these additional costs and, also, unplanned machine stops. In case of RENAULT, each of these types of maintenance activities causes a reduction in production of more than 170 parts.

In case of spindle failure or drift, early detections reduce the overall production costs. Indeed, any abnormal behaviour on the spindle can decrease workpieces qual-

ity. As quality control is realized according to a random sampling law, once a quality problem is detected, several workpieces can be degraded. By instance, in RENAULT cases, spindle abnormal behaviour is detected between 24 and 15 h before alerts. It means that between 130 and 170 parts may be out of specification and must be geometrically controlled by a specific service with a specific machine. These controls increase the overall production costs.

Proactive events also contribute to the reduction of energy consumption of the machine because in most cases abnormal behaviours an equipment will increase its consumption.

16.8 Scenario of Use 5: Quality Control

RENAULT makes quality monitoring using QDAS quality management system (www.us.q-das.de/en/applications/). There is currently no interaction between the quality data stored in QDAS and the manufacturing processes.

Due to short cycle times in automotive use case, it is not possible to measure the 100% of the machined parts. Normally, one part is measured by working turn (every 8 h). If incorrect parts are machined between measurements, they are not detected.

16.8.1 Local Machine Tool and Process Monitoring and Control Device

By using the monitoring infrastructure of Twin-Control, and integrating QDAS data inside, a correlation between process parameters and quality measurement can be done. This should allow 100% scrap detection and reduce measurement work power.

16.8.1.1 Implementation and Results

Figure 16.29 presents the approach followed to integrated quality and process data in Twin-Control project. On the one hand, process data is collected from each machining centre through the installed ARTIS monitoring hardware. On the other hand, data from 3D measurement machines is managed in QDAS.

For each part, all physical process parameters, which are monitored, are retrieved and identified through the part number. The same part number is used to identify the quality measurement file (dfq extension) from QDAS. ARTIS has developed a converter to get process data in QDAS format. This allows the integration in the same environment (Fig. 16.30).

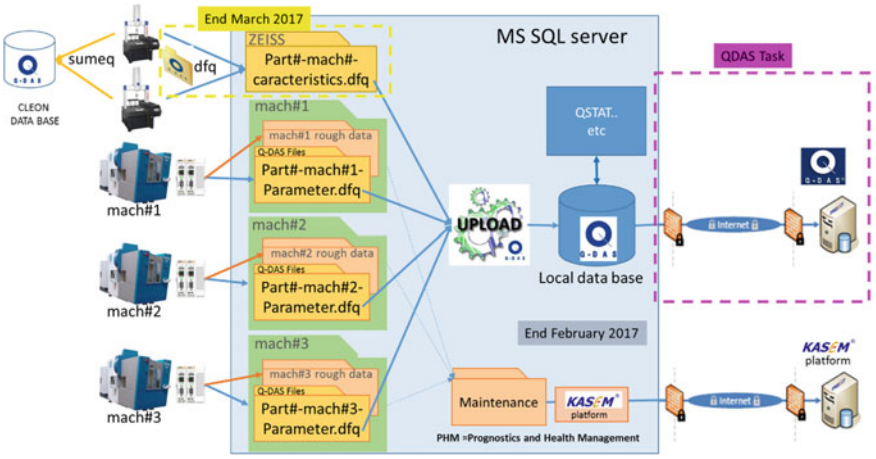

Fig. 16.29 QDAS and process data integration approach

A first application covers the big boring machining of the automotive validation scenario, presented in Fig. 16.8. Figure 16.31 shows the first results of the integration of process (spindle torque) with quality (cylindricity and diameter) data in KASEM®.

After a long period of analysis by QDAS and ARTIS, it has been observed that a lot of characteristics could be predictable. More than the half of characteristics have a correlation ratio R^2 between the model and the real values more than 0.8 (Fig. 16.32).

16.8.1.2 Impact

Once the system is implemented and a learning stage is completed, it should allow detecting all bad quality parts from process monitoring data (faster response time). This leads to:

- Reduce the measurement work load by 2: The need to measure the part quality should be reduced because the model would be enough robust to predict the quality.
- Improve process robustness and detect quality deviation for process correction and maintenance. Scrap parts will be reduced.

16.9 Conclusions

This chapter summarizes the evaluation of Twin-Control project in an automotive validation scenario. A specific evaluation approach is defined, based on different Scenarios of Use defined in the project. The results and the impact of Twin-Control features are structured according to these Scenarios of Use.

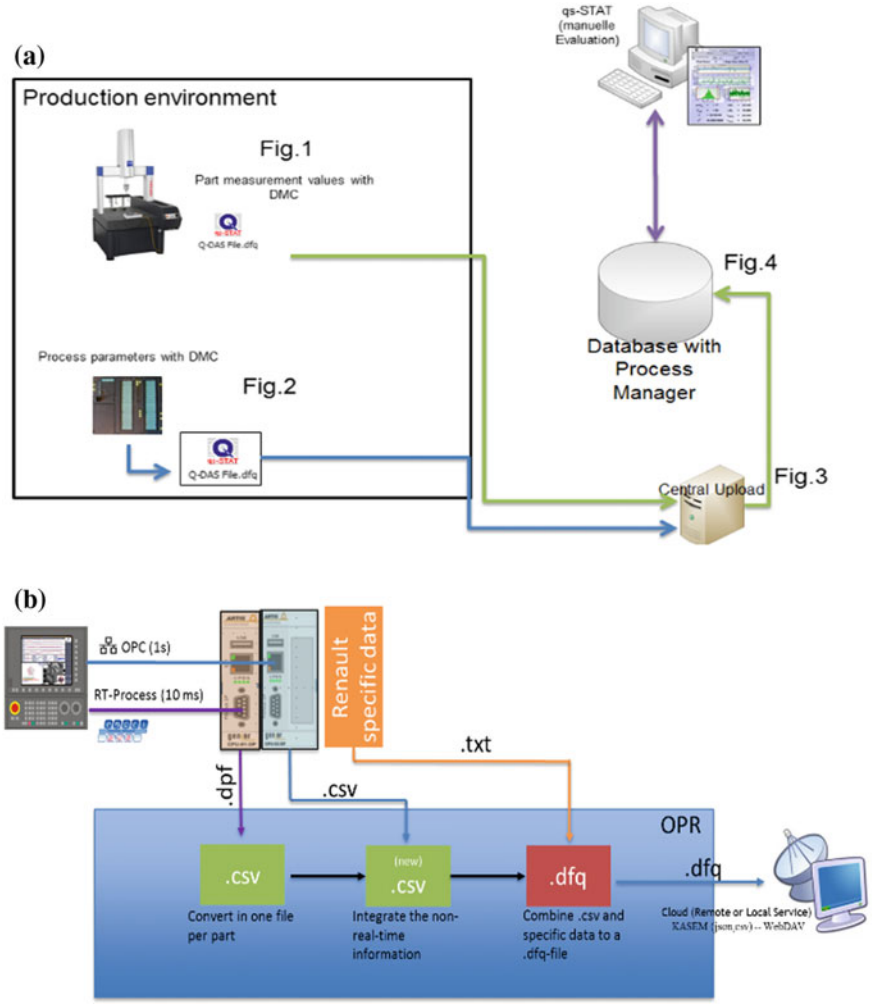

Fig. 16.30 Integration of process and quality data: **a** QDAS data management; **b** conversion of process data from ARTIS to QDAS readable files

The application of Twin-Control in an automotive industrial scenario can potentially affect end-users product development:

- A reduction of a 10% in the total development time of a new machine tool.
- The design of machine tools with a 37% lower energy consumption.
- A reduction of the 11% in the design and set-up of a new process
- A reduction of tooling cost of 5–10%, depending on the part.
- Reduction of energy consumption (35%) of a machine in production by analysing the energy consumption by components.

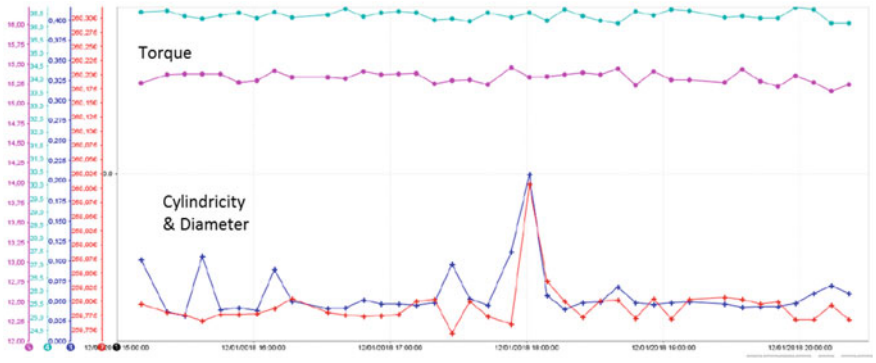

Fig. 16.31 Screenshot of KASEM showing process and quality data comparison

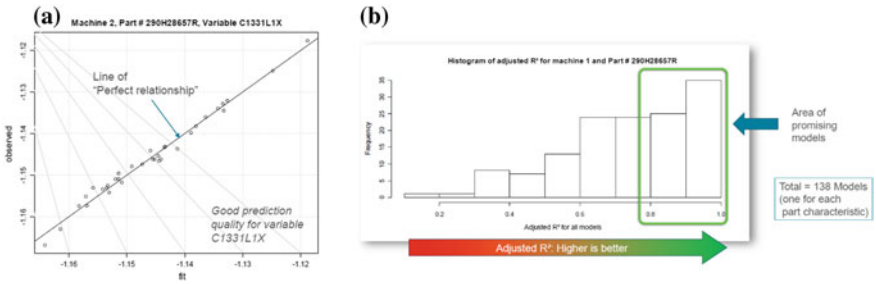

Fig. 16.32 Graphs generated in QDAS reports after integration of process data

– Reduction of machine downtime and maintenance costs thanks to predictive maintenance approach.
– Detect quality deviations, minimize scrap parts and reduce part measurement load by integrating quality and process data.

Conclusions and Next Steps

This book presents the work carried out in Twin-Control project during three years through collaboration of relevant research and industrial partners. Applications and concepts from ICTs have been applied to machine tool industry in all its life cycle, with the objective of increasing the overall equipment efficiency (OEE).

Each development of the project has been validated at research level, showing promising results. However, the aim of Twin-Control, from its gestation, was to provide industrial sense to all this new ICT tools, and hence, a complete industrial validation and evaluation approach has been designed and executed, based in two scenarios from two of the most critical manufacturing sectors in Europe: automotive and aerospace. Twin-Control features have been implemented, validated and evaluated (analysing its impact) in each of the proposed scenarios. The results have been very positive and the impact or potential impact, in case of further utilization of the tools, is very high at all levels: machine tool design, process design, maintenance, process control and quality control.

Developments of the project have been grouped according to their application field and possibilities for joint exploitation:

- A state-of-the-art digital twin of machine tools has been developed. The integrated simulation tool developed in the project is based on a FEA software that integrates the machine structural analysis with the control and the machining process. Results at both research and industrial level are very positive. However, one of the drawbacks is the required long simulation times for some machining operation simulations, which makes it unsuitable for some applications. Further work is required in the optimization of this model. The obtained results should be also used to redefine the digital twin concept proposed in Twin-Control. To cover this drawback, a simulation tool that focuses on the machining process has been developed that perform fast machining simulations by, of course, reducing the available results such as effect of machining process on the structural components on the machine tool.

M. Armendia et al. (eds.), *Twin-Control*,
https://doi.org/10.1007/978-3-030-02203-7

- A local monitoring infrastructure has been developed and implemented. In addition, new features have been developed to provide "intelligence" to the monitoring system and use it to control the manufacturing processes. Depending on the application and/or sector, different features are of interest and can be applied independently.
- Towards application of proactive maintenance, two main issues need to be overcome in the future. First one is the reluctance of machine end-users to share data with third parties. Platform developers and Operations and Maintenance (O&M) providers need to work together to present data monitoring and analytics as a safe and very profitable service for them. Second one is the need of knowledge about the analysed systems before applying a real proactive strategy. In this line, customer must be aware of the need to implement monitoring and data management systems a long time before being able to predict failures. End-users' experience and collaboration potential are very relevant to reduce this learning phase. In this project, thanks to the gathering of machine usage data for almost two years, first correlations of process data with machine tool condition are presented.

The editors of the book, together with all Twin-Control project partners, thank the European Commission for the funding of the project (GA No.: 680725) within the H2020 framework and as part of the Factories of the Future initiative. In the same way, the editors thank all project partners, authors of the book and industrial partners, for the intensive collaboration that contributed to the success of the project, which is represented in this book.

Mikel Armendia
Mani Ghassempouri
Erdem Ozturk
Flavien Peysson